Proceedings of the Thirty-Second
Ohio River Valley Soils Seminar

REGIONAL SEISMICITY AND GROUND VIBRATIONS

October 24, 2001
The Galt House
Louisville, Kentucky

Sponsored by

Kentucky Geotechnical Engineering Group, ASCE

University of Louisville
Department of Civil and Environmental Engineering

University of Kentucky
Department of Civil Engineering
and Kentucky Transportation Center

and

Cincinnati Geotechnical Engineering Group, ASCE

University of Cincinnati
Department of Civil and Environmental Engineering

ORVSS XXXII
ORGANIZING COMMITTEE

Raymond E. Frye, Jr.
Law Engineering and Environmental Services, Inc.

Michael Mattingly
Fuller, Mossbarger, Scott and May Engineers, Inc.

Timothy M. O'Leary
Law Engineering and Environmental Services, Inc.

Troy S. O'Neal
U. S. Army Corps of Engineers, Louisville District

Thomas Rockaway
Qore Property Sciences, Inc.

David G. Sawitzki
AMEC Earth and Environmental, Inc.

Nicholas G. Schnitt
Law Engineering and Environmental Services, Inc.

Mark J. Schuhmann, Chairman
Law Engineering and Environmental Services, Inc.

C. Robert Ullrich, Proceedings Editor
University of Louisville

ORVSS XXXII
EXHIBITORS

Densification, Inc.
40650 Hurley Lane
Paeonian Springs, VA 20129
540-882-4404
www.densification.com

Diedrich Drill, Inc.
1719 State Street
Laporte, IN 46350
219-326-7788
www.diedrichdrill.com

Durham Geo-Slope Indicator
2175 West Park Court
Stone Mountain, GA 30087
770-465-7557
www.slopeindicator.com

Elastizell Systems, Inc.
2475 Arbor Blvd.
Dayton, OH 45439
937-298-1313
www.elastizell.com

Global Drilling Suppliers, Inc.
12101 Centron Place
Cincinnati, OH 45246
800-356-6400
www.globaldrilsup.com

Richard Goettle, Inc.
12071 Hamilton Avenue
Cincinnati, OH 45231
513-825-8100
www.goettle.com

GRL & Associates
4535 Renaissance Pkwy.
Cleveland, OH 44128
216-831-6131
www.pile.com

Keller Foundations, Inc.
1130 Annapolis Road, Suite 202
Odenton, MD 21113
410-551-8200
www.haywardbaker.com

Knauf Polystyrene
2725 Henkle Drive
Lebanon, OH 45036
800-221-6923
www.geoform.ce

Nicholson Construction Company
3085 Perkins Avenue
Morgantown, NC 28655
828-439-8988
www.nicholson-rodio.com

Nicholson Construction Company
12 McClane Street
Cuddy, PA 15031
412-221-4500
www.nicholson-rodio.com

Pile Dynamics, Inc.
4535 Renaissance Pkwy.
Cleveland, OH 44128
216-831-6131
www.pile.com

The Reinforced Earth Company
8614 Westwood Center Drive, Suite 1100
Vienna, VA 22182
703-749-9270
www.reinforcedearth.com

Tensar Earth Technologies
10979 Reed Hartman Hwy., Suite 331A
Cincinnati, OH 45242
513-891-8808
www.tensarcorp.com

ORVSS XXXII
EXHIBITORS

United Dynamics
1301 Fabricon Blvd.
Jeffersonville, IN 47130
812-282-2222
www.ussudi.com

Versa-Lok South
P. O. Box 1138
Murfreesboro, TN 37133
615-867-0030
www.versa-lok.com

Vibra-Tech Engineers
2700 Holloway Road, Suite 113
Louisville, KY 40299
502-240-9900
www.vibra-tech-inc.com

TABLE OF CONTENTS

CENTRAL U.S. EARTHQUAKE HISTORY AND HAZARD

Chris H. Cramer, Ph.D.[1], Martitia P. Tuttle, Ph.D[2], and Eugene S. Schweig III, Ph.D.[1]

ABSTRACT

Assessing earthquake hazard involves a knowledge of earthquake history in a region, a means of estimating the size of future earthquakes and their anticipated ground-motions, and an understanding of the effects of site geology on ground shaking. Seismological research in the last five years has improved our understanding of the potential for major earthquakes in the central U.S. Paleoseismological research in the Mississippi embayment and the southern Illinois basin have clarified the expected recurrence intervals for large damaging earthquakes. In the New Madrid seismic zone, there have been three 1811-1812-type sequences of major earthquakes in the last 1600 years: 900 AD ±100 years, 1450 AD ±150 years, and 1811-1812. This rate is higher than expected by extrapolating the rate of smaller magnitude historic and modern earthquakes to larger magnitudes. On the other hand, for the southern Illinois basin, paleoseismic results suggest that M7 earthquakes occur at the same rate predicted by historical seismicity, which indicates a several-thousand-year recurrence interval.

The recent M7.7 Bhuj, State of Gujarat, India, earthquake of 26 January 2001 provides insight into the seismic hazard of the central U.S. Although the Gujarat geologic setting may not be a perfect analog for New Madrid, seismic-wave attenuation, magnitude vs. rupture-area, magnitude vs. distance of liquefaction, and perhaps earthquake occurrence rates from Gujarat are similar to the central U.S. In particular, for a given rupture area, magnitudes of M>7 intraplate earthquakes are systematically 0.3 units higher than the worldwide average. One possible explanation for this may be that ruptures extend deeper into the lower crust where rock rigidity is higher. For the same-sized rupture area, this implies higher ground motions in the central U.S. and India than in younger crustal settings such as California.

National Seismic Hazard maps provide reasonable probabilistic estimates of strong ground motion for the central U.S. However, these estimates are for firm rock (average shear-wave velocity of 760 m/s for the top 30 m). Hence, ground-motion estimates need to be adjusted for site-specific soil conditions when used in engineering design. State-of-practice methods of making these site-specific adjustments using soil-amplification factors are a hybrid of deterministic and probabilistic methods. For a truly probabilistic result, a fully probabilistic method must be used, which adjusts the hard-rock ground-motion attenuation relations to site-specific relations prior to making hazard calculations. Comparisons are made among site-amplifications from recent central-U.S. research and NEHRP soil site-factors.

INTRODUCTION

Understanding the earthquake hazard in the central U.S. involves not only a knowledge of the earthquake history of the region, but also estimating the size of future earthquakes and their anticipated ground motions. Due to relatively low seismicity and limited earthquake data, observations from analogous regions worldwide are important data for hazard assessement in the central U.S. For engineering design, the effects of site geology on ground shaking should be included.

[1] U.S. Geological Survey, 3876 Central Ave Ste 2, Memphis, TN 38152-3050
[2] M. Tuttle and Associates, 128 Tibbetts Lane, Georgetown, ME 04548

The earthquake history of the Central U.S. starts with the New Madrid series of major earthquakes in 1811 and 1812 (Johnston, 1996). Prehistoric records from dated liquefaction features (e.g., Obermeier, 1998; Tuttle et al., 2001a) extend the history of the largest earthquakes back in time. Research in the last five years has improved our understanding of the potential for major earthquakes and hence the level of seismic hazard in this region. The most recent advance in our understanding of central U.S. seismic hazard has come from halfway around the world. The M 7.7 Bhuj, India earthquake of 26 January 2001 (Bendrick et al., 2001) provides new insights concerning intraplate earthquakes, and can help us estimate the levels of ground shaking to be faced during future major earthquakes in the central U.S.

All of this information must be interpreted in the context of quantifying earthquake hazard. The National Seismic Hazard maps (Frankel et al., 1997) provide a reasonable basis for probabilistic estimates of strong ground-motion for the central U.S. These ground-motion estimates are regional in character and for firm-rock site-conditions (average shear-wave velocity of 760 m/s over the top 30 m). They need to be adjusted for site-specific soil conditions when used in engineering design.

The goals of this paper are 1) to briefly review recent advances in our understanding of major earthquake recurrence rates in the central U.S., 2) to summarize the implications of the Bhuj, India earthquake for eastern North America (ENA) seismic hazard, and 3) to briefly compare a few approaches for determining site-specific ground-motions at soil sites. This is an overview paper and therefore limited to highlighting recent advances and citing references for more detailed information.

RECENT PALEOSEISMIC RESEARCH

Much of the recent progress in understanding central U.S. seismic hazard has come from paleoliqefaction studies. Tuttle et al. (2001a) have presented their most recent findings for the New Madrid seismic zone. Liquefaction features are dated and interpreted in terms of past earthquakes. Figure 1 shows the locations, estimated ages, and measured sizes of all dated liquefaction features. In addition to the historical 1811-1812 sequence of earthquakes, liquefaction features are attributed to events around 1450 AD, 900 AD, 300 AD, and 1370 BC. Liquefaction features attributed to the 1450 AD and 900 AD events have narrow age constraints and are broadly distributed, while those related to the 300 AD and 1370 BC events are poorly constrained in terms of their age and occur in the northern part of the seismic zone. This is illustrated in Figure 2 from Tuttle et al. (2001a), which shows the relative positions of liquefaction features along a NE-SW transect and the dating constraints on the liquefaction features and thus their causative events. The dates of 1450 AD $\pm$ 150 y and 900 AD $\pm$ 100 y correspond well with Kelson et al.'s (1996) dates of 1260 AD - 1650 AD and 780 AD - 1000 AD for two events of ground deformation above the Reelfoot thrust fault.

Field data also suggest that the 1450 AD and 900 AD represent earthquake sequences, similar to what occurred in 1811-1812 (Tuttle et al., 2001a). This finding is important for seismic hazard assessment because New Madrid $M > 7$ earthquakes seem to cluster closely in time when they do occur. Clearly, the last three sequences of $M > 7$ events in the New Madrid seismic zone have occurred with an average recurrence interval of ~500 years. This geologically short time between earthquakes is difficult to reconcile with the low regional strain-rates observed geodetically (Liu et al., 1992; Newman et al., 1999). Kenner and Segall (2000) have attempted to model this kind of behavior with a heterogeneous viscoelastic lower crust.

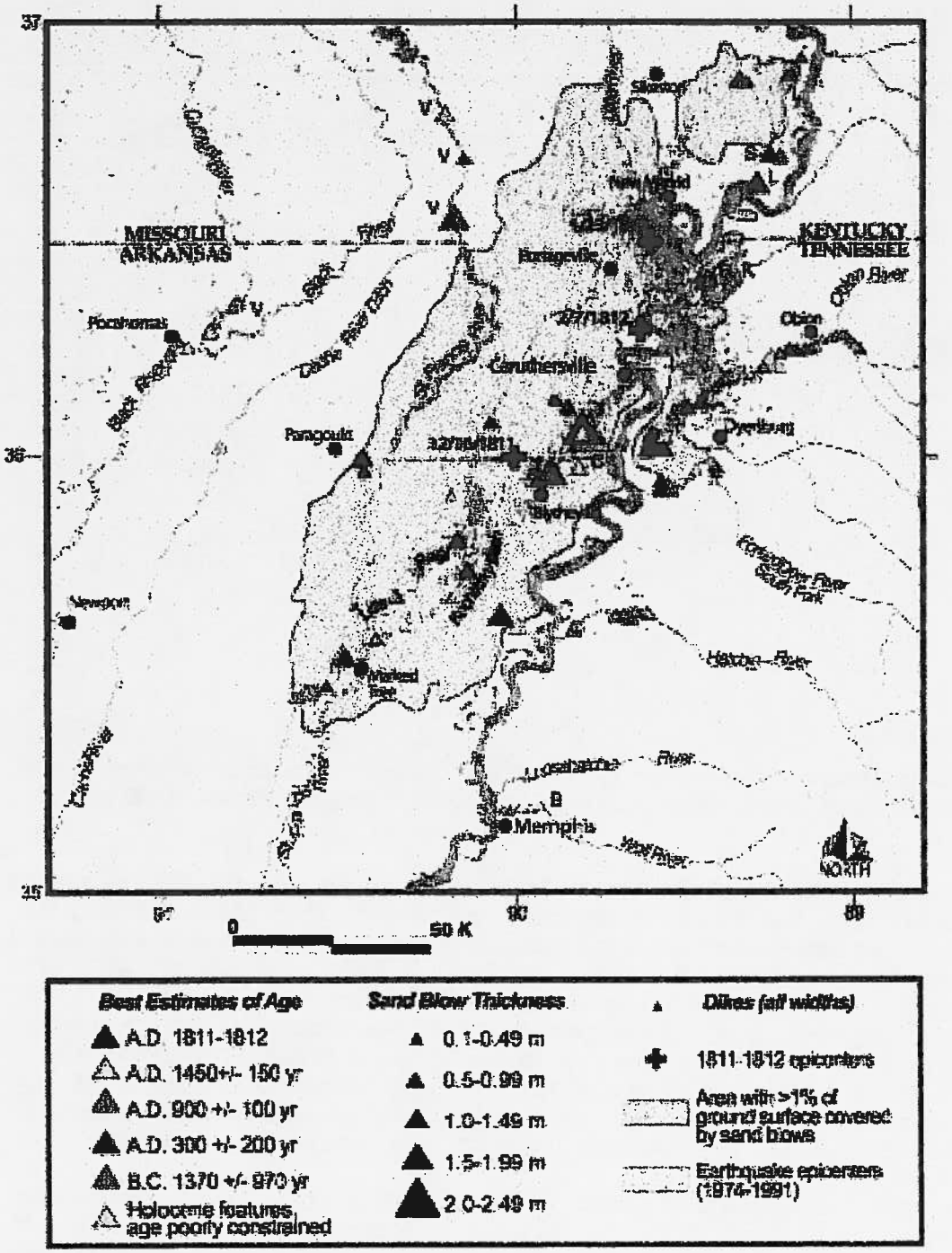

Figure 1: Map of New Madrid seismic zone showing estimated ages and measured sizes of liquefaction features (from Tuttle et al., 2001a).

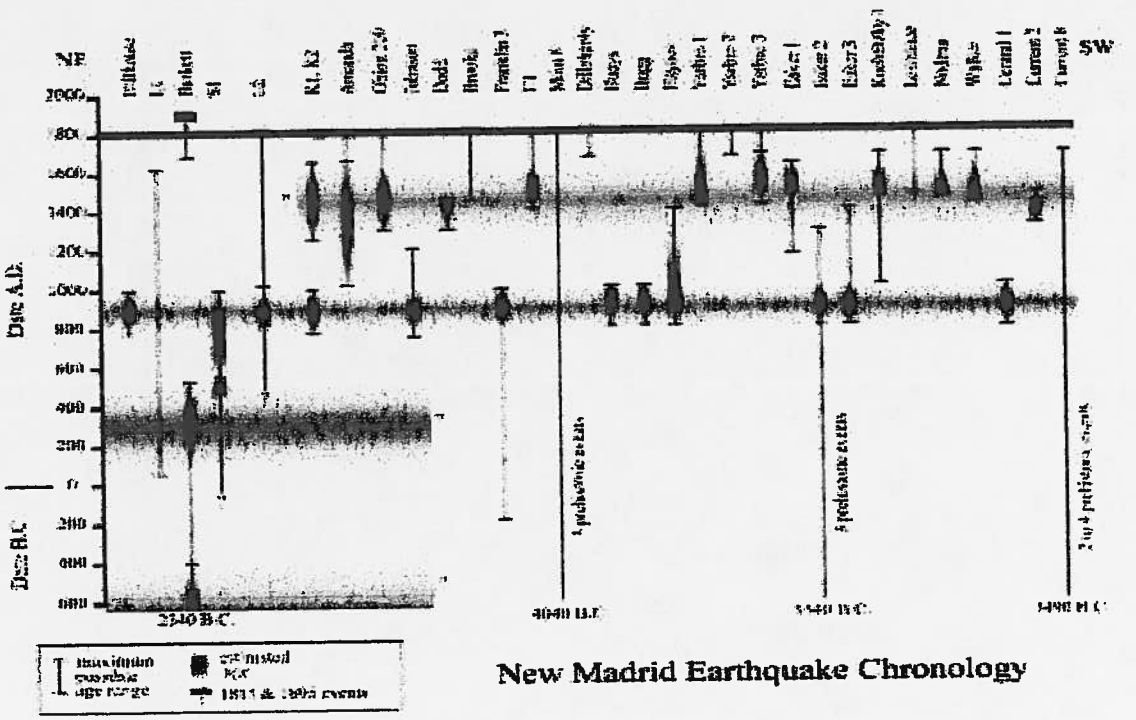

Figure 2: Earthquake chronology for the New Madrid seismic zone from dating and correlation of liquefaction features across the region (from Tuttle et al., 2001a).

Figure 3 compares the rate of M > 7 New Madrid earthquakes with the rates of smaller magnitude events for historical and instrumental catalogs (data from Mueller et al., 1997). The rate of M > 7 earthquakes is an order of magnitude greater than would be extrapolated from the historical earthquake rate. This type of fault behavior is typical of mature fault systems and is often seen in more active areas such as California (Wesnousky, 1994). Basically, it is more efficient to release stored stress in large earthquakes that are produced by similar-sized rupture areas, i.e. characteristic earthquake behavior. The implication for seismic hazard in the central U.S. is that the rate of the largest earthquakes in the New Madrid seismic zone is independent of the rate of smaller earthquakes. The paucity of small earthquakes can lead to a false sense of security as far as society is concerned.

Another earthquake source area of concern in the central U.S. is the southen Illinois basin (also know as the Wabash Valley seismic zone). Obermeier (1998) summarizes the paleoliquefaction research results to date. As shown in Figure 4, the paleoseismic data suggests a rate of large earthquakes that is comparable to that predicted by the rate of smaller earthquakes, unlike the New Madrid seismic zone discussed above. Therefore, the recurrence interval of M 7 earthquakes in the southern Illinois basin is several thousand years. From a seismic hazard point-of-view, the risk of a large earthquake in the southern Illinois basin is lower than in the New Madrid seismic zone.

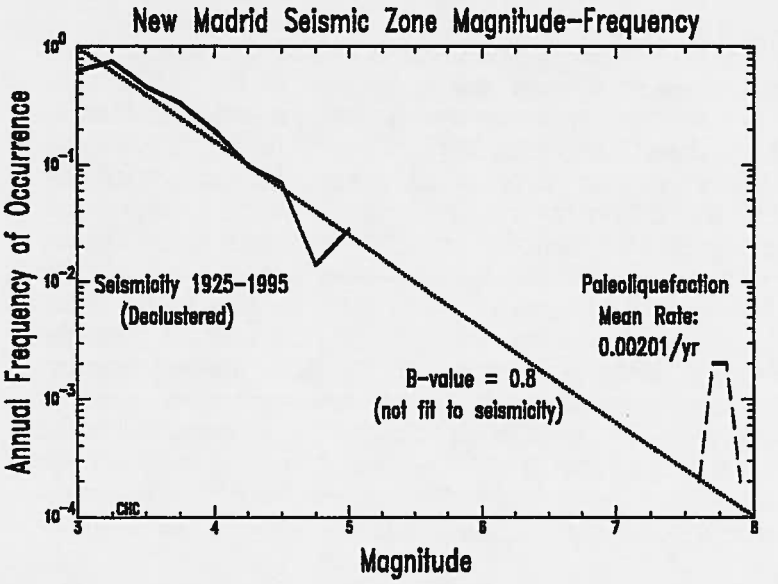

Figure 3: New Madrid seismic zone magnitude frequency plot showing the annual frequency of occurrence from seismicity (solid line) and paleoseismic data (dashed line). The shape of the paleoseismic data emphasizes that the paleoseismic mean rate (top of pyramid shape) is above the projection of the seismicity rate from 1925-1995. A Gutenberg-Richter (exponential) distribution with a b-value (slope) of 0.8 is shown as the projection of the smaller magnitude seismicity rate (dotted line).

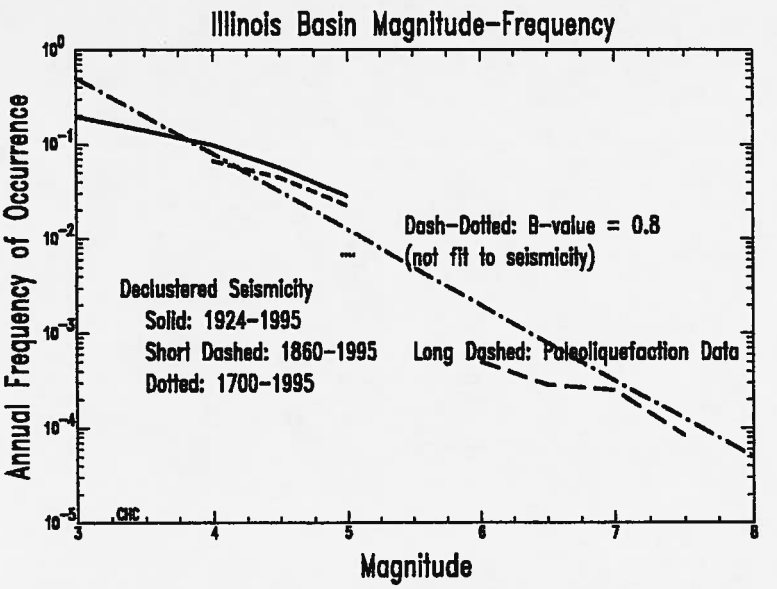

Figure 4: Plot similar to Figure 3 for the southern Illinois basin (Wabash Valley area). Seismicity is shown for different time periods with varying magnitude-thresholds of completeness, including a short, dotted line for M 5 earthquakes in the region since 1700. The paleoseismic data of Obermeier et al. (1998) is plotted as the long-dashed line. A projected Gutenberg-Richter rate of smaller earthquakes with a b-value of 0.8 is shown as a dash-dotted line in this figure.

Other areas of faulting and scattered seismic activity occur in much of the central U.S. Two prominent features of note are the Commerce geophysical lineament (Langenheim and Hildenbrand, 1997) and the East Tennessee seismic zone (Chapman et al., 1997). The Commerce geophysical lineament is a magnetic signature thought to represent a structure in the Precambrian basement (Hildenbrand and Hendricks, 1995). Several faults, including the English Hill fault in the Benton Hills of southeastern Missouri, are spatially associated with the lineament. Hoffman et al. (1996) found Tertiary and Cretaceous deposits juxtapose late Pleistocene Peoria loess across the English Hill fault, the first direct evidence of Quaternary age faulting in the embayment. Large liquefaction features have been found in close association with the Commerce geophysical lineament in the Western Lowlands (Tuttle, 1999). If they are related to a local source and not the New Madrid seismic zone, the liquefaction features might indicate that faults associated with the CGL are seismogenic. Paleoseismological studies have not been conducted in the East Tennessee seismic zone. It is not clear whether the East Tennessee seismic zone is capable of long ruptures and hence large, damaging earthquakes. Seismic hazard can only be estimated in these areas by the rate of smaller events, which leads to some risk associated with these zones of seismicity, especially the East Tennessee seismic zone, as shown by the National Seismic Hazard maps (Frankel et al., 1997) (Figure 5).

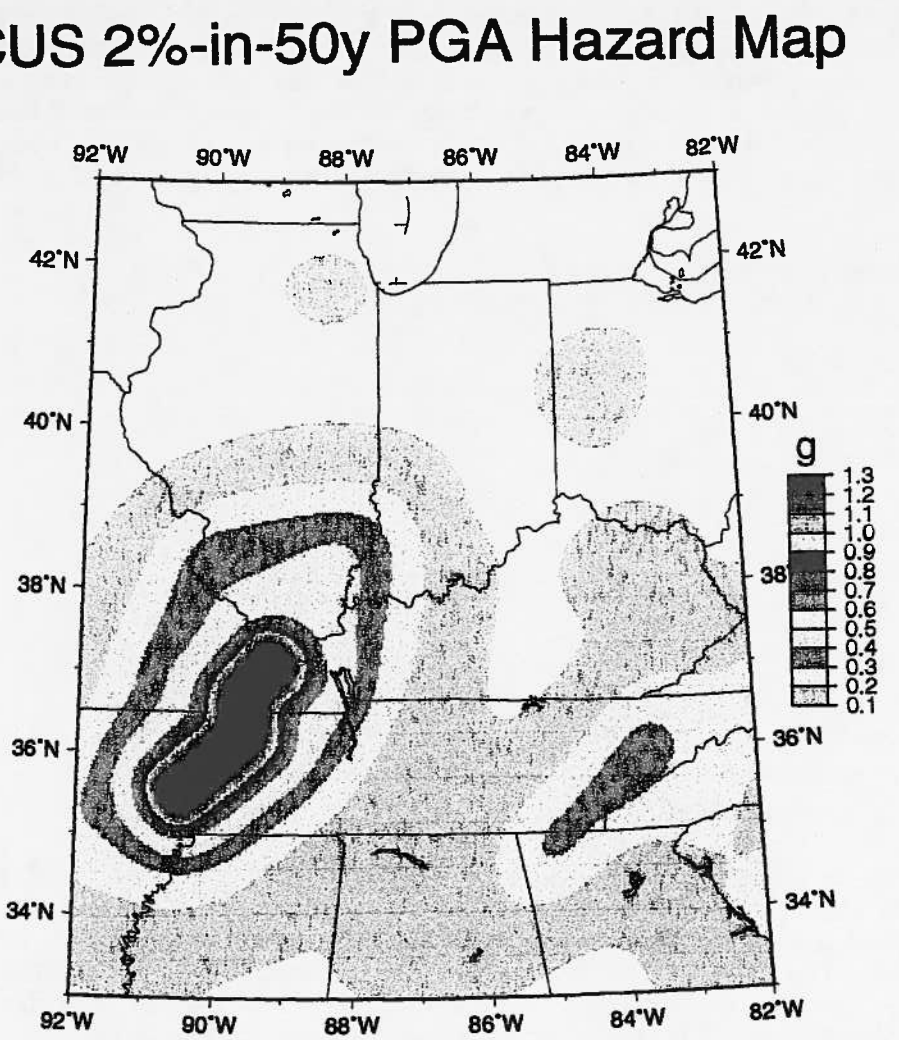

Figure 5: Central U.S. 2%-in-50-year PGA hazard map from Frankel et al. (1997).

BHUJ, INDIA EARTHQUAKE AND ENA SEISMIC HAZARD

The recent M7.7 Bhuj, Gujarat, India earthquake of 26 January 2001 (Bendrick et al., 2001; Tuttle et al., 2001b) also provides insight into the seismic hazard of the central U.S., particularly with regard to seismic-wave attenuation, magnitude vs. rupture area, magnitude vs. distance of liquefaction, and perhaps earthquake occurrence rates. Although the State of Gujarat's geologic setting may not be a perfect analog for New Madrid, there are some striking similarities. Earthquake activity in both regions occurs in thick, colder, Paleozoic crust and within Mesozoic rift structures that have been reactivated in the Cenozoic under regional compression. The tectonic setting, strain rates, and style of deformation may differ, but the rate of earthquake occurrence is fairly low (compared to a plate boundary) in both areas as shown in Table 1. While it is often assumed that seismically active areas should have distinct topography related to repeated fault rupture at the surface, no obvious fault rupture has been documented from the Bhuj, India earthquake or from many large, historical ENA earthquakes. This may be related to the occurrece of deep focus earthquakes beneath the thick sedimentary basins of the Banni Plains in India and the Mississippi embayment in the central U.S. Gujarat is closer to a plate boundary (~300 km to a strike-slip boundary and ~1000 km to the compressional boundary that is the source of the regional compression affecting India) than New Madrid (several thousand km from a plate boundary). But the limited paleoseismic data for Gujarat (Rajendran and Rajendran, 2001) suggest that at least one fault has a ~1000 year recurrence interval for M > 7 earthquakes, which is about an order of magnitude shorter than extrapolated from smaller earthquakes (see Table 1). Paleoseismic results for New Madrid, as already presented above, give similar results, suggesting that in both Gujarat and in the central U.S., low seismicity rates do not necessarily mean low seismic hazard.

Table 1: Seismicity and Recurrence Comparison for Activity Prior to 2001

	Gujarat	New Madrid
Seismicity (with aftershocks removed)		
M 7:	1819	1811-1812
M 6:	1956	1895
M 5:	1903, 1940	1865, 1903
Recurrence of M 7's		
From M 4's:	~10,000 y	~5,000 y
Paleoseismic:	800-1000 y	500 y

The Bhuj earthquake induced liquefaction and related ground failures over an area >15,000 km^2 and possibly up to 250 to 300 km from its epicenter (Tuttle et al., 2001b). Similarly, the 1811-1812 earthquakes are thought to have induced liquefaction over an area of >10,000 km^2 and up to 250 km from their inferred epicenters (Saucier, 1977; Street and Nuttli, 1984; Obermeier, 1989; Johnston and Schweig, 1996). Empirical relations between earthquake magnitude and distance of liquefaction have been developed to assess liquefaction potential during future events (e.g., Youd and Perkins, 1987; Ambraseys, 1988). However, much of the data from which these relations are calculated come from cases in interplate settings where the characteristics of earthquakes and attenuation of ground motions may be different from intraplate regions. The Bhuj earthquake offers the opportunity to measure the maximum distance of liquefaction for a very large intraplate-like earthquake and thus will help to calibrate magnitude-distance relations for intraplate regions.

Seismic-wave attenuation in both India and ENA are also similar. Singh et al. (1999) shows the similarity of seismic-wave attenuation between India and ENA for weak ground-motions

(< 0.1g) (see their Figure 3b). This is not surprising, considering the similar age and geologic history of the crust in both regions. Thus, Indian strong ground-motion recordings can be an important means of understanding expected earthquake ground-motions in the ENA where strong ground-motion records and intensities from large (> M 6) earthquakes are lacking or very limited.

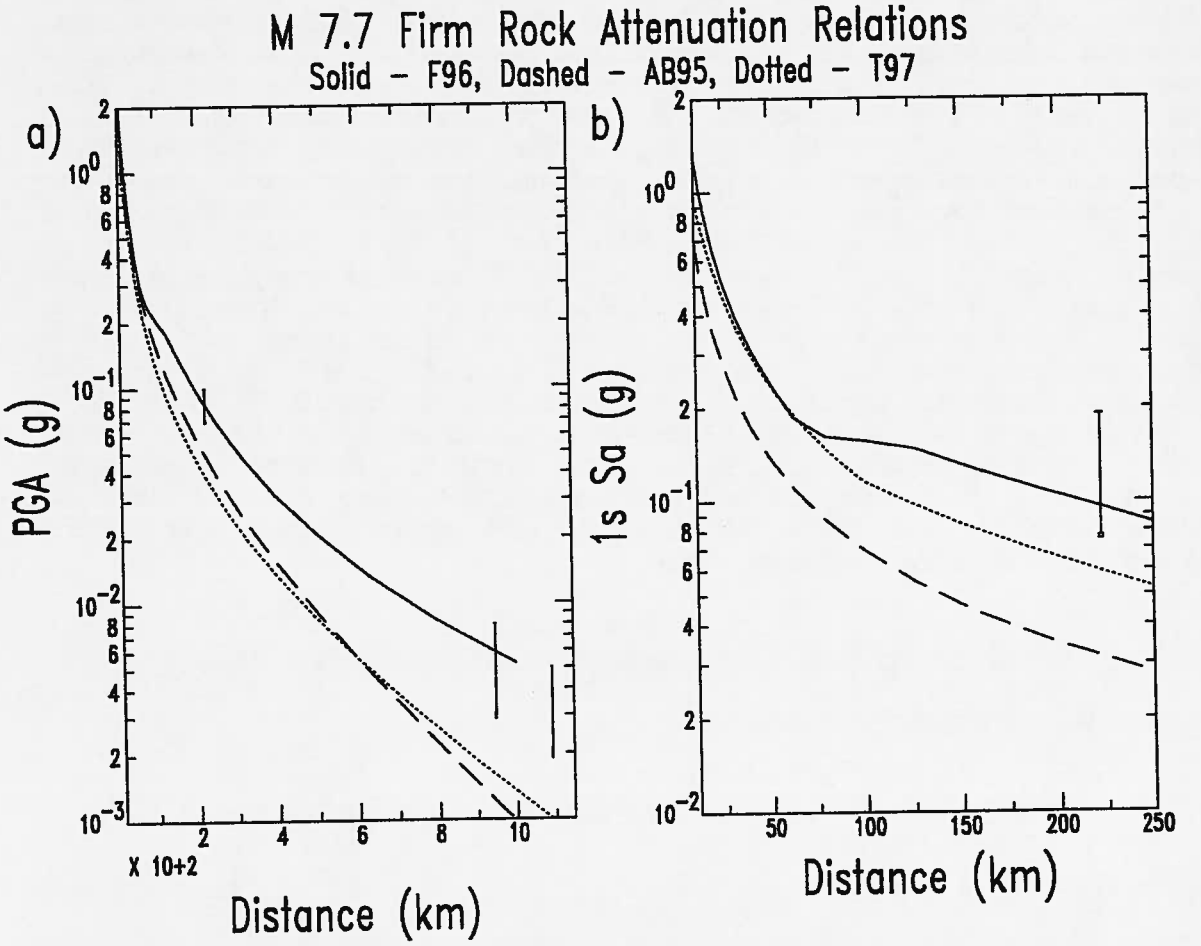

Figure 6: Comparison of the Bhuj, India strong-motion data with the three best-known ENA ground-motion attenuation relations: a) PGA, and b) 1.0 s Sa. The solid curve is for Frankel et al. (1996), the dashed curve is for Atkinson and Boore (1995), and the dotted curve is for Toro et al. (1997). The top of the Bhuj data symbols represents the original strong-motion values at each site and the bottom of the symbols represents that site's value corrected to NEHRP B/C boundary site conditions (firm rock).

The University of Roorkee's Department of Earthquake Engineering has released three Bhuj strong-motion recordings via the web. These records are at Ahmedabad, Delhi, and Roorkee, which are 220 km, 950 km, and 1090 km from the mainshock rupture. Figure 6 shows both peak ground acceleration (PGA) and 1.0 s spectral acceleration (Sa) comparisons for these limited data. All the sites are on deep soil in the first floor of 10-story buildings and are assumed to be NEHRP soil class D sites, which seems likely. In Figure 6, these data are plotted with the top of the symbol at the original level of ground-motion for the site and the bottom of the symbol at the ground-motion level after correction

to the NEHRP B/C boundary conditions. These corrections were done by using the fundamental-period of the strong-motion recordings and the relative site amplification factors using Joyner and Boore (2000) (their Table 3). For PGA and 1.0 s Sa, the available Bhuj earthquake strong-motion data compare favorably with the three well-known ENA ground-motion attenuation relations, and certainly fall well above the western North America relations, which would plot below the ENA relations shown in Figure 6.

Another important factor for central U.S. seismic hazard is the earthquake magnitude generated for a given rupture area. Moment magnitude (M) is a measure of the amount of energy radiated by a rupture and hence the level of strong ground-motion that can be expected. The bigger the magnitude the stronger the expected ground-motion. When coupled with the amount of ground-motion dissipation with distance from the earthquake, which is much less in eastern than in western North America, we can estimate the expected, damaging ground-motions from a given earthquake.

The Bhuj, India earthquake can contribute to our understanding of expected ENA magnitudes from a given size fault rupture. For the same size rupture area, Somerville and Saikia (2000) have suggested, from the limited number of available ENA earthquake data, that ENA earthquakes can have seismic moments that are twice as large as the worldwide average, which translates to 0.3 moment magnitude units larger. For $M > 7$ earthquakes away from plate boundaries, the Wells and Coppersmith (1994) data also support Somerville and Saikia (Figure 7). The magnitude vs. rupture-area data from the Bhuj earthquake also falls along this same trend (Figure 7) and is the first instrumentally recorded earthquake with $M > 7.5$ of this data set.

Why would larger than average magnitudes be the case, particularly for larger intraplate earthquakes? Seismic moment (Mo), and hence moment magnitude, depends on rigidity (u), rupture area (A), and average displacement (D): $Mo = uAD$. For $M > 7$ earthquakes, equidimensional scaling relations between rupture area and average displacement are no longer appropriate because seismogenic width limits rupture in the vertical or down-dip direction. Instead, scaling relations are rectangular and are either limited by seismogenic width (remain constant) or scale with increasing seismogenic length (increase with M) (Hanks and Bakun, 2001). That is, the larger earthquakes tend to rupture the whole seismogenic width of the crust. Johnston (1996) has argued for deeper ruptures in an intraplate setting than for a transform-plate-boundary setting because the 300° C and 450 ° C isoterms are deeper. This would imply thicker seismogenic widths for intraplate earthquakes than the worldwide average. Aftershocks of the Bhuj earthquake down to 40 km depths also suggest this possibility. Crustal rigidity increases with depth and is a measure of the crust's ability to store seismic energy, if the crust is not too hot. In California, crustal rigidity averages $3.0\text{-}3.3 \times 10^{10}$ Nt/sq-m over seismogenic widths (0-15 km). In the CEUS and Gujarat, lower crustal rigidity (below 15 km) increases to $4.2\text{-}4.5 \times 10^{10}$ Nt/sq-m. Thus, the trend of larger earthquakes to completely rupture the seismic portion of the crust and, for intraplate regions, to sustain deeper ruptures into the lower crust where rigidity is higher, could in part explain increased magnitudes for a given size of earthquake rupture in an intraplate setting.

Clearly, then, a lot can be learned about the seismic hazard of eastern North America from the Bhuj, India earthquake. Similarities in seismic attenuation and earthquake magnitude for a given rupture area, allow the Bhuj results to be applied to the central U.S. Lower than average ground-motion attenuation and larger than average magnitudes for a given rupture area, suggest higher expected ground-motions from ENA earthquakes than from worldwide earthquakes in general and from younger crustal settings, such as California, in particular.

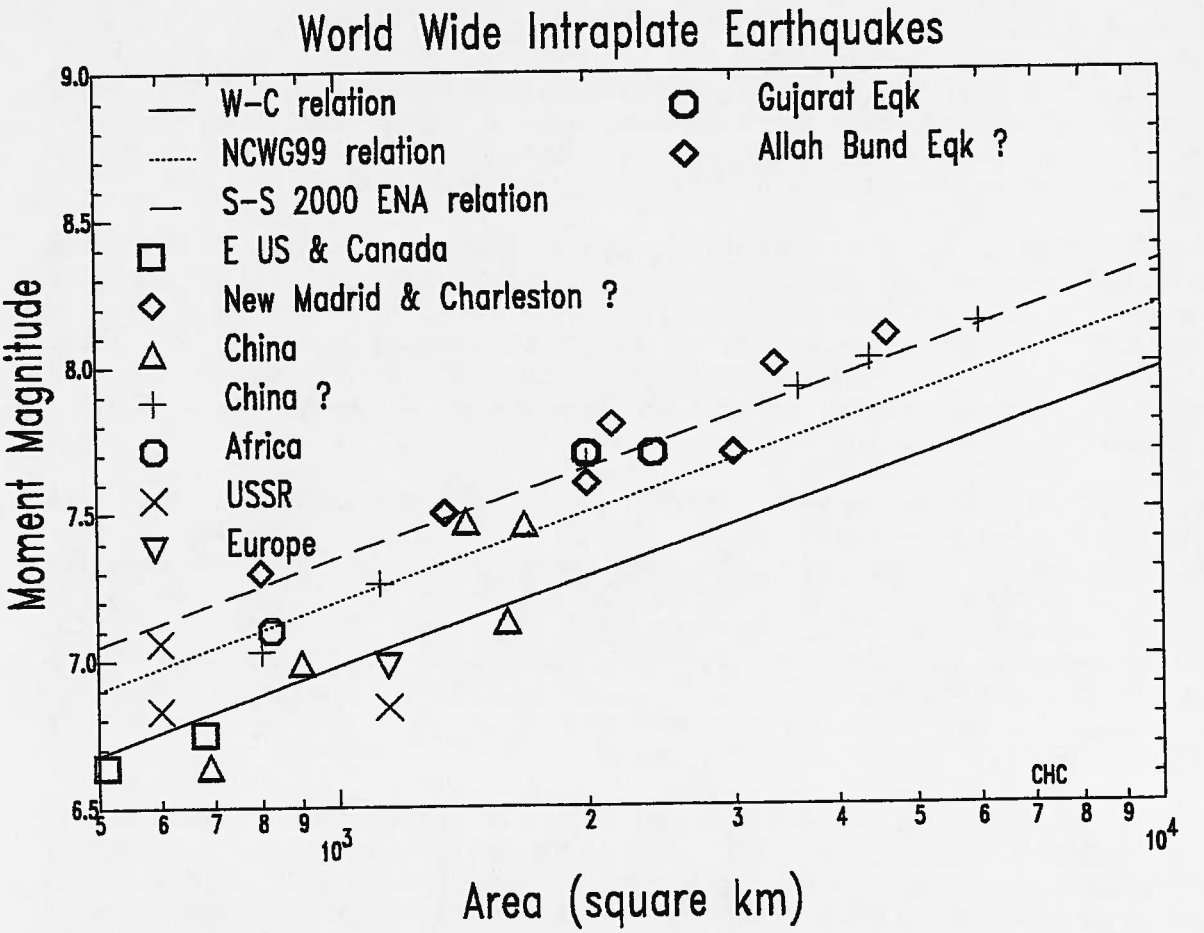

Figure 7: Magnitude versus rupture-area data for intraplate earthquake settings worldwide plotted along with three relations: worldwide average (Wells and Coppersmith, 1994), California M > 7 (WGCEP, 1999), and Somerville and Saikia (2000). Two estimates of rupture area based on University of Tokyo slip inversions and on aftershock distributions are plotted as the dark octagons. Also three estimates for the 1819 Allah Bund (Kutch), India earthquake are also shown as the dark diamonds. These multiple data points represent the uncertainty in the magnitude-area data for these two events.

SITE SPECIFIC HAZARD ANALYSIS

Probabilistic seismic hazard maps and assessments are needed for risk-based decision making. The National Seismic Hazard maps (Frankel et al., 1997), like the one in Figure 5, provide reasonable estimates of strong ground-motion for the central U.S. But these ground-motion estimates are regional in character and for firm-rock site-conditions (average shear-wave velocity of 760 m/s over the top 30 m). They need to be adjusted for site-specific soil conditions when used in engineering design.

The state-of-practice is to develop site-specific amplification factors to adjust hard-rock ground-motions to site-specific ground-motions. Given the geotechnical properties of soils, including shear-wave velocity, damping, density, and modulus-reduction curves, site-amplification factors can be determined using non-linear or equivalent-linear approaches.

An alternative approach is to use the NEHRP site-factors that have been developed to adjust ground-motions according to the NEHRP site classes (Joyner and Boore, 2000).

Figure 8 compares the NEHRP site-factors of Joyner and Boore (2000) for a NEHRP D soil-site with recently published site-amplification estimates at various frequencies for a deep-soil site (1000 m) in the Mississippi embayment. A non-linear, time-domain estimate from Hashash and Park (2001) is compared with an equivalent-linear, frequency-domain estimate from Toro and Silva (2001). Hashash and Park only constrained their time-domain input ground-motions to have a PGA of 1.0 g. For periods longer than 0.1 s, their input ground-motions have values less than 1.0 g, falling to less than 0.2 g at periods greater than 1.0 s. The frequency-domain site-amplification-factors of Toro and Silva are based on input motions of 0.75 g at all periods. The median PGA site-amplification estimates of Hashsh and Park (2001) and Toro and Silva (2001) agree well in Figure 8. At periods longer than 0.1 s, the Hashash and Park site-amplification estimates are larger than those of Toro and Silva. The NEHRP site-factors tend to be conservative estimates because they generally are larger than the site-specific estimates, although in Figure 8 at 0.3 s this is not the case.

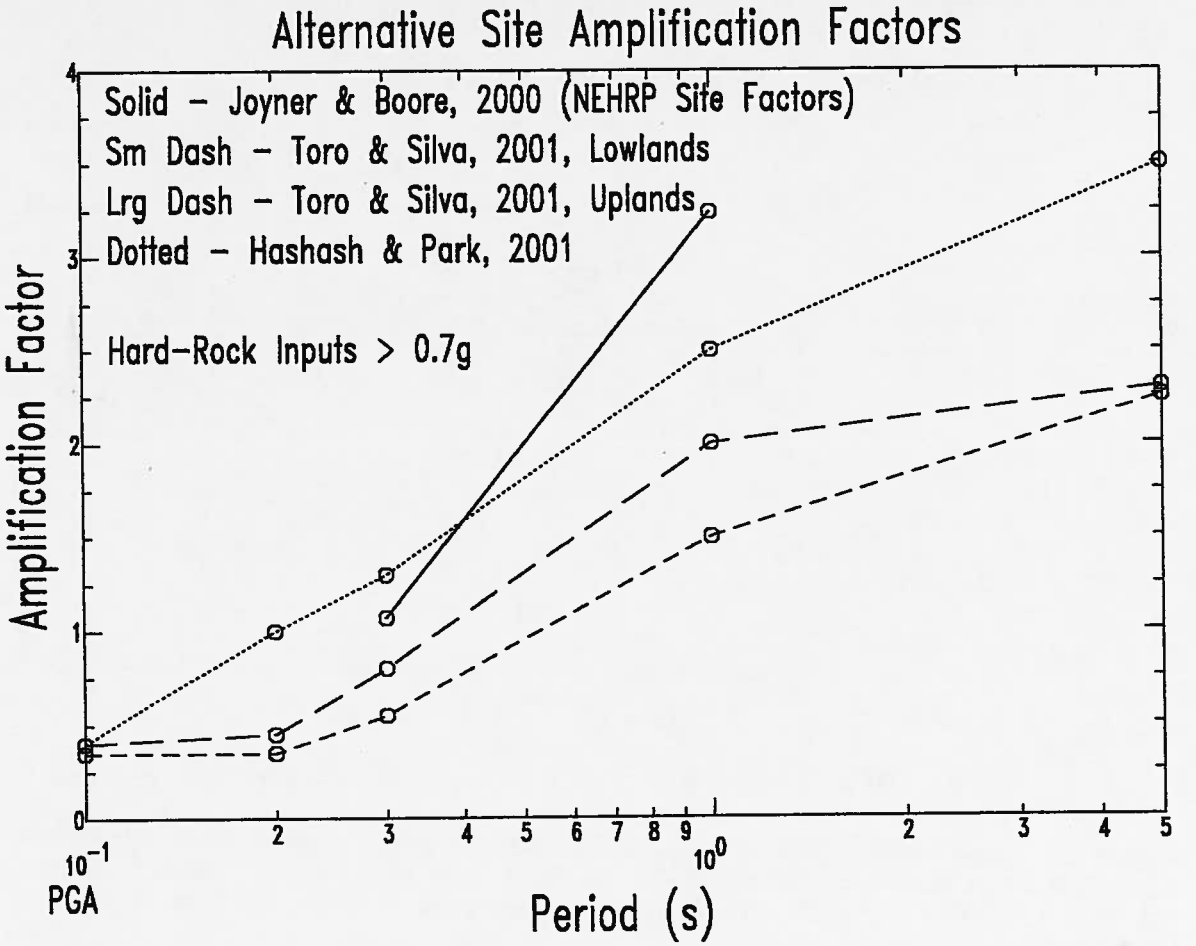

Figure 8: Comparison of recent results of site-amplification studies for the central U.S.

State-of-practice has been to apply median site-amplification factors to hard-rock probabilistic ground-motion estimates to derive probabilistic site-specific ground-motions

and uniform-hazard spectra (UHS). But this approach applies a deterministic estimate of site-amplification to a probabilistic estimate of ground-motion and results in a hybrid estimate of site-specific ground-motion that is not probabilistic and, moreover, is an underestimate for the following reasons. Suppose one is considering a probability level in which a hard-rock ground-motion has a 1-in-2475 chance of being exceeded. In the hybrid approach this is multiplied by a median site-amplification, which by definition has a 1-in-2 chance of being exceeded. The probability of exceeding the resulting site-specific ground-motion is no longer 1-in-2475 but now is greater. In other words, the hybrid estimate actually is more likely than the original probability level selected. Picking a different deterministic level, like the 84th percentile, for the site-amplification will not guarantee a specific probabilistic result because the chosen deterministic site-amplification factor could very well be above or below the desired chance-of-exceedence.

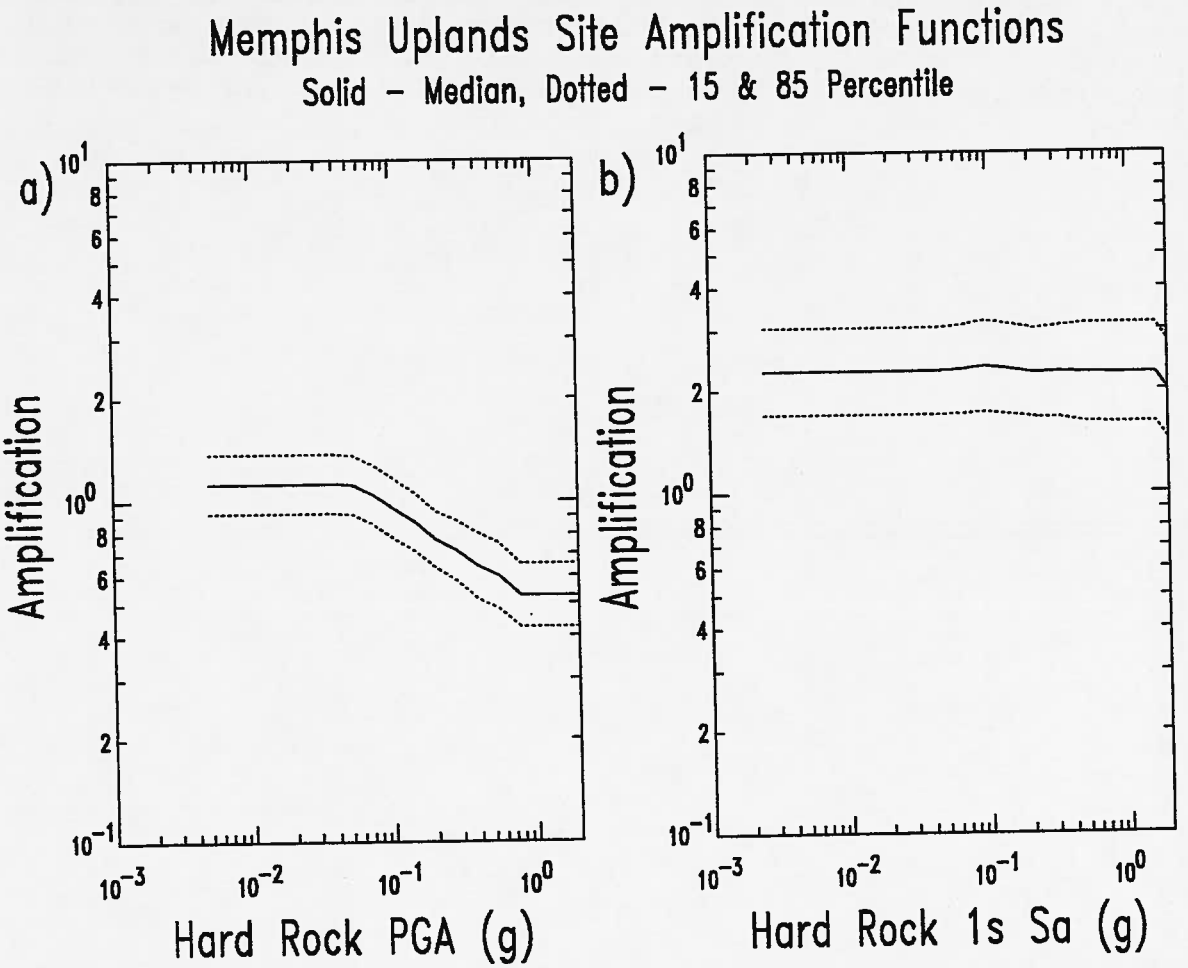

Figure 9: Site-amplification functions for the uplands region near Memphis, Tennessee from Toro and Silva (2001): a) PGA, and b) 1.0 s Sa. These functions are for a 1000m of soft Mississippi embayment sediments over Paleozoic limestones.

If a truly probabilistic value is desired, the site-specific ground-motion must be calculated probabilistically. A state-of-the-art procedure for calculating probabilistic site-specific ground-motions is to adjust the hard-rock ground-motion attenuation relations by the site-specific amplification distributions (Figure 9) to obtain a site-specific ground-motion

attenuation relation. These site-specific attenuation relations are then used in the probabilistic seismic hazard calculations (see Appendix).

To apply this state-of-the-art procedure to deep-soil sites for PGA and 1.0 s Sa, site-amplification distributions like those of Figure 9 should be used. Note that the site-amplification distributions of Figure 9 are dependent on the input hard-rock ground-motion and are represented by median, and 15 and 85 percentile amplification factors. The National Hazard Mapping Project hazard calculation codes have been modified to adjust the input attenuation relations by a given site-amplification distribution to obtain site-specific attenuation relations prior to making the probabilistic seismic hazard calculations. This has been done for Memphis, Tennessee. The resulting PGA and 1.0 s Sa hazard curves are shown in Figure 10. As discussed above, these fully probabilistic curves always fall above the hazard curves derived by multiplying the hard-rock ground-motions by the median site-amplifications. For Memphis, Tennessee, 2%-in-50y (1-in-2475 chance of being exceeded) probabilistic hard-rock input ground-motions are 0.5 g and 0.3 g for PGA and 1.0 s Sa, respectively. The fully probabilistic motions with site conditions for PGA and 1.0 s Sa are 0.35 g and 0.8 g respectively, while the hybrid calculation gives 0.30 g and 0.7 g respectively. In this example, the difference between the probabilistic and hybrid-method results may seem small, but such differences can have engineering significance.

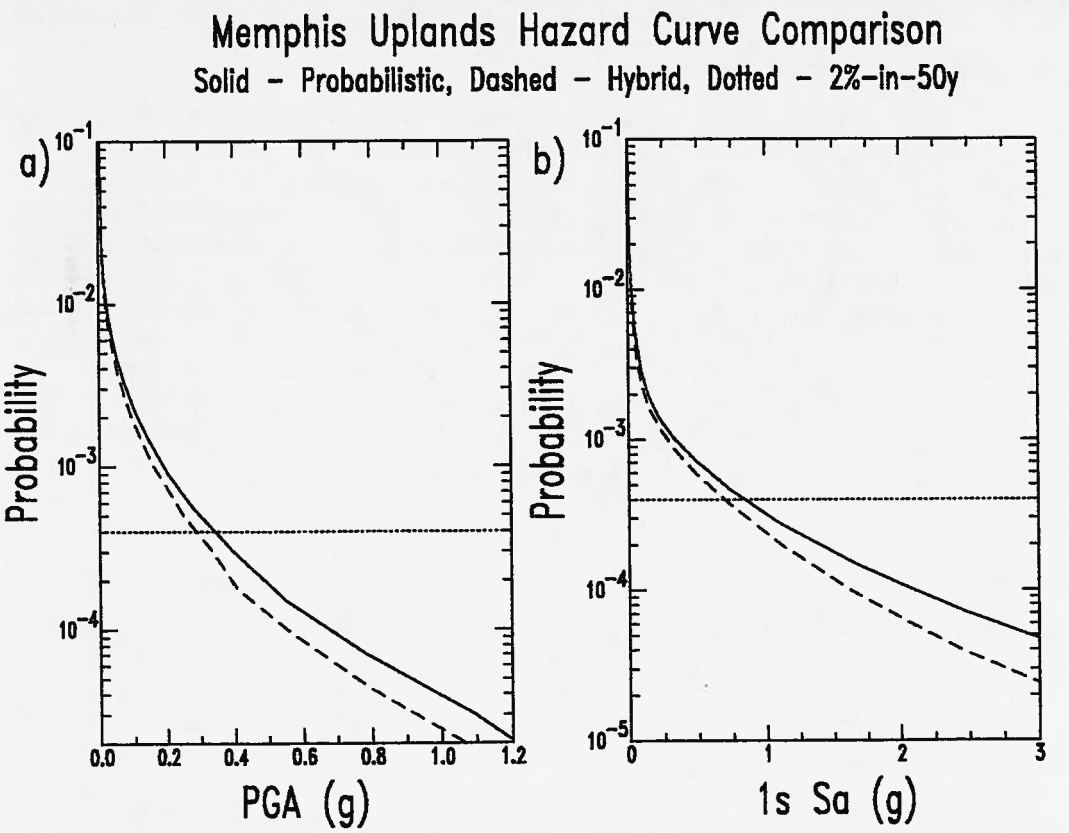

Figure 10: Comparison of hazard curves for the Memphis, Tennessee upland region derived from a state-of-the-art probabilistic methodology described in this paper (solid line) and a state-of-practice hybrid methodology (dashed line): a) PGA, and b) 1.0 s Sa. The reference dotted line indicates the level of probability of exceedence associated with 2%-in-50-year seismic hazard.

SUMMARY

A review of the paleoseismological research in the last five years shows recurrence intervals for M > 7 earthquakes in the New Madrid region and southern Illinois basin have been refined. There have been three episodes of clustered M > 7 earthquakes in the New Madrid seismic zone in the last 1600 years: ~900 AD, ~1450 AD, and 1811-1812 AD. This implies a 500 year average recurrence interval, which is a much higher rate than extrapolated from lower magnitude earthquake activity. In contrast, paleoseismic evidence for the southern Illinois basin suggests a recurrence interval of several thousand years for M > 7 earthquakes, which is in keeping with current seismicity rates. For New Madrid at least, low seismicity rates do not necessarily imply low seismic hazard.

Additionally, the 26 January 2001 Bhuj, India earthquake in the State of Gujarat provides important insights into the seismic hazard of the central U.S. Although the Gujarat geologic setting may not be a perfect analog for New Madrid, seismic-wave attenuation, magnitude vs. rupture-area, magnitude vs. distance of liquefaction, and perhaps earthquake occurrence rates from Gujarat are similar to the central U.S. In particular, for a given rupture area, magnitudes of M > 7 intraplate earthquakes are systematically 0.3 units higher than the worldwide average. One possible explanation for this may be that ruptures extend deeper into the lower crust where rock rigidity is higher. For the same-sized rupture area, this implies higher ground motions in the central U.S. and India than in younger crustal settings such as California.

National Seismic Hazard maps provide reasonable probabilistic estimates of strong ground motion for the central U.S. for uniform firm-rock site conditions. They need to be adjusted for site-specific soil conditions when used in engineering design. State-of-practice approaches use a hybrid method of adjusting probabilistic hard-rock ground-motions with deterministic site-amplification factors. But site-amplification at a specific-site is modeled as a distribution of factors dependent on input ground-motions. Hence, a probabilistic methodology of adjusting hard-rock ground-motion attenuation relations to site-specific attenuation relations before calculating seismic hazard should be used to obtain truly probabilistic results. Comparisons of recent site-amplification research in the central U.S. suggest that frequency-domain methods can provide lower site-amplification factors than time-domain methods. Additionally, NEHRP soil site-factors are generally larger, and more conservative, than estimates from site-specific calculations.

REFERENCES

Ambraseys, N.N. (1988) "Engineering Seismology: Earthquake Engineering and Structural Dynamics" *Earthquake Eng. And Struct. Dyn.* **17**, 1-105.

Atkinson, G.M. and D.M. Boore (1995) "Ground Motion Relations for Eastern North America" *Bull. Seis. Soc. Am.* **85**, 17-30.

Bendick, R., R. Bilham, E. Fielding, V.K. Gaur, S.E. Hough, G. Kier, M.N. Kulkarni, S. Martin, K. Mueller, and M. Mukul (2001) "The 26 January 2001 'Republic Day' Earthquake, India" *Seis. Res. Letters* **72**, 328-335.

Chapman, M.C., C.A. Powell, G. Vlahovic, and M.S. Sibol (1997) "A Statistical Analysis of Earthquake Focal Mechanisms and Epicenter Locations in the Eastern Tennessee Seismic Zone" *Bull. Seis. Soc. Am.* **87**, 1522-1536.

Frankel, A., C. Mueller, T. Barnhard, D. Perkins, E.V. Leyendecker, N. Dickman, S. Hanson, and M. Hopper (1996). National Seismic-Hazard Maps: Documentation June 1996, U.S. Geological Survey, Open-File Report 96-532.

Frankel, A., C. Mueller, T. Barnhard, D. Perkins, E.V. Leyendecker, N. Dickman, S. Hanson, and M. Hopper, (1997). Seismic-hazard Maps for the Conterminous United States: U.S. Geological Survey, Open-File Report 97-131, 12 sheets, scale 1:7,000,000.

Hanks, T.C. and W.H. Bakun (2001) "Bilinear Source-Scaling Relations for M – log A Observations of Continental Earthquakes" *Bull. Seis. Soc. Am.*, (in press).

Hashash, Y.M.A., and D. Park (2001) "Non-linear One-dimensional Seismic Ground Motion Propagation in the Mississippi Embayment" *Engineering Geology* (in press).

Hildenbrand, T. G., and J.D. Hendricks, (1995). Geophysical Setting of the Reelfoot Rift and Relations Between Rift Structures and the New Madrid Seismic Zone, U.S. Geological Survey, Professional Paper 1538-E, 30 p.

Hoffman, D., J. Palmer, J. Vaughn, and R. Harrison, (1996) "Late Quaternary Surface Faulting at English Hill in Southeastern Missouri" *Seis. Res. Letters* **67**, 41.

Johnston, A.C. (1996) "Seismic Moment Assessment of Earthquakes in Stable Continental Regions – III. New Madrid 1811-1812, Charleston 1886 and Lisbon 1755" *Geophys. J. Int.* **126**, 314-344.

Johnston, A. C., and E. S. Schweig (1996) "The Enigma of the New Madrid Earthquakes of 1811-1812" *Ann. Rev. Earth Planet. Sci.* **24**, 339-384.

Joyner, W.B., and D.M. Boore (2000) "Recent Developments in Earthquake Ground Motion Estimation", Proceedings of the Sixth International Conference on Seismic Zonation, Earthquake Engineering Research Institute, California.

Kelson, K.I., Simpson, G.D., Van Arsdale, R.B., Haraden, C.C., and Lettis, W.R. (1996) "Multiple Late Holocene Earthquakes Along the Reelfoot Fault, Central New Madrid Seismic Zone" *J. Geophys. Res.* **101**, 6151-6170.

Kenner, S., and P. Segall (2000) "The Mechanics of Intraplate Earthquake Generation with Application to the New Madrid Seismic Zone" *Science* **286**,

Langenheim, V.E. and T.G. Hildenbrand (1997) "Commerce Geophysical Lineament – Its Source, Geometry, and Relation to the Reelfoot Rift and New Madrid Seismic Zone" *Geol. Soc. Am. Bull.* **109**, 580-595.

Liu, L., Zoback, M.D., and Segall. P. (1992) "Rapid Intraplate Strain Accumulation in the New Madrid Seismic Zone" *Science* **257**, 1666-1669.

Mueller, C., M. Hopper, and A. Frankel (1997). Preparation of Earthquake Catalogs for the National Seismic-Hazard Maps: Contiguous 48 States, U.S. Geological Survey, Open-File Report 97-464.

Newman, A., Stein, S., Weber, J., Engelin, J., Mao, A., and Dixon, T. (1999) "Slow Deformation and Lower Seismic Hazard at the New Madrid Seismic Zone" *Science* **284**, 619-621.

Obermeier, S.F. (1989). The New Mardrid Earthquakes: An Engineering-Geologic Interpretation of Relict Liquefaction Features, U.S. Geologic Survey Prof. Paper 1336-B, 114p.

Obermeier, S.F. (1998) "Liquefaction Evidence for Strong Earthquakes of Holocene and Latest Pleistocene Ages in the States of Indiana and Illinois, USA" *Engineering Geology* **50**, 227-254.

Rajendran, C.P., and K. Rajendran (2001) "Characteristics of Deformation and Past Seismicity Associated with the 1819 Kutch Earthquake, Northwestern India" *Bull. Seis. Soc. Am.* **91**, 407-426.

Saucier, R. T. (1977). Effects of the New Madrid Earthquake Series in the Mississippi Alluvial Valley, U.S. Army Eng. Waterways Experiment Station Misc. Paper S-77-5.

Singh, S.K., M. Ordaz, R.S. Dattatrayam, and H.K. Gupta (1999) "A Spectral Analysis of the 21 May 1997, Jabalpur, India, Earthquake (Mw = 5.8) and Estimation of Ground Motion from Future Earthquakes in the Indian Shield Region" *Bull. Seis. Soc. Am.* **89**, 1620-1630.

Somerville, P., and Saikia, C. (2000). Ground Motion Attenuation Relations for the Central and Eastern United States, Progress Report to the USGS, January 28, 2000, URS Greiner Woodward Clyde, Pasadena: 10p.

Street, R., and O. Nuttli (1984) "The Central Mississippi Valley Earthquakes of 1811-1812" *in* Proceedings of the Symposium on "The New Madrid Seismic Zone," U.S. Geological Survey Open-File Report 84-770, 33-63.

Toro, G., N. Abrahamson, and J. Schneider (1997) "Model of strong ground motions from earthquakes in central and eastern North America: best estimates and uncertainties" *Seis. Res. Letters* **68**, 41-57.

Toro, G.R., and W.J. Silva (2001). Scenario Earthquakes for Saint Louis, MO, and Memphis, TN, and Seismic Hazard Maps for the Central United States Region Including the Effect of Site Conditions, Final Technical Report to the USGS, January 10, 2001, Risk Engineering, Inc., Colorado.

Tuttle, M. P. (1999). Late Holocene Earthquakes and their Implications for Earthquake Potential of the New Madrid Seismic Zone, Central United States, Ph.D. dissertation, University of Maryland, 250 p.

Tuttle, M.P., E.S. Schweig, J.D. Sims, and R.H. Lafferty (2001a) "The Earthquake Potential of the New Madrid Seismic Zone" *Bull. Seis. Soc. Am.* (submitted).

Tuttle, M. P., J. Hengesh, and W. Lettis (2001b). Liquefaction Induced by the 2001 Bhuj Earthquake in India, *Earthquake Spectra* (in press).

Wells, D.L., and Coppersmith, K.J. (1994) "New Empirical Relationships among Magnitude, Rupture Length, Rupture Width, Rupture Area, and Surface Displacement", *Bull. Seis. Soc. Am.* **84**, 974-1002.

WGCEP (1999). Earthquake Probabilities in the San Francisco Bay Region: 2000 to 2030 – A Summary of Findings, U.S. Geological Survey, Open File Report 99-517: 60pp.

Wesnousky, S.G. (1994) "The Gutenberg-Richter or Characteristic Earthquake Distribution, Which is it?" *Bull. Seis. Soc. Am.* **84**, 1940-1959.

Youd T. L., and J.B. Perkins (1987) "Mapping of Liquefaction Severity Index" *Journal of Geotechnical Engineering*, **113**, 1374-1392.

APPENDIX

The following is a brief explanation of the procedure implemented to properly combine site-amplifications distributions with hard-rock attenuation relations to obtain probabilistic seismic hazard analyses including site geological effects.

We assume that the site-amplification-function is a function of rock ground Motion, Ar. Specifically, we have the site-specific probability density function (pdf) Pa(As | Ar). Pa is assumed to be given as a median amplification and its natural-lognormal standard deviation at several values of Ar. In the modified hazard-calculation programs, the attenuation relation is given as a median ground motion and its standard deviation in natural log space. Normally, we derive a hazard curve at each magnitude (M) and distance (R) of interest. The hazard curve is a complimentary cumulative probability function (CCP) that provides the probability if a ground-motion A exceeding Ar given M and R [P(A>Ar | M,R)], but we can just as easily derive its pdf for a given set of rock ground motion levels, Pr(A=Ar | M,R). To modify an attenuation relation to a site specific attenuation relation using Pa at every M and R of interest, the site-specific attenuation pdf, Ps(A=As | M,R), is given by the summation over Ar of the products Pa(As | Ar) * Pr(A=Ar | M,R) at each of the As of interest. The hazard curve CCPs = P(A>As | M,R) needed as part of the site-specific attenuation relation in the hazard calculation is then derived from Ps, a pdf.

GEOLOGIC HISTORY OF THE NORTHERNMOST MISSISSIPPI EMBAYMENT AND SOUTHERN ILLINOIS BASIN[1]

W. John Nelson[2] and John H. McBride[3]

ABSTRACT

The northernmost Mississippi embayment, north of New Madrid, Missouri, has a history of tectonic activity dating back at least 550 Ma. Near the end of Precambrian time a dogleg-shaped rift structure, comprising the northeast-trending Reelfoot Rift and east-trending Rough Creek Graben, developed in what is now the northern part of the embayment and the southern part of the Illinois basin. Faults in the rift were reactivated repeatedly in response to tectonic events elsewhere in North America. Events that triggered fault movements included the Acadian orogeny during the Devonian Period, the Ancestral Rockies orogeny during the Pennsylvanian Period, the Alleghanian Orogeny during the Permian Period, and the breakup of Pangaea with initial formation of the Atlantic Ocean during the Triassic and early Jurassic Periods. Fault movements in the northern embayment continued through the Cretaceous and Tertiary Periods, even though no plate-tectonic activity was taking place closer than the Rocky Mountains. Earth movements have continued into the Quaternary Period, the most recent 1.8 Ma of Earth's history. In western Kentucky and southern Illinois, numerous early to mid-Quaternary (more than 125 ka old) faults trend mostly northeast and outline narrow down-dropped blocks. This area has undergone minor Late Pleistocene Epoch activity, but much of it apparently has been inactive in the Holocene Epoch, the last 11 ka. In contrast, faults in southeastern Missouri, particularly along the Commerce fault zone in the Benton Hills, display evidence of Holocene activity. In one case a fault appears to have moved during the New Madrid earthquakes of 1811 and 1812. All indications are that little stress is required to cause new activity in this highly fractured region. The locus of concentrated activity has frequently moved around the northern embayment and southern Illinois basin, and is currently centered in the New Madrid seismic zone.

INTRODUCTION

In this paper we review the geologic record of earth movements in the northern part of the New Madrid seismic zone, defined as that portion of the Mississippi embayment lying north of New Madrid, Missouri (Fig. 1). The Mississippi embayment, a northward extension of the Gulf Coastal Plain, is underlain by loose to weakly lithified clay, silt, sand, and gravel of Cretaceous and Tertiary age (Fig. 2). These sediments in turn are largely covered by unlithified Quaternary fluvial,

---

[1]Publication authorized by the Chief, Illinois State Geological Survey.

[2] Illinois State Geological Survey, 615 E. Peabody Drive, Champaign, IL 61820

[3] Illinois State Geological Survey and Department of Geology, University of Illinois at Urbana-Champaign, 615 E. Peabody Drive, Champaign, IL 61820

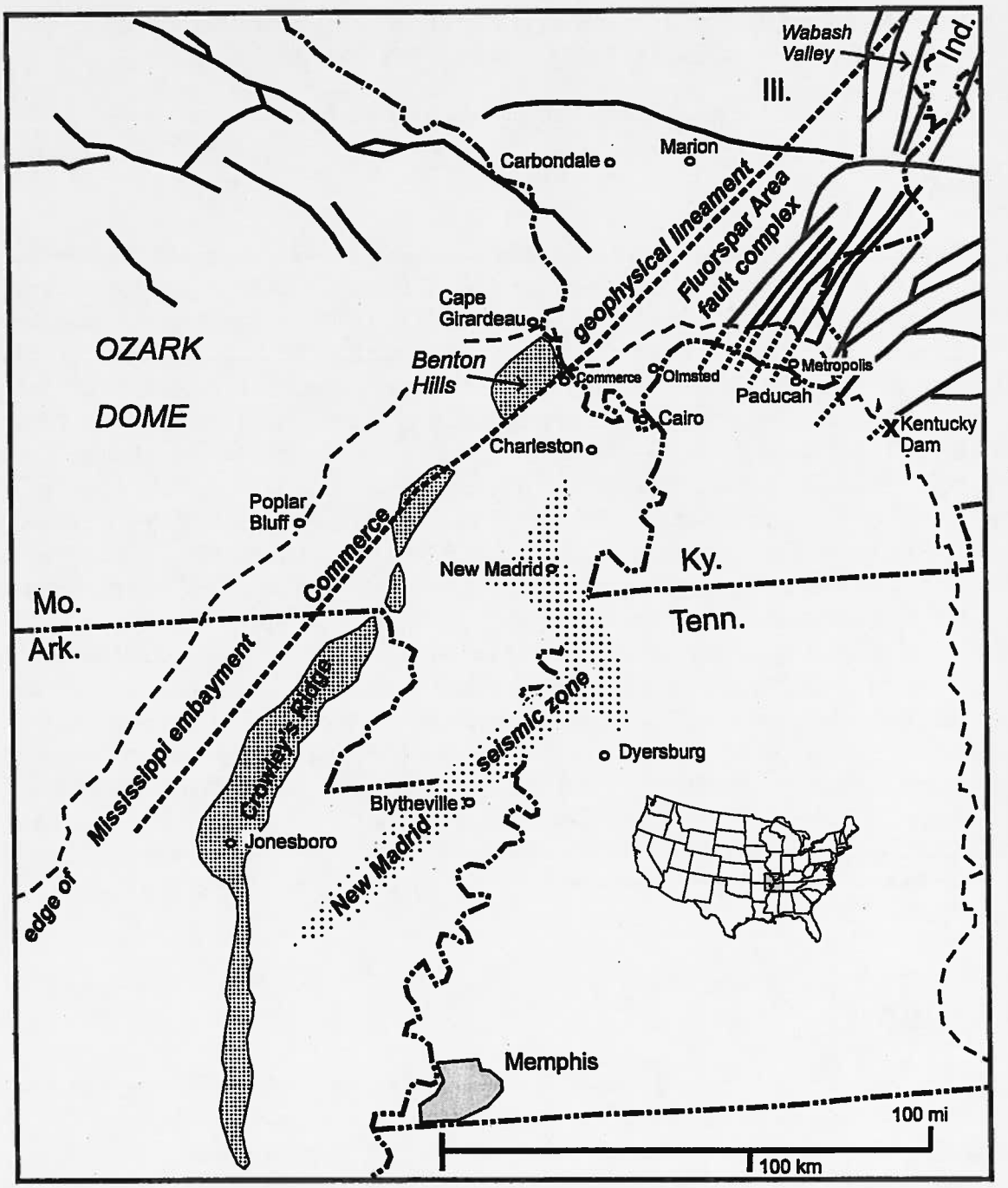

Figure 1: Schematic location map showing northern Mississippi embayment, southern Illinois basin, New Madrid seismic zone, and prominent geologic structures. Also shown are place names referred to in the text.

lacustrine, and wind-blown deposits. Most of the northern embayment is level to gently rolling lowlands, but several upland sections are included, notably the Benton Hills and the northern part of Crowley's Ridge in Missouri (Fig. 1).

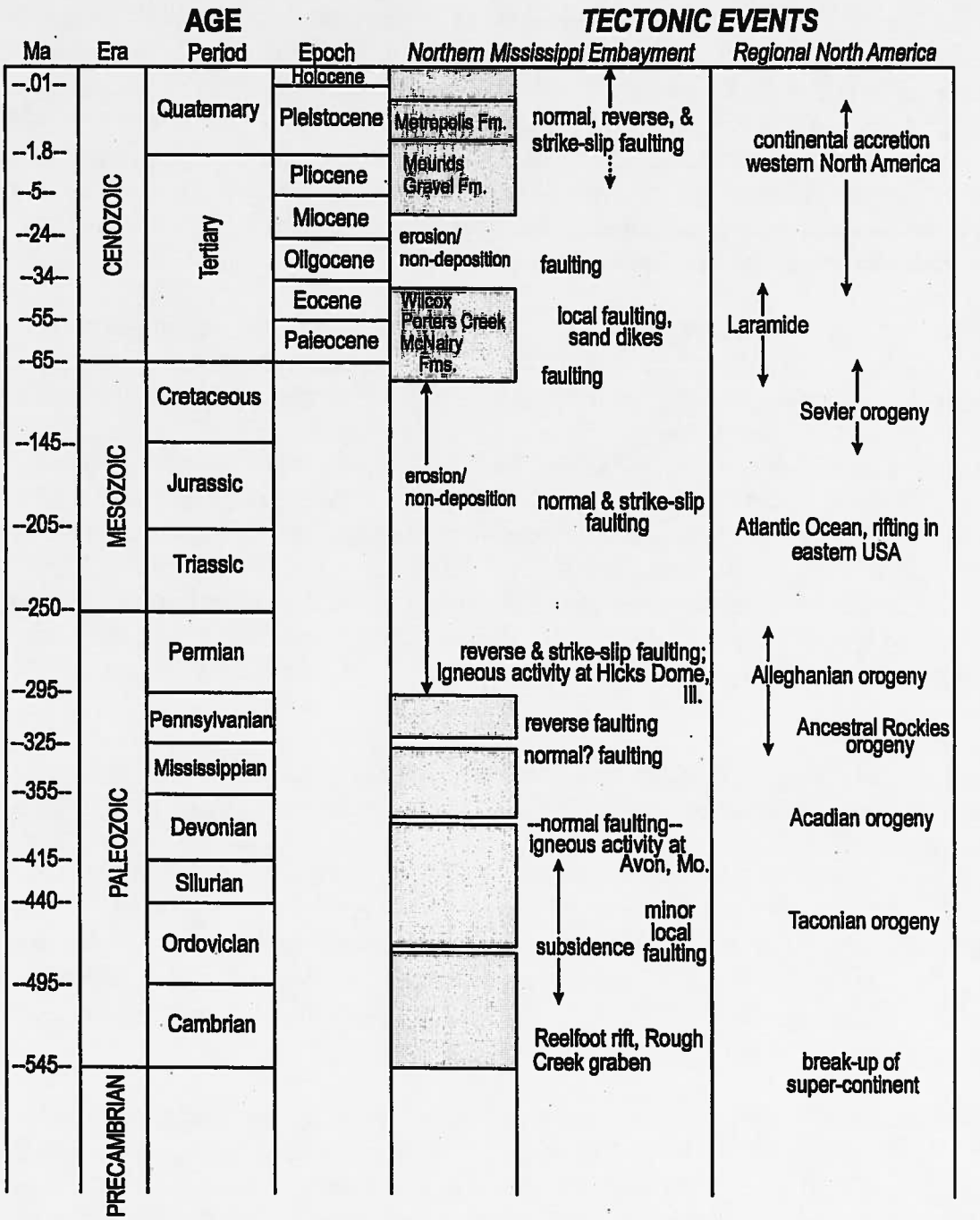

Figure 2: Geologic time chart indicating key tectonic events in northern Mississippi embayment and elsewhere in North America.

Previous Studies

The Mississippi embayment is not conducive to traditional geologic field work. The land is mostly level and intensively farmed in row crops. Thick deposits of alluvium and loess (wind-blown silt) conceal the underlying materials. Outcrops are confined to deep ravines in the few upland areas, such as Crowley's Ridge, and to artificial excavations, which are not numerous. The faults that may host seismicity in the New Madrid area cannot be directly observed and monitored like faults in, say,

California. Hence, remote sensing methods, such as geophysical surveys and drilling boreholes, must be brought to bear. Although well documented (e.g. Fuller, 1912), the great New Madrid earthquakes of 1811 and 1812 were poorly understood by geologists until the 1970s. Before the late 20th century many geologists regarded the New Madrid quakes as somewhat an anomaly within the "stable craton" of the North American Midcontinent. Knowledge that this region has a long history of crustal instability did not begin to grow until the 1940s. For example, beyond the immediate vicinity of the New Madrid seismic zone, the area has traditionally been thought to have experienced no significant tectonism after the Cretaceous Period.

Kentucky. One of the earliest reports of post-Cretaceous faulting in the region is that of Rhoades and Mistler (1941). They documented faults displacing Cretaceous strata near Kentucky Dam on the Tennessee River, along the northeast margin of the embayment (Fig. 1). Also, they described sand- and clay-filled dikes traversing Eocene sediments and Pliocene(?) terrace gravels[4] and attributed these structures to seismic shaking. Their findings were corroborated by later geologists who mapped all of western Kentucky at 1:24,000 scale. Three quadrangle maps show faults displacing the Miocene to early Quaternary "continental deposits" (Mounds Gravel) in the Lockhart Bluff graben of Livingston County (Amos, 1967; 1974; Amos and Wolfe, 1966). The Lockhart Bluff structure crosses Mississippian bedrock uplands at the northeast margin of the embayment. Within the embayment proper, faults displace various Tertiary units and clastic dikes of possible seismic origin crosscut the Porters Creek Clay of Paleocene age (Olive, 1980; Smath and Davidson, 2000).

Missouri. Grohskopf (1955, p. 26-28) described several places where Tertiary and Quaternary strata are faulted or strongly folded on Crowley's Ridge and in the Benton Hills (Fig. 1). For example, regarding the English Hill fault in the Benton Hills (Scott County), Grohskopf wrote, "The loess is down faulted against a sand in the basal Wilcox in the form of a graben..." The Wilcox Formation is Eocene and the loess presumably is Pleistocene. In her catalogue of structural features in Missouri, McCracken (1971) repeated Grohskopf's observations and added some by subsequent authors. Her entry (p. 20) on the "Commerce anticlinorium", located on the Mississippi River bluff at the village of Commerce (Fig. 1) in Scott County, includes the statement, "The structure lies in an active seismic area and deformation may still be in progress".

Recent investigations show that the statements quoted above do not exaggerate (Harrison and Schultz, 1994; Harrison et al., 1999; Nelson et al., 1999b). The studies include surface geologic mapping, geophysical surveys, drilling, and trenching at numerous sites on Crowley's Ridge and in the Benton Hills. They provide widespread evidence for Holocene fault movements as shown by displacement of late Pleistocene loess and Holocene colluvium, the age of the latter being confirmed by radiocarbon dating. In fact, some faults exposed in a trench at "Sassafras Canyon" (part of the Commerce anticlinorium of McCracken (1971)) may have been reactivated during the New Madrid

---

[4] Reddish-brown chert gravels of late Miocene to early Pleistocene age are widespread throughout the northern Mississippi embayment. These deposits are variously called "terrace gravels", "continental deposits" (in Kentucky), Lafayette Gravel (Tennessee), and Mounds Gravel (Illinois and Missouri). The name Mounds Gravel is used in this paper.

earthquakes of 1811 and 1812 (Harrison et al., 1999). The most intense recent deformation appears to be along a northeast-trending zone of faults that follow the steep southeast margin of Crowley's Ridge and the Benton Hills. The fracture zone, named the Commerce fault or fault zone, exhibits right-lateral strike-slip displacement (Harrison et al., 1999), which is the same as shown on northeast-trending segments of the New Madrid seismic zone and is consistent with slip under the current regional tectonic stress regime. The Commerce fault zone coincides with part of a linear trend of magnetic and gravity anomalies called the Commerce geophysical lineament (Fig. 1). Approximately 12 earthquakes having body-wave magnitudes of 3.0 or greater appear to be associated with the Commerce fault zone and lineament running from northeastern Arkansas through Missouri into southern Illinois (Harrison and Schultz, 1994; Langenheim and Hildenbrand, 1997).

Illinois. Ross (1963; 1964) was the first geologist who explicitly postulated post-Cretaceous tectonic faulting within the Mississippi embayment in Illinois. He asserted that some faults displaced the Mounds Gravel and that geomorphic relationships suggested movements continued later into the Pleistocene. Ross did not find much evidence to support his statements, listing only one place where the Mounds Gravel showed "steep dips".

Kolata et al. (1981) carried out a regional study of structure in the embayment of southern Illinois and also investigated several sites where Ross or other geologists suggested neotectonic faulting. They found no positive evidence for post-Cretaceous faulting. Where Cretaceous and younger strata were deformed, they viewed landsliding, solution-collapse, and other non-tectonic processes as plausible.

New investigations during the 1990s showed that southern Illinois does indeed have post-Cretaceous tectonic faults; some are as young as late Pleistocene. Geophysical surveys, drilling, and excavations in Massac and Pulaski Counties reveal widespread faulting of the Mounds Gravel and a younger Pleistocene alluvial deposit, the Metropolis Formation. Most of the faults strike northeast, and in many cases they outline small grabens. Strike-slip or wrenching movement is suspected, but not proven. Some small faults may displace Wisconsinan (late Pleistocene) deposits, but none to date are known to show Holocene activity (Nelson et al., 1997; 1999a; b).

GEOLOGIC HISTORY

Pre-Cretaceous

The structural grain of the northern embayment is ancient. More than 550 Ma ago, during Precambrian time, North America was part of a "super-continent" (Fig. 2). Under plate-tectonic stresses this great landmass began to break apart, with oceans forming along the southern and eastern margins of North America. During this continental breakup, a rift zone extended into the interior of North America in the location of the present Mississippi embayment. This northeast-trending rift (Fig. 3) was named the Reelfoot rift in reference to Reelfoot Lake, which formed during the New Madrid earthquakes of 1811 and 1812 (Ervin and McGinnis, 1975). An eastward extension of the Reelfoot rift into Kentucky is called the Rough Creek graben (Soderberg and Keller, 1981). During the Cambrian Period (~545 to 495 Ma), the Reelfoot rift and Rough Creek graben became a deep, narrow inlet of the ocean, and thousands of meters of marine sediments accumulated therein. These structures are known as "failed rifts" because the continent failed to break apart completely. The

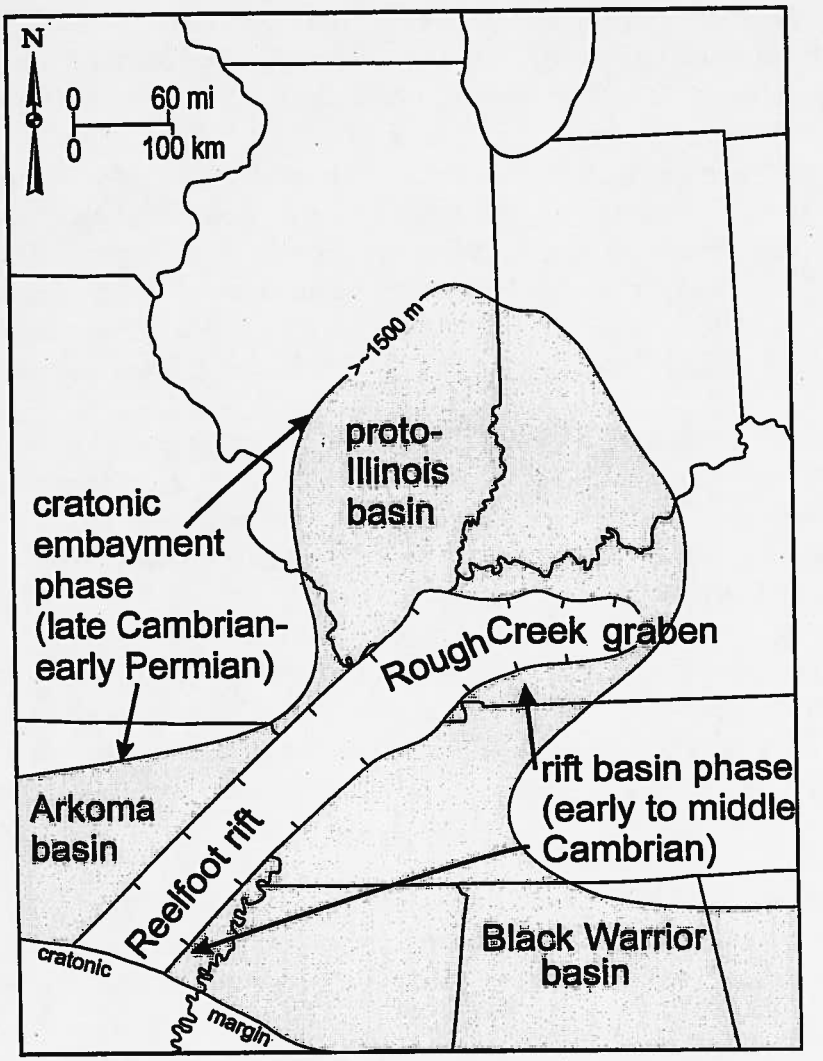

Figure 3: Map showing development of rift basin and subsequent formation of the proto-Illinois basin centered over the rift junction. Shading indicates Paleozoic strata thicker than ~1500 m (modified from Kolata and Nelson (1991)).

rifts gradually were filled with sediment, as shallow seas spread across most of North America by Late Cambrian time. However, the underlying fault zones became permanent zones of weakness in the earth's crust, ready to be reactivated under new stress regimes.

During the Ordovician (495 to 440 Ma) and Silurian (440 to 415 Ma) Periods, faults in the rift generally were inactive, but the rift continued to subside more rapidly than the surrounding region (Fig. 2). As a result, an elongate ocean basin, open to the southwest, was centered over the rift (Fig. 3). This basin may be considered a proto-Illinois basin (Schwalb, 1969; Kolata and Nelson, 1991). Sedimentary rocks deposited in the basin at this time are largely limestone and dolomite, with lesser amounts of shale and sandstone.

Fault activity was renewed in Kentucky, Illinois, and Missouri during the Devonian Period (415 to 355 Ma). Among the faults that moved were portions of the Rough Creek and Pennyrile fault

systems, which respectively form the northern and southern margins of the Rough Creek graben (Fig. 4), as evidenced by dramatic changes in the thickness of Devonian formations on opposites sides of faults (Freeman, 1951; Nelson and Marshak, 1996). In the southern Illinois basin, the Ste. Genevieve and Waterloo-Dupo anticlines were active during Devonian time. In southeastern Missouri, a cluster of igneous intrusions known as the Avon diatremes are dated radiometrically as Middle Devonian (Nelson and Marshak, 1996) (Fig. 4). The Acadian orogeny, a major mountain-building episode, was taking place in eastern North America during the Devonian and it is likely that this induced fault movements in the Midcontinent (Fig. 2).

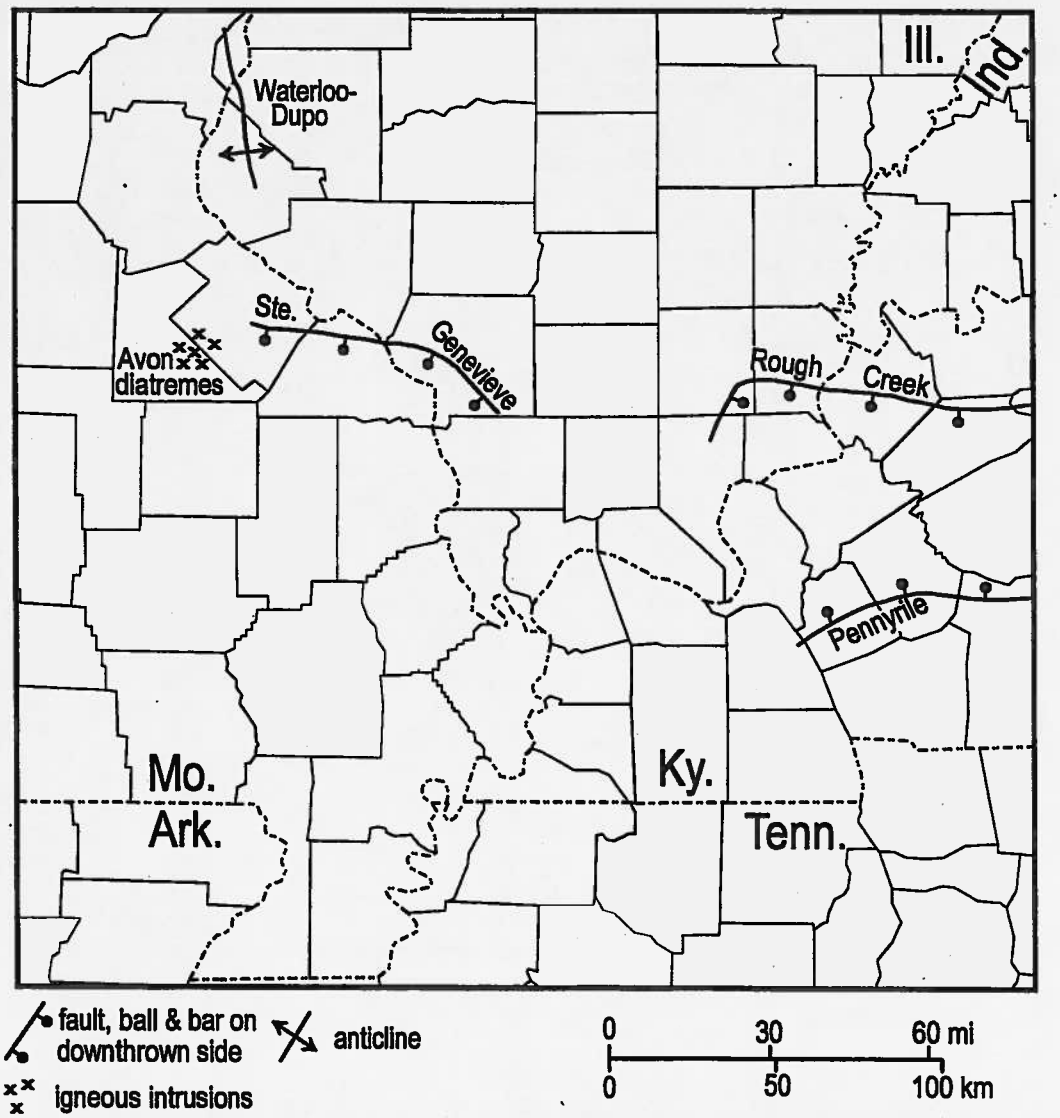

Figure 4: Map showing structures active during Devonian Period (Nelson and Marshak, 1996).

The shallow marine basin or "ramp" open to the southwest persisted into Mississippian time (355 to 325 Ma). As before, the deepest water and fastest subsidence were centered over the Reelfoot rift. Lower Mississippian rocks are mostly limestone, whereas upper Mississippian (Chesterian Series) strata are alternating sandstone, shale, and limestone. Detailed mapping from outcrops and boreholes in southeastern Illinois reveals abrupt changes of the thicknesses and rock types of certain

Chesterian formations on opposite sides of northeast-trending faults near the northern end of the Reelfoot rift (Fig. 5). These changes are evidence that the fault blocks moved during Chesterian deposition (Nelson et al., in press). For example, along the Ste. Genevieve fault zone and Waterloo-Dupo anticline, locally deformed strata and angular unconformities suggest late Mississippian activity for part of these structures. The occurrence of multiple, superimposed channels of thick sandstone implies grabens that developed in the Wabash Valley of southwestern Indiana and in the Dixon Springs graben of southern Illinois (Nelson et al., in press) (Fig. 5).

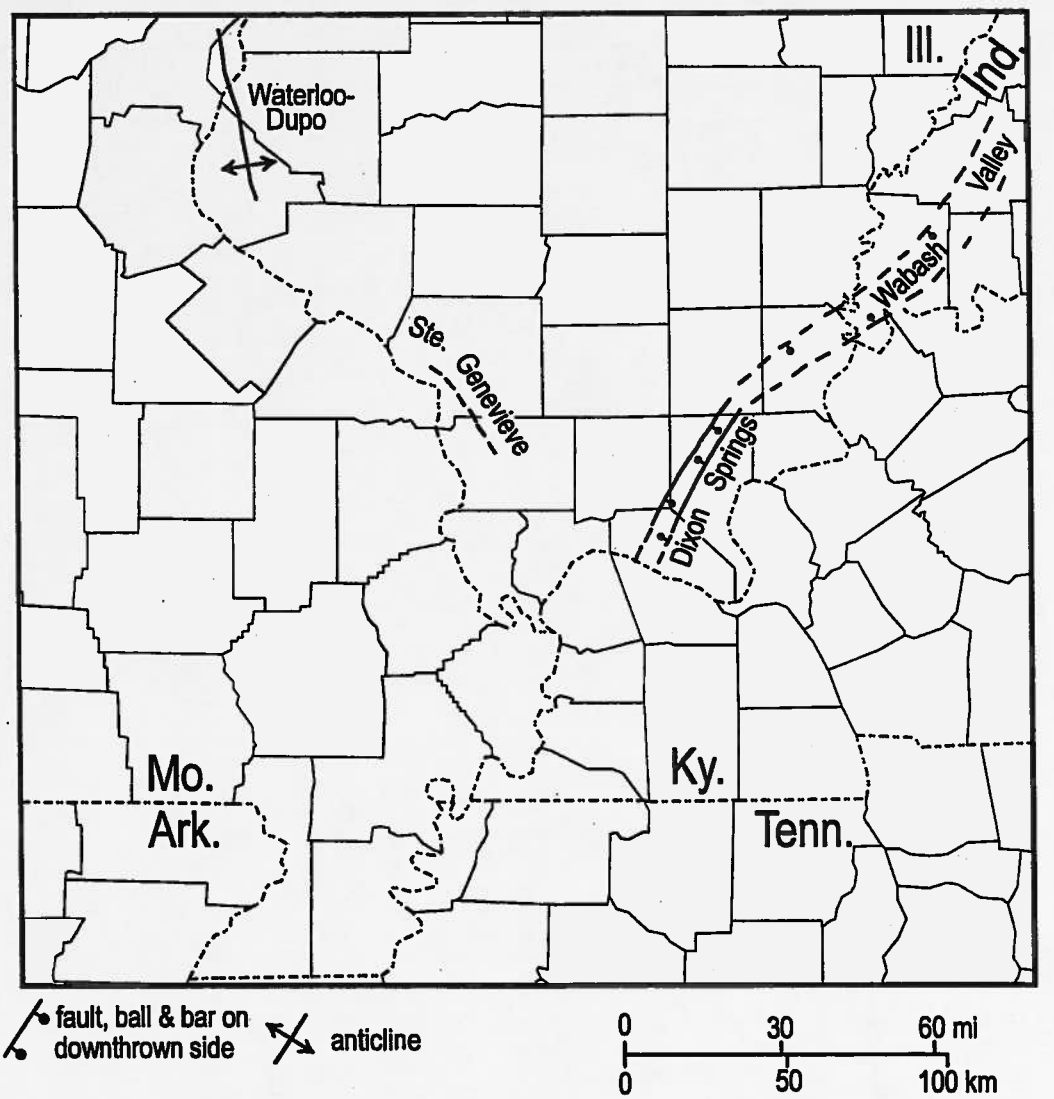

Figure 5: Map showing structures active during Mississippian Period (Nelson et al., in press).

The Pennsylvanian System, comprising rocks that formed 325 to 295 Ma ago, is noted for its valuable coal deposits in Illinois, Indiana, and western Kentucky. This was also a time of widespread, major earth movements throughout the western and central United States. This tectonic episode is called the Ancestral Rockies orogeny (Fig. 2) because it produced many mountainous uplifts, separated by deep and narrow fault-bounded basins, in the area of the present Rocky

Mountains of Colorado, New Mexico, and Utah. Equally impressive fault movements created major Midcontinent structures such as the Permian basin in Texas, the Arbuckle and Wichita Mountains in Oklahoma, and the Nemaha uplift in Kansas. Many faults in Missouri and Illinois were active during the Pennsylvanian, some undergoing displacements of several thousand meters. Many great oil-producing anticlines and domes in the Illinois basin may be products of the Ancestral Rockies orogeny (Fig. 6). The prevalent structural pattern in Illinois and Missouri involves reverse faults that strike north to northwest in the Precambrian "basement", accompanied by elongate domes, anticlines, and monoclines in the Paleozoic sedimentary rocks (McBride and Nelson, 1999). Many faults in the Reelfoot rift and Rough Creek graben were reactivated during the Ancestral Rockies orogeny, although in most cases the displacements were small. The evidence for Pennsylvanian

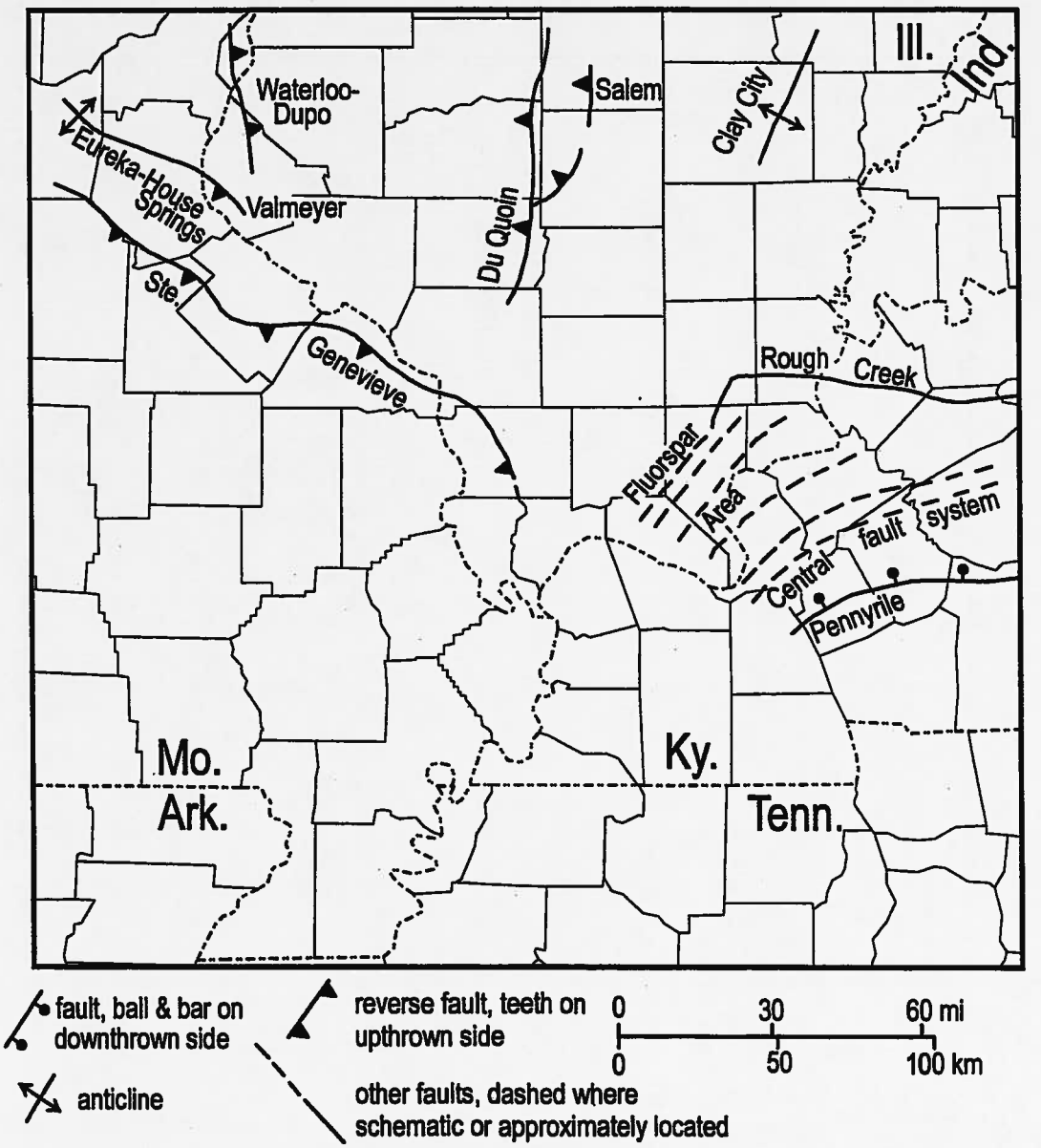

Figure 6: Map showing structures active during Pennsylvanian Period, mostly in connection with the Ancestral Rockies orogeny (McBride and Nelson, 1999).

faulting includes thickness changes of coal beds and other strata, linear alignment of ancient river and deltaic channels along faults, and widespread ancient landslides and clastic dikes close to faults (Nelson and Lumm, 1987; Kolata and Nelson, 1991).

Dramatic deformation took place in the rift area during the Permian Period (295 to 245 Ma). This was the time of the culmination of the Alleghanian orogeny, when the collision of eastern North America with exotic tectonic plates created the Appalachian Mountains. Stresses resulting from this collision were transmitted far into the continental interior. In general, the collision produced a regional compressive stress oriented northwest-southeast. Many faults that originated as normal faults under crustal extension or rifting now became reverse faults. Formerly down-dropped blocks in the Rough Creek graben and Reelfoot rift were uplifted (Fig. 7). Vertical displacements as great

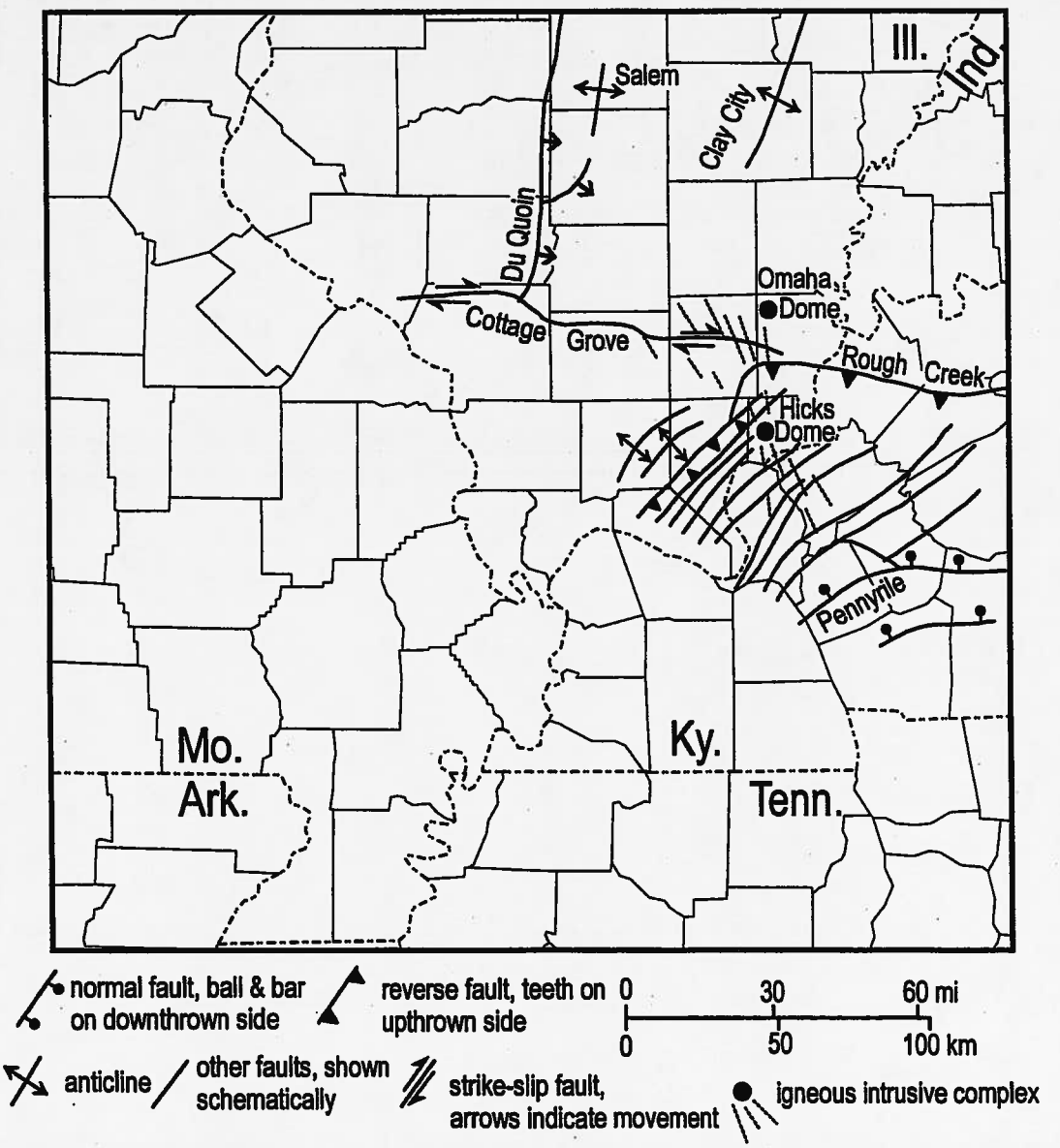

Figure 7: Map showing structures active during the Alleghanian orogeny (Permian Period) (Kolata and Nelson, 1991). Activity within the Mississippi embayment is unknown.

as ~1070 m took place on segments of the Rough Creek graben, juxtaposing Devonian and Pennsylvanian rocks (Nelson and Lumm, 1987). Many northeast-trending faults near the northern end of the Reelfoot rift also underwent reverse displacements. At the same time, magma invaded the intensely fractured area near the rift junction. Igneous activity culminated at Hicks Dome, a nearly circular structure in Hardin County, Illinois (Figs. 2 and 7). Outcrop and borehole data show that Hicks Dome is the product of explosive igneous activity that greatly shattered the bedrock (Bradbury and Baxter, 1992; Potter et al., 1995). Hundreds of small Permian igneous dikes and breccia pipes radiate from Hicks Dome into southern Illinois and western Kentucky. Although not shown on our map (Fig. 7), many structures in southeastern Missouri were also active during the Permian, but fault movements cannot be dated owing to the absence of rocks younger than Ordovician in most places.

Although no Triassic (245 to 205 Ma) or Jurassic (205 to 145 Ma) rocks are preserved in the northern part of the rift, tectonism continued apace. Continents that coalesced during the Alleghanian orogeny pulled apart, and the Atlantic Ocean began to open. Many Triassic to Lower Jurassic rift basins formed inland from the Atlantic coast in the eastern United States. Within the Midcontinent, the regional stress regime reverted from compressional to extensional. Hence, faults that underwent reverse displacements during the Alleghanian orogeny now experienced normal displacements, and a multitude of new normal faults formed (Fig. 8). The intricate network of largely northeast-trending normal faults of the rift junction are known as the Fluorspar Area fault complex, because they are mineralized with fluorite as well as lead, zinc, barite, and other minerals (Kolata and Nelson, 1991; Potter et al., 1995).

Cretaceous and Tertiary

The most significant event in the region during the Cretaceous Period (145 to 65 Ma) was the development of the elongate depression that became the Mississippi embayment (Fig. 9). The embayment at this time was literally a bay off the Gulf of Mexico. The tectonic mechanism by which this feature formed is not clear, but undoubtedly the highly fractured, weakened rock along the Reelfoot rift's axis played a role.

As the embayment subsided, sediments were deposited within it and along its margins. This process did not begin in the northern embayment until late in the Cretaceous, specifically the middle to late Campanian Stage of 80 to 75 Ma ago (Harrison and Litwin, 1997). A basal gravel, the Post Creek Formation, was succeeded by clay, silt, and fine sand of the McNairy Formation (Fig. 2). There is evidence that some faults were active during deposition of the McNairy. Most notably, well records indicate that the McNairy is more than 100 m thicker on the northwest, downthrown side of a northeast-trending fault near Olmsted in Pulaski County, Illinois (Fig. 1). The full extent of tectonism during this time interval is poorly documented because so few exposures exist of sediments of this age.

With minor interruptions, sedimentation in the northern embayment continued into early Tertiary time. Paleocene and Eocene deposits (65 to 35 Ma) are partly marine, partly deltaic and marginal-marine. A gap in sedimentation covers the Oligocene and early Miocene Epochs, about 35 to10 Ma ago, during which time the sea gradually withdrew from the embayment. By late Miocene time, large braided rivers became established in the northern embayment. The master stream appears to

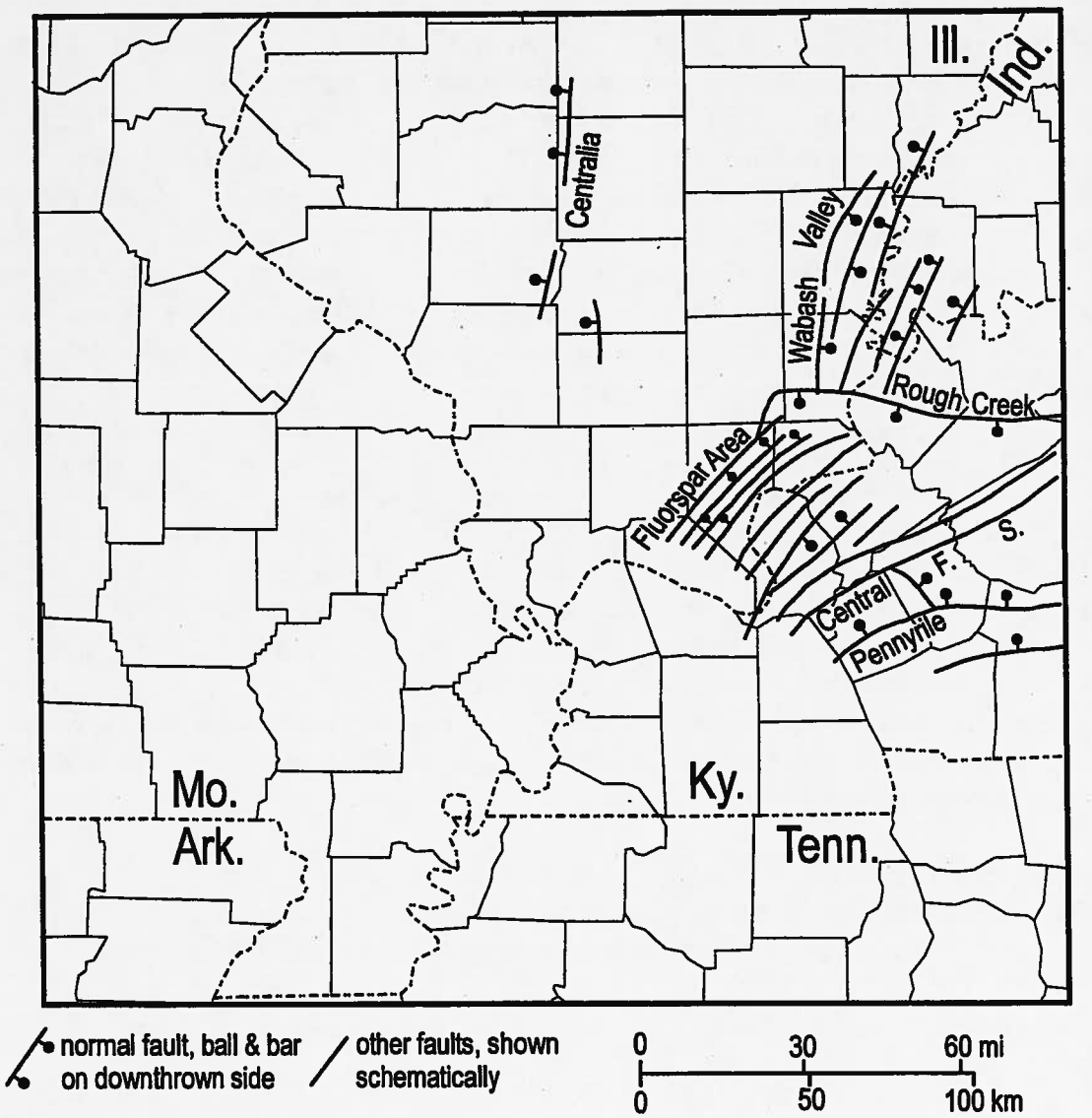

Figure 8: Map showing structures active during Triassic and Jurassic Periods (Kolata and Nelson, 1991).

have been an ancestral Tennessee River (Nelson et al., 1999b). The coarse reddish-brown chert gravel laid down by these rivers is the Mounds Gravel (Fig. 2). Although the age of the Mounds is poorly constrained, it probably encompasses all of Pliocene time (10 to 2 Ma) and extends at least locally into the Quaternary (less than 2 Ma).

Portions of the Fluorspar Area fault complex of southern Illinois and the Commerce fault zone in Missouri were active at times during the Tertiary. Trench exposures in the Benton Hills show that Paleocene and Eocene strata are present in some fault blocks and absent in others. Also, there are cases of early Tertiary strata that are folded and faulted and overlain by Mounds Gravel that is not deformed or less strongly deformed (Harrison et al., 1999). In Illinois, we have found Paleocene and Eocene units preserved in down-faulted blocks, outside of which those units were eroded before the

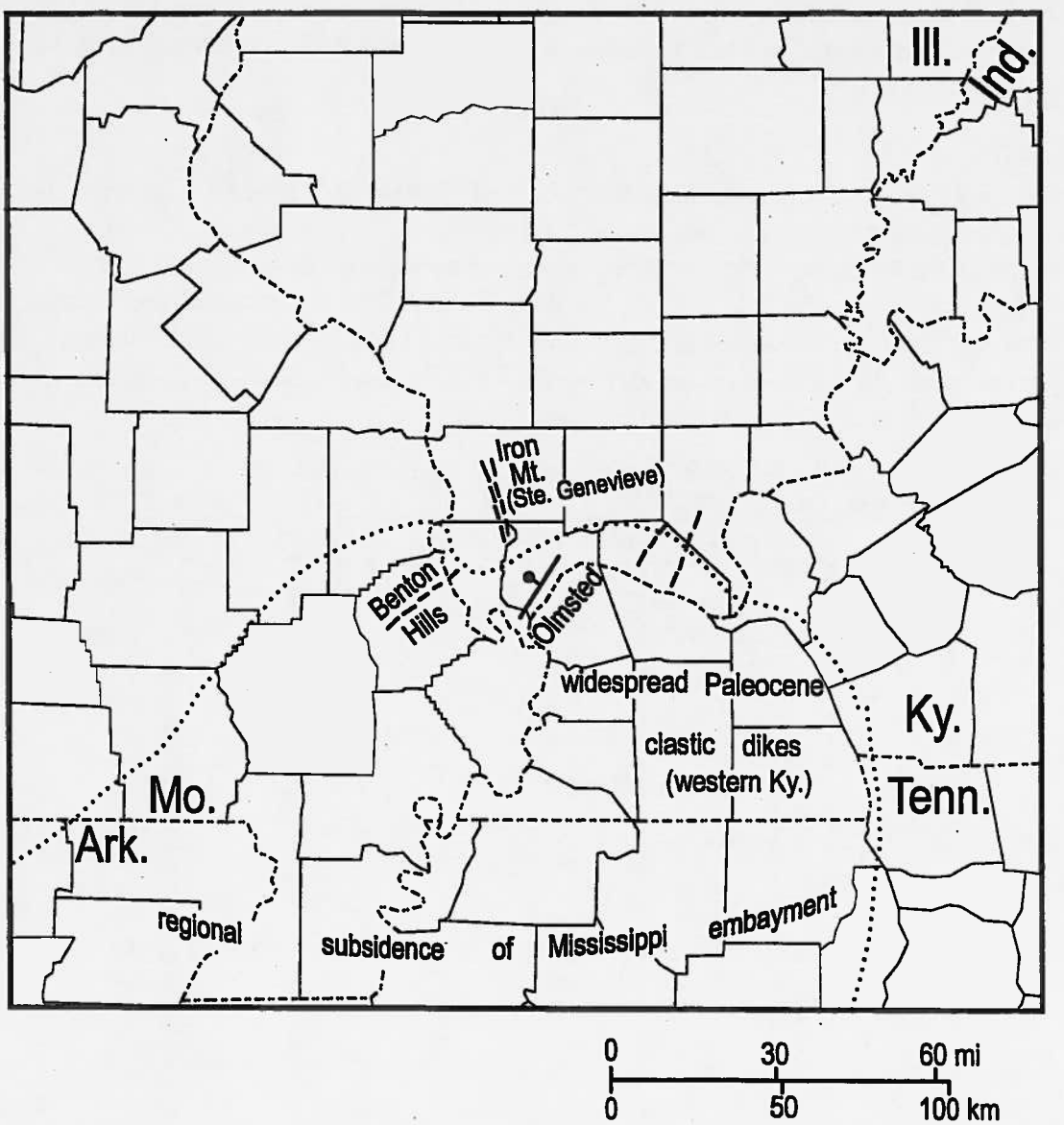

Figure 9: Map showing structures active during Cretaceous and early Tertiary Periods (pre Mounds Gravel (i.e., pre-Miocene)).

Mounds Gravel formed. Other faults displace the Cretaceous McNairy Formation, but not the Mounds Gravel (Nelson et al., 1999a). In Kentucky, sand dikes that appear to be earthquake-liquefaction features are common in the Porters Creek Clay, a Paleocene unit (Olive, 1980; Smath and Davidson, 2000) (Fig. 2).

Putting together a coherent story from these scattered observations is difficult. Evidently fault movements and seismic shaking took place during the Paleocene Epoch, and also between Eocene and Miocene or Pliocene time. The western United States has experienced continuous and intense tectonic activity since the late Jurassic Period, when the Rocky Mountains began to form. After initial Atlantic rifting during the late Triassic and Jurassic Periods, eastern North America has been

relatively quiet tectonically, as it is today. The great New Madrid earthquakes tell us that nearby mountain-building episodes are not required to trigger fault activity in the northern part of the Mississippi embayment.

Quaternary

The Quaternary Period covers approximately the last 2 Ma of earth's history. The period is divided into two unequal epochs: the Pleistocene and the Holocene. The Holocene (also called Recent) Epoch began about 10 ka ago (Fig. 2). The Pleistocene is best known as the time when continental glaciers advanced across Canada and the northern U.S. Three divisions of the Pleistocene are currently recognized: pre-Illinoian, Illinoian, and Wisconsinan (Fig. 10), excluding Sangamonian. No glaciers reached the Mississippi embayment. The Illinoian ice sheet came closest, advancing within about 30 km of the embayment's northern edge.

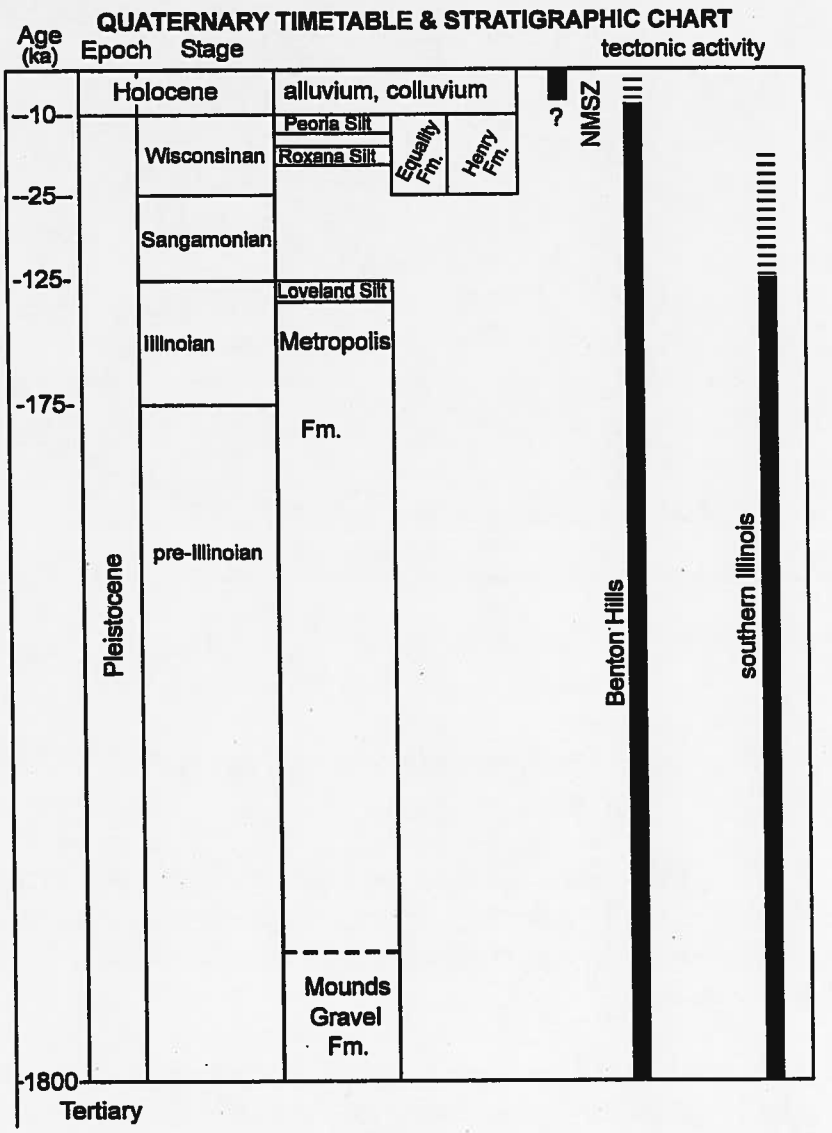

Figure 10: Chart of Quaternary showing subdivisions, key stratigraphic units, and episodes of tectonic activity in different areas of the northern Mississippi embayment.

Many faults in the northern embayment displace the Plio-Pleistocene Mounds Gravel. Intricate faulting of the Mounds has been mapped in the Benton Hills of Missouri (Harrison and Schultz, 1994; Harrison, 1999; Harrison et al., 1999). In Illinois, faulted Mounds is found along every fault zone that reaches the embayment in the Fluorspar Area fault complex. At the Massac Creek site, north of Metropolis, Illinois (Fig. 1) drilling showed a narrow fault zone with the Mounds Gravel down-dropped ~150 m (Nelson et al., 1997; 1999a). Faulted Mounds Gravel is shown on geologic maps in Kentucky (Amos, 1967; 1974; Amos and Wolfe, 1966), but has not been subjected to further study. The age of the Mounds remains a big question. The unit is too old for radiocarbon dating, and no other minerals suitable for other forms of absolute dating have been found. As in most gravel deposits, fossils are rare. The only relevant reports are two finds of fossil pollen in Kentucky by Olive (1980), who cited analyses indicating possible late Miocene to early Pleistocene age. This finding agrees well with inferences made by authors such as Willman and Frye (1970), who equate the Mounds with similar gravels of the southern Gulf Coastal Plain. In the latter area, the gravels are sandwiched by deposits of known age and thereby determined to be Pliocene to early Pleistocene. Hence, any fault displacing the Mounds is potentially a Quaternary fault.

Wherever Quaternary deposits are deformed, non-tectonic mechanisms must be considered. Landslides and solution collapse (collapse of sinkholes or caverns in limestone) commonly deform overlying soils and sediments. For example, impressive faults in Pleistocene strata at Mounds, Illinois were caused by ancient landslides along a former bluff of the Ohio River (Kolata et al., 1981). But earthquakes can trigger landslides, and tectonic fractures in limestone can be widened by groundwater solution. Quaternary-age structures along portions of Post Creek, located east of Metropolis, Illinois (Fig. 1), appear to involve a combination of tectonic faulting and solution collapse (Nelson et al., 1999a).

Pre-Illinoian and Illinoian strata of the northern embayment are largely fluvial and alluvial sediments. Extensive sand and gravel deposits of those ages underlie the alluvial plain of the Mississippi River, which encompasses virtually all of the lowlands within the embayment in Missouri. The Mississippi migrated widely on this plain throughout the Pleistocene, flowing at times northwest of Crowley's Ridge and gradually working its channel eastward to its present position (Fisk, 1944; Johnson, 1985). Illinoian and older sand and gravel also occur at depth in the Cache Valley of southern Illinois, where the Ohio River flowed prior to the Holocene (Fisk, 1944; Esling et al., 1989). Distinguishing among sediments of different ages in these areas is difficult, and outside of the immediate New Madrid area, Holocene faulting has not been documented.

The Metropolis Formation (Pleistocene Epoch), observed along the Ohio and Tennessee Rivers in Illinois and Kentucky (Nelson et al., 1999a), overlies the Mounds Gravel and is composed of a mixture of clay, silt, sand, and gravel, most of which is well compacted and weakly layered. The Metropolis appears to represent alluvium of small, meandering streams and is Illinoian and pre-Illinoian in age. Many faults of the Fluorspar Area fault complex in Illinois displace the Metropolis Formation. Some faults in the Metropolis, confirmed by drilling, have displacements of at least 30 m. Hence it is clear that there was significant tectonic activity in southernmost Illinois during Illinoian and earlier Pleistocene time (Nelson et al., 1997, 1999a; b; McBride and Nelson, 2001). Sediments that resemble the Metropolis occur also in the Benton Hills of Missouri, and are offset along the Commerce fault zone (Harrison et al., 1999).

Wisconsinan sediments in the northern embayment include fluvial sand and gravel (Henry Formation), lacustrine silt and clay (Equality Formation), and wind-blown silt or loess (Roxana and Peoria Silts) (Fig. 10). To date, no tectonic faults have been found that clearly displace any of these units in Kentucky or Illinois. A few small (less than 1.5 m of throw) faults in Illinois displace alluvial sediments that appear to be younger than the Metropolis Formation, but the ages of these faults cannot be verified (Nelson et al., 1997, 1999a; b). Southeastern Missouri is the place to see faults displacing Wisconsinan loess. Trenching in the Benton Hills revealed many faults that offset the youngest Wisconsinan loess, the Peoria Silt (Harrison et al., 1999), as first reported by Grohskopf (1955). Another site in Missouri where Peoria Silt is faulted is Holly Ridge on the southeast face of Crowley's Ridge (Fig. 1). At the time of writing, however, questions remain as to whether the faults at Holly Ridge are tectonic or the products of landslides (Nelson et al., 1999b). The Peoria Silt being 25 to 10 ka old, any faults offsetting this unit would be latest Wisconsinan to Holocene.

Outside of the immediate vicinity of New Madrid, the only place in the northern Mississippi embayment having known tectonic faults in Holocene sediment is the Benton Hills (Fig. 1). In addition to Peoria Silt, Holocene colluvium is faulted in trenches at English Hill. Charcoal from the faulted colluvium yielded radiocarbon ages that range from about 5.0 to 1.2 ka before present. In a trench at Sassafras Canyon, also in the Benton Hills, a small reverse fault juxtaposed Tertiary strata with Holocene colluvium. Charcoal from the colluvium yielded ages of 160 to 210 a, which suggests that this fault moved during the New Madrid quakes of 1811 and 1812 (Harrison et al., 1999). On Crowley's Ridge, excavations at Holly Ridge showed faulted Peoria loess, but as noted above, these faults could represent non-tectonic landslides.

CURRENT SEISMICITY

During the Winter of 1811-1812, the Mississippi Valley centered over the fledgling settlement of New Madrid in the Missouri bootheel was convulsed by a powerful series of earthquakes with an estimated moment magnitude of 8.0 or more. Since 1812, the largest earthquake in the region was centered near Charleston, Missouri in 1895 (Fig. 1). An estimated magnitude of 6.5 is based on published accounts of the physical effects of the quake, which correspond to an MM intensity of VIII. These effects included minor and localized eruptions of sand blows near Charleston. Today, well-defined seismicity patterns in the New Madrid seismic zone (NMSZ) (Fig. 1) indicate a relatively discrete zone of strike-slip faulting, while a more dispersed zone of seismicity continues farther north into the southern Illinois basin and southeastern Missouri (Fig. 11). Despite the high degree of knowledge about the immediate tectonic setting of the NMSZ and the fact that the southern Illinois region has had larger and deeper twentieth-century earthquakes than the NMSZ (Langer and Bollinger, 1991), it is unclear how the very different patterns of seismicity in the two areas are related. The southeastern Illinois area over the past half-century has hosted several instrumentally recorded events of magnitude (m_{bLg}) 3.0 or greater (e.g., 1968, 1974, 1987; Fig. 12), of which the magnitude 5.5 1968 event is the largest and one of the deepest. No known surface faulting or liquefaction was associated with any of these events. Nevertheless, the larger magnitude twentieth-century earthquakes and paleoliquefaction sites in southern Illinois and Indiana imply a major seismic zone that may approach the NMSZ in terms of earthquake hazard (Langer and Bollinger, 1991; Obermeier, 1998). In fact, Braile et al. (1997) and Hinze et al. (1988) have argued that the

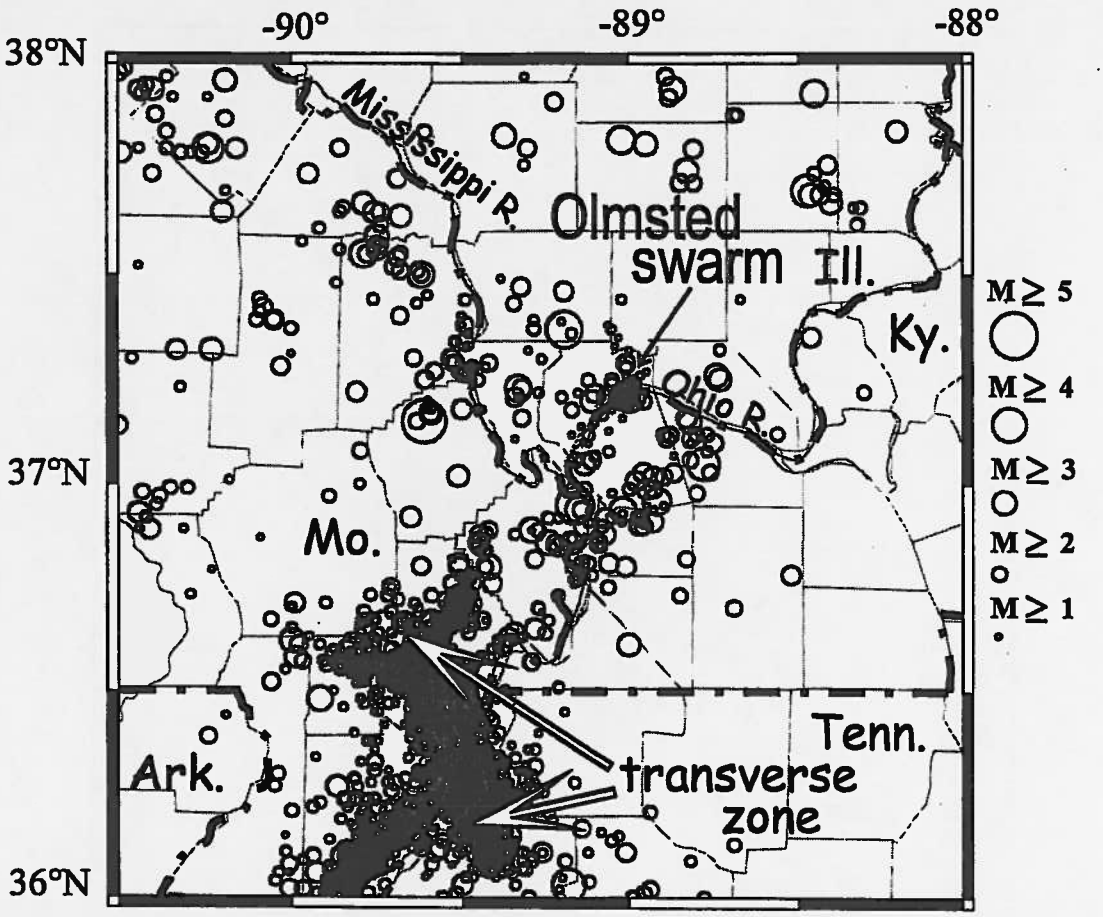

Figure 11: Epicenter map of instrumentally recorded earthquakes in the study area, 1974 to 2001, based on the Saint Louis University and Central Mississippi Valley Earthquake Bulletins, the Tennessee Earthquake Information Center earthquake bulletin, and continuous monitoring by Saint Louis University and the Center for Earthquake Research and Information, University of Memphis. The relative location accuracy is not indicated.

structures underlying and controlling the NMSZ extend well beyond the central part of the zone into southern Illinois and vicinity.

For the northern half of the NMSZ just northeast of the Missouri bootheel, the pattern of seismic epicenters indicates a northwest-trending transverse zone (dominated by thrust faulting) and two northeast-trending zones (dominated by near-vertical strike-slip faulting) (Chiu et al., 1992); however, two northeast-trending epicenter alignments can also be recognized further to the northeast: (1) an eastern "prong" in western Kentucky and (2) a western "prong" under a straight segment of the Ohio River around Cairo, Illinois (Fig. 11) that takes in the 1984 Olmsted, Illinois, earthquake swarm (more than 200 events between November 1983 and April 1984), which included body-wave magnitudes up to 3.6. These patterns suggest that the NMSZ extends into southernmost Illinois and western Kentucky. In map view, the Olmsted epicenters plot to an ellipse with the long axis northeast, suggesting a northeast-trending fault (Stauder et al., 1984; Stover, 1988).

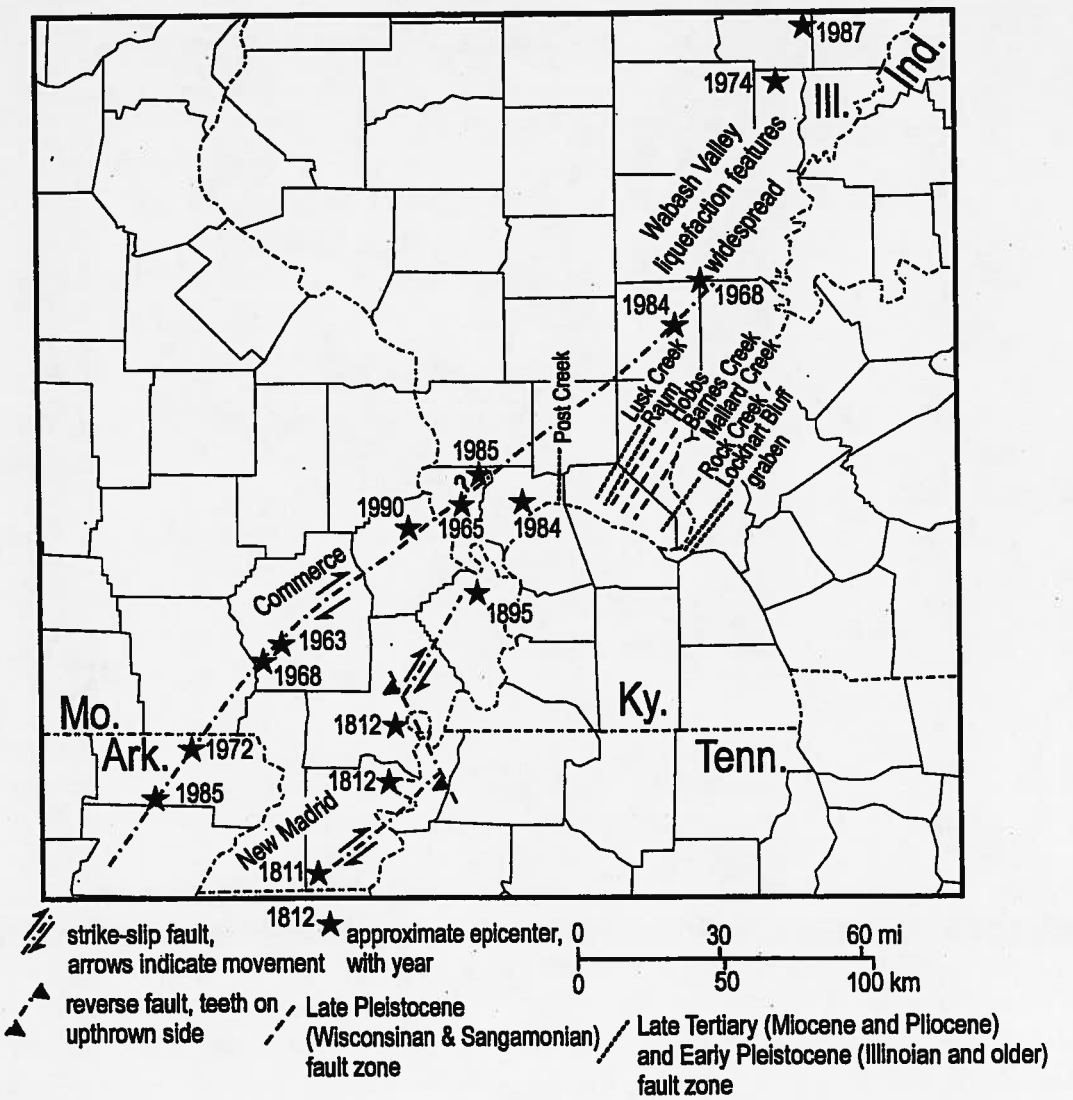

Figure 12: Map showing features active in (1) Illinoian and older Pleistocene, (2) Wisconsinan and Sangamonian, and (3) Holocene. Also shown are locations of significant earthquakes mentioned in the text.

DISCUSSION

A long-standing paradigm for the North American stable continental region is that earthquakes here tend to occur by reactivation of existing faults (Marshak and Paulsen, 1996). This is especially true for the northern Mississippi embayment and southern Illinois basin, which have been tectonically active through more than half a billion years of earth's history. An aborted rifting event of late Precambrian time produced a permanent zone of weakness subject to reactivation under different stress regimes. The region is shattered by intricate networks of fractures, many of which have displacements of hundreds to thousands of meters (Kolata and Nelson, 1997). In many instances, the same faults underwent opposing senses of slip under different stress regimes.

During Quaternary time, different areas of the northern embayment seem to have conflicting histories. Although current seismicity is concentrated in the well-defined New Madrid seismic zone, late Cenozoic deformation in the Midcontinent affects a much larger region (Harrison and Schultz, 1994). Studies of surface deformation in the New Madrid seismic zone suggest seismic faulting as old as only about 65 ka (Pratt, 1994; Schweig and Ellis, 1994). Indeed, geologists have remarked that such conditions cannot have continued for long, or else there would be far greater topographic manifestation of fault movement in the New Madrid area.

The Benton Hills of southeastern Missouri record the next youngest series of large earth movements. Studies reveal extensive displacement of Wisconsinan loesses, and local faulting of Holocene sediments. In one place, a small movement may have occurred in 1811 or 1812. Overall, southeastern Missouri may be characterized as having had major tectonic activity during the late Pleistocene with only localized Holocene activity.

In southernmost Illinois, the Illinoian and older Pleistocene units are faulted in many places, and with displacements larger than any seen in the central New Madrid seismic zone. The record indicates at most, minor disturbance during the Wisconsinan and none yet detected during the Holocene.

We suggest that the differing Quaternary-Holocene deformation histories in the greater New Madrid seismic zone region indicate that seismicity and tectonic activity migrate around from one place to another within the northern Mississippi embayment. This conclusion implies that activity will continue to migrate in the future - as it has done for more than 500 Ma.

ACKNOWLEDGMENTS

This work was supported in part by the Earthquake Engineering Research Centers Program of the National Science Foundation under Award Number EEC-9701785. The paper was formally reviewed by the Editorial Board of the Illinois State Geological Survey. The authors gratefully acknowledge reviews by J. H. Goodwin, D. R. Kolata, and Z. Lasemi.

REFERENCES

Amos, D.H., 1967, Geologic Map of Part of the Smithland Quadrangle, Livingston County, Kentucky: *U.S. Geological Survey, Map GQ-657,* 1 sheet, scale 1:24,000.

Amos, D.H., 1974, Geologic Map of the Burna Quadrangle, Livingston County, Kentucky: *U.S. Geological Survey, Map GQ-1150,* 1 sheet, scale 1:24,000.

Amos, D.H., and Wolfe, E.W., 1966, Geologic Map of the Little Cypress Quadrangle, Kentucky-Illinois: *U.S. Geological Survey, Map GQ-554,* 1 sheet, scale 1:24,000.

Bradbury, J.C. and Baxter, J.W., 1992, Intrusive Breccias at Hicks Dome, Hardin County, Illinois: *Illinois State Geological Survey, Circular 550,* 23 p.

Braile, L.W., Hinze, W.J., and Keller, G.R., 1997, New Madrid Seismicity, Gravity Anomalies, and Interpreted Ancient Rift Structures: *Seismological Research Letters*, v. 68, p. 599-610.

Chiu, J.M., Johnston, A.C., and Yang, Y.T., 1992, Imaging the Active Faults of the Central New Madrid seismic Zone Using PANDA Array Data: *Seismological Research Letters*, v. 63, p. 375-393.

Ervin, P.C. and McGinnis, L.D. 1975, Reelfoot Rift - Reactivated Precursor to the Mississippi Embayment: *Geological Society of America Bulletin,* v. 86, p. 1287-1295.

Esling, S.P., Hughes, W.B., and Graham, R.C., 1989, Analysis of the Cache Valley Deposits in Illinois and Implications Regarding the Late Pleistocene - Holocene Development of the Ohio River Valley: *Geology,* v. 17, p. 434-437.

Fisk, H.N., 1944, Geological Investigation of the Alluvial Valley of the Lower Mississippi River: *U.S. Army Corps of Engineers, Mississippi River Commission, Vicksburg, Mississippi,* 78 p.

Freeman, L.B., 1951, Regional Aspects of Silurian and Devonian Stratigraphy in Kentucky: *Kentucky Geological Survey, Series IX, Bulletin 6,* 565 p.

Fuller, M., 1912, The New Madrid Earthquake: *U.S. Geological Survey Bulletin 494.*

Grohskopf, J.G., 1955, Subsurface Geology of the Mississippi Embayment of Southeast Missouri: *Missouri Geological Survey,* V. 37, 2nd Series, 133 p. and 9 plates.

Harrison, R.W., 1999, Geologic Map of the Thebes Quadrangle, Illinois and Missouri: *U.S. Geological Survey, Geologic Quadrangle Map GQ-1779,* 1 sheet, scale 1:24,000.

Harrison, R.W. and R.J. Litwin, 1997, Campanian Coastal-plain Sediments in Southeastern Missouri and Southern Illinois - Significance to the Early Geologic History of the Northern Mississippi Embayment: *Cretaceous Research,* v. 18, p. 687-696.

Harrison, R.W. and Schultz, A., 1994, Strike-slip Faulting at Thebes Gap, Missouri and Illinois: Implications for New Madrid Tectonism: *Tectonics,* v. 13, no. 2, p. 246-257.

Harrison, R.W., Hoffman, D., Vaughn, J.D., Palmer, J.R., Wiscombe, C.L., McGeehin, J.P., Stephenson, W.J., Odum, J.K., Williams, R.A., and Forman, S.L., 1999, An Example of Neotectonism in a Continental Interior - Thebes Gap, Midcontinent, United States: *Tectonophysics,* v. 305, p. 399-417.

Hinze, W.J., Braile, L.W., Keller, G.R., and Lidiak, E.G., 1988, Models for Midcontinent Tectonism; an Update: *Reviews of Geophysics*, v. 26, p. 699-717.

Johnson, W.D., Jr., 1985, Geologic Map of the Scott City Quadrangle and Part of the Thebes Quadrangle, Scott and Cape Girardeau Counties, Missouri: *U.S. Geological Survey, Miscellaneous Field Studies Map MF-1803,* 2 sheets, scale 1:24,000.

Kolata, D.R. and Nelson, W.J., 1991, Tectonic History of the Illinois Basin: *American Association of Petroleum Geologists, Memoir 51*, p. 263-285.

Kolata, D. R., and Nelson, W. J., 1997, Role of the Reelfoot Rift-Rough Creek Graben in the Evolution of the Illinois Basin. In: Ojakangas, R. W., Dickas, A. B., and Green, J. C., eds., Middle Proterozoic to Cambrian Rifting, Central North America: Geological Society of America Special Paper 312, p. 287-298.

Kolata, D.R., Treworgy, J.D., and Masters, J.M., 1981, Structural Framework of the Mississippi Embayment of Southern Illinois: *Illinois State Geological Survey, Circular 526,* 38 p.

Langenheim, V.E. and Hildenbrand, T.G., 1997, Commerce Geophysical Lineament - Its Source, Geometry, and Relation to the Reelfoot Rift and New Madrid Seismic Zone: *Geological Society of America Bulletin,* v. 109, no. 5, p. 580-595.

Langer, C.J. and Bollinger, G.A., 1991, The Southeastern Illinois Earthquake of 10 June 1987: the Later Aftershocks: *Bulletin of the Seismological Society of America,* v. 81, p. 423-445.

Marshak, S. and Paulsen, T., 1996, Midcontinent U. S. Fault and Fold Zones; a Legacy of Proterozoic Intracratonic extensional tectonism?: *Geology,* v. 24, p. 151-154.

McBride, J.H. and Nelson, W.J., 1999, Style and Origin of Mid-Carboniferous Deformation in the Illinois Basin, USA - Ancestral Rockies Deformation? *Tectonophysics,* v. 305, p. 249-273.

McBride, J.H. and Nelson, W.J., 2001, Seismic Reflection Images of Shallow Faulting, Northernmost Mississippi Embayment, North of the New Madrid Seismic Zone: *Bulletin of the Seismological Society of America,* v. 91, no. 1, p. 128-139.

McCracken, M.H., 1971, Structural Features of Missouri: *Missouri Geological Survey, Report of Investigations No. 49,* 99 p. and 1 plate.

Nelson, W.J., Denny, F.B., Devera, J.A., Follmer, L.R., and Masters, J.M., 1997, Tertiary and Quaternary Tectonic Faulting in Southernmost Illinois: *Engineering Geology,* v. 46, no. 3-4, p. 235-258.

Nelson, W.J., Denny, F.B., Follmer, L.R., and Masters, J.M., 1999a, Quaternary Grabens in Southernmost Illinois: Deformation Near an Active Intraplate Seismic Zone: *Tectonophysics,* v. 305, p. 381-397.

Nelson, W.J., Harrison, R.W., and Hoffman, D., 1999b, Neotectonics of the Northern Mississippi Embayment: *Illinois State Geological Survey, Guidebook 30,* 34 p.

Nelson, W.J. and Marshak, S., 1996, Devonian Tectonism of the Illinois Basin Region, U.S. Continental Interior: *Geological Society of America, Special Paper 308,* p. 169-180.

Nelson, W.J. and Lumm, D.K., 1987, Structural Geology of Southeastern Illinois and Vicinity: *Illinois State Geological Survey, Circular 538,* 70 p. and 2 plates.

Nelson, W.J., Smith, L.B., and Treworgy, J.D., in press, Sequence Stratigraphy of Lower Chesterian (Mississippian) Strata of the Illinois Basin: *Illinois State Geological Survey, Bulletin 107.*

Obermeier, S.F., 1998, Liquefaction Evidence for Strong Earthquakes of Holocene and Latest Pleistocene Ages in the States of Indiana and Illinois, USA: *Engineering Geology,* v. 50, p. 227-254.

Olive, W.W., 1980, Geologic Maps of the Jackson Purchase Region, Kentucky: *U.S. Geological Survey, Miscellaneous Investigations Series, Map I-1217,* 1 sheet and 11-page pamphlet.

Potter, C.J., Goldhaber, M.B., Heigold, P.C., and Drahovzal, J.A., 1995, Structure of the Reelfoot-Rough Creek Rift System, Fluorspar Area Fault Complex, and Hicks Dome, Southern Illinois and Western Kentucky - New Constraints from Regional Seismic Reflection Data: *U.S. Geological Survey, Professional Paper 1538-Q,* 19 p. and 1 plate.

Pratt, T.L., 1994, How Old is the New Madrid Seismic Zone?: *Seismological Research Letters,* v. 65, p. 172-179.

Rhoades, R. and Mistler, A.J., 1941, Post-Appalachian Faulting in Western Kentucky: *Bulletin of the American Association of Petroleum Geologists,* v. 25, no. 11, p. 2046-2056.

Ross, C.A., 1963, Structural Framework of Southernmost Illinois: *Illinois State Geological Survey, Circular 351,* 28 p.

Ross, C.A., 1964, Geology of the Paducah and Smithland Quadrangles in Illinois: *Illinois State Geological Survey, Circular 360,* 32 p. and map, scale 1:62,500.

Schwalb, H.R., 1969, Paleozoic Geology of the Jackson Purchase Region, Kentucky: *Kentucky Geological Survey, Series X, Report of Investigations 10,* 40 p.

Schweig, E. S. and Ellis, M. A., 1994, Reconciling Short Recurrence Intervals with Minor Deformation in the New Madrid Seismic Zone: *Science,* v. 264, p. 1308-1311.

Smath, R.A. and Davidson, B., 2000, Economic and Engineering Geology of the Jackson Purchase Area, Kentucky: *Year 2000 Annual Field Conference of the Kentucky Society of Professional Geologists,* 19 p. and 2 plates.

Soderberg, R.K. and Keller, G.R., 1981, Geophysical Evidence for Deep Basin in Western Kentucky: *American Association of Petroleum Geologists Bulletin,* v. 65, no. 2, p. 226-234.

Stauder, W., Herrmann, R., Chulick, J., Mascarenas, M.J., John, V., Leu, P.L., Shin, T.C., Yepes, H., and Finn, C., 1984, Central Mississippi Valley Earthquake Bulletin, Quarterly Bulletin No. 39, First Quarter 1984, *Department of Earth and Atmospheric Sciences, St. Louis University*, 83 p.

Stover, C.W., 1988, United States Earthquakes, 1984: *U.S. Geological Survey, Bulletin 1862,* 179 p.

Willman, H.B. and Frye, J. C., 1970, Pleistocene Stratigraphy of Illinois: *Illinois State Geological Survey, Bulletin 94,* 204 p.

STRONG-MOTION RECORDINGS, SHEAR-WAVE VELOCITIES, AND LINEAR SITE EFFECTS IN THE NEW MADRID SEISMIC ZONE

Ron Street[1]
Edward Woolery[2]
Zhenming Wang[3]

ABSTRACT

Strong-motion stations in the Upper Mississippi Embayment are underlain by several tens to several hundreds of meters of loose to semi-consolidated sediments. Site effects resulting from these sediments are expected to be profound and highly variable. Twelve years of strong-motion monitoring by the University of Kentucky in the embayment provides direct observations of these variabilities; observations are necessary for testing and validating future ground-motion modeling.

Shear-wave velocity models for six of the strong-motion stations are developed using direct *P*- and *S*-wave measurements, and the converted *Sp*-wave that is generated at the bedrock/sediment interface in the embayment. Site effects, for the case of low strains (i.e., $<10^{-4}$ percent), were estimated using the one-dimensional computer program SHAKE91, the horizontal-to-vertical spectral ratios of earthquake induced *S* waves, and the horizontal-to-vertical ambient noise spectral ratios for five of the strong-motion station sites. The analyses were conducted for the frequency range of 0.5 to 10 Hz. The results from the three techniques, in general, do not coincide with each other. At one site where the results from the three techniques correspond reasonably well in predicting the frequencies at which the ground motions will be amplified, the levels of amplifications do not coincide.

INTRODUCTION

The University of Kentucky has monitored strong motions in the New Madrid seismic zone of the Upper Mississippi Embayment for 12 years, in an effort to determine the site effects at the strong-motion stations. The Upper Mississippi Embayment is a broad southwest-plunging trough filled with several tens to several hundreds of meters of post-Paleozoic unconsolidated and semi-consolidated sediments overlying limestones and dolomites of Ordovician and Cambrian age (Fig. 1). The region has undergone long-term tectonism, including rifting, uplifting, and subsidence, as well as the ongoing processes of erosion and deposition. Because of these processes, as well as localized areas of intense sediment deformation as a result of movement in the bedrock

---

[1]Assoc. Prof., Emeritus, Dept. of Geological Sciences, University of Kentucky, Lexington, Ky.
[2]Assistant Prof., Dept. of Geological Sciences, University of Kentucky, Lexington, Ky.
[3]Kentucky Geological Survey, University of Kentucky, Lexington, Ky.

along active faults, and liquefaction in the uppermost sediments (≤30 m), the properties and velocity structures of the sediments in the region are highly variable. These variabilities, along with the sediment thickness in the embayment, the dynamic properties of the near-surface soft soils, the damping of the deeper stiff soils at high confining pressures, and basin-generated surface waves, are some of the properties and aspects of the embayment that are expected to have a profound influence on the propagation of seismic waves generated by earthquakes in the seismic zone.

STRONG-MOTION RECORDS ACQUIRED AT THE UNIVERSITY OF KENTUCKY STATIONS

The University of Kentucky strong-motion array began operating in the fall of 1989. Station abbreviations, coordinates, the instrumentation used at each station, as well as some brief comments about the stations, are given in Table 1. In the decade during which the strong-motion stations have been operating, we have acquired 107 digital records of 67 reported earthquakes in New Madrid seismic zone, ranging in magnitude from 1.6 to 4.5 $m_{b,Lg}$. Epicenters of the earthquakes with respect to the stations are shown in Figure 2. Table 2 is a list of the strong-motion records (in the chronological order in which they were acquired), the epicentral location and magnitude of the earthquakes, and instrument-corrected peak horizontal and vertical ground accelerations and velocities. The five character code used to identify the records is explained at the bottom of the table. Data for the records were uniformly collected at 200 samples per second on Kinemetrics FBA-13 or -23 accelerometers, and SSA-1, SSA-2, SSR-1, or K-2 accelerographs.

The records were processed using Kinemetrics' software programs, Seismic Workstation® (Version 1-E, 1989) and Strong Motion Processing Software® (1998). High-frequency filtering was done with a transition band of 45 to 50 Hz. Anti-aliasing for the Kinemetrics accelerographs used in this study was accomplished by a two-pole, 50-Hz Butterworth filter. The transition band used in the low-frequency filtering varied, depending upon the record length, the magnitude of the event, and noise levels. Typically for the smaller events (< 3 m_{bLg}), the low-frequency transition band was set at 2 to 4 Hz, whereas for the larger events, the low-frequency transition band was set at 0.6 to 0.8 Hz or less.

The distribution of the magnitudes of the earthquakes and their processed peak ground accelerations and velocities are summarized in Figure 3. The majority of the records have a peak acceleration (PA) of <10 cm/s^2, and peak velocity (PV) of < 1 cm/s. The largest PA and PV values in the data set are 330 cm/s^2 and 3.32 cm/s for a 2.7 $m_{b,Lg}$ event that occurred within 5 km of station VSAB on December 2, 1997. The acceleration and velocity traces for the event are shown in Figure 4. The earthquake was felt over a few square kilometers, and was described by homeowners in the immediate vicinity of the epicenter as being a violent jar that shook their houses and everything in them (i.e., MM IV). As indicated in Figure 4, the PA and PV values for the event are associated with the P-wave on the vertical component and the S-wave on the 250° component, respectively. The frequency of the PA is ~21 Hz, whereas for PV it is ~7 Hz. The strain level at the site resulting from the earthquake is estimated to be 2.4×10^{-4} percent, which is obtained by dividing the observed peak ground velocity, 3.32

cm/s, by the shear-wave velocity of the soil, 122 m/s (Hays, 1980). Peak ground accelerations from earthquakes within 10 to 15 km of station VSAB are typically associated with P-waves on the vertical component, and high-frequency phenomena.

Parameters other than the peak accelerations and peak velocities were reviewed for the study. One of the parameters that is of interest to those involved with seismic hazard mitigation is the 0.2 s spectral response acceleration at 5% critical damping (S_s), which is used in the 1997 National Earthquake Hazards Reduction Program (NEHRP) provisions for seismic regulations for new buildings (Federal Emergency Management Agency, 1997). Of the 107 records reviewed for this study, 23 had S_s values in excess of 10^{-2}% g and two had S_s values in excess of 10^{-1}% g. The largest S_s value recorded to date is $2x10^{-1}$% g, for the December 2, 1997, event at station VSAB; this is the same earthquake and recording from which we obtained the largest PA and PV values.

Another ground-motion parameter that is occasionally mentioned in the literature and was reviewed for this study is the ratio of the vertical-to-horizontal peak accelerations (Z/H). Figure 5 illustrates the Z/H ratios of the ground motions as a function of their hypocentral distances. Although there is considerable scatter in the data, the general trend of the Z/H ratios decreases with increasing hypocentral distance. A notable exception is the Z/H ratio for the 4.3 m_b earthquake of November 29, 1996, at station VSAB. The epicentral distance between the earthquake and VSAB is 81 km. The 12 km focal depth of the event is typical of other earthquakes in the seismic zone. The peak acceleration for the earthquake is the 8-Hz converted *Sp*-wave indicated on the vertical trace of the accelerogram.

P- and S-WAVE VELOCITIES OF THE POST-PALEOZOIC SEDIMENTS IN THE UPPER MISSISSIPPI EMBAYMENT

P-Wave Velocities

A thorough understanding of site effects in an area that has thick layers of sediments, such as those found in the Upper Mississippi Embayment, requires a detailed knowledge of the *P*- and *S*-wave velocity structure of the sediments. *P*-wave seismic reflection and refraction velocity profiles can be used to determine the depth to the top of the water table, and for imaging subsurface topography in the sediments and at the sediment/bedrock interface. The depth to the top of the water table is needed for determining the effective stress in the sediments, and for estimating the frequency of the *P*-wave resonance between the top of the water table and the surface (Cranswick *et al.*, 1990).

P-wave velocities of the formations that make up the sediments in the Upper Mississippi Embayment are reasonably well known from the extensive number of commercial and scientific *P*-wave CDP seismic profiles and soundings, and sonic logs, that have been acquired in the embayment. Figure 6, taken from Gao *et al.* (in press), shows the *P*-wave velocity profiles at the three sites in southeastern Missouri near the Arkansas/Missouri boundary. *P*-wave velocities in the figure are typical of the *P*-wave velocities of the sediments found throughout the Upper Mississippi Embayment.

S-Wave Velocities of the Near-Surface Sediments (≤ 100 m)

In contrast to the *P*-wave velocities, the *S*-wave velocities of the sediments in the Upper Mississippi Embayment are not well determined. *S*-wave velocities of the near-surface sediments (< 150 m) for sites throughout the embayment can be found in Street *et al.* (in press), for sites in western Tennessee in Liu *et al.* (1997), and for sites in the Memphis, Tenn., metropolitan area in Williams *et al.* (in press). However, *S*-wave velocities of the sediments between the near-surface sediments and the top of the Paleozoic bedrock in the embayment have not been determined, except at a few scattered sites along the edges of the embayment (Sykora and Davis, 1993; Harris *et al.*, 1994; Street *et al.*, 1995, 1997).

Near-surface S-wave velocity data can be used to characterize the soil stiffness, damping, and impedance boundaries that might result in resonances. Soil stiffness is a function of the shear modulus, G_{max}, and the manner in which the ratio of the secant shear modulus (G) to G_{max} varies with cyclic strain amplitudes (Kramer, 1996). G is derived from laboratory tests on soil samples, whereas G_{max} is determined by the relationship

$$G_{max} = \rho V_s^2 \qquad (1)$$

in which ρ is the density (kg/m^3) and V_s is the shear-wave velocity (m/s) of the sediments. Near-surface velocity data can be used to estimate the in situ damping (τ) of seismic shear waves at low strains (i.e., < 10^{-4}%). Damping in a soil is related to the specific quality factor, Q_s, by

$$\tau \approx (2\ Q_s)^{-1} \qquad (2)$$

(Mok *et al.*, 1988), and the site-specific Q_s can be estimated from the pulse broadening of first-arrival SH-wave refractions (Ricker, 1953; Hatherly, 1986; Wang *et al.*, 1994). Impedance is the resistance to particle motion, and for a vertically propagating polarized shear wave (*SH*), the impedance of a formation is defined as the product of the density and shear-wave velocity. Since particle velocity is inversely proportional to the square root of the impedance, particle velocities tend to be greater in lower-velocity soils than they are in stiff soils or rock, assuming other factors being equal (Reiter, 1990). Impedance boundaries at the interfaces between sediments of distinctly different densities and velocities are expected to play a significant role in site effects because of resonances resulting from trapped seismic waves (Williams *et al.*, 1999, 2000).

Near-surface *S*-wave seismic reflection and refraction investigations are capable of imaging topography and impedance boundaries in the near-surface sediments. Figure 7, taken from Woolery and Street (in press), shows the near-surface *S*-wave velocity models at two sites in northeastern Arkansas, and the respective H/V ambient noise spectra (discussed below). In Figure 7a, the contact between the 258 and 551 m/s velocities is nearly horizontal, and there is a well-defined resonance at ~1 Hz in the H/V spectra. In Figure 7b, the contact between the 780 and 454 m/s velocities is irregular, and there is no well-defined resonance in the H/V ambient noise spectra. Ground motions at the two sites resulting from an earthquake are expected to behave

similarly; that is, the near-surface *S*-wave velocity structure at the first site would be expected to induce a high-amplitude resonance at ~1 Hz, whereas at the second site, the near-surface *S*-wave velocity structure would not induce a resonance.

S-Wave Velocities of the Deeper Sediments and the Bedrock

For most sites in the Upper Mississippi Embayment, the thickness of the post-Paleozoic sediments exceeds 100 m (Fig. 1). Studies, such as those by Bard and Chávez-García (1993), Anderson *et al.* (1996), Hartzell *et al.* (1997), and Wald and Mori (2000), have shown that variations in site effects are the result of the properties and velocity structures in both the near-surface and deeper sediments.

Chiu *et al.* (1992) pointed out that the average *S*-wave velocities (V_s) of the post-Paleozoic sediments at sites in the Upper Mississippi Embayment can be estimated from the travel-time differences between the direct *S* and converted *Sp* waves generated by earthquakes in the New Madrid seismic zone. Assuming that the raypaths in the sediments for the two waves are nearly vertical and almost identical, the average V_s of the sediments can be estimated from the equation

$$H/V_s - H/V_p \simeq t_S - t_{Sp} \qquad (3)$$

where H is the thickness, and V_p is the average *P*-wave velocity of the sediments, and $t_S - t_{Sp}$ is the arrival time difference between the *S* and *Sp* waves. Since H, Vp, and $t_S - t_{Sp}$ can be determined for the University of Kentucky strong-motion station sites, the average V_s of the post-Paleozoic sediments at the sites can be determined. Furthermore, since the thickness and *S*-wave velocities of the near-surface sediments are known, the average *S*-wave velocities of the sediments between the near-surface sediments and the top of the Paleozoic bedrock can be determined.

Figure 8 shows the near-surface *S*-wave velocity models, depth to bedrock, average *P*-wave velocities (V_{Pave}) of the post-Paleozoic sediments, and the $t_S - t_{Sp}$ time differences for the University of Kentucky strong-motion station LATN (Fig. 2). The near-surface *S*-wave model is from Street *et al.* (1995), the depth to the top of the bedrock is from Wheeler *et al.* (1994), and the $t_S - t_{Sp}$ time is for seismograph station MFRT, provided to us by Dr. Chiu of the University of Memphis (personal communication); the seismograph station is ~4 km from LATN. The average *P*-wave velocities, V_{Pave}, is based on the intercept time shown in Street *et al.* (1995) and the depth to bedrock. Using the appropriate values in equation 2, the average *S*-wave velocity of the post-Paleozoic sediments at LATN is determined to be 628 m/s (±21 m/s). The average *S*-wave velocity to a depth of 80 m, based on the near-surface *S*-wave model, is 297 m/s. The average *S*-wave to a depth of 231 m, based on an *S*-wave vibroseis record (not shown), is 433 m/s. The interval *S*-wave velocity between 80 and 231 m is, therefore, 536 m/s, and the interval *S*-wave velocity of the sediments between 231 and 770 m is estimated to be 691 m/s.

The average *S*-wave velocities for the deeper sediments at strong-motion stations COKY, HIKY, and VSAB (Fig. 9), were estimated in a similar manner. The *S*-wave velocity model at strong-motion station VSAP is based on drill hole and surface *SH*-wave seismic reflection and refraction profiles (Sykora and Davis, 1993; Harris *et al.*, 1994).

The *S*-wave model at strong-motion station WIKY in Figure 9 is based on surface seismic reflection and refraction *P*- and *SH*-wave velocity profiles.

The 3,520 m/s *S*-wave velocity for the Paleozoic bedrock for most of the strong-motion stations shown in Figure 9 is from Catchings (1999). He determined the *S*-wave velocities of the upper crust in the Upper Mississippi Embayment from a 400-km-long seismic refraction profile that ran from Memphis, Tenn., to a location just east of St. Louis, Mo. The 2,743 m/s is based on *S*-wave velocity measurement near Paducah, Ky. It is expected that some of the *S*-wave velocities assigned to the bedrock in Figure 9 will be changed once we complete our Vibroseis *SH*-wave measurements at the sites.

SITE EFFECTS AT THE UNIVERSITY OF KENTUCKY STRONG-MOTION STATIONS

Estimating Site Effects of Engineering Interest at the University of Kentucky Strong-Motion Stations

One of our primary objectives in collecting strong-motion records in the Upper Mississippi Embayment is to determine the site effects within the frequency range of general engineering interest; i.e., 0.5 to 10 Hz. With the exception of VSAP, three methods were used in this study to estimate the site effects for strong-motion stations whose velocity profiles are shown in Figure 9. The three methods are the one-dimensional computer program SHAKE91 (Idriss and Sun, 1992), the horizontal-to-vertical spectral ratio (HVSR) of *S*-waves from earthquakes recorded at the stations, and the HVSR of ambient noise. At VSAP, where we have accelerometers at the top of the bedrock and at the surface, site effects were also estimated using the ratios of the ground motions measured at the two accelerometers.

Input parameters for SHAKE91 are G_{max}, γ_{max}, densities (ρ), sublayer thickness, and G-ϵ and γ-ϵ curves. ϵ is the shear strain. G_{max}, sublayer thicknesses, and the damping ratios were derived from the shear-wave velocity models developed for the individual strong-motion stations (Fig. 9), whereas Q_s is based the relationship:

$$Q_s = 0.08\ V_s + 6.99\ (\pm 12.10) \qquad (4)$$

(Wang *et al.*, 1994). The G-ϵ and γ-ϵ curves for clay, silt, and sand used in this study are standard curves provided in the SHAKE91 package (Idriss and Sun, 1992). For an input ground motion at the base of the soil columns shown in Figure 9, we used a cosine-tapered, band-limited (0.3 to 30 Hz) white-noise acceleration record, with a peak acceleration of 25 cm/s^2. Site effects defined as the ratio of the Fourier spectrum of the ground motions at the surface to the Fourier spectrum of the input ground motions at the base of the soil columns.

Site effects at the strong-motion stations shown in Figure 9 were also calculated from H/V ratios of a 6 s window of accelerograms at the station. The window was chosen so that it began shortly before the arrival of the *S*-wave in the accelerogram. Similar studies, with slight variations, by Lermo and Chávez-García (1993), Field and Jacob (1995), Lachet *et al.* (1996), Castro *et al.* (1997), Chávez-García *et al.* (1999), Triantafyllidis *et al.* (1999), and others have shown the success of H/V ratios in

determining the fundamental period at a sediment-filled site. Figure 10 is the strong-motion record obtained at VSAB for the May 27, 1995, western Tennessee earthquake. Indicated in the figure is the 6 s window used in the H/V analysis. The 6 s window used in our analysis was chosen because it excluded the *S*-to-*P* converted wave commonly seen in the vertical traces of ground motions in the New Madrid seismic zone (Chiu *et al.*, 1992). The windows were tapered with a 5% cosine filter, padded to 8,192 points, and the horizontal and vertical components were transformed into the frequency domain. Prior to taking the horizontal to vertical ratios, the transforms were smoothed using a running average of 0.4 Hz (17 samples). Only strong-motion records that clearly exhibited a signal-to-noise ratio greater than 3 were used. Since many of the accelerograms obtained to date are of 3.0 $m_{b,Lg}$ or smaller earthquakes, the signal-to-noise constraint limited the number of records that could be used.

The third technique used in this study for estimating site effects is generally referred to as Nakamura's (1989) technique. In this technique, it is assumed that the vertical component of ambient noise is relatively uninfluenced by sediments, and that by taking the ratio of the horizontal-to-vertical components of the ambient noise recordings, the resulting ratio can be used to identify the fundamental frequency of the resonant S-wave of the sediment. This method has been successfully used by Lermo and Chávez-García (1993), Field and Jacob (1995), and Seht and Wohlenberg (1999), among others. Bodin and Horton (1999) used this technique to estimate the fundamental period of resonance at sites along an east-west profile across that part of the Upper Mississippi Embayment in western Tennessee. They found that the fundamental period of resonance varied from ~1.5 s near the eastern edge of the embayment to ~4.6 s at Memphis, which is near the center of the embayment.

In our studies with Nakamura's (1989) technique, we used an engineering seismograph and a three-component Mark Products L-4-3D seismometer with a natural period of 1 s. The useable frequency range of our L-4-3D was 0.5 to 10 Hz; the signal was truncated in the field by an active filter at 12 Hz. Our objective was to check for resonances in the near-surface sediments caused by layering. In particular, we were interested in resonances of general engineering interest, which we defined as 0.5 to 10 Hz. Data at the sites in our study were recorded at a sampling interval of 4 ms.

Results

Figures 11a through 11f show the site effects for the six strong-motion stations discussed in this study based on the results from SHAKE91, the HVSR of the *S*-waves from accelerograms, and the HVSR of ambient noise. With the exception of COKY, there is a rough correlation between the HVSR of the *S*-waves from accelerograms recorded at the strong-motion stations and the general trend of the results obtained using SHAKE91 and the soil columns developed for the sites in this study. The next step in the study will be to adjust the damping in the soil layers to bring the results in SHAKE91 more into agreement with the HVSR of the *S*-wave results. Damping of the soil column as a whole will be compared to Q_S for the total soil column estimated from the high-frequency decay of the acceleration spectra of earthquakes recorded at the site (Anderson and Hough, 1984).

The general trends for the site effects at COKY using SHAKE91 and the HVSR of the *S*-waves from accelerograms recorded at the station (Fig. 11c), are distinctly different. We interpret this to mean that the *S*-wave model derived for the strong-motion station is substantially incorrect. Additional *P*- and *SH*-wave reflection and refraction data will be collected to check our velocity model.

SUMMARY

Because the thick layers of sediments in the Upper Mississippi Embayment, are expected to be a significant factor in damages resulting from an earthquake, site effects in the New Madrid seismic zone are of considerable importance. The purpose of this ongoing study is to determine the site effects at the University of Kentucky strong-motion stations in the Upper Mississippi Embayment (Fig. 2). Our approach to determining the site effects at the strong-motion staions is to utilize as many field and modeling techniques as possible at each site, and to compare the results as means of improving the interpretations.

REFERENCES CITED

Anderson, J.G., and Hough, S.E. (1984). "A Model for the Shape of the Fourier Amplitude Spectrum of Acceleration at High Frequencies," *Bulletin of the Seismological Society of America.* Vol. 74, 1969-1993.

Anderson, J.G., Lee,Y., Zeng, Y., and Day, S. (1996). "Control of Strong Motion by the Upper 30 Meters," *Bulletin of the Seismological Society of America.* Vol. 86, 1749-1759.

Bard, P.-Y., and Chávez-Garciá, F.J. (1993). "On the Decoupling of Surfical Sediments from Surrounding Geology at Mexico City," *Bulletin of the Seismological Society of America.* Vol. 83, 1797-1991.

Bodin, P., and Horton, S. (1999). "Broadband Microtremor Observation of Basin Resonance in the Mississippi Embayment, Central US," *Geophysical Research Letters.* Vol. 26, 903-906.

Castro, R.R., Mucciarelli, M., Pacor, F., and Petrungaro, C. (1997). "*S*-Wave Site-Response Estimates Using Horizontal-to-Vertical Spectral Ratios," *Bulletin of the Seismological Society of America.* Vol. 87, 256-260.

Catchings, R.D. (1999). "Regional *Vp, Vs, Vp/Vs*, and Poisson's Ratios across Earthquake Source Zones from Memphis, Tennessee, to St. Louis, Missouri," *Bulletin of the Seismological Society of America.* Vol. 89, 1591-1605.

Chávez-Garciá, F.J., Stephenson, W.R., and Rodríguez, M. (1999). "Lateral Propagation Effects Observed at Parkway, New Zealand, a Case History to Compare 1D Versus 2D Site Effects," *Bulletin of the Seismological Society of America.* Vol. 89, 718-732.

Chiu, J.M., Johnston, A.C., and Yang, Y.T. (1992). "Imaging the Active Faults of the Central New Madrid Seismic Zone Using PANDA Array Data," *Seismological Research Letters.* Vol. 63, 375-393.

Cranswick, E., King, K., Carver, D., Worley, D., Williams, R., Spudich, P., and Banfill, R. (1990). "Site Response across Downtown Santa Cruz, California," *Geophysical Research Letters.* Vol. 17, 1793-1796.

Federal Emergency Management Agency (1997). 1997 NEHRP Recommended Provisions for Seismic Regulations for New Buildings. Washington D.C., developed by the Building Seismic Safety Council for the Federal Emergency Management Agency.

Field, E.H., and Jacob, K.H. (1995). "A Comparison and Test of Various Site-Response Estimation Techniques, Including Three that Are Not Reference-Site Dependent," *Seismological Research Letters.* Vol. 85, 1127-1143.

Gao, F.C., Chiu, J.M., Schweig, E., and Street, R. (in press). "Three-Dimensional P- and S-Wave Velocity Structure in the Sedimentary Basin of the Upper Mississippi Embayment," *Engineering Geology.*

Harris, J., Street, R., Kiefer, J., Allen, D., and Wang, Z. (1994). "Modeling Site Response in the Paducah, Kentucky, Area," *Earthquake Spectra.* Vol. 10, 519-538.

Hartzell, S., Cranswick, E., Frankel, A., Carver, D., and Meremonte, M. (1997). "Variability in Site Response in the Los Angeles Urban Area," *Bulletin of the Seismological Society of America.* Vol. 87, 1377-1400.

Hatherly, P.J. (1986). "Attenuation Measurements on Shallow Seismic Refraction Data," *Geophysics*. Vol. 51, 250-254.

Hays, W.W. (1980). "Procedures for Estimating Earthquake Ground Motions," *U.S. Geological Survey Professional Paper 114*.

Idriss, I.M., and Sun, J.L. (1992). *User's Manual for SHAKE91*, Center for Geotechnical Modeling, Department of Civil and Environmental Engineering, University of California, Davis.

Kramer, S.L. (1996). *Geotechnical Earthquake Engineering*, Prentice-Hall, Inc., Upper Saddle River, N.J., 653 p.

Lachet, C., Hatzfeld, D., Bard, P.-Y., Theodulidis, N., Papaioannou, C., and Savvaidis, A. (1996). "Site Effects and Microzonation in the City of Thessaloniki (Greece), Comparison of Different Approaches," *Bulletin of the Seismological Society of America*. Vol. 86, 1692-1703.

Lermo, J., and Chávez-García, F.J. (1993). "Site Effects Evaluation Using Spectral Ratios with Only One Station," *Bulletin of the Seismological Society of America*. Vol. 83, 1574-1594.

Liu, H.-P., Hu, Y., Dorman, J., Chang, T.-S., and Chiu, J.-M. (1997). "Upper Mississippi Embayment Shallow Seismic Velocities Measured In Situ," *Engineering Geology*. Vol. 46, 313-330.

Mok, Y.J., Sanchez-Salinero, I., Stoke, K.H., and Rosset, J.M. (1988). "In-Situ Damping Measurements by Crosshole Seismic Methods," *Earthquake Engineering and Soil Dynamics II - Recent Advances in Ground Motion Evaluation, Proc. of the A.S.C.E. Specialty Conference*, June 27-30, Park City, Utah, 103-155.

Nakamura, Y. (1989). "A Method for Dynamic Characteristics Estimation of Subsurface Using Microtremor on the Ground Surface," *QR Railway Technical Research Institute*. Vol. 30, 1.

Nuttli, O.W. (1973). "Seismic Wave Attenuation and Magnitude Relations for Eastern North America," *Journal of Geophysical Research*. Vol. 78, 876-885.

Reiter, L. (1990). *Earthquake Hazard Analysis: Issues and Insights*, Columbia University Press, New York, 254 p.

Ricker, N. (1953). "The Form and Law of Propagation of Seismic Wavelets," *Geophysics*. Vol. 18, 10-40.

Seht, M.I.-V., and Wohlenberg, J. (1999). "Microtremor Measurements Used to Map Thickness of Soft Sediments," *Bulletin of the Seismological Society of America*. Vol. 89, 250-259.

Seismic Image Software Ltd. (1996). VISTA 7.0 Notes, 477 pp.

Street, R., Woolery, E., Wang, Z., and Harris, J. (1995). "A Short Note on Shear-Wave Velocities and Other Site Conditions at Selected Strong-Motion Stations in the New Madrid Seismic Zone," *Seismological Research Letters*. Vol. 66, 56-63.

Street, R., Wang, Z., Woolery, E., Hunt, J., and Harris, J. (1997). "Site Effects at a Vertical Accelerometer Array near Paducah, Kentucky," *Engineering Geology*. Vol. 46, 369-367.

Street, R., Woolery, E., Wang, Z. (in press). "NEHRP Soil Classifications for Estimating Site-Dependent Seismic Coefficients in the Upper Mississippi Embayment," *Engineering Geology*.

Sykora, D.W., and Davis, J.J. (1993). "Site-Specific Earthquake Response Analysis for Paducah Gaseous Diffusion Plant, Paducah, Kentucky," U.S. Army Corps of Engineers, Waterways Experiment Station, *Miscellaneous Paper GL-93-14*, 116 pp.

Triantafyllidis, P., Hatzidimitriou, P.M., Theodulidis, N., Suhadolc, P., Papazachos, C., Raptakis, D., and Lontzetidis, K. (1999). "Site Effects in the City of Thessaloniki (Greece) Estimated from Acceleration Data and 1D Local Soil Profiles," *Bulletin of the Seismological Society of America*. Vol. 89, 521-537.

Wald, L.A., and Mori, J. (2000). "Evaluation of Methods for Estimating Linear Site-Response Amplifications in the Los Angeles Region," *Bulletin of the Seismological Society of America*. Vol. 90(6B), S32-S42.

Wang, Z., Street, R., Harris, J., and Woolery, E. (1994). "Q_s Estimation for Unconsolidated Sediments Using First-Arrival SH-Wave Critical Refractions," *Journal of Geophysical Research*. Vol. 90, 13543-13551.

Wheeler, R., Rhea, S., and Dart, R.L. (1994). "Map Showing Structure of the Mississippi Valley Graben in the Vicinity of New Madrid, Missouri," U.S. Geological Survey, Miscellaneous Field Studies Map MF-2264-D.

Williams, R.A., Stephenson, W.J., Frankel, A.D., and Odum, J.K., (1999). "Surface Seismic Measurements of Near-Surface *P*- and *S*-Wave Seismic Velocities at Earthquake Recording Stations, Seattle, Washington," *Earthquake Spectra*. Vol. 15, 565-584.

Williams, R.A., Stephenson, W.J., Frankel, A.D., Cranswick, E., Meremonte, M.E., and J.K. Odum (2000). "Correlation of 1- to 10-Hz Earthquake Resonances with Surface Measurements of *S*-wave Reflections and Refractions in the Upper 50 m," *Bulletin of the Seismological Society of America*. Vol. 90, 1323-1331.

Williams, R., Wood, S., Stephenson, W., Odum, J., and Street, R. (in press). "Surface Seismic-Refraction/Reflection Measurements of *P*- and *S*-Wave Velocities, Memphis, Tennessee," *Engineering Geology*.

Woolery, E., and Street, R. (in press). "3D Near-Surface Soil Response of Earthquake Engineering Interest from H/V Ambient Noise Ratios," *Journal of Soil Dynamics and Earthquake Engineering*.

TABLE 1

Station	Location °N/°W	Instrumentation[a]	Installation
COKY	36.763/89.108	SSA-1/K-2	Free-field
HNBK[b]	36.333/89.296	SSA-1	Free-field
HIKY	36.551/89.183	SSA-1	Concrete floor[c]
HIKY2	36.554/89.170	K-2	Free-field and -21 m
LATN	36.125/89.399	SSA-1/K-2	Free-field
RIDG[b]	36.264/89.481	K-2	Free-field and -35 m
RLTN	36.396/89.320	SSA-2	Free-field
VSAB	36.528/89.509	Kentucky Box	Free-field and -99 m
		SSA-2	Free-field
VSAP	37.124/88.822	SSR-1/SSA-1	Free-field and -41 m -102 m
WIKY	36.971/89.092	SSA-1	Free-field

a. Strong-motion instrumentation are registered trademarks of Kinemetrics, Inc.
b. Strong-motion stations HNBK and RIDG were installed by Lamont Doherty Observatory in 1988. In January 2001, the University of Kentucky took over the operation and maintenance of the two strong-motion stations.
c. The SSA-1 at HIKY was attached to the concrete floor of the National Guard Armory at the northwest corner of the building.

TABLE 2

Year	Record[1]	No.	Epicenter °N/°W	Mag[2] $m_{b,Lg}$	Dist (km)	PHA cm/s^2	PHV cm/s	PVA cm/s^2	PVV cm/s
1990	SE26H	1	37.16/89.58	4.5	76	2.98	.075	2.47	.044
	SE26W	2	37.16/89.58	4.5	48	32.3	1.71	18.5	.355
1991	MY04C	3	36.56/89.82	4.5	67	1.88	.042	1.34	.024
	MY04H	4	36.56/89.82	4.5	57	1.43	.050	1.88	.022
	JE07C	5	36.75/89.27	2.5	14	2.43	.020	1.46	.013
	JY07H	6	36.66/91.65	3.8	220	0.43	.016	0.35	.008
	DE29C	7	36.69/89.12	2.9	8	1.24	.012	0.46	.005
1992	AP30C	8	36.83/90.36	2.8	111	0.48	.007	0.24	.003
	MY11C	9	36.82/88.98	2.7	13	1.13	.021	0.81	.011
	AU18P-41	10	37.12/88.85	2.0	3	20.6	.117	5.27	.046
	OC02P-41	11	37.12/88.76	2.0	8	4.07	.02	1.52	.01
	OC02P	12	37.12/88.76	2.0	8	8.03	.06	3.07	.03
1993	JA08H	13	35.93/90.03	3.5	102	4.34	.31	1.83	.14
	FE06H	14	36.66/89.73	3.3	50	9.69	.35	4.22	.16
	FE06R	15	36.66/89.73	3.3	47	2.84	.03	4.97	.04
	FE06W	16	36.66/89.73	3.3	66	2.49	.03	1.81	.01
	FE24L	17	36.16/89.46	2.7	7	5.23	.08	8.51	.09
	MR02C	18	36.67/89.49	3.0	35	1.30	.03	1.32	.01
	MR02H	19	36.67/89.49	3.0	30	2.06	.03	1.61	.01
	MR02B-102	20	36.67/89.49	3.0	16	7.79	.07	3.34	.03
	MR02B	21	36.67/89.49	3.0	16	10.5	.11	13.6	.11
	MR31C	22	36.80/89.43	3.1	29	3.40	.04	2.78	.03
	MR31H	23	36.80/89.43	3.1	35	1.26	.02	1.99	.02
	AP02W	24	37.01/89.00	2.8	9	5.97	.04	1.58	.02
	AP02W	25	37.02/89.02	2.8	8	3.15	.04	3.26	.02
	AP28C	26	36.20/89.44	3.7	68	1.32	.03	1.05	.02
	AP28H	27	36.20/89.44	3.7	45	0.94	.02	0.93	.01
	AP28L	28	36.20/89.44	3.7	9	13.8	.31	14.8	.16
	JY05L	29	36.08/89.32	1.9	9	2.04	.02	4.47	.04
	AU05C	30	36.01/89.89	3.0	108	0.73	.01	0.47	.01
1994	FE05H	31	37.37/89.19	4.2	91	5.13	.05	9.91	.04
	FE05R	32	37.37/89.19	4.2	108	2.75	.09	2.53	.06
	FE05P-102	33	37.37/89.19	4.2	42	5.53	.07	2.57	.04
	FE05P-41	34	37.37/89.19	4.2	42	13.5	.19	5.38	.08
	FE05P	35	37.37/89.19	4.2	42	21.8	.34	9.18	.16
	FE05W	36	37.37/89.19	4.2	45	6.05	.13	4.55	.07
	MR21C	37	36.86/89.17	3.1	12	6.79	.12	3.90	.06
	JE04P-102	38	37.08/88.86	2.0	6	5.46	.03	2.39	.01
	JE04P-41	39	37.08/88.86	2.0	6	11.6	.07	2.00	.01
	JE04P	40	37.08/88.86	2.0	6	12.8	.09	5.15	.04

	SE26C	41	36.96/88.92	3.6	28	3.18	.06	1.99	.02
	SE26H	42	36.96/88.92	3.6	51	0.86	.016	0.79	.009
	SE26W	43	36.96/88.92	3.6	15	9.41	.12	34.0	.29
	DE31B	44	36.49/89.55	2.0	5	3.05	.051	7.75	.041
1995	JA22B	45	36.60/89.35	1.5	16	2.88	.027	3.86	.024
	JA31B	46	36.51/89.56	2.3	5	1.76	.031	2.77	.029
	AP15C	47	36.76/89.11	1.9	0	1.96	.018	1.64	.014
	AP24B	48	36.68/89.58	2.3	18	1.47	.025	2.68	.026
	AP27B	49	36.70/89.49	2.8	19	4.17	.066	14.2	.126
	MY27C	50	36.18/89.44	3.8	70	2.75	.035	1.58	.018
	MY27H	51	36.18/89.44	3.8	47	1.60	.046	1.53	.024
	MY27L	52	36.18/89.44	3.8	7	19.0	.413	17.3	.202
	MY27R	53	36.18/89.44	3.8	26	5.40	.139	6.96	.094
	MY27B	54	36.18/89.44	3.8	39	7.95	.122	10.4	.110
	MY27W	55	36.18/89.44	3.8	93	1.52	.027	7.04	.058
	JE06C	56	36.22/89.47	3.2	68	0.79	.011	0.70	.010
	JE06H	57	36.22/89.47	3.2	45	0.61	.012	0.61	.007
	JE06L	58	36.22/89.47	3.2	12	6.15	.135	3.90	.045
	JE06R	59	36.22/89.47	3.2	24	2.02	.059	3.95	.040
	JE06B	60	36.22/89.47	3.2	34	3.59	.054	4.34	.056
	JE29B	61	36.59/89.77	2.8	24	6.21	.072	5.63	.059
	JY20B	62	36.55/89.58	2.7	7	29.4	.312	20.4	.223
	AU17L	63	36.22/89.33	3.0	12	5.82	.111	7.22	.090
	AU25L	64	36.19/89.47	2.5	10	5.57	.059	2.66	.032
	OC04B	65	36.42/89.48	1.9	12	4.45	.042	4.83	.040
	NO24B	66	36.55/89.81	2.8	27	6.48	.071	6.54	.060
	DE20B	67	36.52/89.61	2.2	9	16.9	.200	36.5	.200
1996	FE17B	68	36.52/89.68	2.4	15	14.3	.254	20.2	.162
	NO29C	69	35.90/89.97	4.3	122	2.72	.059	2.14	.071
	NO29H	70	35.90/89.97	4.3	100	5.57	.208	2.34	.042
	NO29R	71	35.90/89.97	4.3	80	5.14	.113	6.15	.115
	NO29B	72	35.90/89.97	4.3	81	37.9	1.07	50.3	1.19
	NO29W	73	35.90/89.97	4.3	142	3.62	.087	5.02	.132
	NO29R	74	36.34/89.40	3.5	9	2.20	.063	2.21	.035
	NO29B	75	36.34/89.40	3.5	23	3.76	.055	3.48	.049
1997	SE24B	76	36.65/89.73	3.2	24	2.45	.023	2.83	.022
	SE27L	77	36.18/89.41	3.2	6	4.61	.093	3.92	.025
	DE02B	78	36.57/89.51	2.7	5	212.	3.32	330.	2.88
1998	JA09B	79	36.56/89.52	2.2	4	80.3	1.01	68.7	.696
	FE12B	80	36.14/89.71	3.0	46	2.06	.037	1.70	.025
	FE19B	81	36.54/89.57	2.7	6	21.3	.479	22.7	.215
	FE19B	82	36.48/89.56	1.9	7	7.55	.087	9.42	.079
	FE26B	83	36.36/89.58	2.5	20	24.1	.316	21.6	.171
	MR13B	84	36.26/89.61	2.0	31	5.14	.049	8.57	.040
	MR21B	85	36.15/89.47	1.6	42	2.69	.029	3.54	.030
	AP08B	86	36.92/89.02	3.0	61	2.15	.036	3.01	.034

	AP09B	87	36.43/89.53	2.7	11	6.73	.085	7.22	.066
	JY15B	88	36.69/89.52	3.1	18	22.1	.350	18.3	.295
1999	MR18B	89	36.53/89.61	2.3	9	15.7	.175	10.9	.094
	AP16B	90	36.46/89.52	1.6	8	4.34	.044	5.11	.039
	JE22B	91	36.50/89.53	2.1	4	4.90	.069	13.9	.084
	AU01B	92	36.53/89.54	2.3	3	8.24	.140	9.40	.081
	AU23L	93	36.26/89.52	3.2	18	4.26	.075	2.23	.025
	AU23B	94	36.26/89.52	3.2	30	9.40	.136	7.70	.064
	SE03B	95	36.42/89.52	2.3	12	5.71	.068	8.33	.093
	SE11B	96	36.46/89.55	2.1	8	8.04	.113	6.44	.047
	SE13B	97	36.48/89.48	2.6	6	4.67	.084	5.84	.094
	SE15B	98	36.56/89.48	2.5	4	70.5	.687	97.4	.589
	OC21L	99	36.49/91.02	3.9	150	1.71	.042	0.68	.014
	OC21B	100	36.49/91.02	3.9	134	4.23	.108	4.13	.067
	NO11B	101	36.82/89.54	2.5	0	2.83	.041	8.99	.083
	DE09B	102	36.58/89.60	2.4	10	11.2	.142	7.4	.063
2000	JA13L	103	36.13/89.41	2.2	1	2.20	.042	4.77	.043
	JA27B	104	36.53/89.49	2.8	2	41.9	.775	26.4	.195
	FE22B	105	36.55/89.70	2.2	17	3.92	.055	3.60	.033

1. The five letter code used to identify the strong-motion recordings consists of two letters for the month, two numbers for the day, and a single letter for the strong-motion station. The abbreviations for months and stations are as follows:

   Months: JA=January, FE=February, MR=March, AP=April, MY=May, JE=June, JY=July, AU=August, SE=September, OC=October, NO=November, and DE=December.
   Stations: B=VSAB, C=COKY, H=HIKY, G=RIDG, K=HNBK, L=LATN, P=VSAP, R=RLTN, and W=WIKY.

2. Lg-wave magnitude scale (Nuttli, 1973).

GUIDELINES FOR ANALYZING AND MITIGATING SOIL LIQUEFACTION

Marshall Lew, Ph.D., G.E.[1]

ABSTRACT

Liquefaction is a seismic hazard that must be evaluated in regions of moderate to high seismicity. The combination of the presence of active seismic faults, young loose alluvium, and shallow ground water are the ingredients that are found in many seismically active areas of the United States, and not just in California. Because of the devastating effects of liquefaction in the 1989 Loma Prieta earthquake, among other earthquake effects, the state of California, through the Seismic Hazards Mapping Act of 1990, has mandated that liquefaction hazard be determined for new construction. In addition, the Uniform Building Code since 1994 has provisions requiring the determination of liquefaction potential and mitigation for the consequences, such as settlement, flow slides, lateral spreading, ground oscillation, sand boils, and loss of bearing capacity. The state of practice in the new field of "liquefaction geotechnical engineering" has now evolved that there are field exploration methods and analytical techniques to estimate the liquefaction potential with a good degree of confidence. In addition, the ability to evaluate the possible consequences arising from the occurrence of liquefaction triggering in the soils has also developed nicely. There are, however, some areas that still need further research. Mitigation techniques for liquefaction have become more commonplace and confidence in these techniques have been increased based on relatively successful performance of improved sites in several past major earthquakes. The purpose of this paper is to inform the practitioners of "liquefaction geotechnical engineering" about the present state-of-practice in liquefaction analysis and mitigation, and to increase his or her knowledge about the options available to mitigate the liquefaction hazard to structures if potential for liquefaction exists.

INTRODUCTION

Liquefaction is a process by which sediments below the water table temporarily lose stiffness and strength and behave as a viscous liquid rather than a solid. The types of sediments most susceptible are clay-free deposits of sand and silts; occasionally, gravel liquefies. The actions in the soil which produce liquefaction are as follows: seismic waves, primarily shear waves, passing through saturated granular layers, distort the granular structure, and cause loosely packed groups of particles to progressively densify. Densification increases the pore-water pressure between the grains if drainage cannot occur. If the pore-water pressure rises to a level approaching the weight of the overlying soil, the granular layer temporarily behaves as a viscous liquid rather than a solid and thus, liquefaction occurs.

In response to large earthquake losses, the State of California has enacted a series of legislative acts in the hope of reducing future earthquake-related losses. In 1990, the Seismic Hazards Mapping Act of 1990 became California law in 1991. The purpose of the Act is to protect public safety from the effects of strong ground shaking, liquefaction, landslides, or other ground failure, or other hazards caused by earthquakes. The Seismic Hazards Mapping Act is a companion and complement to the 1972 Alquist-Priolo Earthquake Fault Zoning Act, enacted after the 1971 San Fernando earthquake, which addresses only surface fault-rupture hazards.

As part of the implementation of the Seismic Hazards Mapping Act, the California Department of Conservation, Division of Mines and Geology published Special Publication 117 (SP 117), in 1997, which presents guidelines for evaluation of seismic hazards other than surface fault-rupture and for recommending mitigation measures. The guidelines in SP 117 provide, among other things, definitions, caveats, and general considerations for earthquake hazard mitigation, including soil liquefaction. It should also be noted that Section 1804.5 of the Uniform Building Code (International Conference of Building Officials, 1994

---

[1] Senior Principal and Vice President, Law/Crandall, a LAWGIBB Group Member, Los Angeles, California

and 1997) also requires an evaluation of the liquefaction potential of a site for new construction in zones of high seismicity.

SP 117 provides a summary overview of analysis and mitigation of liquefaction hazards. The document also provide guidelines for the review of site-investigation reports by regulatory agencies who have been designated to enforce the Seismic Hazards Mapping Act. However, building officials in Southern California desired to have more definitive guidance to aid their agencies in the review of geotechnical investigations that must address seismic hazards and mitigations. Specifically, the building officials sought assistance in the development of recommendations for dealing with earthquake-induced liquefaction and landslide hazards.

An "Implementation Committee" was convened under the auspices of the Southern California Earthquake Center (SCEC) at the University of Southern California. It was decided to address the issue of liquefaction first, with the landslide hazards to be addressed after the liquefaction implementation guidelines had been completed. (At the time of this writing, a draft report on landslide hazards has been published and is in the review process.) The Liquefaction Implementation Committee has participating members from the practicing professional, academic, and regulatory communities. This Implementation Committee published a technical report through SCEC entitled "Recommended Procedures for Implementation of DMG Special Publication 117 – Guidelines for Analyzing and Mitigating Liquefaction Hazard in California" (Martin and Lew, 1999)

The purpose of the SCEC report was two-fold. The first purpose is to present information that will be useful and informative to Building Officials so that they can properly and consistently review and approve geotechnical reports that address liquefaction hazard and mitigation. The second purpose is to provide a broad-brush survey of some of the most common methods of analyses and mitigation techniques that will be useful to geotechnical engineers, engineering geologists, building officials, and other affected parties including owners, architects, and structural engineers. This paper is intended to summarize that information that should be known by geotechnical engineers and engineering geologists about the current state-of-the-practice in liquefaction hazard analysis and mitigation.

LIQUEFACTION HAZARD ZONES

The State Geologist of California is required under the Seismic Hazards Mapping Act to delineate various "seismic hazard zones," including those for liquefaction. The criteria for delineating Liquefaction Zones were developed by the Seismic Hazards Mapping Act Advisory Committee for the California State Mining and Geology Board in 1993, and are contained in a document entitled "Guidelines For Delineating Seismic Hazard Zones" (CDMG, 1999). Under those criteria, Liquefaction Zones are areas meeting one or more of the following:

1. Areas where liquefaction has occurred during historical earthquakes.
2. Areas of uncompacted or poorly compacted fills containing liquefaction-susceptible materials that are saturated, nearly saturated, or may be expected to become saturated.
3. Areas where sufficient existing geotechnical data and analyses indicate that the soils are potentially susceptible to liquefaction.
4. For areas where geotechnical data are lacking or insufficient, zones are delineated using one or more of the following criteria:
    a) Areas containing soil of late Holocene age (less than 1,000 years old, current river channels and their historical flood plains, marshes, and estuaries) where the ground water is less than 40 feet deep and the anticipated earthquake peak ground acceleration (PGA) having a 10% probability of being exceeded in 50 years is greater than 0.1g.
    b) Areas containing soils of Holocene age (less than 11,000 years old) where the ground water is less than 30 feet below the surface and the PGA (10% probability of exceedance in 50 years) is greater than 0.2g.

c) Areas containing soils of latest Pleistocene age (11,000 to 15,000 years before present) where the ground water is less than 20 feet below the surface and the PGA (10% probability of exceedance in 50 years) is greater than 0.3g.

It should be noted that the ground-water levels used for the purposes of zoning are the historically shallowest (highest) ground-water levels using the results of ground-water studies. Sediments deposited on canyon floors are presumed to become saturated during wet seasons and shallow water conditions can occur in narrow stream valleys that can receive an abundance of water runoff from canyon drainages and tributary streams during periods of high precipitation.

Seismic Hazard Zones for potentially liquefiable soils within a region based on these criteria are presented on 7.5-minute quadrangle sheet maps at a scale of 1:24,000. The Seismic Hazard Zone Maps are developed using a combination of historical records, field observations, and computer-mapping technology. These maps may not identify all areas that have potential for liquefaction; a site located outside of a zone of required investigation is not necessarily free from liquefaction hazard. The zones do not always include lateral spread run-out areas.

Seismic Hazard Zone maps are in the process of being released by the California Department of Conservation, Division of Mines and Geology. The maps present zones of identified landslide and liquefaction hazards as determined by the criteria established by the Seismic Hazards Mapping Act Advisory Committee. Currently, these maps are available for portions of southern California (mostly Los Angeles and Orange Counties) and parts of the San Francisco Bay region.

PRELIMINARY SCREENING FOR LIQUEFACTION

The SP 117 Guidelines state that an investigation of the potential seismic hazards at a site can be performed in two steps: (1) a screening investigation and (2) a quantitative evaluation. The screening investigation should include a review of relevant topographic, geologic and soils engineering maps and reports, aerial photographs, ground-water contour maps, water well logs, agricultural soil survey maps, the history of liquefaction in the area, and other relevant published and unpublished reports. The purpose of the screening investigations for sites within zones of required study is to eliminate sites that have no potential or low potential for liquefaction.

The following screening criteria may be applied to determine if further quantitative evaluation of liquefaction hazard potential is not required:

- If the estimated maximum-past-, current-, and maximum-future-ground-water-levels (i.e., the highest ground-water level applicable for liquefaction analyses) are determined to be deeper than 50 feet below the existing ground surface or proposed finished grade (whichever is deeper), liquefaction assessments are not required.
- If "bedrock" or similar lithified formational material underlies the site, those materials need not be considered liquefiable and no analysis of their liquefaction potential is necessary.
- If there are prior subsurface explorations and if the corrected standard penetration blow count, $(N_1)_{60}$, is greater than or equal to 30 in all samples with a sufficient number of tests, additional qualitative liquefaction assessments may not required. If cone penetration test soundings are made, the corrected cone penetration test tip resistance, q_{c1N}, should be greater than or equal to 160 in all soundings in sand materials.
- If clayey soil materials were encountered during prior site exploration, those materials may be considered non-liquefiable. For purposes of this screening, clayey soils are those that have a clay content (particle size <0.005 mm) greater than 15 percent. However, based on the so-called "Chinese Criteria," (Seed and Idriss, 1982) clayey soils having all of the following characteristics may be susceptible to severe strength loss:
  - Percent finer than 0.005 mm less than 15 percent

- Liquid Limit less than 35
- Water content greater than 0.9 x Liquid Limit

If the screening investigation clearly demonstrates the absence of liquefaction hazards at the project site and the lead agency technical reviewer concurs, the screening investigation will satisfy the site investigation report requirement for liquefaction hazards. If not, a quantitative evaluation will be required to assess the liquefaction hazards.

FIELD INVESTIGATIONS FOR LIQUEFACTION HAZARD EVALUATION

Field (or geotechnical) investigations are routinely performed for new projects as part of the normal development and design process. Geologic site reconnaissance and subsurface explorations are normally performed as part of the field exploration program, even when liquefaction does not need to be investigated.

Geologic Reconnaissance

Geologic research and reconnaissance are important to provide information to define the extent of unconsolidated deposits that may be susceptible to liquefaction. Such information should be presented on geologic maps and cross sections, and provide a description of the formations present at the site that includes the nature, thickness, and origin of Quaternary deposits with liquefaction potential. There also should be an analysis of ground-water conditions at the site that includes the highest recorded water level and the highest water level likely to occur under the most adverse foreseeable conditions in the future.

During the field investigation, the engineering geologist should map the limits of unconsolidated deposits with liquefaction potential. Liquefaction typically occurs in cohesionless silt, sand, and fine-grained gravel deposits of Holocene to late Pleistocene age in areas where the ground water is shallower than about 50 feet. Common geologic settings include unlithified sediments in coastal regions, bays, estuaries, river floodplains and basins, areas surrounding lakes and reservoirs, and wind-deposited dunes and loess. In many coastal regions, liquefiable sediments occupy back-filled river channels that were excavated during Pleistocene low stands of sea level, particularly during the most recent glacial stage. Among the most easily liquefiable deposits are beach sand, dune sand, and clean alluvium that were deposited following the rise in sea level at the start of the Holocene age, about 11,000 years ago.

Shallow ground water may exist for a variety of reasons, which may be of natural and or man-made origin. Ground water may be shallow because the ground surface is only slightly above the elevation of the ocean, a nearby lake or reservoir, or the sill of a basin. Another concern is man-made lakes and reservoirs that may create a shallow ground-water table in young sediments that were previously unsaturated.

Subsurface Explorations

Subsurface explorations are routinely performed using borings; cone penetration tests (CPTs) are also becoming more commonplace to supplement or replace borings. The scope of the field exploration program will depend on the type of development or building planned. It might be expected that a high-rise building may require an array of closely spaced exploratory borings (and/or CPTs), whereas a large housing tract will have an array of exploratory borings or pits (and/or CPTs) that may be more distantly spaced.

There are various methods for evaluation of liquefaction potential. The most popular and common methods relate in situ soil indices, such as the standard penetration test (SPT) or the cone penetration test, to observed liquefaction occurrence or non-occurrence during major earthquakes. These indices can generally be routinely and economically obtained. In the case of silts or sandy silts, liquefaction evaluation may require the cyclic testing of soil samples, which can be obtained by high quality sampling techniques during the field exploration program.

The normal field exploration program may need to be expanded to evaluate the potential for liquefaction. Additional and/or deeper SPT-borings and CPTs may be warranted, or the field exploration program may be augmented with other forms of exploration. The exploration program should be planned to determine the soil stratigraphy, ground-water level, and indices that could be used to evaluate the potential for liquefaction by either in situ testing or by laboratory testing of soil samples. Good engineering judgment will need to be exercised in determining the exploration program needed to obtain adequate and sufficient geotechnical information to evaluate the potential for liquefaction. An inadequate exploration program could lead to either overly conservative or unconservative conclusions and actions.

Depth of Analysis for Liquefaction Evaluation

Traditionally, a depth of 50 feet (about 15 m) has been used as the depth of analysis for the evaluation of liquefaction. The Seed and Idriss EERI Monograph on "Ground Motions and Soil Liquefaction During Earthquakes" (1982) does not recommend a minimum depth for evaluation, but notes 40 feet (12 m) as a depth to which some of the numerical quantities in the "simplified procedure" can be estimated reasonably. Liquefaction has been known to occur during earthquakes at deeper depths than 50 feet (15 m) given the proper conditions such as low-density granular soils, presence of ground water, and sufficient cycles of earthquake ground motion.

Experience has shown that the 50-foot (15 m) depth may be adequate for the evaluation of liquefaction potential in most cases, however, there may be situations where this depth may not be sufficiently deep.

It is recommended that a minimum depth of 50 feet (15 m) below the existing ground surface or lowest proposed finished grade (whichever is lower) be investigated for liquefaction potential. Where a structure may have subterranean construction or deep foundations (e.g., caissons or piles), the depth of investigation should extend to a depth that is a minimum of 20 feet (6 m) below the lowest expected foundation level (e.g., caisson bottom or pile tip) or 50 feet (15 m) below the existing ground surface or lowest proposed finished grade, whichever is deeper.

If, during the subsurface investigation, the indices to evaluate liquefaction indicate that the liquefaction potential may extend below that depth, the exploration should be continued until a significant thickness (at least 10 feet or 3 m, to the extent possible) of nonliquefiable soils are encountered.

Liquefaction Assessment by Use of the Standard Penetration Test (SPT)

One of the most widely used semi-empirical procedures for estimation of liquefaction potential utilizes Standard Penetration Test (SPT) N-values to estimate a soil's liquefaction resistance.

Primarily because of their inherent variability, sensitivity to test procedure, and uncertainty, SPT N-values have the potential to provide misleading assessments of liquefaction hazard, if the tests are not performed carefully. The engineer who wants to utilize the results of SPT N-values to estimate liquefaction potential should become familiar with the details of SPT sampling as given in ASTM D 1586 (ASTM, 2000a) and ASTM D 6066-96 (ASTM, 2000b) in order to avoid, or at least reduce, some of the major sources of error.

The semi-empirical procedures that relate SPT N-values to liquefaction resistance use an SPT blow count that is normalized to an effective overburden pressure of 100 KPa (or 1.044 ton per square foot). This normalized SPT blow count is denoted as N_1, which is obtained by multiplying the uncorrected SPT blow count by a depth correction factor, C_N. A correction factor may be needed to correct the blow count for an energy ratio of 60%, which has been adopted as the average SPT energy for North American geotechnical practice. Additional correction factors may need to be applied to obtain the corrected normalized SPT N-value, $(N_1)_{60}$. It has been suggested that the corrections should be applied according to the following formula:

$$(N_1)_{60} = N_m C_N C_E C_B C_R C_S$$

Where N_M = measured standard penetration resistance
C_N = depth correction factor
C_E = hammer energy ratio (ER) correction factor
C_B = borehole diameter correction factor
C_R = rod length correction factor
C_S = correction factor for samplers with or without liners

A useful reference, which discusses energy delivery and the SPT, is Seed et al. (1985). A summary of the recommended procedure for performing the SPT is given in Table 1. Table 2 presents the correction factors for the field SPT "N" values.

The SPT tests should be performed to investigate the liquefaction potential of the soils to the minimum depths recommended earlier. However, if the SPT tests indicate that there is a potential for liquefaction to extend below the minimum depth, SPT tests should be continued until a significant thickness of nonliquefiable soils are encountered. This thickness is recommended to be at least 10 feet or 3 meters.

SPT Testing in Gravel Deposits

SPT tests are difficult, at best, to perform in gravel deposits. Because of the coarse size of the particles, as compared to the size of the sampler, those deposits have the potential to provide misleadingly high N-values.

An alternative in gravel deposits is to obtain Becker Hammer blow counts, which have been correlated to the standard penetration test blow count. Another alternative would be to measure the shear wave velocities of the gravel deposits to determine the liquefaction potential.

Table 1. Recommended SPT Procedure

Borehole size	66 mm < Diameter < 115 mm
Borehole support	Casing for full length and/or drilling mud
Drilling	Wash boring; side discharge bit Rotary boring; side or upward discharge bit Clean bottom of borehole*
Drill rods	A or AW for depths of less than 15 m N or NW for greater depths
Sampler	Standard 51 mm O.D. +/- 1 mm 35 mm I.D. +/- 1 mm >457 mm length
Penetration Resistance	Record number of blows for each 150 mm; N = number of blows from 150 to 450 mm penetration
Blow count Rate	30 to 40 blows per minute

* Maximum soil heave within casing <70 mm

Table 2. Corrections to Field SPT N-Values (modified from Youd and Idriss, 1997)

Factor	Equipment Variable	Term	Correction
Overburden Pressure		C_N	$(P_a / \sigma'_{vo})^{0.5}$; $0.4 \leq C_N \leq 2$ *
Energy Ratio	Safety Hammer Donut Hammer Automatic Trip Hammer	C_E	0.60 to 1.17 0.45 to 1.00 0.9 to 1.6
Borehole Diameter	65 mm to 115 mm 150 mm 200 mm	C_B	1.0 1.05 1.15
Rod Length**	3 m to 4 m 4 m to 6 m 6 m to 10 m 10 m to 30 m >30 m	C_R	0.75 0.85 0.95 1.0 <1.0
Sampling Method	Standard Sampler Sampler without liners	C_S	1.0 1.2

* The Implementation Committee recommends using a minimum of 0.4.

** Actual total rod length, not depth below ground surface

Liquefaction Assessment by Use of the Cone Penetration Test (CPT)

This section presents suggested minimum requirements for Cone Penetration Test or CPT-based liquefaction evaluation.

The primary advantages of the CPT method are:

1. The method provides an almost continuous penetration resistance profile that can be used for stratigraphic interpretation.
2. The repeatability of the test is very good.
3. The test is fast and economical compared to drilling and laboratory testing of soil samples.

The limitations of the method are:

1. The method does not routinely provide soil samples for laboratory tests.
2. The method provides approximate interpreted soil behavior types and not the actual soil types according to ASTM Test Methods D2488 (Visual Classification) or D2487 (USCS Classification) [ASTM, 2000a].
3. The test cannot be performed in gravelly soils and sometimes the presence of hard/dense crusts or layers at shallow depths makes penetration to desired depths difficult.

The CPT method should be performed in general accordance with ASTM D3441 (ASTM, 2000a).

The recent proceedings from the January 1996 NCEER workshop (Youd and Idriss, 1997) on the evaluation of liquefaction resistance of soils represent the most up-to-date consensus among some of the

foremost experts in the liquefaction field. That document will likely set the standard of practice for liquefaction potential evaluation for the next several years. A summary report on the 1996 NCEER workshop and a later 1998 NCEER/NSF follow-up workshop has been prepared by Youd and Idriss (2001).

Historically, CPT-based liquefaction evaluations typically use a CPT-SPT correlation to estimate the SPT blow count values from CPT data. This method of liquefaction evaluation is also considered acceptable according to the NCEER report (Youd and Idriss, 1997). However, direct use of CPT may have supplanted these procedures.

The NCEER report identifies the CPT as a prime candidate for reconnaissance exploration and indicates that the CPT can be used to develop preliminary soil and liquefaction resistance profiles for site investigations. These preliminary profiles should always be checked by the use of selected boring samples retrieved during site investigations.

In practice, site investigations are seldom performed solely for the purpose of evaluating liquefaction potential. Soil samples from exploratory borings both disturbed and "relatively undisturbed," are usually needed to perform laboratory tests for typical geotechnical studies. Therefore, typically CPTs alone will not be sufficient to provide the geotechnical consultant with all the information needed to prepare a complete geotechnical report.

The following suggestions on the use of CPT soundings for liquefaction study are made:

- CPT soundings should be extended to the minimum depth needed for proper evaluation of liquefaction potential (i.e., the same minimum depth recommendations used for the SPT evaluation should be met).

  The minimum recommended depth of investigation is 50 feet (15 m). When a structure may have subterranean construction or deep foundations, the depth should extend to a minimum of 20 feet (6 m) below the lowest expected foundation level (bottom of caisson or pile) or 50 feet (15 m) below the ground surface, whichever is deeper. If there is a potential for liquefaction to extend below the minimum depth, CPTs should be continued until a significant thickness (at least 10 feet or 3 m) of nonliquefiable soils are encountered. The CPT tip resistance in that zone should exceed a corrected value of 160 tsf (16 MPa) in coarse-grained soils or the soils should be demonstrated to be nonliquefiable.

- As a minimum, one boring used for sampling and testing (for providing other geotechnical recommendations) should be performed immediately adjacent to one of the CPT soundings to check that the CPT-soil behavior type interpretations are reasonable for the project site. The boring and CPT sounding should not be spaced so closely that stress relief would significantly affect the results; therefore, consideration should be given to the sequence of the explorations. This boring should be extended to at least the same depth as the CPT sounding. Soil samples should be taken at least every 2½ or 3 feet using SPT, Modified California Drive, or other appropriate samplers, or at changes in soil stratigraphy. Blow-counts from the Modified California or other samplers should not be relied upon. Any differences between the SPT and CPT should be reconciled before proceeding with liquefaction analyses.

- Additional confirmation borings may be necessary if the site is large or the subsurface conditions vary significantly within the site. If an additional boring(s) is performed for other geotechnical design purposes, it may serve as confirmation boring(s). The need for and the number of additional borings shall be determined by the project geotechnical consultant, subject to the review of the appropriate regulatory agencies.

Liquefaction Assessment Using Other In Situ Indices

As data and correlations are being developed and verified with other in situ indices, alternative methods of assessment may become available. A limited amount of data have been collected and correlated to relate the liquefaction potential to shear wave velocities (Youd and Idriss, 1997). In particular, the shear wave

velocity approach may be an alternative method to the Becker Hammer method (Youd and Idriss, 1997) for evaluating the liquefaction potential of gravelly deposits.

Overburden Corrections For Differing Water Table Conditions

To perform analyses of liquefaction triggering, liquefaction settlement, seismically induced settlement, and lateral spreading, it is necessary to develop a profile of SPT blow-counts or CPT q_c-values that have been normalized using the effective overburden pressure. That normalization should be performed using the effective stress profile that existed at the time the SPT or CPT testing was performed. Then, those normalized values are held constant throughout the remainder of the analyses, regardless of whether or not the analyses are performed using higher or lower water-table conditions. Although the possibility exists that softening effects due to soil moistening can influence SPT or CPT results if the water table fluctuates, it is commonly assumed that the only effect that changes in the water table have on the results are due to changes in the effective overburden stress.

Raw, field N-values (or q_c-values) obtained under one set of ground-water conditions should not be input into an analysis where they are then normalized using C_N correction factors based on a new (different) water table depth.

GROUND MOTIONS FOR LIQUEFACTION ANALYSES

To perform analyses of liquefaction triggering, liquefaction settlement, seismically induced settlement, and lateral spreading, an earthquake magnitude, a peak horizontal ground acceleration, and a distance are needed. To obtain those values, consultants can perform a site-specific seismic hazard analysis.

There are two basic approaches for calculating site-specific design ground motions: deterministic and probabilistic. In the deterministic approach, a specific scenario earthquake is selected (i.e., with a particular magnitude and location) and the ground motion is computed using applicable attenuation relations. Even when the earthquake is specified in terms of its magnitude and distance to the site, there is still a large range of potential ground motions that could occur at the site. This variability of the ground motions can be characterized by the standard deviation of the attenuation relation. Traditionally, in deterministic analyses, either the median (50th percentile) or median-plus-one-standard-deviation (84th percentile) ground motion is selected for use as design ground motion.

In the probabilistic approach, multiple potential earthquakes are considered. That is, all of the magnitudes and locations believed to be applicable to all of the presumed sources in an area are considered. Thus, the probabilistic approach does not consider just one scenario, but all of the presumed possible scenarios. For a normal probabilistic analysis, the rate of earthquake occurrence (how often each scenario earthquake occurs) and the probabilities of earthquake magnitudes, locations, and rupture dimensions, also are considered. Also, rather than just considering a median or 84th percentile ground motion, the probabilistic approach considers all possible ground motions for each earthquake and their associated probabilities of occurring based on the variability of the ground motion attenuation relation. In addition, more elaborate probabilistic analyses can be performed using logic tree or Monte Carlo simulations to consider modeling uncertainty.

To lessen the burden of performing site-specific probabilistic seismic hazard analyses, the use of a set of standardized ground-motion maps may be considered as a procedure to estimate ground motion for liquefaction analyses. The United States Geologic Survey (USGS), through the National Seismic Hazard Mapping Project, has prepared estimates of the peak ground acceleration (PGA) for the entire United States (Frankel et al., 1996). The PGA has been estimated for three different risk levels: 10 percent probability of exceedance in 50 years; 5 percent probability of exceedance in 50 years; and 2 percent probability of exceedance in 50 years. The PGA values have been determined for a 0.1 degree grid spacing for the entire country; for California, Nevada, and most of Utah, PGA values have been determined for a 0.05 degree grid spacing. In addition, the seismic hazard corresponding to 2 percent probability of exceedance has been deaggregated by moment magnitude (M_w) and by epicentral distance in the Central and Eastern U.S. and by hypocentral distance in the Western U.S. Thus it is possible by using the USGS information to obtain an

estimate of the PGA, the corresponding moment magnitude, and distance for a liquefaction analysis for a 2 percent probability of exceedance in 50 years. For other levels of risk, a site-specific probabilistic seismic hazard analysis would have to be performed. The USGS PGA and deaggregation estimates can be found at the web address: http://geohazards.cr.usgs.gov/eq/.

Let us consider a site in Louisville, Kentucky for example; the site can be located by latitude and longitude or by a zip code. Let the site be in zip code 40223. The USGS National Seismic Hazard Mapping Project website will return the PGA at the nearest 0.1 degree grid point at 38.3 degrees north latitude and 85.5 degrees west longitude. The PGAs for three levels of risk are returned as given in the Table 3. Note that PE is the abbreviation for "probability of exceedance." It should be noted that the USGS ground motion predictions are based on the assumption that the soil profile will be a NEHRP B-C boundary condition. Estimates of ground motion would need to be adjusted for local site conditions.

Table 3. Estimated Peak Ground Accelerations (in gravity) for Zip Code 40223 (Louisville, Kentucky)

Risk Level	10% PE in 50 years	5% PE in 50 years	2% PE in 50 years
PGA in g's	0.0356	0.0553	0.0953

Figure 1 shows a USGS evaluation of the PGA in the Central and Eastern United States for a 2 percent probability of exceedance in 50 years; the contours on the map show that the PGA near Louisville is about 0.10g.

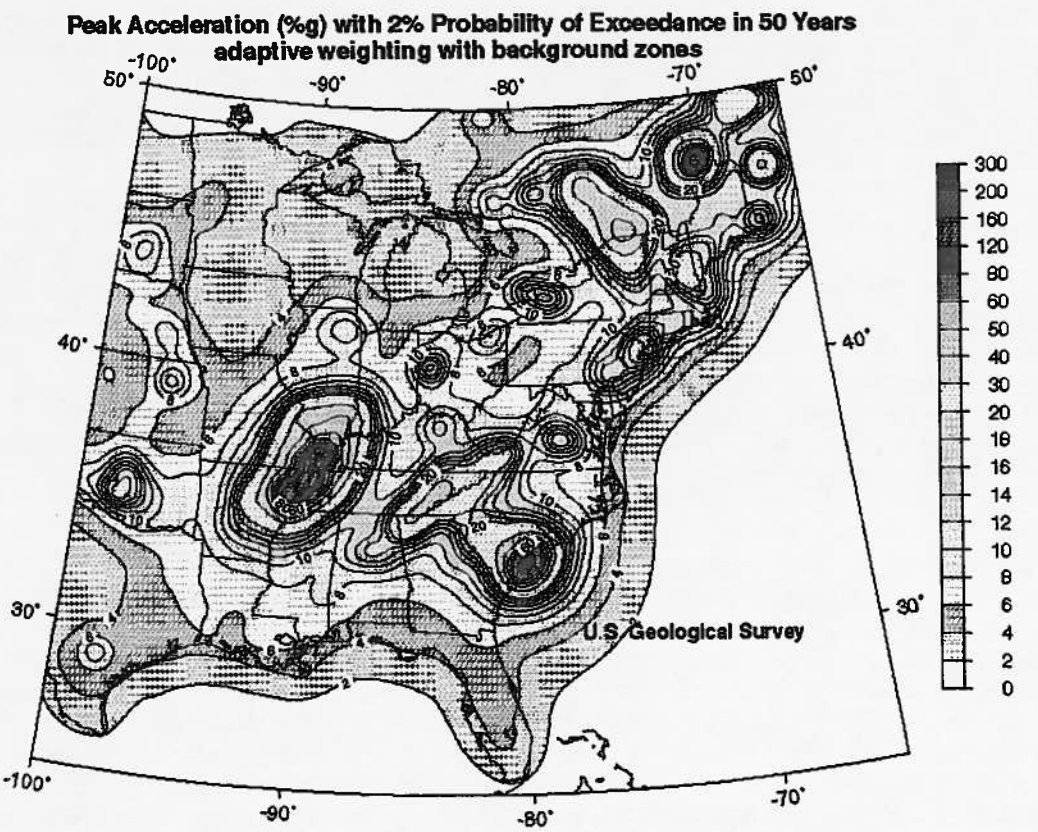

Figure 1. PGA with 2 percent probability of exceedance in 50 years (Frankel et al., 1996)

Figure 2 shows the probabilistic seismic deaggregation for the PGA in Louisville. It is clearly evident that the seismic hazard is dominated by a large distant event; from Figure 2, the hazard is dominated by a magnitude 8 event at a distance of about 350 kilometers. This event would be from the New Madrid region as can be seen in Figure 1.

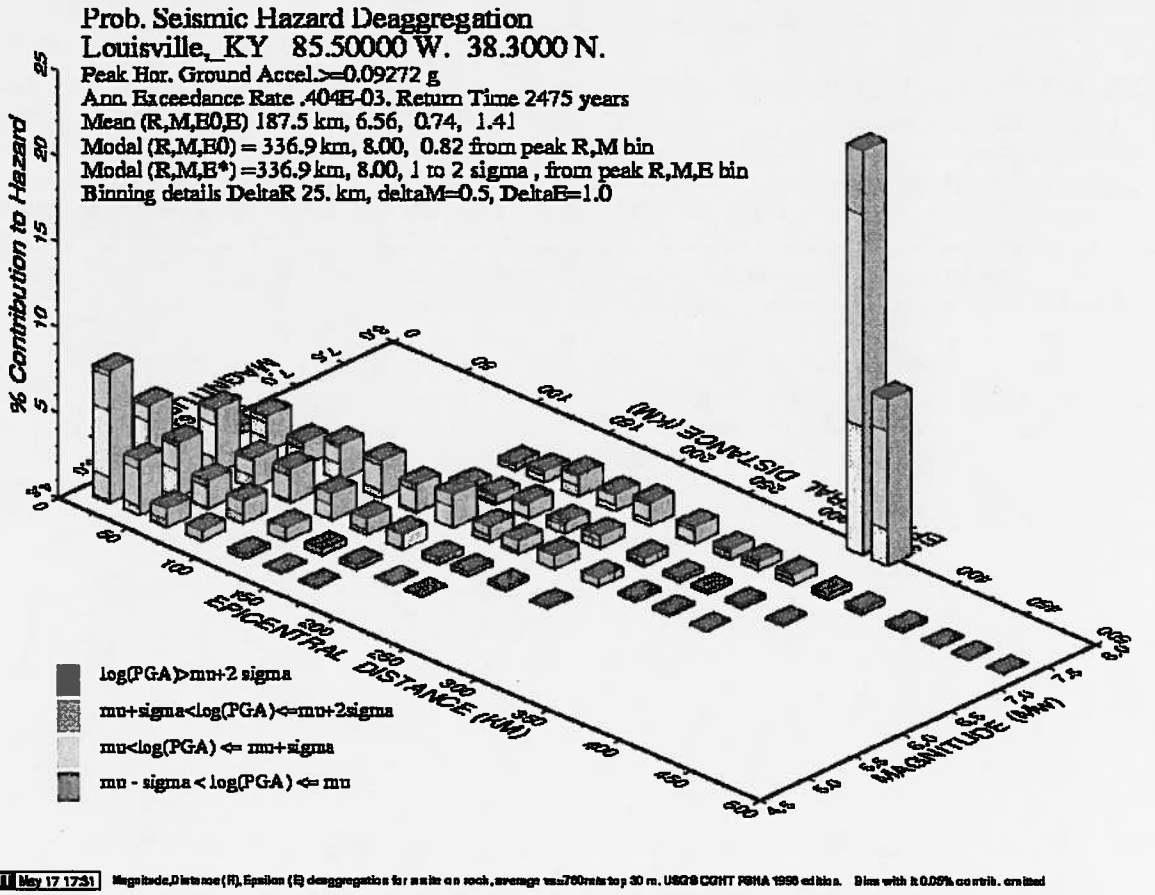

Figure 2. Probabilistic seismic hazard aggregation for the peak ground acceleration for Louisville, Kentucky for risk level of 2 percent probability of exceedance in 50 years.

EVALUATION OF LIQUEFACTION HAZARDS

Liquefaction Potential

The most basic procedure used in engineering practice for assessment of site liquefaction potential is that of the "Simplified Procedure" originally developed by Seed and Idriss (1971, 1982) with subsequent refinements by Seed et al. (1983), Seed et al. (1985), Seed and De Alba (1986), and Seed and Harder (1990). That procedure compares the cyclic resistance ratio (CRR) [the cyclic stress ratio required to induce liquefaction for a cohesionless soil stratum at a given depth] with the earthquake-induced cyclic stress ratio (CSR) at that depth from a specified design earthquake (defined by a peak ground surface acceleration and an associated earthquake moment magnitude at a given distance). The cyclic stress ratio, CSR, for the soil at a particular depth below the ground surface is computed by the following equation:

$$CSR = \tau_{av} / \sigma'_o = 0.65 \, (a_{max} / g) \cdot (\sigma_o / \sigma'_o) \cdot r_d$$

where a_{max} = maximum acceleration at the ground surface from the design earthquake with given moment magnitude

σ_o = total overburden pressure at depth under consideration

σ_o' = effective overburden pressure at depth under consideration

r_d = stress reduction coefficient

Values of CRR were originally established from empirical correlations using extensive databases for sites that did or did not liquefy during past earthquakes where values of $(N_1)_{60}$ could be correlated with liquefied strata. The current version of the baseline chart defining values of CRR as a function of $(N_1)_{60}$ for moment magnitude 7.5 earthquakes is shown on Figure 3. That chart was recently established by a consensus at the 1996 NCEER Workshop (Youd and Idriss, 1997). A corresponding chart documenting revised magnitude scaling factors was also developed, and is shown on Figure 4. Note that there are significant increases in scaling factors for moment magnitudes less than 7.5, compared to the original values. The new scaling factors supersede those in previous documents, for example: Seed et al. (1985).

For estimating values of the earthquake-induced cyclic stress ratio, CSR, the NCEER Workshop recommended essentially no change to the original simplified procedure (Seed and Idriss, 1971), where the use of a mean r_d factor defining the reduction in CSR with depth is usually adopted for routine engineering practice, as shown in Figure 5. As an alternative, a site-specific response analysis of the ground motions can be performed. Then values of CRR and CSR once established for a soil stratum at a given depth, allow a factor of safety against liquefaction, CRR/CSR, to be computed.

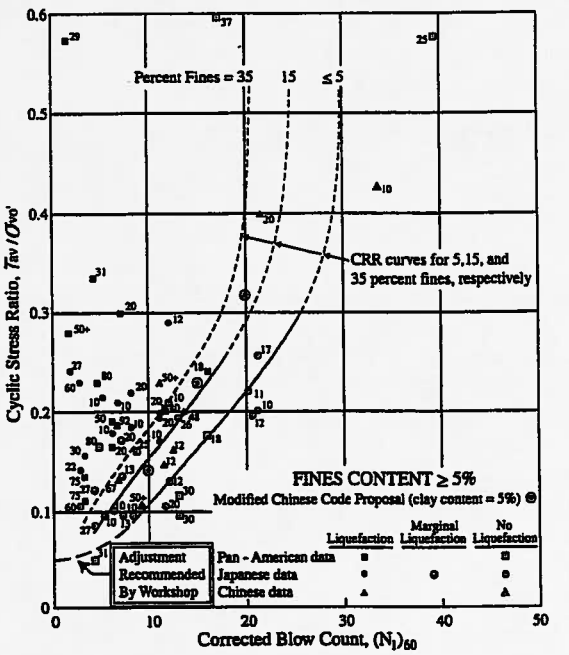

Figure 3. Simplified Base Curve Recommended for Determination of CRR from SPT Data for Moment Magnitude 7.5 Along with Empirical Liquefaction Data (after Youd and Idriss, 1997)

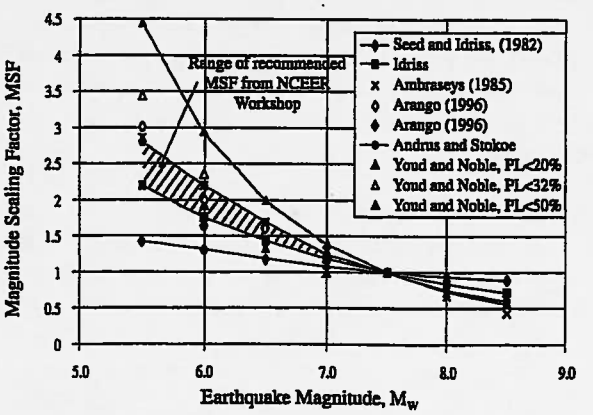

Figure 4. Magnitude Scaling Factors Derived by Various Investigators (After Youd and Idriss, 1997)

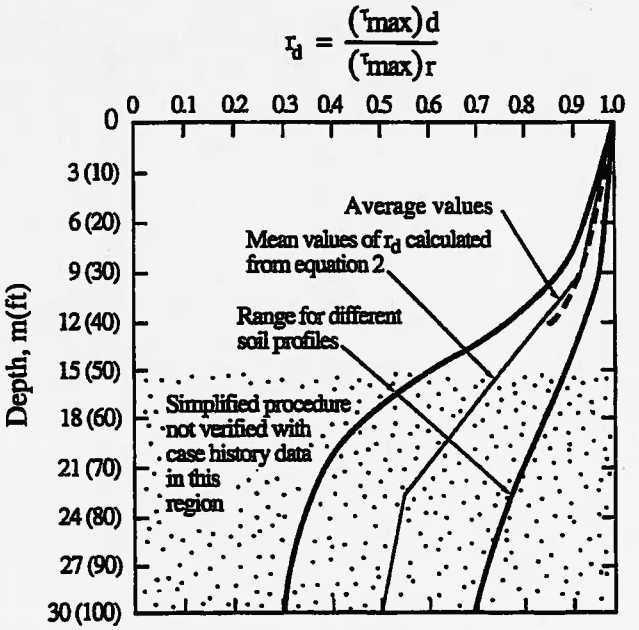

Figure 5. r_d Versus Depth Curves Developed by Seed and Idriss (1971) with Added Mean Value Lines (After Youd and Idriss, 1997)

The procedure given above should be regarded as the minimum requirement for evaluating site liquefaction potential where SPT data are used as a basis for determining liquefaction strengths. However, the use of the CPT is now recognized as one of the preferred investigation tools to estimate liquefaction strengths. It has the advantage of providing continuous data with depth, and the relatively low cost of performing multiple soundings over a site enable continuity of liquefiable strata to be assessed. The latter advantage is particularly important in determining the potential for lateral spreads and significant differential post-liquefaction settlements.

Historically, in using CPT data to establish liquefaction strengths, CPT data have been converted to equivalent SPT blow counts using procedures such as described by Martin (1992). With such an approach, confirmation of correlations is essential using at least one SPT borehole (required for laboratory classification tests) adjacent to a CPT sounding. An example of such a verification study is illustrated in

Figure 6. SPT blow counts at 5 foot intervals and corrected for fines content (using the procedure described by Seed et al. [1985]), are compared to CPT-derived blow count data derived using the correlation chart described by Martin et al. (1991). In general, the CPT-derived SPT data are seen to be in reasonable agreement with the measured SPT data. However, note that the five-foot sampling interval used for the SPT lacks the ability to pick up the significant variations in blow counts with depth, typical of interbedded sedimentary stratigraphy.

As discussed in the NCEER Workshop Proceedings, increased field performance data have become available at liquefaction sites investigated with CPT in recent years. Those data have facilitated the development of CPT-based liquefaction resistance correlations. These correlations allow direct calculation of CRR, without the need to convert CPT measurements to equivalent SPT blow counts and then applying SPT criteria.

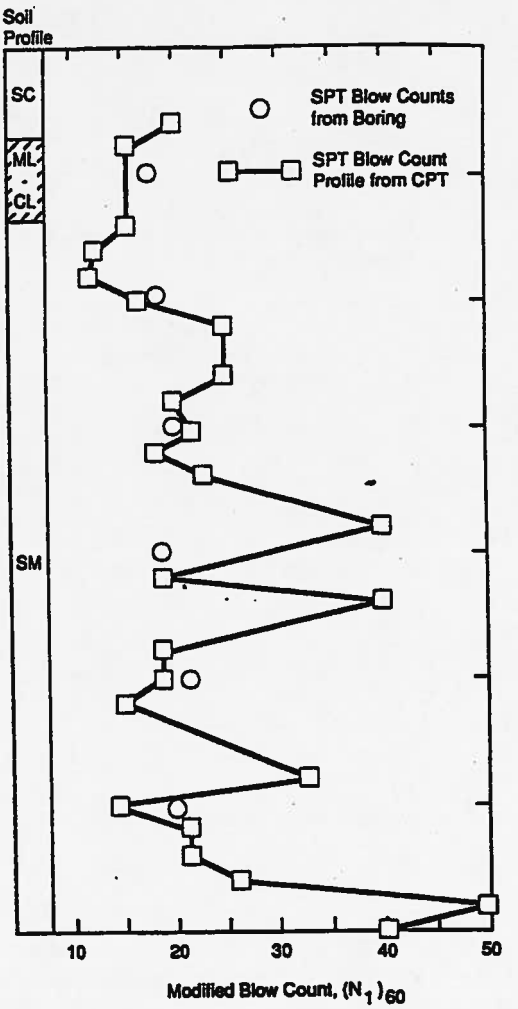

Figure 6. Comparison of Blow Counts from SPT and Those Derived from CPT Soundings (After Martin et al., 1991)

Figure 7 shows a chart developed by Robertson and Wride (Youd and Idriss, 1997) for determining liquefaction strengths for clean sands (fines content, FC, less than or equal to 5%) from CPT data. The chart, which is only valid for moment magnitude 7.5 earthquakes, shows calculated cyclic stress ratios

plotted as a function of corrected and normalized CPT resistance, q_{c1N}, from sites where liquefaction effects were or were not observed following past earthquakes. A curve separates regions of the plot with data indicative of liquefaction from regions indicative of nonliquefaction. Dashed curves showing approximate cyclic shear strain potential, γ_c, as a function of q_{c1N} are shown to emphasize that cyclic shear strain and ground deformation potential of liquefied soils decrease as penetration resistance increases.

The NCEER Workshop Proceedings provide an explicit commentary on how the new Robertson and Wride CPT procedure should be used for liquefaction evaluations. Because there is not complete consensus about this procedure, it is recommended that the method be used with care. As stated previously, a parallel borehole immediately adjacent to one CPT sounding; this will allow for a check of the soil classification, particularly for clayey silts where the Chinese liquefaction criteria may be applicable.

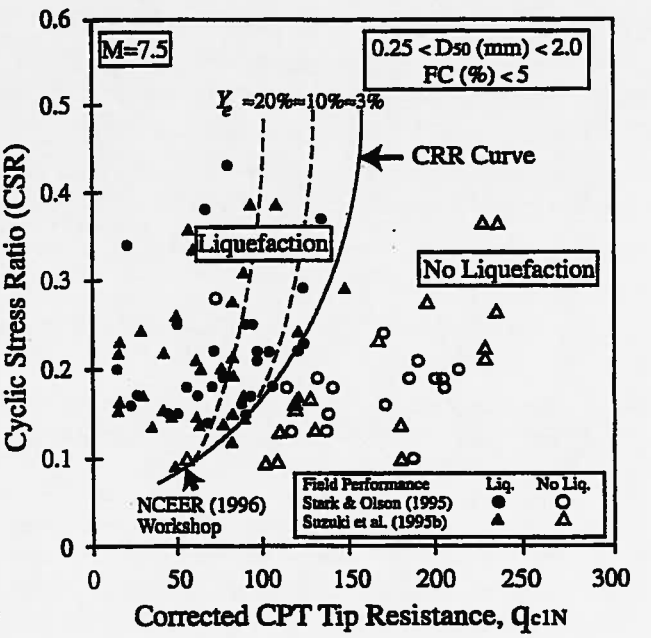

Figure 7. Curve Recommended for Determination of CRR from CPT Data Along with Empirical Liquefaction Data (After Robertson and Wride, 1997)

Hazard Assessment

The report on liquefaction assessment at a given site should include logs of the borings, field and corrected SPT blow counts, and classification test results, if SPT tests are performed. If CPT tests are performed, field and normalized CPT data (tip resistance, sleeve friction, and friction ratio) should be provided. The CPT data also should be interpreted to estimate soil behavior types. Values of $(N_1)_{60}$ and/or q_{c1N} required to resist liquefaction for a factor of safety equal to 1.0 should be determined. The site liquefaction potential should be evaluated for a specific design earthquake magnitude and peak ground acceleration.

In using such data to evaluate mitigation needs and to establish appropriate factors of safety for analyses, four principal liquefaction-related potential hazards need to be considered:

1. Flow slides or large translational or rotational site failures mobilized by existing static stresses (i.e., the site static factor of safety drops below unity (1.0) due to low strengths of liquefied soil layers).
2. Limited lateral spreads of the order of feet or less triggered and sustained by the earthquake ground shaking.

3. Ground settlement.
4. Surface manifestation of underlying liquefaction.

Each of those hazards and their potential should be addressed in the site report, along with mitigation options, if appropriate. In evaluating the need to address the above hazards, an acceptable factor of safety needs to be chosen. Often the acceptable factor of safety is chosen arbitrarily. The Special Publication 117 guidelines suggest a minimum factor of safety of 1.3. Clearly, no single value can be cited in a guideline, as considerable judgment is needed in weighing the many factors involved in the decision. Several of those factors are noted below:

1. The type of structure and its vulnerability to damage. In some situations, structural mitigation solutions may be more economical than ground remediation.
2. Levels of risk accepted by the owner or governmental regulations associated with questions related to design for life safety, limited structural damage, or essentially no damage.
3. Damage potential associated with the particular liquefaction hazards. Clearly flow failures or major lateral spreads pose more damage potential than differential settlement. Hence, factors of safety could be adjusted accordingly.
4. Damage potential associated with the design earthquake magnitude. It is obvious that a magnitude 7.5 event is far more damaging than a magnitude 6.5 event.
5. Damage potential associated with low SPT values, i.e., soils with low blow counts have a greater cyclic strain potential than soils with higher blow counts.
6. Uncertainty in SPT- or CPT- derived liquefaction strengths used for evaluations. Note that a change in silt content from 5 to 15% could change a factor of safety from 1.0 to 1.25.
7. For high levels of design ground motion, factors of safety may be indeterminant. For example, if $(N_1)_{60} = 20$, M = 7.5 and fines content = 35%, liquefaction strengths cannot be accurately defined due to the vertical asymptote on the empirical strength curve.

Factors of safety in the range of about 1.1 may be acceptable for single family dwellings where the potential for lateral spreading is very low and differential settlement is the hazard of concern, and where post-tensioned floor slabs are specified. On the other hand, factors of safety of 1.3 may be more appropriate for assessing hazards related to flow failure potential for large magnitude earthquake events.

The final choice of an appropriate factor of safety must reflect the particular conditions associated with a specific site and the vulnerability of site related structures. Table 4 provides a generalized guide that reflects many of the factors noted above.

These suggested factors of safety in Table 4 remain open for discussion. There was not a complete consensus on these factors of safety within the Implementation Committee; a minority position favors setting the factors of safety in the range between 1.25 and 1.5.

Table 4. Suggested Factors of Safety for Liquefaction Hazard Assessment

Consequence of Liquefaction	$(N_1)_{60}$ for clean sand	Factor of Safety
Settlement	≤15 >30	1.1 1.0
Surface Manifestation	≤15 >30	1.2 1.0
Lateral Spread	≤15 >30	1.3 1.0

MITIGATION OF LIQUEFACTION HAZARDS

Liquefaction and its related effects are likely to occur in saturated loose, cohesionless soils when subjected to strong ground motion. Soil densification methods, modifications leading to improving the cohesive properties of the soil (hardening or mixing), removal and replacement, or permanent dewatering can reduce or eliminate liquefaction potential. Other methods such as reinforcement of the soil or the use of shallow or deep foundations designed to accommodate the occurrence of liquefaction and associated vertical and horizontal deformations may also achieve an acceptable level of risk.

Often a mitigation measure may involve the implementation of a combination of techniques or concepts such as soil densification, reinforcement, and mixing. Shallow or deep foundations may also be designed to work with partial ground improvement techniques in order to reduce cost while achieving an acceptable level of risk.

As stated in SP 117, mitigation should provide suitable levels of protection with regard to potential large lateral spread or flow failures, and more localized problems including bearing failure, settlements, and limited lateral displacements.

The choice of mitigation methods will depend on the extent of liquefaction and the related consequences. Also, the cost of mitigation must be considered in light of an acceptable level of risk. Youd (1998) has suggested that structural mitigation for liquefaction hazards may be acceptable where small lateral displacements (say less than 1 foot or 0.3 meter) and vertical settlement (say less than 4 inches or 10 centimeters) are predicted. Youd cites evidence that houses and small buildings with reinforced perimeter footings and connected grade beams have performed well in Japan, and similar performance should be expected in the United States.

Performance Criteria

Liquefaction mitigation and performance criteria vary according to the acceptable level of risk for each structure type and human occupation considerations.

Implementation of mitigation measures should be designed to either eliminate all liquefaction potential or to allow partial improvement of the soils, provided the structure in question is designed to accommodate the resulting liquefaction-induced vertical and horizontal deformations. In some cases, the owners and engineers may decide to design mitigation measures to prevent liquefaction of certain soil types and allow limited deformations in others (i.e., allow some liquefaction).

During the initial site investigation and liquefaction evaluation, the engineer will determine the extent of liquefaction and potential consequences such as bearing failure, and vertical and/or horizontal deformations. Similarly, the engineer will determine the liquefaction hazard in terms of depth and lateral extent affecting the structure in question. The lateral extent affecting the structure will depend on whether there is potential for large lateral spreads toward or away from the structure and the influence of liquefied ground surrounding mitigated soils within the perimeter of the structure. Large lateral spread or flow failure hazards may be mitigated by the implementation of containment structures, removal or treatment of liquefiable soils, modification of site geometry, or drainage to lower the ground-water table.

Provided the potential for lateral spreads is addressed and level ground conditions exist, the extent of lateral mitigation beyond the structure footprint is related to bearing capacity and seepage conditions during and after the earthquake event (Port and Harbor Research Institute, 1997). Because liquefaction mitigation is likely to treat the ground underneath the structure to a sufficient depth, in most cases the bearing capacity reduction due to liquefiable ground outside the structure is not likely to govern the design. Instead, the propagation of excess pore pressures from liquefied to improved ground will determine the lateral extent of improvement required. Studies by Iai et al. (1988) indicate that, in the presence of liquefiable clean sands, an area of softening due to seepage flow occurs to a distance beyond the improved ground on the order of two-thirds of the liquefiable thickness layer.

The performance criteria for liquefaction mitigation, established during the initial investigation, may be in the form of a minimum, or average, penetration resistance value associated with a soil type (fines content, clay fraction, USCS classification, CPT soil behavior type index I_c, normalized CPT friction ratio), or a tolerable liquefaction settlement. Soils meeting the discussed Chinese criteria can be excluded from vertical deformation calculations, but they should be carefully considered for loss of strength and potential bearing failure or lateral deformations.

Soil Improvement Options

Soil liquefaction improvement options can be characterized as densification, drainage, reinforcement, mixing, or replacement. As noted above, the implementation of these techniques may be designed to fully, or partially, eliminate the liquefaction potential, depending on input forces and the amount of deformation that the structure in question can tolerate. With regards to drainage techniques for liquefaction mitigation, only permanent dewatering works satisfactorily. The use of gravel or prefabricated drains, installed without soil densification, is unlikely to provide adequate pore pressure relief during strong earthquakes and may not prevent excessive settlement. Their use should be evaluated with extreme caution. The following soil improvement methods have demonstrated successful performance in past earthquakes.

Densification Techniques

The most widely used techniques for in-situ densification of liquefiable soils are vibro-compaction, vibro-replacement (also known as vibro-stone columns), deep dynamic compaction, and compaction (pressure) grouting (Hayden and Baez, 1994).

Vibro-compaction and vibro-replacement techniques use similar equipment, but use different backfill material to achieve densification of soils at depth. In vibro-compaction; a sand backfill is generally used, whereas in vibro-replacement, stone is used as backfill material. Vibro-compaction is generally effective if the soils to be densified are sands containing less than approximately 10 percent fine-grained material passing the No. 200 sieve. Vibro-replacement is generally effective in soils containing less than 15 to 20% fines. However, recent experience (Luehring et al., 1998) has verified that even non-plastic sandy silts can be densified by a combination of vibro-replacement and vertical band (wick) drains. In such a case, the vertical band drains are installed at the midpoint of stone column locations prior to installation of vibro-replacement. Due to the usual variation of liquefiable soil types in a given profile and economy of the system, vibro-replacement is typically the most widely used liquefaction countermeasure used in North America (Hayden and Baez, 1994).

Deep dynamic compaction involves the use of impact energy on the ground surface to densify and compact subsurface soils. Weights typically ranging from 10 to 30 tons are lifted with standard, modified, or specialty machines and dropped from about 50 to 120 feet heights. Free-fall impact energy is controlled by selecting the weight, drop height, number of drops per point and the spacings of the grid. Empirical relationships are available to design deep dynamic compaction programs to treat specific site requirements and reconstitute liquefiable soils to a denser condition (Lukas, 1986). In general, treatment depths of up to 35 feet may be achievable in granular soils. If surficial saturated cohesive soils are present or the ground-water table is within 3 to 5 feet of the surface, a granular layer is often needed to limit the loss of impact energy and transfer the forces to greater depths. The major limitations of the method are vibrations, flying matter, and noise. For these reasons, work often requires 100 to 200 feet clearance from adjacent occupied buildings or sensitive structures.

Displacement or compaction grouting involves the use of low slump, mortar-type grout pumped under pressure to densify loose soils by displacement. Compaction grouting pipes are typically installed by drilling or driving steel pipes of 2-inch internal diameter or greater. Injection of the stiff, 3-inch or less slump, cement grout is accomplished with pressures generally ranging from 100 to 300 pounds per square inch (psi). Refusal pressures of 400 to 500 psi are common in most granular soil projects where liquefaction is the problem. Grout pipes are installed in a grid pattern that usually ranges from 5 to 9 feet. The use of primary spacing patterns with secondary or tertiary intermediate patterns infilled later is

effective to achieve difficult densification criteria. Grouting volumes can typically range from 3 to 12 percent of the treated soil volume in granular soils, although volumes up to 20 percent have been reported for extremely loose sands or silty soils. Inadequate compaction is likely to occur when sufficient vertical confinement (less than 8 to 10 feet of overburden) is not present. Theory and case histories on this technique can be found in Graf (1992), Baez and Henry (1993), and Boulanger and Hayden (1995), among others.

Hardening (Mixing) Techniques

Hardening and/or mixing techniques seek to reduce the void space in the liquefiable soil by introducing grout materials either through permeation, mechanical mixing, or jetting. These techniques are known as permeation grouting, soil mixing, or jet grouting.

Permeation grouting involves the injection of low viscosity liquid grout into the pore spaces of granular soils. The base material is typically sodium silicate or microfine cements where the D_{15} of the soil should be greater than 25 times D_{85} of the grout for permeation. With successful penetration and setting of the grout, a liquefiable soil with less that approximately 12 to 15 percent fine-grained fraction becomes a hardened mass. Use of this method in North America has been limited to a few projects such as the bridge pier in Santa Cruz, California (Mitchell and Wentz, 1991), and a tunnel horizon in downtown San Francisco. Design methodology and implementation of this technique are described in detail by Baker (1982) and Moseley (1993).

Jet grouting forms cylindrical or panel shapes of hardened soils to replace liquefiable, settlement sensitive, or permeable soils with soil-cement having strengths up to 2,500 psi. The method relies on up to 7,000 psi water pressure at the nozzle to cut soils, mix in place cement slurry and lift spoils to the surface. Control of the drill rotation and pull rates allows treatment of variable soils as described by Moseley (1993). Lightweight drill systems can be used in confined spaces such as inside existing buildings that are found to be at risk of liquefaction after construction.

Deep soil-mixing is a technique involving mixing of cementitious materials using a hollow-stem-auger and paddle arrangement. Gangs of 1 to 5 shafts with augers up to 3 feet or more in diameter are used to mix to depths of 100 feet or more. As the augers are advanced into the soil, the hollow stems are used as conduits to pump grout and inject into the soil at the tip. A trencher device has also been used successfully in Japan. Confining cells are created with the process as the augers are worked in overlapping configurations to form walls. Liquefaction is controlled by limiting the earthquake induced shear strains, and re-distributing shear stresses from soils within the confining cells to the walls. As with jet grouting, treatment of the full range of liquefiable soils is possible and shear strengths of 25 psi or more can be achieved even in silty soils. The method has been used for liquefaction remediation in only a few cases in North America, including Jackson Lake dam in Wyoming (Ryan and Jasperse, 1989). However, the method has found more extensive use in Japan (Schaefer, 1997).

Structural Options

In some cases, structural mitigation for liquefaction effects may be more economical than soil improvement mitigation methods. However, structural mitigation may have little or no effect on the soil itself and may not reduce the potential for liquefaction. With structural mitigation, liquefaction and its related ground deformations will still occur. A competent licensed structural engineer that is familiar with seismic design principles with an understanding of liquefaction effects should design the structural mitigation. The structural mitigation should be designed to protect the structure from liquefaction-induced deformations, recognizing that the structural solution may have little or no improvement on the soil conditions that cause liquefaction. The appropriate means of structural mitigation may depend on the magnitude and type of soil deformation expected because of liquefaction. If liquefaction-induced flow slides or significant lateral spreading is expected, structural mitigation may not be practical or feasible in many cases. However, if the soil deformation is expected to be primarily vertical settlement, structural mitigation may be economically and technically feasible.

Where the structure is small (in building footprint) and light in weight, such as in typical single family residential houses, a post-tensioned slab foundation system may be beneficial. A post-tensioned slab should have sufficient rigidity to span over voids that may develop under the slab due to differential soil settlement. Light buildings also may be supported on continuous spread footings having isolated footings interconnected with grade beams. For heavier buildings with a low profile and relatively uniform mass distribution, a mat foundation may be feasible. The mat should be designed to bridge over local areas of settlement.

Piles or caissons extending to non-liquefiable soil or bedrock below the potentially liquefiable soils may be feasible. Such designs should take into account the possible downdrag forces on the foundation elements due to settlement within the liquefiable and upper soils. Design must also accommodate seismic lateral forces that must be transmitted from the structure to the supporting soils and displacement demand, due to lateral ground deformations. As there may be a considerable loss of lateral soil stiffness and capacity, the piles or caissons will have to transmit the lateral loads to the deeper supporting soils. Experience from the 1989 Loma Prieta earthquake (Benuska, 1990) have shown that battered piles to resist lateral loads are not effective in seismic conditions and should not be used in general. Floor slabs supported on grade should be expected to undergo settlements in sympathy with the liquefaction-induced settlements of the ground. If such floor settlements are not acceptable, the ground level floor slabs could be structurally supported on the pile or caisson system.

Subterranean wall structures retaining potentially liquefiable soils may be subjected to substantially greater than normal active or at-rest lateral soil pressures. An evaluation should be made to determine the appropriate lateral earth pressures and structural design for this condition.

It should be recognized that structural mitigation may not reduce the potential of the soils to liquefy during an earthquake. There will remain some risk that the structure could still suffer damage and may not be useable if liquefaction occurs. Utilities and lifeline services provided from outside the structure could still suffer disruption unless mitigation measures are employed that would account for the soil deformations that could occur between the structure and the supporting soils. Repair and remedial work should be anticipated after a liquefaction event if structural mitigation is used.

Quality Assurance

Soil improvement techniques generally use specialized equipment and require experienced personnel. As such, they should be implemented by specialty construction companies with a minimum of 5 years experience in similar soils and job conditions as those considered for the project in question. Minimum quality assurance requirements will vary significantly depending on the technique being implemented.

For dynamic compaction, measurement of energy being delivered to the ground, sequence and timing of drops, as well as ground response in the form of crater depth and heave of the surrounding ground are important quality control parameters. Similarly, the location of the water table and presence of surface "hard pans" could greatly affect the quality and outcome of the densification process. Pore water pressures of an area recently treated should be allowed to dissipate before secondary treatments are implemented.

Vibro-compaction and vibro-replacement are generally performed with electric or hydraulic powered depth vibrators. When electric vibrators are used, the "free hanging" amperage as well as the amperage developed during construction are strong indicators of the likely success of the densification effort. The equipment should be capable of delivering the appropriate centrifugal force to cause densification. Stone backfill materials should be generally clean and hard with minimum durability index of about 40 (Caltest method 229). When the engineer relies on the stone backfill material to provide reinforcement for vertical or horizontal deformations, the stone should be crushed and have a suitable angle of internal friction. In some cases, computer data acquisition systems may be desired to monitor the depth of the vibrator, stone usage, and amperage developed.

Compaction grouting requires the verification of slump and consistency of the mix, as well as careful monitoring of grout volumes, injection pressures, and ground movement at the surface or next to sensitive

structures. Critical projects also monitor pore water pressure and deep ground heave (borros points) development during the compaction grouting procedures. Because grout is typically injected in stages from the bottom up, at each stage a stopping criteria of grout volume, pressure, or heave should be followed before proceeding with the next stage. Usage of grout casing with less than 2 inches in internal diameter should be avoided as it could cause detection of high back pressures before sufficient grout is injected. Over injection of grout in a primary phase may lead to early ground heave and may diminish densification effectiveness. Spacing and sequence of the grout points may also affect the quality of densification or ground movement achieved.

In general, the geotechnical engineer of record or his/her representatives conducts on-site inspection of all the procedures mentioned above. Testing locations are selected at random and tend to be located in the middle of a grid pattern formed by the densification locations. This is somewhat conservative and more realistic average results can be obtained by testing closer to the densification points. To permit excess pore pressure dissipation, a minimum of 48 to 72 hours after soil improvement is implemented should be allowed for prior to testing.

Soil mixing and jet grouting are also constructed with specialized equipment; this equipment is capable of adjustment of the rate of rotation and lifting rate of the injection ports. The grout or binder may include cement, fly ash, quicklime, or other components and additives designed to obtain the desired strength properties of the mixed soil. The binders are controlled for quality by checking consistency as measured by specific gravity. This is generally checked with mud balance or hydrometer devices. Pumping pressures and rates are designed to achieve production and strength requirements of the product. Installed columns are usually tested by wet sampling, coring with a minimum 3-inch core, CPT, pressuremeter, or seismic devices. Variation in quality and strength should be expected in the final product.

GEOTECHNICAL REPORTING OF RESULTS

The liquefaction evaluation report should be prepared under the direction of and signed by a competent registered professional civil (or geotechnical) engineer with the aid of a certified engineering geologist, having competence in the field of liquefaction hazard evaluation and mitigation. The geotechnical report should contain site-specific evaluations of the liquefaction hazard affecting the "project," and should identify portions of the site affected by the liquefaction hazard. The contents of the report should include, but shall not be limited to, the following:

1. Project description.
2. A description of the geologic and geotechnical conditions at the site, including an appropriate site location map. The descriptions should also include information regarding the site and near-site topography; topographic maps, geologic maps, and cross sections may be helpful.
3. Evaluation of the site-specific liquefaction hazard based on the geological and geotechnical conditions, in accordance with the current standards of practice.
4. Recommendations for appropriate mitigation measures.
5. Logs of field explorations. Detailed description of field test procedures, such as SPT and CPT should be given.
6. A description of laboratory tests conducted on soil/rock samples and summary of test results.
7. A summary of the assumptions used in analysis. Calculations should be submitted to facilitate review.

The report should contain a complete description of the test procedures used to evaluate liquefaction potential and the method of analysis used to evaluate the site-specific hazard. Assumptions should be clearly presented as well as supporting reference data.

If liquefaction countermeasures or mitigation techniques to improve the soil are used, generally the geotechnical engineer is responsible for geotechnical observation and testing to provide assurance of

conformance to the project specifications and achieving the desired soil improvements and performance objectives. The report should fully describe the construction methods and the quality assurance program used. All testing should be documented.

CONCLUDING REMARKS

The practice of liquefaction geotechnical engineering has advanced and matured. There is an ever-increasing awareness that liquefaction is not just a problem in California, but is an earthquake hazard that must be considered in other seismically active regions of the United States, including the central U.S. The state of the practice will continue to evolve and advance at an ever-increasing pace and it is a certainty that new methodologies in liquefaction geotechnical engineering will develop from future research and the inevitable observations in future occurrences in earthquakes to come.

It is the hope of the author that this paper will provide geotechnical professionals with more knowledge and understanding about the current state-of-the-practice of liquefaction analysis, evaluation, and mitigation. With this knowledge and understanding, better informed decisions can be made regarding the available options to eliminate or reduce the effects of liquefaction hazards. More detailed information can be found in the SCEC Implementation Committee report (Martin and Lew, 1999) which is available by download in Adobe PDF format at the Southern California Earthquake Center website at the following address: http://www.scec.org/outreach/products/liqreport.pdf.

ACKNOWLEDGEMENTS

The Liquefaction Implementation Committee was supported by funding from the Southern California Earthquake Center (SCEC) at the University of Southern California. SCEC is funded by NSF Cooperative Agreement EAR-8920136 and USGS Cooperative Agreements 14-08-0001-A0899 and 1434-HQ-97AG01718. The Implementation Committee was formed through the Geotechnical Group of the Los Angeles Section of the American Society of Civil Engineers.

The members of the Implementation Committee were: Geoffrey R. Martin and Marshall Lew, co-chairs, K. Arulmoli, Juan I. Baez, Thomas F. Blake, Johnnie Earnest, Fred Gharib, J. Goldhammer, David Hsu, Steve Kupferman, Jim O'Tousa, Charles R. Real, Wes Reeder, Ebrahim Simantob, and T. Leslie Youd.

REFERENCES

American Society for Testing and Materials, 2000, Soil and Rock, ASTM Standards, v. 4.08.

American Society for Testing and Materials, 2000, Soil and Rock, ASTM Standards, v. 4.09.

Baez, J.I., and Henry, J.F., 1993, "Reduction of Liquefaction Potential by Compaction Grouting at Pinoplis Dam, SC," Proceedings of the Geotechnical Practice in Dam Rehabilitation Conference, ASCE Geotechnical Special Publication No. 35, p. 493-506, Raleigh, N.C.

Baker, Wallace H., 1992, "Planning and Performing Structural Chemical Grouting," Grouting in Geotechnical Engineering, ASCE Specialty Conference, New Orleans, p. 515-540.

Benuska, K.L. (editor), 1990, "Loma Prieta Earthquake Reconnaissance Report," Earthquake Engineering Research Institute.

Boulanger, R.W. and Hayden, R.F., 1995, "Aspects of Compaction Grouting of Liquefiable Soil," Journal of Geotechnical Engineering, ASCE, Vol. 121, No. 12, p. 844-855.

California Department of Conservation, Division of Mines and Geology, 1997, "Guidelines For Evaluating and Mitigating Seismic Hazards in California," CDMG Special Publication 117.

California Department of Conservation, Division of Mines and Geology, 1999, "Recommended Criteria for Delineating Seismic Hazard Zones in California," CDMG Special Publication 118.

Frankel, A., Mueller, C., Bernhard, T., Perkins, D., Leyendecker, E.V., Dickman, N., Hanson, S., and Hopper, M., "National Seismic-Hazard Maps: Documentation – June 1996," United States Geological Survey, Open-File Report 96-532.

Graf, E.D., 1992, "Compaction Grout, 1992," *Grouting, Soil Improvement and Geosynthetics*, ASCE Geotechnical Special Publication No. 30, p. 275-287.

Hayden, R.F., and Baez, J.I., 1994, "State of Practice for Liquefaction Mitigation in North America," Proceedings of the 4th U.S.-Japan Workshop on Soil Liquefaction, Remedial Treatment of Potentially Liquefiable Soils, PWRI, Tsukuba City, Japan, July-4-6.

Iai, S., Noda, S., and Tsuchida, H., 1988, "Basic Considerations for Designing the Area of the Ground Compaction as a Remedial Measure Against Liquefaction," Proceedings of the U.S.-Japan Workshop on Soil Liquefaction, Remedial Treatment of Potentially Liquefiable Soils, San Francisco.

International Conference of Building Officials, 1994, Uniform Building Code, ICBO, Whittier, CA.

International Conference of Building Officials, 1997, Uniform Building Code, ICBO, Whittier, CA.

Luehring, R., Dewey, B., Mejia, L., Stevens, M. and Baez, J., 1998, "Liquefaction Mitigation of Silty Dam Foundation Using Vibro-Stone Columns and Drainage Wicks – A Test Section Case History at Salmon Lake Dam," Proceedings of the 1998 Annual Conference Association of State Dam Safety Officials, Las Vegas, NV, October 11-14.

Lukas, R.G., 1986, "Dynamic Compaction for Highway Construction, Volume I: Design and Construction Guidelines," Federal Highway Administration Report No. FHWA/RD-86/133.

Martin, G.R., 1992, "Evaluation of Soil Properties for Seismic Stability Analyses of Slopes," ASCE Geotechnical Publication No. 31, Stability and Performance of Slopes and Embankments, Vol. 1, p. 116-142.

Martin, G.R. and Lew, M., editors, 1999, "Recommended Procedures for Implementation of DMG Special Publication 117 – Guidelines for Analyzing and Mitigating Liquefaction Hazard in California," Southern California Earthquake Center, University of Southern California, Los Angeles, CA.

Martin, G. R., Tsai, C-F., and Arulmoli, K., 1991, "A Practical Assessment of Liquefaction Effects and Remediation Needs," Proceedings, 2nd International Conference on Recent Advances in Geotechnical Earthquake Engineering and Soil Dynamics, St. Louis, Missouri, March 11-15.

Mitchell, J.K., and Wentz, F.L., 1991, "Performance of Improved Ground During the Loma Prieta Earthquake," Report No. UCB/EERC-91/12, Earthquake Engineering Research Center, University of California, Berkeley.

Moseley, M.P. (Editor), 1993, *Ground Improvement*, CRC Press, Inc., Boca Raton, Florida.

Petersen, M.D., Bryant, W.A., Cramer, C.H., Cao, T., Reichle, M.S., Frankel, A.D., Lienkaemper, J.J., McCrory, P.A., and Schwartz, D.P., 1996, "Probabilistic Seismic Hazard Assessment for the State of California," California Division Mines and Geology, Open File Report 96-08, 59p.

Port and Harbour Research Institute, PHRI, (1997*), "Handbook on Liquefaction Remediation of Reclaimed Land*," A.A. Balkema Publishers, Brookfield, VT, USA.

Robertson, P.K. and Wride, C.E., 1998, "Cyclic Liquefaction and Its Evaluation Based on the SPT and CPT," *in* Proceedings edited by Youd and Idriss, 1998, p. 41-88.

Ryan, C.R., and Jasperse, B.H., 1989, "Deep Soil Mixing at the Jackson Lake Dam," Foundation Engineering: Current Principles and Practices, Proceedings of an ASCE Congress, Geotechnical Special Publication No. 22, Vol. 1, p. 354-367.

Schaefer, V.R., 1997, Ground Improvement, Ground Reinforcement, Ground Treatment Developments 1987-1997, Geotechnical Special Publication No. 69, ASCE, Logan, UT.

Seed, H.B. and DeAlba, P., 1986, "Use of SPT and CPT Tests for Evaluating the Liquefaction Resistance of Sands," *in* Clemence, S.P., editor, "Use of In Situ Tests in Geotechnical Engineering," New York, ASCE Geotechnical Special Publication No. 6, p. 281-302.

Seed, H.B. and Idriss, I.M., 1971, "Simplified Procedure for Evaluating Soil Liquefaction Potential," Journal of the Soil Mechanics and Foundations Division, ASCE, Vol. 97, No. SM9, p. 1249-1273.

Seed, H.B. and Idriss, I.M., 1982, "Ground Motions and Soil Liquefaction During Earthquakes," Earthquake Engineering Research Institute Monograph.

Seed, H. B., Idriss, I. M., and Arango, I., 1983, "Evaluation of Liquefaction Potential Using Field Performance Data," Journal of the Geotechnical Engineering Division, ASCE, Vol. 109, No. 3, March.

Seed, H. B., Tokimatsu, K., Harder, L. F., and Chung, R. M., 1985, "Influence of SPT Procedures in Soil Liquefaction Resistance Evaluations," Journal of the Geotechnical Engineering Division, ASCE, Vol. 111, No. 12, December.

Seed, R.B. and Harder, L.F., Jr., 1990, "SPT-Based Analysis of Cyclic Pore Pressure Generation and Undrained Residual Strength," *in* Proceedings, H. Bolton Seed Memorial Symposium, BiTech Publishers, Ltd., p. 351-376.

Youd, T.L., 1998, personal communication, August.

Youd, T. L. and Idriss, I.M. (Editors), 1997, Proceedings of the NCEER Workshop on Evaluation of Liquefaction Resistance of Soils, Salt Lake City, UT, January 5-6, 1996, NCEER Technical Report NCEER-97-0022, Buffalo, NY.

Youd, T.L. and Idriss, I.M., 2001, "Liquefaction Resistance of Soils: Summary Report from the 1996 NCEER and 1998 NCEER/NSF Workshops on Evaluation of Liquefaction Resistance of Soils," Journal of Geotechnical and Geoenvironmental Engineering, Vol. 127, No. 4, April.

Liquefaction Evaluations and Seismic Rehabilitation
an
Overview of Case Histories

Greg Yankey, P.E.[1], Jeffrey Schaefer, Ph.D., P.G. P.E.[2]

ABSTRACT

The United States Army Corps of Engineers conducts rigorous assessments of their civil works projects through the use of a phased approach. The first phase is non-invasive and includes an assessment of all existing data for an identification of project features that may be susceptible to earthquake ground motions. Projects that are deemed acceptable are not subjected to further study. Remaining projects are investigated through the use of site-specific studies that include drilling, laboratory testing and engineering analyses. Finally, projects identified to have an unacceptable risk of failure are rehabilitated. This paper will focus on these investigation phases through the use of case histories. Corps of Engineers projects in Indiana and Kentucky will be reviewed. Typical investigation and assessment methodologies will be provided along with key considerations. Finally, an overview of rehabilitation techniques commonly employed in practice will be provided.

INTRODUCTION

Numerous state and federal agencies are responsible for the seismic safety of dams that they own and/or regulate. A cost-effective process for assessing seismic safety of dams includes multiple stages with increasing levels of sophistication. In this fashion, a safe dam can be identified with a reduced effort and eliminated from further study. The United States Army Corps of Engineers (USACE) operates such a program (ER 1110-2-1155) that effectively evaluates existing structures through a phased approach. Figure 1 presents the location of three projects that will be used as case histories herein to illustrate the USACE's method.

SEISMIC ANALYSIS PROCESS

Figure 2 illustrates the phases of USACE's approach. Generally, the level of effort increases with each phase. The first phase is called a seismic safety review (SSR). The purpose of the SSR is to identify critical project features that could become damaged or weakened (such as soils) during an earthquake using available project documentation. The sole outcome of the SSR is the decision of whether or not a Phase 1 investigation is required.

[1] Associate, Fuller, Mossbarger, Scott and May Engineers, Inc. of Lexington, Kentucky
[2] Senior Geotechnical Engineer, Louisville District Corps of Engineers, Louisville, Kentucky

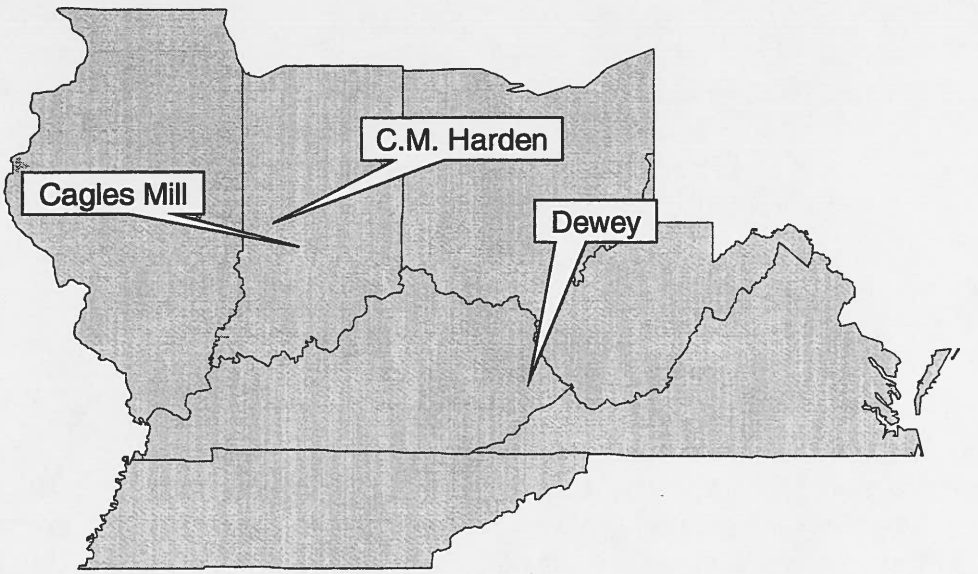

Figure 1. Project Locations.

A Phase 1 investigation is typically very comprehensive and it represents the primary data gathering effort for all future studies. Typical components include a geotechnical investigation and subsequent laboratory testing to characterize material types, extents and density. Geophysical techniques are often employed to estimate shear wave velocity profiles for the site at several locations. A site specific ground motion study is usually performed at this stage to provide time histories of acceleration for use in seismic assessments. These assessments, at a minimum include an identification of liquefaction potential of foundation and/or embankment materials, the potential for embankment deformation and the capacity of the intake tower to resist design loadings. If it is concluded that the dam cannot withstand the maximum credible earthquake (MCE) without uncontrolled loss of the pool, a Phase 2 study is planned.

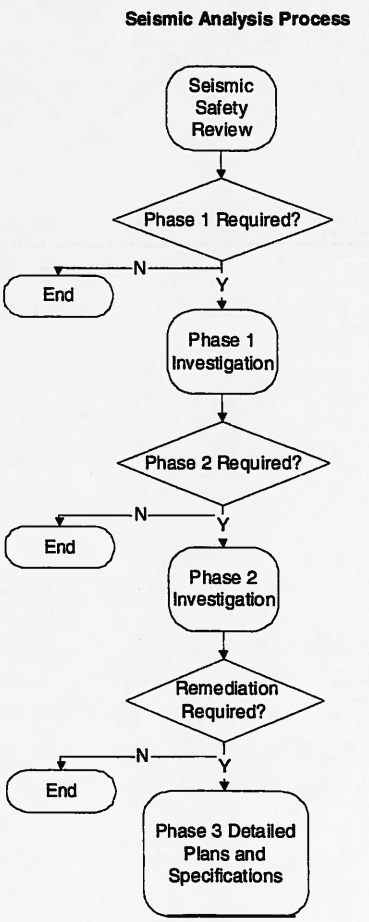

Figure 2. Seismic Analysis Process.

The Phase 2 study provides an opportunity to employ more sophisticated analysis techniques if it is believed that undue conservatism exists in previous

analyses. The more advanced techniques include finite element or centrifuge studies, among others. If problems are still identified, Phase 2 serves as a precursor to the preparation of final design(s), plans and specifications. Several remediation options are usually identified and carried through the preliminary design stage including venture level cost estimates. One alternative is selected as the most cost effective that meets the design constraints. The last phase includes carrying the selected alternative through final design including the preparation of detailed plans and specifications. Common components of construction include test sections to verify that products meet design expectations.

EXAMPLE PROJECTS – Cagles Mill Lake Dam - SSR

Cagles Mill Lake Dam is located on Mill Creek, 2.9 miles upstream of its confluence with the Eel River, and approximately 25 miles east of Terre Haute, Indiana. The dam is utilized primarily for flood control purposes in the Eel and White River watersheds, and further downstream to the Ohio River. The structure is a 900-foot long zoned earth and rock embankment with a maximum height of 150 feet and crest width of 30 feet. The embankment slopes are 2 horizontal (H) to 1 vertical (V) along the entire length of the structure. The embankment section includes an impervious core with upstream and downstream shells of rock fill with gravel filters separating the clay core and rock fill zones of the dam. A cutoff trench along the dam centerline was extended to bedrock during dam construction. The dam foundation upstream and downstream of the core consists of cyclic sequences of silt, sand and rock fragments, and it varies in thickness from five to thirty five feet. The outlet works consist of a 161-foot tall intake tower with three, five by ten-foot rectangular shaped sluice gates and one low-flow 30-inch diameter discharge pipe. Figure 3 illustrates a photograph of Cagles Mill Lake Dam and a typical section.

Based on a review of the available design and construction information in conjunction with an SSR, the primary concern is the presence of potentially liquefiable foundation materials beneath the upstream and downstream slopes. These materials are believed to consist of relatively young alluvial deposits of sands and silts associated with the former Mill Creek. Little post-construction boring information is available for review and borings that have been advanced, did not contain standard penetration tests (SPTs). Consequently, a reliable assessment of liquefaction potential could not be completed. However, an approach that was implemented included a back-calculation of acceptable N-values that could be used as a gauge in later field efforts. In this fashion, quick determination of acceptable in-situ densities could be estimated based on an empirical approach. Another consideration was the fact that the site is positioned near two commonly accepted seismic sources: the New Madrid and Wabash Valley seismic zones. Additional complicating factors related to seimicity include the recent discovery of the Commerce Geophysical Lineament (CGL) and paleoliquefaction features in the upper Wabash River valley. Some experts believe that the CGL is seismogenic. The paleoliquefaction features suggest that relatively large (compared to documented historical seismicity) earthquakes occur about every 4,000 years in the Wabash Valley Seismic Zone. As a result of these considerations, Cagles Mill Lake Dam was recommended to be advanced to the Phase 1 level wherein site specific information could be utilized to evaluate the structure. SPT N-values will be collected and compared to the threshold values determined in the SSR.

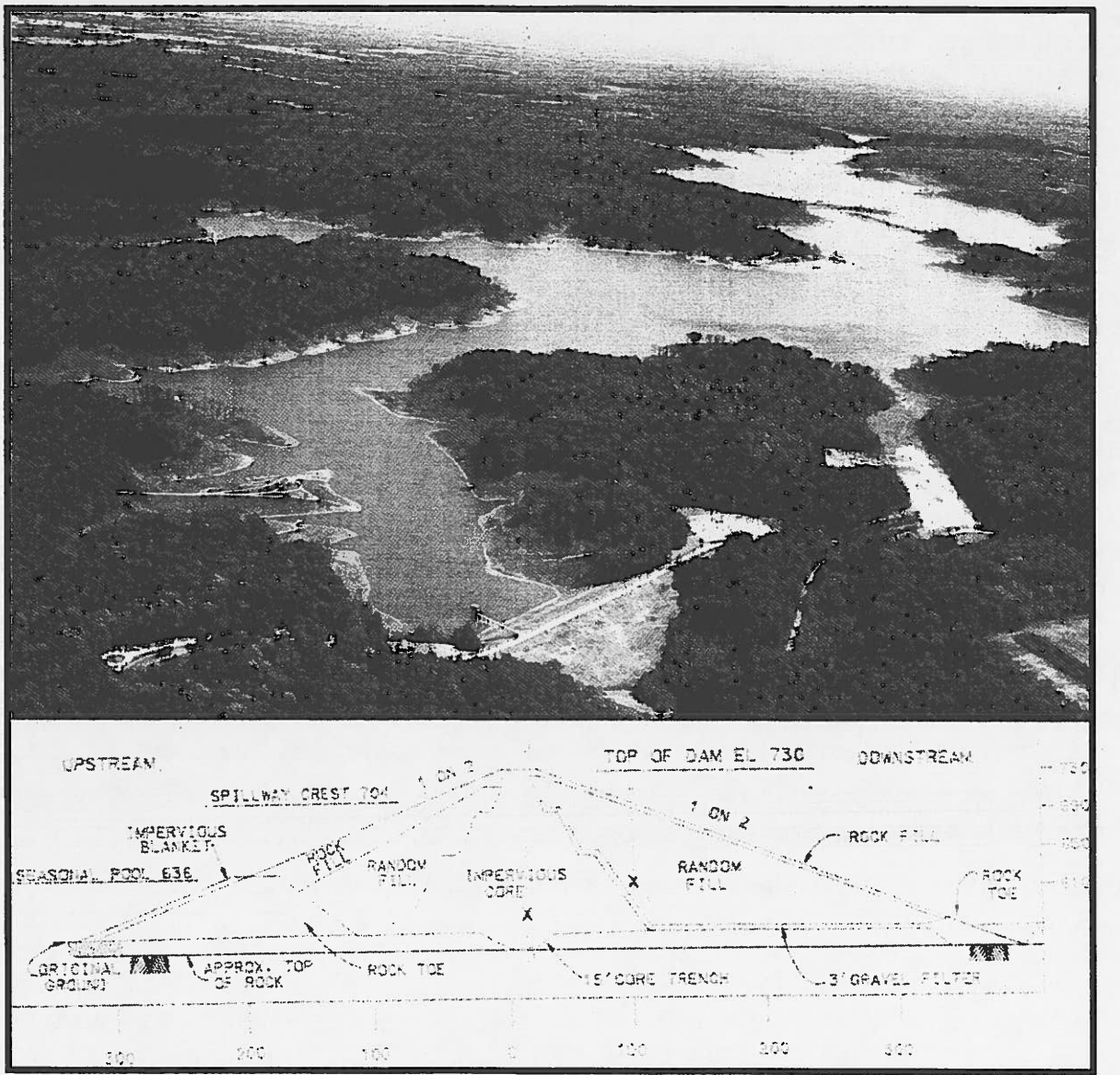

Figure 3. Aerial Photograph and Cross-Section of Cagles Mill Dam

EXAMPLE PROJECTS – C.M. Harden Lake Dam – Phase 1

C. M. Harden Lake Dam is located on Raccoon Creek in Parke County Indiana, 33 miles upstream of its confluence with the Wabash River and approximately 25 miles northeast of Terre Haute, Indiana. The dam is a rolled earth fill structure approximately 119 feet in height. The dam has a crest length and width of 1,860 feet and 30 feet, respectively. Both upstream and downstream slopes vary from 2.27 Horizontal (H) : 1 Vertical (V) near the crest to 3.5H:1V near the toe of the slopes. A 10-foot thick impervious blanket is present upstream of the dam. The blanket extends approximately 500-feet upstream of the toe and helps to limit underseepage. The dam foundation consists of cyclic sequences of sands and gravels varying in thickness from five feet at the abutments to approximately fifty feet in

the valley sections. The outlet works consist of a 153-foot tall concrete intake structure located near the right (west) abutment. A dike, which closes a low portion of the reservoir rim, is located approximately one-half mile southwest of the dam. The 1600–foot long dike is an earth fill structure with a maximum height of approximately 30 feet. During normal lake stages, the upstream toe of the dike is approximately 20 feet above the reservoir pool elevation. The dike foundation consists primarily of sandy lean clays having an approximate thickness of 100 feet.

Because C.M. Harden Lake Dam was founded on approximately 50 feet of alluvial sands and gravels (Figure 4), it was advanced to the Phase 1 level without completing a SSR. This permitted the timely collection of site specific information in a piece-wise fashion prior to initiating comprehensive studies. Once begun, the Phase 1 effort at this site included the following elements:

- Estimating subsurface conditions through a compilation of previous site characterization efforts that included rotary boring techniques with standard penetration tests and undisturbed sampling as well as seismic crosshole testing for shear wave velocity profiling;
- Describing the local and regional geologic structures, tectonic history, and physiographic characteristics of the C. M. Harden Lake area to provide the geologic and seismologic setting for the dam site;
- Recommending specific seismic source zones to be utilized for the project area;
- Establishing the Operating Basis Earthquake and Maximum Credible Earthquake by using deterministic methods;
- Developing the time histories and ground motions (accelerations, velocities and displacement) for both the OBE and MCE as well as the response spectra for both events;
- Predicting the shear stresses required to cause liquefaction within the embankment, foundation and in the dike using site specific geotechnical data;
- Summarizing the results of an earthquake response analysis for the site, and compares the shear stresses required to cause liquefaction with shear stresses induced by the design earthquakes;
- Predicting the permanent deformations of the embankment induced by the design earthquakes;
- Predicting the seismic response of the intake structure by utilizing a simplified lumped-mass two mode approximation.

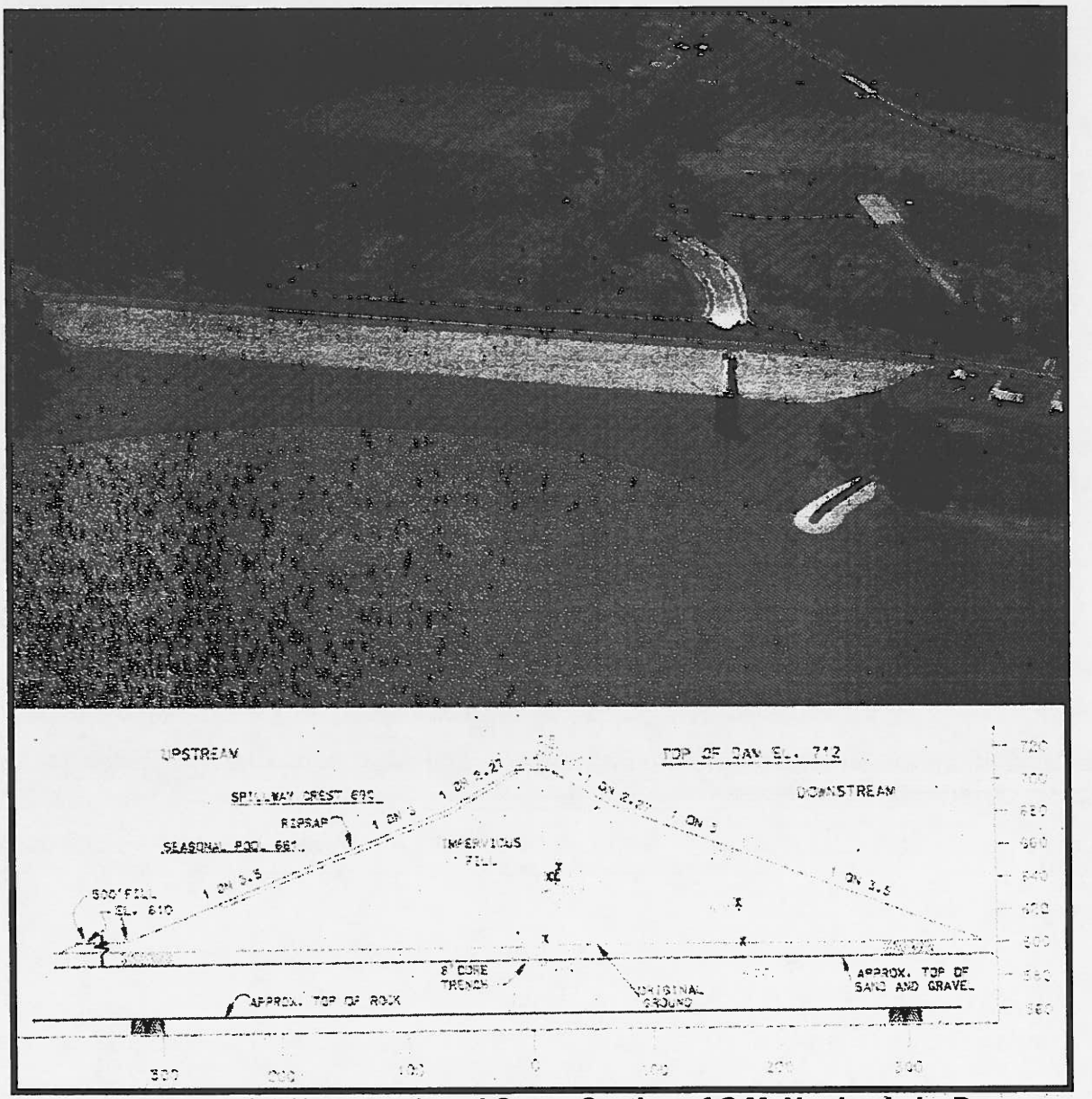

Figure 4. Aerial Photograph and Cross-Section of C.M. Harden Lake Dam.

During completion of the study, it was discovered that C. M. Harden Lake Dam is positioned within an area of Indiana exhibiting relatively moderate seismicity. No active faults are known to exist within the immediate vicinity of the site. The closet area of potential seismicity to the dam is the Wabash Valley Seismic Zone. Extensive reviews of the local and regional geology, tectonic history, local and regional seismicity as well as seismic risk hazards resulted in the definition of the Operating Basis and Maximum Credible Earthquakes for the C.M. Harden Lake Dam site as follows:

Operating Basis Earthquake

Magnitude	- 5.5
Modified Mercalli Intensity	- VII
Peak Horizontal Acceleration	- 0.14g
Peak Horizontal Velocity	- 3.1 cm/sec
Bracketed Duration of Event	- ≤ 5 sec

Maximum Credible Earthquake

Magnitude	- 6.2
Modified Mercalli Intensity	- VIII
Peak Horizontal Acceleration	- 0.21g
Peak Horizontal Velocity	- 4.7 cm/s
Bracketed Duration of Event	- ≤ 9 sec

A third design earthquake was also defined, and its impact to the site was evaluated because this event is estimated to have a 19 to 29 percent probability of occurring by the year 2035. The parameters modeled for this earthquake are as follows:

- Magnitude - 6.5
- Modified Mercalli Intensity - VI
- Peak Horizontal Acceleration - 0.02
- Peak Horizontal Velocity - 1.11 cm/s

Site specific soil profiles were developed using the results of drilling and foundation conditions beneath the dam and dike. All borings were drilled downstream of the dam centerline. As a result of the drilling and testing programs, zones of soil deposits were then identified as exhibiting the potential to liquefy when subjected to the design earthquake loads. The dam foundation was characterized as potentially liquefiable because it consists of SP and SM type materials. The normalized SPT N-values ranged from approximately 10 to 20 blows per foot and the shear wave velocity ranged from 600 feet per second (near the surface) to 1200 feet per second near the bedrock contact. Cyclic stress ratios and the ultimate shear stresses required to cause liquefaction within these deposits were estimated using corrected SPT N-values and empirical correlations between the modified N-values, cyclic stress ratios and overburden pressures. Earthquake response analyses were then conducted using the ProShake computer model. These analyses predicted the shear stresses that would be induced in the foundation soils when subjected to the design earthquakes.

The shear stresses predicted by the earthquake response analyses were compared to those required to cause liquefaction in order to determine a soil's susceptibility to significant strength loss. Safety factors against liquefaction were estimated for each deposit, as applicable. A soil was considered to undergo significant (>20%) strength loss if the estimated safety factor was less than or equal to 1.4. The results of these evaluations indicate that the foundation soils at the C.M. Harden Lake Dam site will not exhibit a tendency to liquefy (i.e. safety factors greater than 1.4) when subjected to the design earthquake loadings.

A Newmark-type analysis was performed to estimate the permanent deformation that the main dam may experience from the design earthquake events. As a result of this analysis, no significant permanent deformation of the embankment was predicted (i.e. the yield accelerations were greater than expected embankment accelerations). Additionally, the preliminary computations performed relative to the intake's ability to withstand design earthquake loadings indicate adequate capacity. From the results of the liquefaction potential and deformation computations, more in-depth seismic reviews of C.M. Harden Lake Dam at the Phase II level were not recommended.

EXAMPLE PROJECTS – Dewey Lake Dam – Phase II

Dewey Dam is positioned on John's Creek, in Floyd County, Kentucky, approximately five miles northeast of Prestonsburg. The dam is located 5.4 miles upstream from the confluence of John's Creek and Levisa Fork, which is 46.8 miles above the confluence of Tug and Levisa Forks, and 74 miles above the mouth of the Big Sandy River. The reservoir created by Dewey Dam is the central attraction of Jenny Wiley State Park. The 913 foot long dam is an impervious rolled embankment having a maximum height of 118 feet, a top width of 30 feet, and a base width of 680 feet. The design geometry of the upstream slope varies from 4H:1V to 2.5H:1V, while the downstream slope varies from 3H:1V to 2.5H:1V. The dam was founded on a cut-off trench excavated into rock at each abutment. The center section was founded on an alluvial deposit approximately 50 feet in thickness and consisting primarily of silty sands with lesser amounts of silts and clays.

Figure 5 illustrates an aerial photograph and typical section for the Dewey Dam embankment. The scope of work for analyzing the existing condition performance of Dewey Dam included liquefaction potential evaluations using state of the art procedures. These evaluations were performed using both SPT and seismic cone penetration (SCPT) tests conducted as a part of 1984-1985, 1996 and 1998 geotechnical explorations. The explorations indicate that the foundation of Dewey Dam consists of loose sands (SM type materials) having SPT N-values as low as 4 near the embankment toes, and shear wave velocities as low as 400 feet per second. Both the Operating Basis Earthquake (OBE) and MCE were utilized in the existing condition analysis. The OBE was a natural event (Perry Plant Time History) while the MCE was a scaled version of the 1971 San Fernando earthquake having a peak acceleration of 0.18g (and a low frequency). The lateral and vertical extents of potentially liquefiable materials and appropriate soil strengths for further dynamic stability and deformation analyses were estimated. Assessments of impacts of recently collected (1996 and 1998) data on liquefaction potential evaluations, changes in the state of the art prior to the last evaluation, and comparisons between SPT and SCPT results were part of the scope of work. The results of this work illustrated that Dewey Dam could potentially permit uncontrolled release of the pool during a severe earthquake event. The results of the existing condition analyses were assembled in an "Interim Summary Report" which briefly outlined the methodology and results of liquefaction potential evaluations and material parameter selections. Plan, profile and cross-section drawings were prepared to convey the results of the calculations and the limits of liquefiable materials. The Interim Summary Report was presented to USACE-LRH (Huntington District COE) and Dr. W.D.

Liam Finn of PEACS, Ltd. in a joint meeting held in Vancouver, British Columbia. Dynamic stability and deformation analyses of the existing embankment and foundation soils comprising Dewey Dam were then performed using large strain formulations in the TARA programs [Finn et al, 1986, 1989]. Additionally, bearing capacity and settlement analyses of the existing facility using dynamic strength parameters were completed. The results indicate large deformations (>60' upstream) and crest settlements (20'-40').

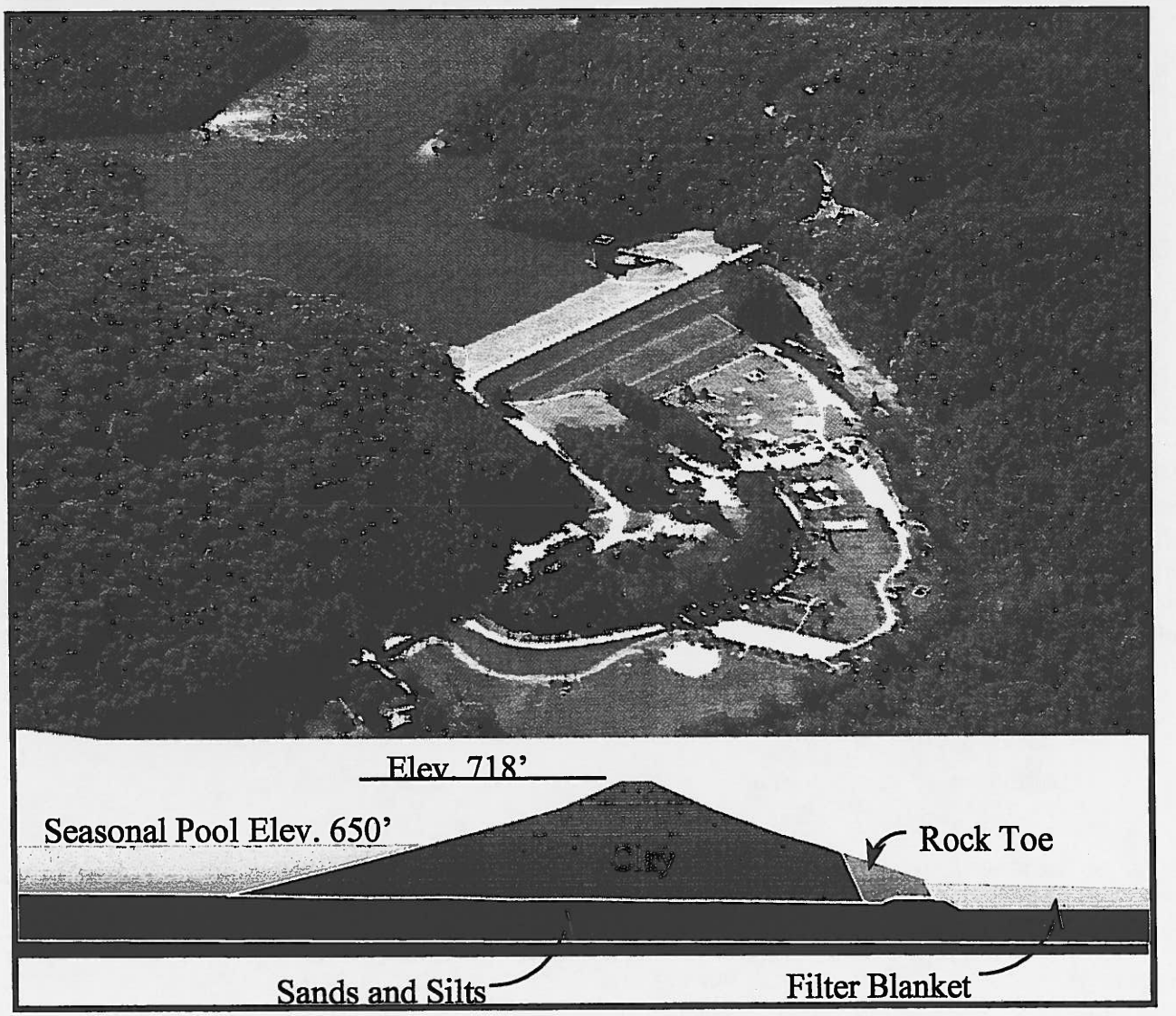

The results of the analyses performed by PEACS, Ltd. and the Interim Summary Report prepared by FMSM were utilized, along with available project data, to prepare a "Concept Meeting Review Package". The package was supplied to two seismic rehabilitation experts, one seismic expert facilitator, and a panel of USACE-LRH and FMSM personnel. The panel then met in Cincinnati, Ohio for a one-day "Concept Meeting". The meeting goal was to brainstorm all possible alternatives and then identify the three remediation options most worthy of further study.

After reviewing the existing conditions and establishing the ground rules for the conduct of the meeting, the panel of USACE-LRH representatives, seismic experts and FMSM proceeded into a brainstorming session. Solutions proposed by the group are shown below.

Summary of Proposed Remediation Concepts			
No.	Description	No.	Description
1.	Grout foundation soils	14.	Explosive compaction
2.	Upstream berm and shear key	15.	Dynamic compaction downstream
3.	Sheet pile structures	16.	Anchor tie downs
4.	Stone columns	17.	Armoring downstream slope
5.	Vibro-compaction	18.	Remove and replace foundation soils
6.	Piles (augured, pipe, concrete, H-piles)	19.	Raise embankment crest elevation
7.	Downstream berm with drain	20.	Upstream internal tieback wall
8.	Strengthen downstream (includes berms)	21.	Drainage boundary improvement
9.	Strengthen downstream foundation soils	22.	Gallery drain in foundation soils
10.	Continuous internal caissons	23.	Gallery drain in dam
11.	Flatten slopes	24.	Micro-tunneling
12.	Deep soil mixing	25.	Temporary upstream de-watering
13.	Jet grouting	26.	Anchored slab on grade

After breaking the proposed alternatives into four categories (stabilize upstream section, add to dam geometry, improve downstream section and improve foundation soils), attendees were asked to fill out an evaluation matrix. The purpose of the matrix was to get the attendees thinking about the available possibilities for various alternatives. Alternatives were scored under each of the four main categories mentioned above using the following criteria:

- Adversely affect facility during construction.
- Confidence in alternative.
- Constructibility.
- Eliminate liquefaction.
- Mitigate settlement.
- Limit slope stability problems / lateral displacement.
- Control seepage.
- Minimize costs.
- Pool constraints during construction.

Scores were to be 1 for least confidence and 5 for most confidence in a particular solution or alternative. Participants were asked to put a dash for unfamiliar categories. A weighted average was calculated for categories where respondents placed a dash. Normalized composite scores were reduced by all attendees. The five highest scoring alternatives were chosen for further discussion by the group. These alternatives included:

1. Downstream berm with filter drain.
2. Compaction piles.
3. Piles (Upstream).
4. Stone Columns (Upstream).
5. Stone Columns (Downstream).

The primary purpose of the evaluation matrix was to start the group considering all the available alternatives. After further discussion, debate and combining particular alternatives from the evaluation matrix, the group narrowed the field of options to three worthy of further study. Final suggested solutions generated by the group are as follows (Option 1 was added in the final debate of which alternatives to evaluate):

- Option 1 - Upstream cellular sheetpile structure.
- Option 2 - Upstream stone columns.
- Option 3 - Upstream stone columns, downstream berm, filter and shear key.

The group agreed that all options could be combined with an upstream berm, if necessary, to achieve global stability.

Each of the three options identified in the concept meeting were evaluated based on relevance to the site, operation and maintenance constraints, constructibility, dynamic performance, seepage, stability and capital construction costs. The dynamic stability and deformation characteristics of each option were assessed by PEACS, Ltd. using the large strain finite element formulations in the TARA programs [Finn, et al, 1986, 1989]. The seepage and stability impacts were quantified using limited empirical relationships based on published data. At the completion of the dynamic analyses, the options were revised, as appropriate, to improve dynamic performance. Conceptual drawings showing each alternative in plan, profile and cross-section were prepared along with relevant details. Finally, capital construction cost estimates and ranking of the alternatives based on evaluation factors were completed.

FMSM's opinions regarding the various options were formulated into a ranking scheme, specifically geared toward scoring the options in an objective fashion. The primary evaluation items were assembled, assigned a score of zero through ten, and then weighted. A score of zero represented the worst performance in a particular category while ten represented the best. Capital construction cost and dynamic performance were weighted the highest with 20 percent. Constructibility and permanence were assigned a weight of 15 percent, while

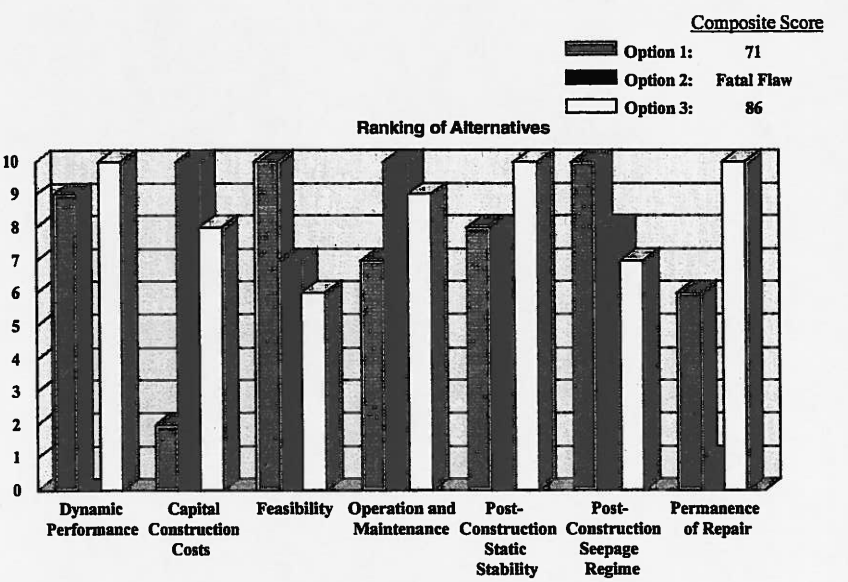

Figure 5. Ranking of Alternatives.

the remaining factors were assigned a weight of ten percent. Because Option 2 performed poorly and was demonstrated to possibly permit catastrophic failure of the dam, it was considered to have a "fatal flaw". Consequently, the scores for this option were not totaled. Based on the simple rating scheme, it appears that Option 3 is the most promising concept as shown in Figure 5.

Closure

This paper presented the USACE's typical approach for assessing seismic safety of their dams. The approach consisted of four basic steps from a screening analysis all the way to final design. These steps were illustrated through the use of case histories of the Cagles Mill, C.M. Harden, and Dewey Lake Dam projects. Primary influencing factors on the advancement of a project through the evaluation process include the presence and consistency of liquefiable materials in the embankment or foundation, and the seismologic setting. Projects that are demonstrated to be safe, such as C.M. Harden Lake Dam, can be eliminated from further study. Other projects appropriately advance through the study process.

Bibliography

1. Finn, W.D. Liam, Yogendrakumar, M., Yoshida, N., and Yoshida, H., (1986). "TARA-3: A Program for Nonlinear Static and Dynamic Effective Stress Analysis", Soil Dynamics Group, University of British Columbia, Vancouver, B.C., Canada.
2. Finn, W.D. Liam, Yogendrakumar, M., (1989). "TARA3-FL: Program for Analysis of Liquefaction Induced Flow Deformations", Department of Civil Engineering, University of British Columbia, Vancouver, B.C., Canada.
3. ER 1110-2-1155, Dam Safety Assurance Program, United States Army Corps of Engineers, September 12, 1997.

OVERVIEW OF SITE-SPECIFIC SEISMIC STUDIES

David Bentler, Ph.D.[1] and Greg Yankey, P.E.[2]

ABSTRACT

Over the last two decades, the awareness of earthquake hazards in the Central and Eastern United States has increased dramatically. Therefore, many geotechnical-oriented projects in this region now include a component that estimates the seismic hazard at a particular site and for a specific structure. This paper focuses on the methodology typically employed in site specific seismic studies. Regulatory requirements observed by the United States Corps of Engineers, Bureau of Reclamation, highway officials and other sources will be summarized and contrasted in terms of approach and acceptable risk. An overview of the results of several site specific studies conducted in the Ohio River Valley will be provided. Finally, a summary of pitfalls encountered in practice by the authors will be given. These will include issues ranging from the study methodology to the use of ground motion time histories.

INTRODUCTION

Over the last 150 years, we have be fortunate to observe only a few damaging earthquakes in the Central and Eastern United States (Figure 1). In the last ten years, paleoliquefaction data has revealed that certain areas of the Ohio River Valley region have experienced periodic large events (Munson et al., 1997; Obermeier et al., 1992; Pond and Martin, 1997). Awareness of the seismicity of the New Madrid Seismic Zone has also increased in recent years (Street and Nuttli, 1990; Street and Green, 1984). Consequently, state and federal governments now recognize earthquake hazards in this region as low probability – high consequence events. With this new awareness, new structures and retrofits of existing structures are now designed to resist ground motions based on our current understanding of seismic hazards. The methodologies dictated by governing agencies vary significantly from the use of national seismic hazard maps to sophisticated, site-specific studies. Accordingly, the regulatory requirements on acceptable levels of seismic risk are expected to differ substantially depending on the agency and consequence of failure. With these differing methodologies and requirements on acceptable risk, the results of seismic studies performed for projects that are in the same general vicinity can often be significantly different. Some of the inconsistencies may be attributable to site differences, but often the majority is due to specific criteria and methodology utilized. There is often disproportionate conservatism for structures that offer little risk to society in the event of a failure. The challenge in the coming years will be for state and federal governments to derive a uniform means to assess seismic hazards and implement design standards that are consistent with the risk to society.

[1] Senior Geotechnical Engineer, Fuller, Mossbarger, Scott and May Engineers, Inc., Lexington, Kentucky
[2] Associate, Fuller, Mossbarger, Scott and May Engineers, Inc., Lexington, Kentucky

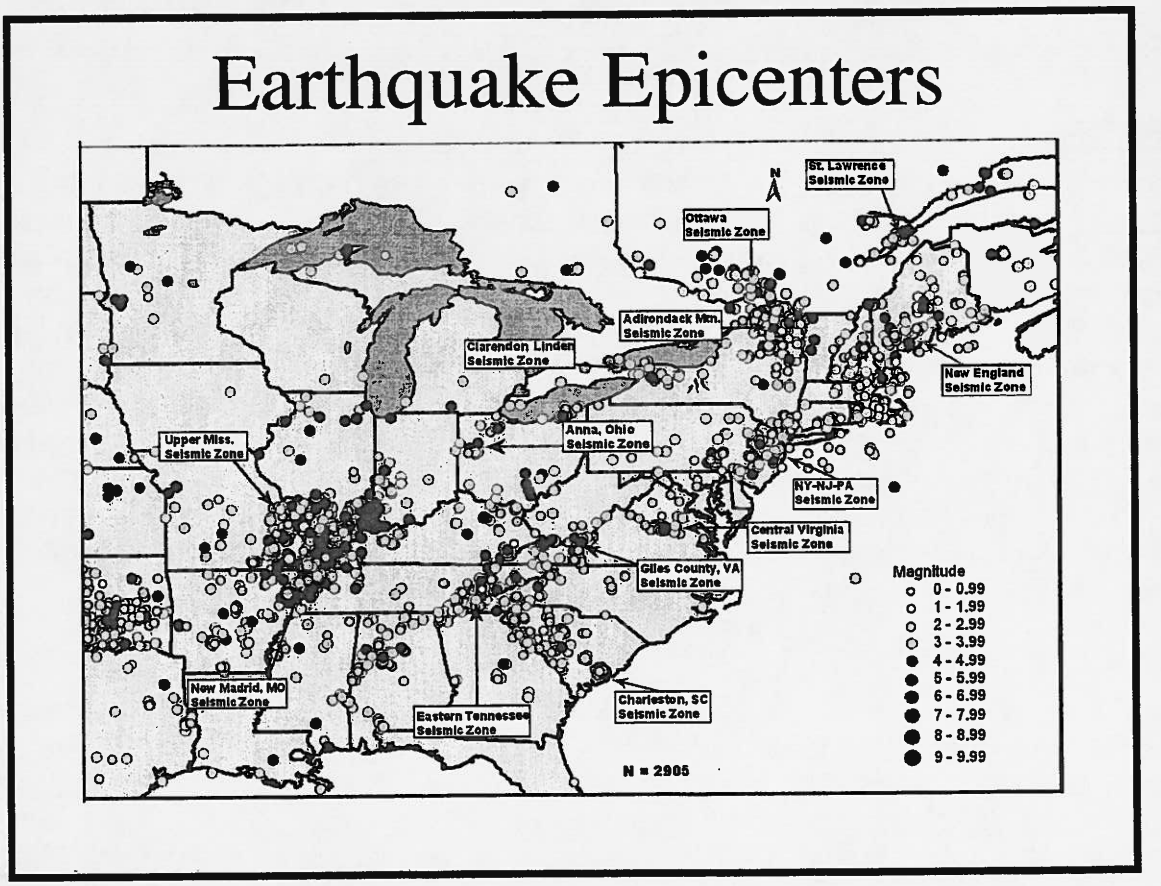

Figure 1 Earthquake Epicenters and Magnitudes in the Central and Eastern United States

Methodologies

National Seismic Hazard Maps

The National Earthquake Hazard Reduction Program (NEHRP) Maps are prepared by the United States Geological Survey for the Building Seismic Safety Council of FEMA, the Federal Emergency Management Agency (Building Seismic Safety Council, 1998a). The purpose of NEHRP maps is to reduce earthquake risks in the United States by improving the design and construction of new buildings. The NEHRP maps are used in the seismic design portions of the International Building Code and International Residential Code.

The USGS maps, which are described by Frankel et al. 2000, provide the basis for the NEHRP maps (USGS, 2001). The complete NEHRP map set, can be obtained at no cost from the FEMA Report Distribution Center by calling 1-800-480-2520. The 1997 and 2000 *NEHRP Recommended Provisions for Seismic Regulations for New Buildings* are also available on line at http://www.bssconline.org. The NEHRP maps can also be downloaded in electronic format from the USGS ftp site ftp://ghtftp.cr.usgs.gov/pub/hazmaps/design/nehrp/. The USGS Earthquake Hazard Mapping Program web site provides interactive maps.

Engineers can use the NEHRP maps to roughly assess earthquake risks to a project. However, the NEHRP maps do not consider the influence of site conditions on ground motions.

Deterministic Seismic Hazard Analysis

Deterministic seismic hazard analyses (DSHA) are often employed as a basic technique to complete a site-specific seismic study. Figure 2 illustrates the four steps of a DSHA. These four steps can be summarized as follows:

1. Define the earthquake source or sources. These may range from clearly understood and defined faults to area sources that are not well understood (typical of central and eastern United States).
2. Select the maximum earthquake from the sources defined in Step 1. This could be the largest earthquake that could reasonably be expected or some other definition. The criterion chosen is one of the most important elements in determining the general level of conservatism. Along with the selected earthquake(s), source to site distances are also identified.
3. Obtain the ground motion characteristics at the site for the earthquake event identified in step 2. Considerations include attenuation of ground motion, which is a function of source to site distance, earthquake magnitude, and dynamic properties of the geo-materials along the travel path of the seismic waves.
4. Define the hazard at the site in terms of peak acceleration, velocity and/or displacement for the design earthquake.

DSHA provides a very direct approach to determining seismic hazard, however it involves some subjective judgements of the seismologists, seismic geologists, engineers, and others involved in the study. Kramer, 1997 and Reiter, 1990 provide additional details on DSHA.

A key step in a DSHA is the selection of the maximum or design earthquake event (i.e. step 2). Because the selection of the maximum earthquake event has a large influence on the calculated hazard, many of the agencies that utilize DSHA provide guidance for this step. Terms such as maximum credible earthquake (MCE), design base earthquake (DBE), safe shutdown earthquake (SSE), maximum design earthquake (MDE), and operating basis earthquake (OBE) are often used by agencies to guide the selection of a controlling earthquake event that is consistent with the role of the project. Some of these terms are unique to particular agencies or industries, while others are common. One must be aware that although two agencies may use the same or a very similar term, the term may be defined differently. Definitions of the relevant controlling earthquake term are usually provided, but are subject to the interpretation and judgement of the person(s) performing the DSHA.

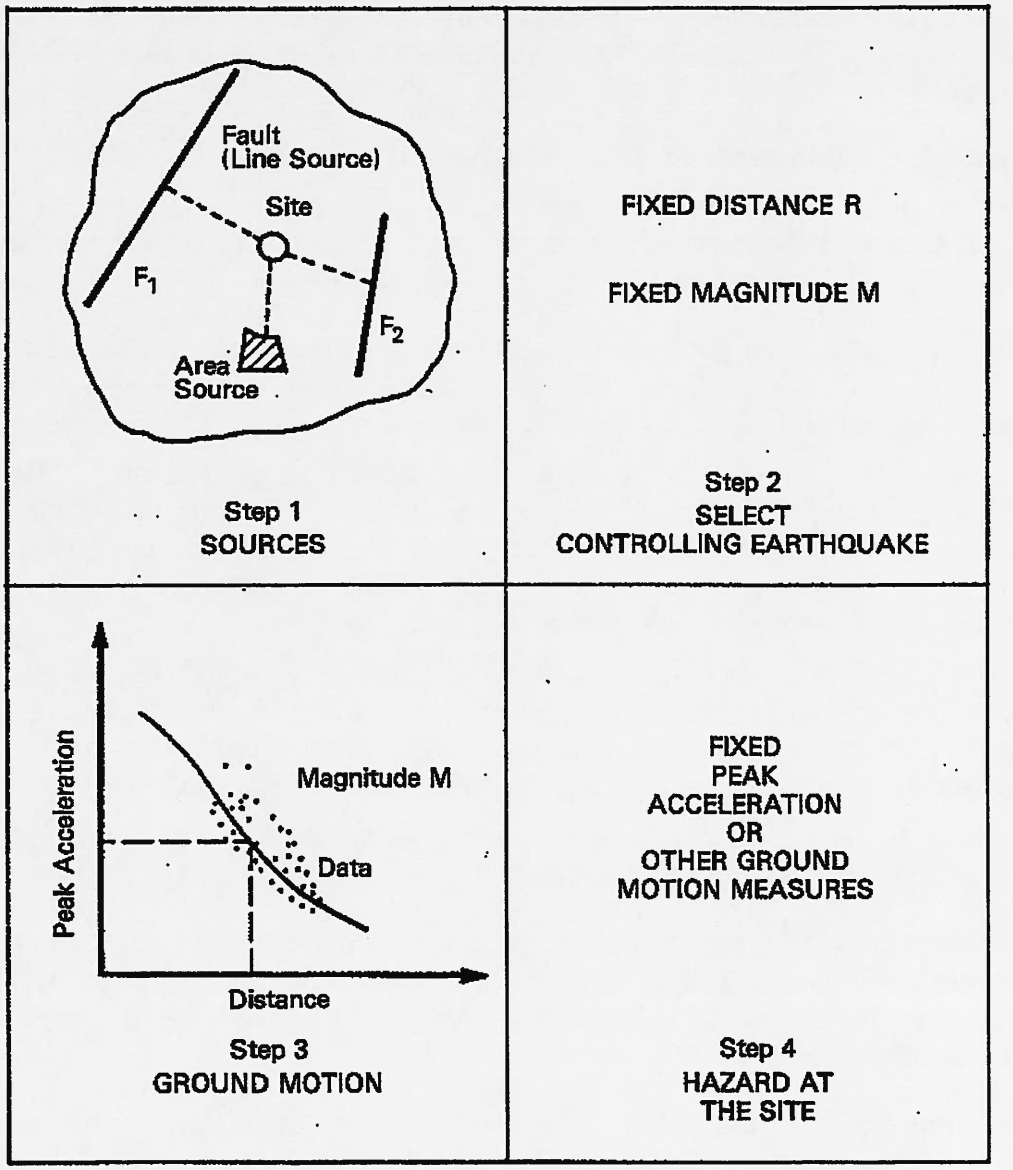

Figure 2 Basic Steps in a Deterministic Seismic Hazard Analysis (after Reiter, 1990)

Probabilistic Seismic Hazard Analysis

Some of the uncertainties involved in a seismic hazard analysis include the size, location, recurrence rate of earthquakes, and variations in ground motions. The DSHA methodology does not address these uncertainties. Probabilistic seismic hazard analysis (PSHA) utilizes probabilistic theory to account for these uncertainties when characterizing seismic hazard. The basic steps of the PSHA are shown in Figure 3 and are described as follows:

1. Define the earthquake sources. This is generally similar to Step 1 of the DSHA.

2. Define the recurrence rate for earthquake of various magnitudes from each source. This is fundamentally different than Step 2 of the DSHA where only maximum magnitude events are prescribed.
3. Estimate the effects at the site for multiple earthquakes from each source.
4. Identify the seismic hazard at the site. This step is substantially different from the DSHA. In this case, the effects of all the earthquakes of various sizes, occurring at different locations at different probabilities of occurrence, are integrated into one relationship that shows the probability of exceeding different levels of ground motion at the site during a specified time period.

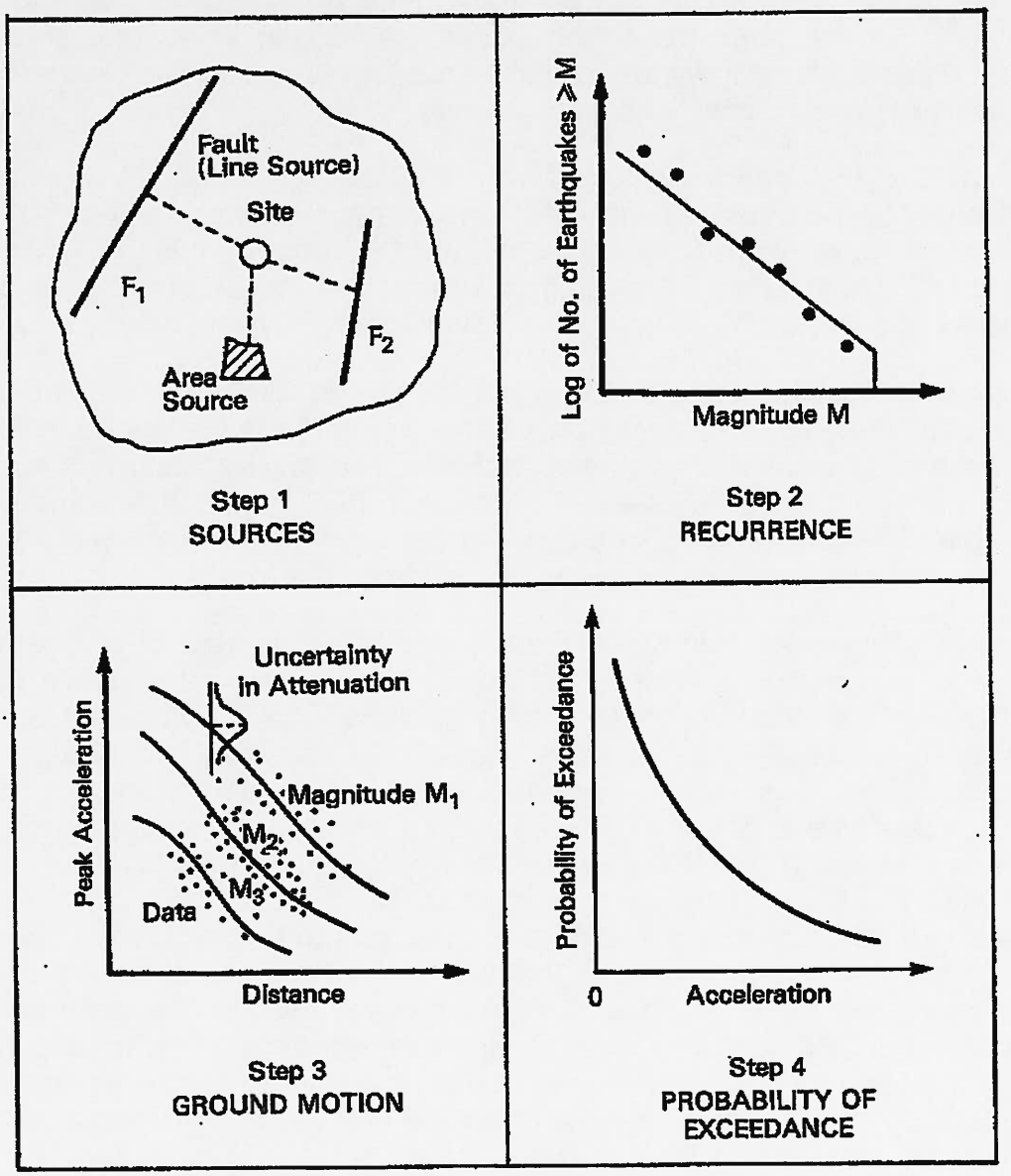

Figure 3 Basic Steps in a Probabilistic Seismic Hazard Analysis (after Reiter, 1990)

All of the uncertainties in a seismic hazard analysis can not be addressed with the probabilistic calculations in a PSHA. PSHA require that the person(s) performing the study make decisions that are subject to uncertainty. For example, there is often more than one characterization of earthquake sources that is reasonably consistent with the available information. Logic trees are often employed in PSHA as a means to incorporate multiple models for decision factors such as earthquake sources and attenuation models.

Regulatory Requirements

Requirements of different agencies for the performance of site specific seismic studies vary greatly. Agencies are separated into two categories, "self-regulated" and "review", for the purposes of this paper. A number of various entities are discussed within each category to provide the reader with background information on basic requirements and acceptable levels of risk.

Self-regulated agencies include those which 1) own and operate their structures, 2) establish their own methodologies and 3) indicate acceptable levels of risk. The United States Army Corps of Engineers (USACE) and Bureau of Reclamation (USBR) fit into this category. The structures that these entities provide oversight of during design, construction and operation include locks and dams among others.

Review agencies include those that regulate the design, construction and operation of certain structures, but they do not own them. Typical review agencies include the Mine Safety and Health Administration (MSHA), Nuclear Regulatory Commission (NuREG), Federal Energy Regulatory Commission (FERC), and state transportation departments. The requirements vary considerably among these agencies, partly due the inherent risk of failure but also due to other inconsistencies.

The Corps of Engineers indicate that usual studies will consist of a deterministic element and a probabilistic element (USACE, 1995). The deterministic study is utilized to select the maximum credible earthquake (MCE). The probabilistic study is normally used to identify the operating basis (OBE) and maximum design (MDE) earthquakes. The MCE is not associated with a return period and the MDE is typically a lesser event than the MCE. The OBE and MDE are usually defined as having return periods of 144 and 950 years, respectively. Some latitude is provided for the latter such that risks can be consistent with economic considerations. Structures are divided into the categories critical and non-critical. Generally speaking, critical structures are those that will likely cause loss of life if they failed. All other structures are non-critical. Critical structures must be designed to remain functional for the OBE, and they must survive and remain safe (i.e. no uncontrolled release of the pool) for the MCE. Non-critical structures must remain functional after the OBE and survive the MDE. People unfamiliar with the classification scheme are often surprised when they learn that large projects such as Olmsted Lock and Dam and J.T. Myers Lock and Dam, two large projects on the Ohio River Navigation System, are classified as non-critical.

The Bureau of Reclamation utilizes a risk-based approach that is keyed to the estimated average annual loss of life. Two tiers are identified with Tier 1 relating to loss of life and Tier 2 dealing with public trust issues and their entire dam inventory. Under Tier 1, three levels of estimate average annual loss of life are indicated. Greater than 0.01 lives per year (or one life per 100 years) is considered as strong justification for short term and long term measures to increase safety. Between 0.01 and 0.001 lives per year is considered strong justification for implementation of long term measures. Less than 0.001 lives per year is indicated to have a diminished justification. Corrective action costs, uncertainties in the loss of life estimate and other issues play an increased role in decision making. Tier 2 guidelines recognize that dam failures and associated large consequences need to be avoided because public trust is jeopardized resulting in costly increases in their expectations. This tier also considers the entire dam inventory and the fact that the risk of failure of any one of their dams if related to the number of dams at the time of exposure. The end result is that each dam is expected to have a maximum combined (all failure mechanisms including earthquake) annual probability of failure of 1 in 10,000.

The Mine Safety and Health Administration regulates numerous coal slurry dams. The federal regulations do not specify a return period for the design earthquake, but rather rely on standard engineering practices. As a result, most engineers define a MCE for use in design.

The Nuclear Regulatory Commission defines an OBE and a SSE, or a safe shutdown earthquake. The OBE is generally an event occurring once every 100 years and the SSE is expected to occur once every 10,000 years. The OBE cannot be less than one-half the SSE in terms of peak horizontal acceleration. The facility is expected to remain functional with the OBE and no release of harmful components with the SSE.

The Federal Energy Regulatory Commission (FERC) oversees many hydropower facilities throughout the United States. FERC relies heavily on USACE guidelines, but prefer to solely utilize DSHA methods.

The American Association of State Highway and Transportation Officials (AASHTO) provides guidelines for the design of highway systems. Embankments, roadways and bridges are to be designed for a single event having a return period of 475 years. Site specific studies are not required and national hazard maps are commonly used to provide design ground motion parameters. On larger projects, site-specific studies are sometime undertaken when site conditions or economic considerations dictate.

Finally, the Environmental Protection Agency (EPA) provides federal regulations for the design and construction of solid waste landfills. Guidance by the EPA, and subsequently adopted by many states including Kentucky, indicates that solid waste landfills should be designed for the maximum horizontal acceleration (MHA) in lithified material at a site for an earthquake having a return period of 2,475 years. The MHA can be obtained from the NEHRP maps or a site-specific study.

Table 1 summarizes the requirements of the agencies considered in this paper.

Table 1. Overview of Seismic Study Requirements								
Agency	Study Elements		Basic EQ Risk Levels			Return Periods (years)		
	DSHA	PSHA						
Self Regulated								
USACE	√	√	OBE	MDE	MCE	144	950	N/A
USBR		√	Risk Based - Related to Average Annual Loss of Life					
Review								
MSHA	√		N/A	N/A	MCE	N/A	N/A	N/A
NUREG		√	OBE	N/A	SSE	100	N/A	10,000
FERC	√		OBE		MCE	144	N/A	N/A
AASHTO		√	Single Event			475		
EPA		√	Single Event			2,475		

Site Specific Study Results

Selected results of site specific seismic studies from the various agencies listed in Table 1 are provided in this section. These results are presented in terms of peak ground acceleration for the various design events as shown in Table 2 and are depicted graphically in Figure 4.

Table 2. Overview of Site Specific Seismic Study Results						
	OBE		MDE		MCE	
Project	PGA (g)	Magnitude	PGA (g)	Magnitude	PGA (g)	Magnitude
1. Muskingum	0.10	5.2 M_b	N/A		0.15	5.5 M_b
2. Haysi	0.01	5-6.5 M_b	0.10	5-6.5 M_b	0.32	6.3 M_b
3. Dewey	0.09	4.9 M_b	0.15	5.3 M_b	0.17	5.5 M_b
4. Marmet L&D	0.01	5-6.5 M_b	0.08	5-6.5 M_b	0.32	6.3 M_b
5. Bluestone	0.14	N/A	N/A		0.29	N/A
6. Fishtrap	0.05	4.5 M_b	N/A		0.10	5.2 M_b
7. Monroe	0.15	5.5 M_b	N/A		0.19	6.2 M_b
8. C.M. Harden	0.15	5.5 M_b	N/A		0.23	6.2 M_b
9. J.T. Myers L&D	0.02-0.03	5-6.5 M_w	0.08-0.17	6-7.5 M_w	N/A	
10. Bridge in Western Ky.	Example: Uniontown Bridge – PGA = 0.07g					
11. SWL in Western Ky.	Example: Uniontown Solid Waste Landfill – PGA = 0.13g					

Table 2 illustrates a relatively large difference in the design peak ground acceleration for the various sites. In particular, the differences in projects 9, 10 and 11 is significant. J.T. Myers Lock and Dam is a pivotal lock and dam on the Ohio River near the confluence with the Wabash River. A tremendous amount of barge traffic passes through its locks every year. Project 10 is a hypothetical bridge at the same

site with a PGA selected from the latest National Earthquake Hazard Reduction Program (NEHRP) maps. Project 11 is a hypothetical solid waste landfill at the same site with a PGA derived from the same mapping.

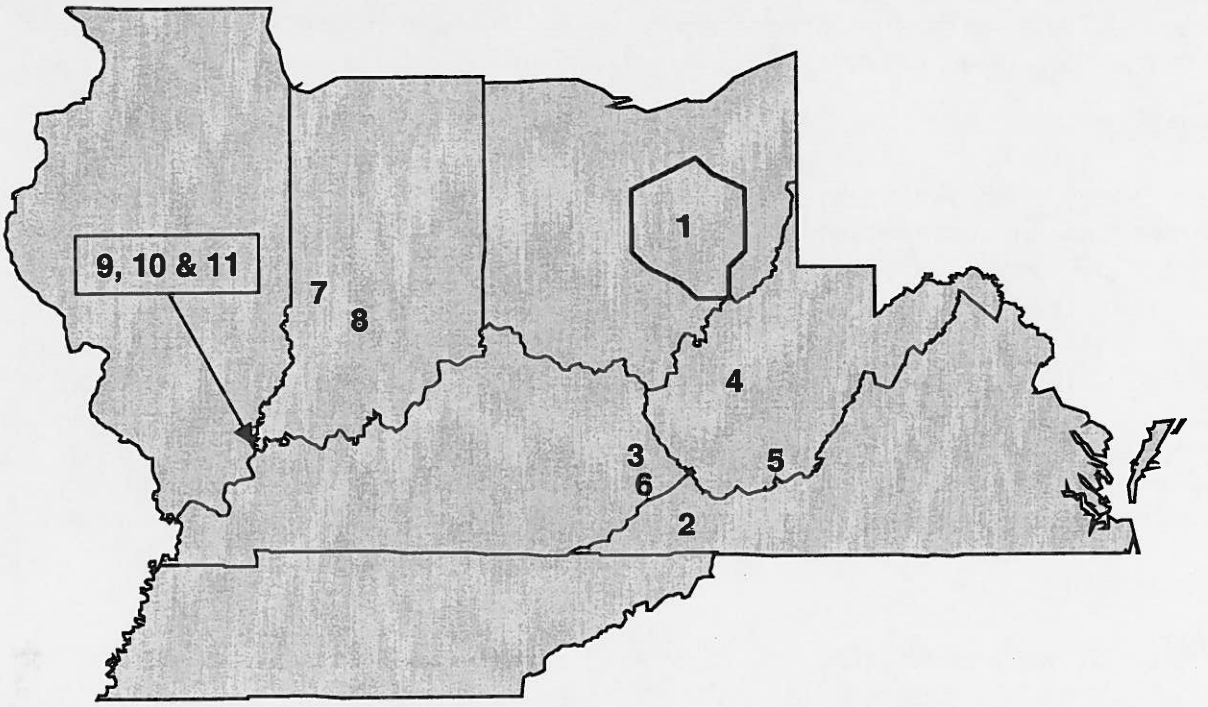

Figure 4 Locations of Projects in Table 2.

It is evident from Table 2 that some disparity exists between structures that offer little risk to the general population if they failed and those that do. Further differences exist in economic considerations in the event of a failure. Specifically, project 9, 10 and 11 illustrate this point. A solid waste landfill (11) would be designed to resist earthquake loadings greater than a nearby bridge and potentially greater than project 9 – a major lock and dam on the Ohio River.

PITFALLS

The biggest pitfalls encountered by the authors include:

- Failure to establish earthquake ground motions prior to initiating the design of critical project elements – this will always result in costly delays.
- Because much of the field of seismicity is subjective, gaining consensus among experts involved in a seismic hazard analysis is sometimes difficult. Peer reviews are almost always complicated by this problem.
- Selected earthquake time histories are sometimes inconsistent with the tectonic region and they have unrealistic accelerations, velocities and/or displacements.

- Failure to be familiar with the requirements of the governing agency for which you are preparing the seismic study. Many times, differences in methodology exist that are significant.

- Unfamiliarity with the processes used to develop the NEHRP maps and terminology used in the maps can lead to misinterpretation.

SUMMARY

Methodologies for assessing site specific ground motions at a particular civil project site typically include deterministic and probabilistic techniques. Some agencies employ one and/or both of these techniques depending on their expectations for design requirements and the degree of subjectively they will allow in specifying ground motions. These expectations are often different and they commonly lead to disproportionate conservatism for sites that offer little risk to the general population.

The challenge for state and federal governments in the coming years is to derive a uniform means to assess seismic hazards and implement design standards that are consistent with the risk to society.

REFERENCES

Building Seismic Safety Council (1998a). NEHRP Recommended Provisions for Seismic Regulations for New Buildings and Other Structures, Part 1 - Provisions, 1997 Edition, FEMA 302, Washington, D. C.

Building Seismic Safety Council (1998b). NEHRP Recommended Provisions for Seismic Regulations for New Buildings and Other Structures, Part 2 - Commentary, 1997 Edition, FEMA 303, Washington, D. C.

Frankel, A.D., Mueller, C.S., Barnhard, T.P., Leyendecker, E.V., Wesson, R.L., Harmsen, S.C., Klein, F.W., Perkins, D.M., Dickman, N.C., Hanson, S.L., and Hopper, M.G. (2000). "USGS National Seismic Hazard Maps", Spectra, Earthquake Engineering Research Institute, Oakland, CA.

Kramer, S.L. (1996). "Geotechnical Earthquake Engineering", Prentice-Hall, New Jersey.

Munson, P.J., Obermeier, S.F., Munson, C.A. and Hajic, E.R. (1997). "Liquefaction Evidence for Holocene and Latest Pleistocene Seismicity in the Southern Halves of Indiana and Illinois: A Preliminary Overview", Seismological Research Letters, v. 68, p. 521-536.

Obermeier, S.F., Munson, P.J., Munson, C.A., Martin, J.R., Frankel, A.D., Youd, T.L. and Pond, E.C. (1992). "Liquefaction evidence for strong Holocene earthquake(s) in the Wabash Valley of Indiana-Illinois", Seismological Research Letters, v. 63, p. 321-335.

Pond, E.C. and Martin, J.R. (1997). "Estimated Magnitudes and Accelerations Associated with Prehistoric Earthquakes in the Wabash Valley Region of the Central United States", Seismological Research Letters, v. 68, no. 4, p. 611-623.

Reiter, L. (1990). "Earthquake Hazard Analysis - Issues and Insights", Columbia University Press, New York, New York.

Street, R. and Green, R.F. (1984). "The Historical Seismicity of the Central United States - 1811-1928", U.S. Geological Survey, Report Contract No. 14-08-001-1251.

Street, R. and Nuttli, O.W. (1990). "The Great Central Mississippi Valley Earthquakes of 1811-1812", Kentucky Geological Survey, Special Publication 14, Series XI, 1990.

U.S. Army Corps of Engineers (1970). "Engineering and Design – Stability of Earth and Rockfill Dams", U.S. Army Corps of Engineers, Engineering Manual 1110-2-1902 (April 1, 1970).

U.S. Army Corps of Engineers (1995). "Earthquake Design and Evaluation for Civil Works Projects", U.S. Army Corps of Engineers, Engineering Regulations 1110-2-1806 (July 31, 1995).

United States Geological Survey National Seismic Hazard Mapping Project Home Page. http://geohazards.cr.usgs.gov/eq/html/nehrp.html

Earthquake Assessment of Typical Transportation Geotechnical Systems

Shamsher Prakash
University of Missouri-Rolla
Rolla, Missouri, 65409 - USA

(THIS PRESENTATION IS BASED ON PAPER NO 8.I3 TO THE FOURTH INTERNATIONAL CONFERENCE ON GEOTECHNICAL EARTHQUAKE ENGINEERIG AND SOIL DYNAMICS , SAN DIEGO CA MARCH 25-31, 2001_)

Abstract

The Missouri Department of Transportation initiated a study of an "emergency vehicle priority access". Detailed earthquake site assessments have been conducted for two critical US 60 roadway bridge sites (Wahite Ditch and St. Francis River Bridge). Liquefaction potential, slope stability, abutment stability, and structure stability analysis were performed at both sites for selected "worst case scenario synthetic bedrock ground motions" based on New Madrid source zone earthquakes with 2% and 10% probabilities of exceedance in fifty years. Site assessments indicate that both the Wahite Ditch and St. Francis River bridges could be rendered unusable by strong ground motion with a 2% probability of exceedance in the next fifty years.

INTRODUCTION

Southeast Missouri experiences relatively small magnitude earthquakes on a regular basis, and is the site of several of the largest magnitude earthquake events to strike North America in recorded history. Experts agree that similar (or greater magnitude) earthquakes will strike this region again. Geologic conditions in southeast Missouri are such as to make this region one of the most seismically susceptible in the country, based on its damage potential from intrinsically susceptible soil, high water levels and vast expanses of flood sensitive ground. If a high magnitude earthquake struck southeastern Missouri today, infrastructure could be devastated. Levees and dams could be breached, bridges across the Mississippi and Meramec rivers could collapse or be otherwise rendered unusable, extended sections of highway would be closed by landslides, floods, soil liquefaction, and the failure of roadway bridges and overpasses. The network of facilities and services required for commerce and public health in south St. Louis, Sikeston, Cape Girardeau and surrounding communities could be devastated. Utilities, including electrical power, communications, oil and gas distribution, sewage, waste disposal and water, could be disabled until emergency repair crews were able to access these communities. SE Missouri could be effectively cut-off from the rest of the world. (Luna et al, 2001).

Preliminary site-specific earthquake assessment of two critical bridge sites along US 60 and the development of an initial geotechnical database were conducted as part of Phase I of this multi-agency initiative.

The goals of the site assessments at these two locations were to:

i) Estimate peak magnitude and duration of ground surface motion (including amplification/damping) associated with various events at each site.

ii) Evaluate the susceptibility of each site to quake-induced slope instability and liquefaction.

iii) Estimate shaking effects on the various types of existing bridge structures at each site.

iv) Compare ground motion and structural response parameters from site specific earthquake analysis method with those from AASHTO response spectrum analysis method and provide preliminary guidance regarding selection of the analysis method at future sites.

v) Determine if site conditions could be exacerbated by localized flooding as a result of canal and/or dam failure.

Only first 3-parts are presented Today

Paper to
OHIO RIVER VALLEY SEMINAR,LOUIVILLE , KY
OCTOBER 24, 2001

Earthquake Assessment of Critical Structures for Route US 60 Missouri

Ronaldo Luna, Genda Chen, Yulman Munaf, Huimin Mu, Shamsher Prakash and Paul Santi
University of Missouri-Rolla
Rolla, Missouri, 65409 - USA

Tom Fennessey
Missouri Dept. of Transportation
Jefferson City, MO 65102 - USA

Dave Hoffman
Missouri Dept. of Natural Resources
Rolla, Missouri 65401- USA

Abstract

The Missouri Department of Transportation initiated a study of that segment of Route US 60 that has been officially designated as "emergency vehicle priority access". The objectives were to establish a current subsurface and earthquake design geographic information systems (GIS) database for the designated US 60 corridor, and to conduct detailed earthquake assessments at two critical bridge sites along US 60. Databases have been established for current subsurface and earthquake data for the US Route 60 corridor in Butler, Stoddard and New Madrid Counties. These databases serve as the beginning of a larger regional or statewide database for future development and usage by MoDOT. Detailed earthquake site assessments have been conducted for two critical US 60 roadway bridge sites (Wahite Ditch and St. Francis River Bridge). Liquefaction potential, slope stability, abutment stability, and structure stability analysis were performed at both sites for selected "worst case scenario synthetic bedrock ground motions" based on New Madrid source zone earthquakes with 2% and 10% probabilities of exceedance in fifty years. Site assessments indicate that both the Wahite Ditch and St. Francis River bridges could be rendered unusable by strong ground motion with a 2% probability of exceedance in the next fifty years. Studies indicate that the bridge themselves would not fail – rather they would probably be rendered unusable because of damage to their abutments and the failure of their approaches (as a result of slope instability and liquefaction). Problems could be exacerbated by the localized flooding as a result of levee failure and/or damage to the Wappapello Dam. A scheme of retrofit of these structures will be developed later.

INTRODUCTION

Southeast Missouri experiences relatively small magnitude earthquakes on a regular basis, and is the site of several of the largest magnitude earthquake events to strike North America in recorded history. Experts agree that similar (or greater magnitude) earthquakes will strike this region again. Geologic conditions in southeast Missouri are such as to make this region one of the most seismically susceptible in the country, based on its damage potential from intrinsically susceptible soil, high water levels and vast expanses of flood sensitive ground. If a high magnitude earthquake struck southeastern Missouri today, infrastructure could be devastated. Levees and dams could be breached, bridges across the Mississippi and Meramec rivers could collapse or be otherwise rendered unusable, extended sections of highway would be closed by landslides, floods, soil liquefaction, and the failure of roadway bridges and overpasses. The network of facilities and services required for commerce and public health in south St. Louis, Sikeston, Cape Girardeau and surrounding communities could be devastated. Utilities, including electrical power, communications, oil and gas distribution, sewage, waste disposal and water, could be disabled until emergency repair crews were able to access these communities. SE Missouri could be effectively cut-off from the rest of the world.

Because of the compelling need to reopen emergency vehicle access routes into St. Louis, Sikeston and Cape Girardeau following a devastating earthquake, the Missouri Department of Transportation (MoDOT) in conjunction with other state agencies have designated specific routes for vehicular access of emergency personnel, equipment and supplies in the event of a major earthquake in southeast Missouri. These routes include portions of US 60 and US 100 (see Figure 1).

Preliminary site-specific earthquake assessment of two critical bridge sites along US 60 and the development of an initial geotechnical database were conducted as part of Phase I of this multi-agency (MoDOT, MoDNR and UMR) initiative. The methodologies developed in this study will be used to establish an assessment protocol. The interpreted geotechnical data will be used for future prioritization and retrofit of deficiencies noted at the bridge sites studied.

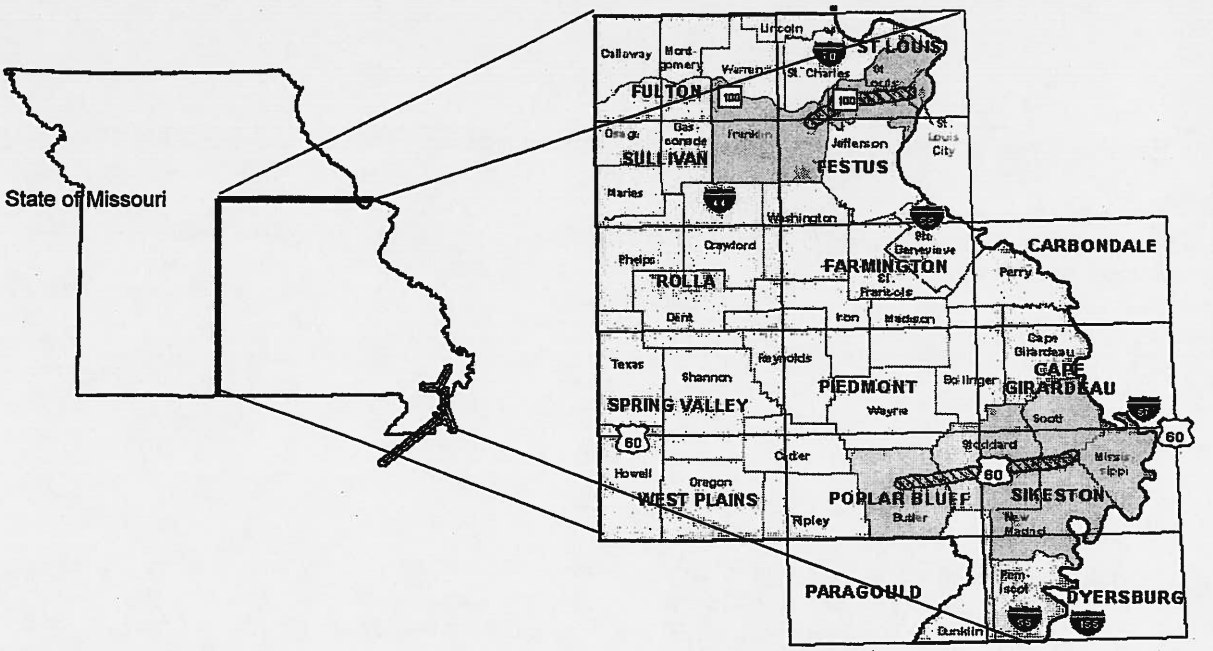

Figure 1 – Vicinity Map and Emergency Vehicle Access Routes

The designated US 60 corridor crosses the Butler, Stoddard and New Madrid Counties and was visited by the members of the MoDOT/MoDNR/UMR research team. Bridge sites with critical roadway features were ranked based upon geologic factors, structural factors and perceived criticality/risk factors. The top two sites with differing geologic settings were selected for detailed site-specific earthquake assessment (Wahite Ditch Number 1 bridge and the Saint Francis River bridge).

Detailed earthquake site assessments were conducted for both critical US 60 roadway sites. Site assessments included: subsurface exploration, and laboratory testing to identify subsurface materials and their engineering properties; evaluation of available seismic records and procedures to characterize the ground motions associated with various design earthquake events; and evaluation of the response of the subsurface materials and the existing bridge structures to the estimated ground motions.

The goals of the site assessments at these two locations were to:

i) Estimate peak magnitude and duration of ground surface motion (including amplification/damping) associated with various events at each site.

ii) Evaluate the susceptibility of each site to quake-induced slope instability and liquefaction.

iii) Estimate shaking effects on the various types of existing bridge structures at each site.

iv) Compare ground motion and structural response parameters from site specific earthquake analysis method with those from AASHTO response spectrum analysis method and provide preliminary guidance regarding selection of the analysis method at future sites.

v) Determine if site conditions could be exacerbated by localized flooding as a result of canal and/or dam failure

EARTHQUAKE GROUND MOTION

Liquefaction potential, slope stability, abutment stability, and structure stability analysis were performed at both sites for selected "worst case scenario bedrock ground motions" with probability of exceedance (PE) of 2% and 10% in 50 years. Ground motion analysis utilized synthetic ground motions for a New Madrid source zone.

In traditional site-specific earthquake hazard assessment, an initial step is to select rock base ground motion(s) at the site. This usually requires a site-specific seismic hazard analysis taking into consideration site conditions and all known earthquake sources (fault zones, epicentral distances, geological conditions, etc.). However, in the central U.S. there is a paucity of recorded strong ground motion from the New Madrid area that can be used for such purposes. Therefore investigators in the research community have resorted to procedures that develop synthetic seismic ground motions at a site (rock base).

A thorough search (literature and via professional contacts) revealed that acceptable, published synthetic ground motions

are available at only three locations in proximity to the bridge sites studied (Saint Louis, MO; Memphis, TN and Carbondale, IL; Wen and Wu, 2000). (These three locations were originally selected due to their population density and level of importance.) These three locations and the bridge sites studied (St. Francis and Wahite) are effectively surrounded by the three locations for which synthetic ground motions are available. A "worst case scenario" (in terms of soil, slope and structure response) was developed for each bridge site (for both PE time periods) based on all available synthetic ground motions (from all three locations) using the one-dimensional wave propagation analysis program SHAKE. A profile of peak accelerations for each soil layer was generated for each bridge site and for each synthetic ground motion. The ground motion with the highest peak ground acceleration (maximum PGA) at the surface (for each of the two PE values) was used to develop a "worst case" scenario for that PE value. It is acknowledged that site-specific synthetic ground motions would probably be preferable to those generated through the "worst case scenario" described above.

SEISMIC RESPONSE OF SOILS

Programs SHAKE and SHAKEDIT were used to transfer the rock motion to the above soil layers. Liquefaction analysis was performed using the Seed and Idriss (1971) simplified method, as modified by Youd et al. (1997).

SHAKE Analysis

Program SHAKE computes the responses in a system of homogenous, viscoelastic layers of infinite horizontal extent subjected to vertically traveling shear waves. The adopted synthetic ground motion is described above. Soil profiles for the St. Francis River and Wahite Ditch bridge sites, with corresponding soil properties of layers of St. Francis and Wahite sites were developed for the analysis. The shear wave velocity (Vs) measured by the seismic cone penetrometer at the St. Francis site was consistently below 400 meters per second within the soil column.

The peak ground motion for each layer above the base rock is larger than the rock ground motion. This means that, the ground motion amplification has occurred for this site. The calculated peak ground motion for each soil layer was plotted against depth. At the ground surface a peak ground motion ranged from 0.22g to 0.4g for the PE 10% and 2% in 50 years, respectively. (Anderson, et al., 2000)

Liquefaction Analysis

Soil Profile

The soil profile at St. Francis Bridge is used in this paper to present the analysis procedures. Boreholes and cone penetrometer tests were located close to the bridge abutment. Soil at this site consists of clay with medium to stiff consistency up to 18 ft depth and about 30 ft thickness of dense to very dense sand layer. A brief description of the soil profile, which includes observed SPT (N) and corrected $(N_1)_{60}$ values are shown in Figure 2. The shear wave velocity profile

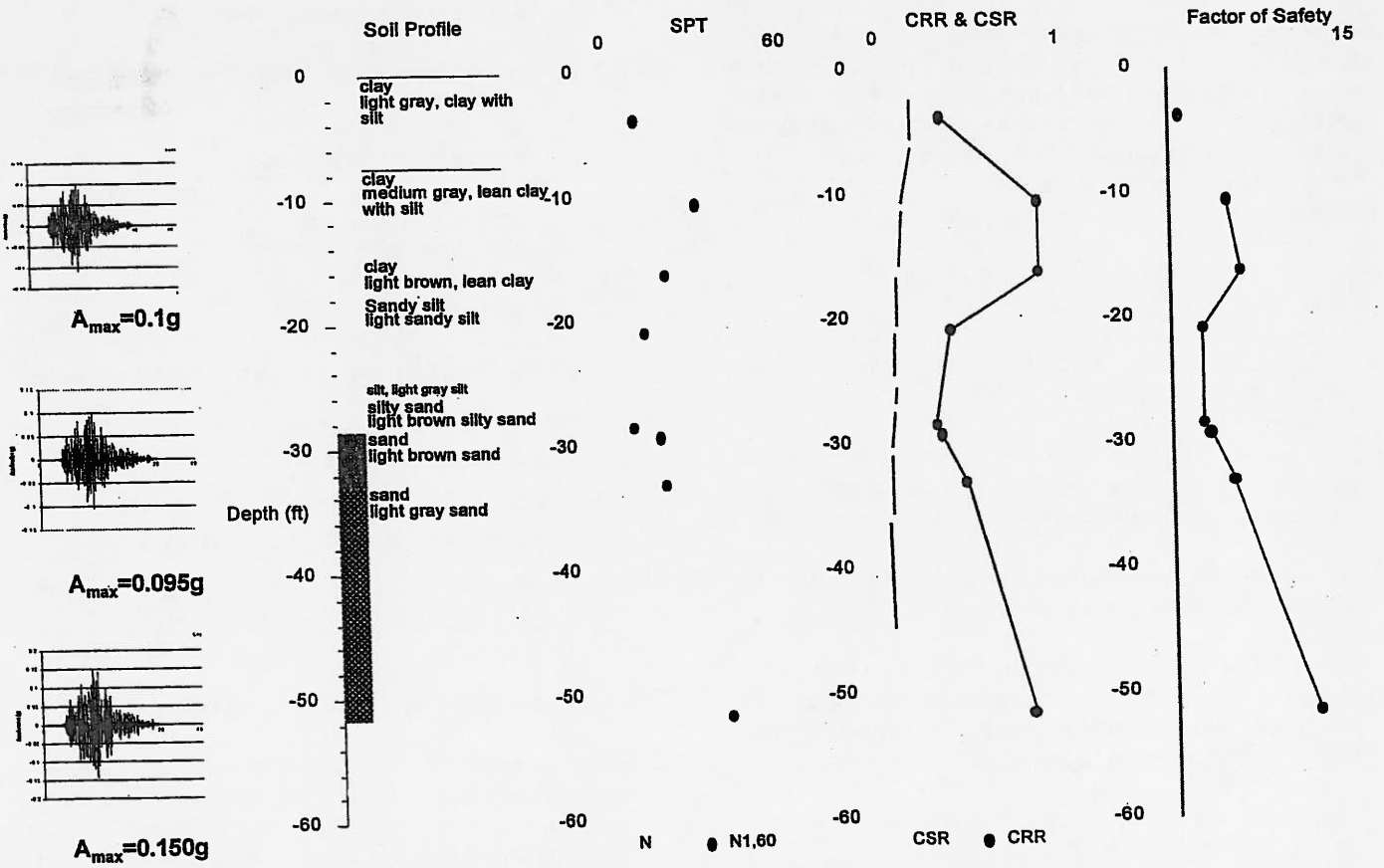

Figure 2 – Soil Profile, seismic ground response and liquefaction at St. Francis site

at this site was measured by CPT test up to about 40 ft of depth.

Wahite Ditch site followed similar analysis procedures. The subsurface soil at this site consists of clay of high plasticity up to 20 ft depth and about 170 ft thickness of medium sand, containing numerous thin gravel lenses.

Liquefaction Evaluation Potential

Liquefaction potential of that site is obtained by comparing the value of Cyclic Resistant Ratio (CRR) and the Cyclic Stress Ratio (CSR) to obtain the factor of safety against liquefaction. Figure 2 shows the plots of the CRR, CSR and factor of safety (FOS) against liquefaction with depth for PE 10% in 50 years of St. Francis site. For PE 10% in 50 years, the factor of safety is higher than that recommended value of 1.4 and those sites will be safe against damage due to liquefaction. However, for PE 2 % in 50 years, the factor of safety is less than 1.4 and the soil liquefied for PE 2% in 50 years at both sites.

SEISMIC RESPONSE OF BRIDGE ABUTMENTS

The older bridge (1978) at the St. Francis site (deck is sitting on the abutments) was analyzed, and a detailed analysis of abutment of this bridge was conducted. The new bridge (1992) has integral abutment with the deck. This requires a highly involved and sophisticated analysis that should be performed in recommended follow-up studies.

Displacements of bridge abutment were computed considering it as a two-degrees-of-freedom (2-DOF) model. Choudhry (1999) and Wu (1999) have proposed methods to calculate displacements of bridge abutment and retaining wall due to earthquake, based on permanent displacement concept. This method/procedure has been modified to predict seismic response of bridge abutment supported on piles.

Procedures of this method are presented as follow:

1. Seismic response of bridge abutment was calculated based on time history of acceleration acting on the base of foundation abutment.

2. The bridge abutment is supported on two rows of vertical and battered piles. The pile provided stiffness and damping and the abutment provides the mass.

3. Two degrees of freedom motion were used to obtain displacement of bridge abutment.

4. Mononobe-Okabe method was used to compute force acting in backfill. Vertical load acting on the bridge abutment was obtained based on reaction force of bridge structure from output analysis of bridge super structure.

5. Non-linear soil properties were used to obtain stiffness and damping parameter of base soil layer.

6. Spring and damping constants were calculated using recommendation of Novak's (1974) and Novak and El-Sharnouby (1983).

7. Point of rotation was assumed at the heel of bridge abutment. (Wu, 1999, Choudhry, 1999).

8. Displacements were calculated based on active state condition. This means that, permanent displacement occurred if acceleration acts towards the fill and the wall move away from the fill.

9. Total displacements at top of bridge abutment are calculated by cumulative of sliding and overturning displacement.

Load Acting on Bridge Abutment

Loads acting on bridge abutment are:

i) Self weight of abutment and time dependent inertia force.
ii) Vertical load of the deck and time dependent inertia force.
iii) Lateral static and time dependent load from backfill of soil .

Vertical load acting on bridge abutment is obtained from reaction force of dead and live load. The seismic motion at subsoil layer 1 (Figure 2) is used in typically this analysis.

Bridge Abutment and Pile Parameters

Bridge abutments and piles are cast in-place concrete with the following properties;

Diameter of pile section	= 0.508 m
Length	= 13.4 m
Unit weight of concrete	= 23.58 kN/m^3
Elastic modulus concrete	= 2.15x10^7 kN/m^2
Poisson ratio (υ)	= 0.3
Moment inertia of pile	= 0.00316 m^4

Table 1 - Soil Properties Used for Abutment Analysis

Backfill soil	Foundation soil around the pile
Unit weight = 19.54 kN/m^3	Unit weight = 21.56 kN/m^3
Internal friction angle (ϕ) = 33°	Internal friction angle (ϕ) = 35°
Friction angle between soil and wall (δ) = 33°	Friction angle between soil and wall (δ) = 23.3°

Calculated Time Dependent Displacement of Abutment

Using the selected synthetic ground motions referenced earlier and soil properties in Table 1, Figure 3 shows the time histories of sliding, rocking and total permanent displacement of bridge abutment. The sliding displacement of bridge abutment is 0.2 to 1.0 ft.

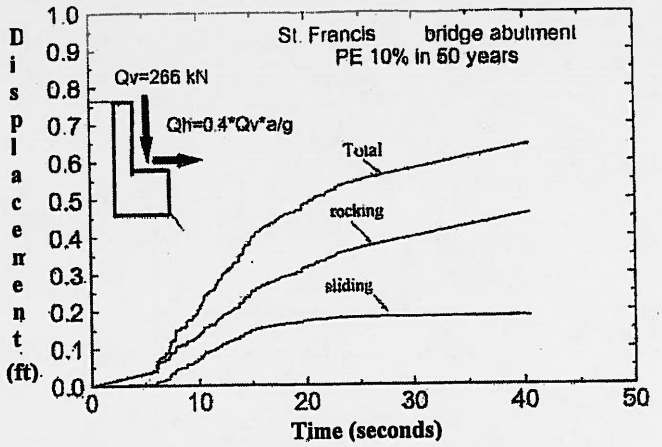

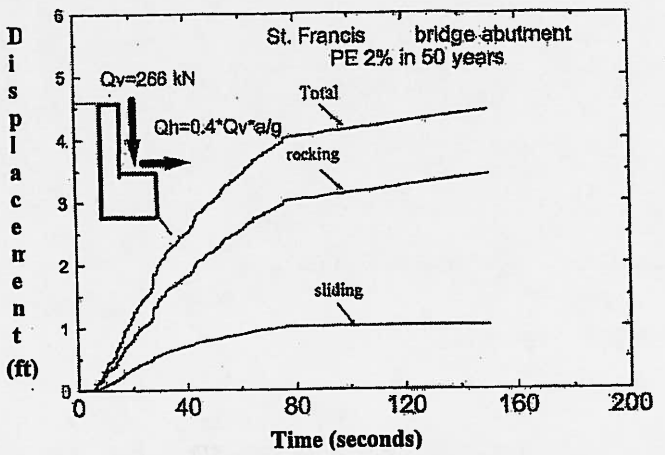

Figure 3 – Time histories of displacement at the abutments (St. Francis River Bridge).

SEISMIC SLOPE STABILITY

For the St. Francis Bridge site, slope stability analyses were completed for seven cross-sections. Each cross-section was analyzed for both low and high ground-water conditions under static analysis and under two pseudo-static earthquake accelerations. Cross-section locations are shown on Figure 4, St. Francis Bridge Site Topography. The cross-section data was then entered into the slope stability program *PCSTABL5* using the pre and post processor *STEDwin*. The slopes were analyzed under static and dynamic conditions using the Modified Bishop Method.

A summary of the St. Francis site analyses is included in Table 2. In general, the site slopes appear to be stable under static conditions, with both low and high ground-water tables, with factors of safety ranging from 1.93 to 3.96. When subjected to an earthquake with a 10% exceedance probability in 50 years (PE) (which would generate horizontal accelerations of 21%g), slopes continue to show stability, with factors of safety dropping to a range of 1.23 to 2.20. When subjected to an earthquake with a 2% PE (38%g), factors of safety less than or approximately equal to one are calculated for section F-F' under low water conditions and all sections under high water conditions. Expected failure planes pass through both the roadway and bridge piers. An example analysis output for cross-section C-C' is shown on Figure 5.

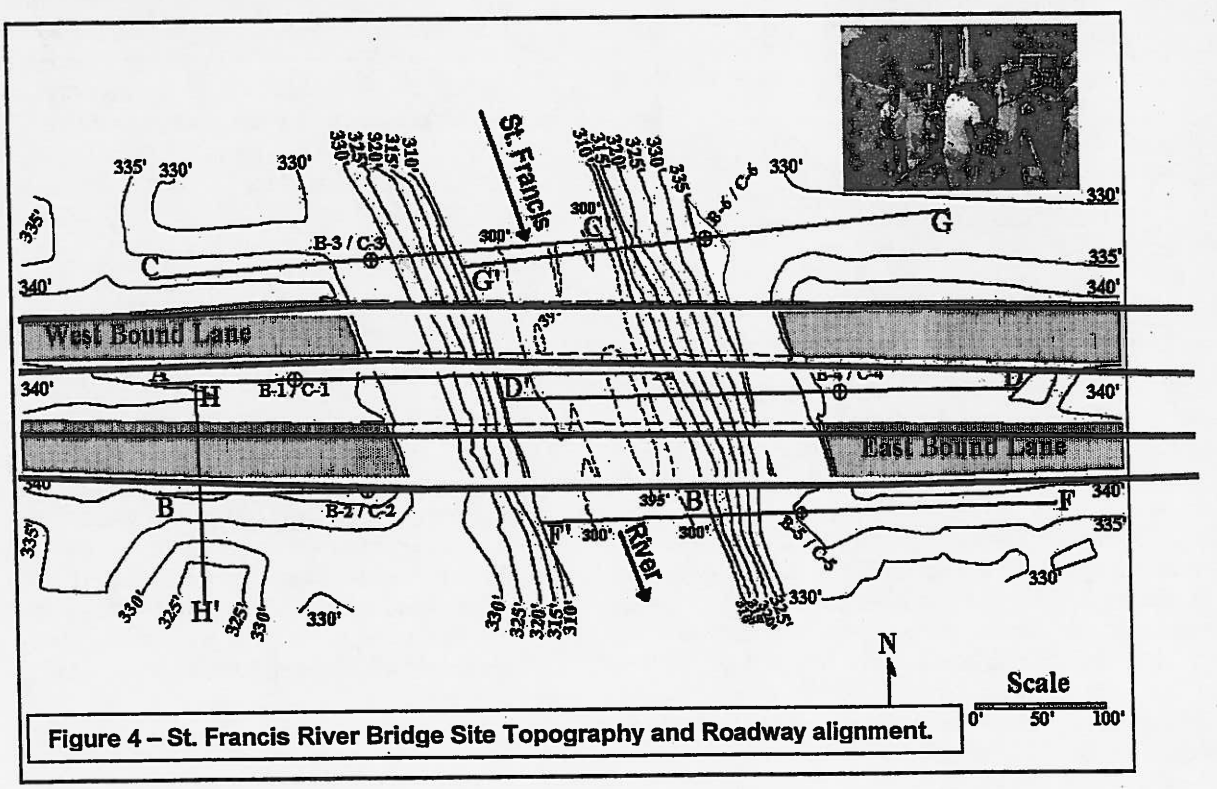

Figure 4 – St. Francis River Bridge Site Topography and Roadway alignment.

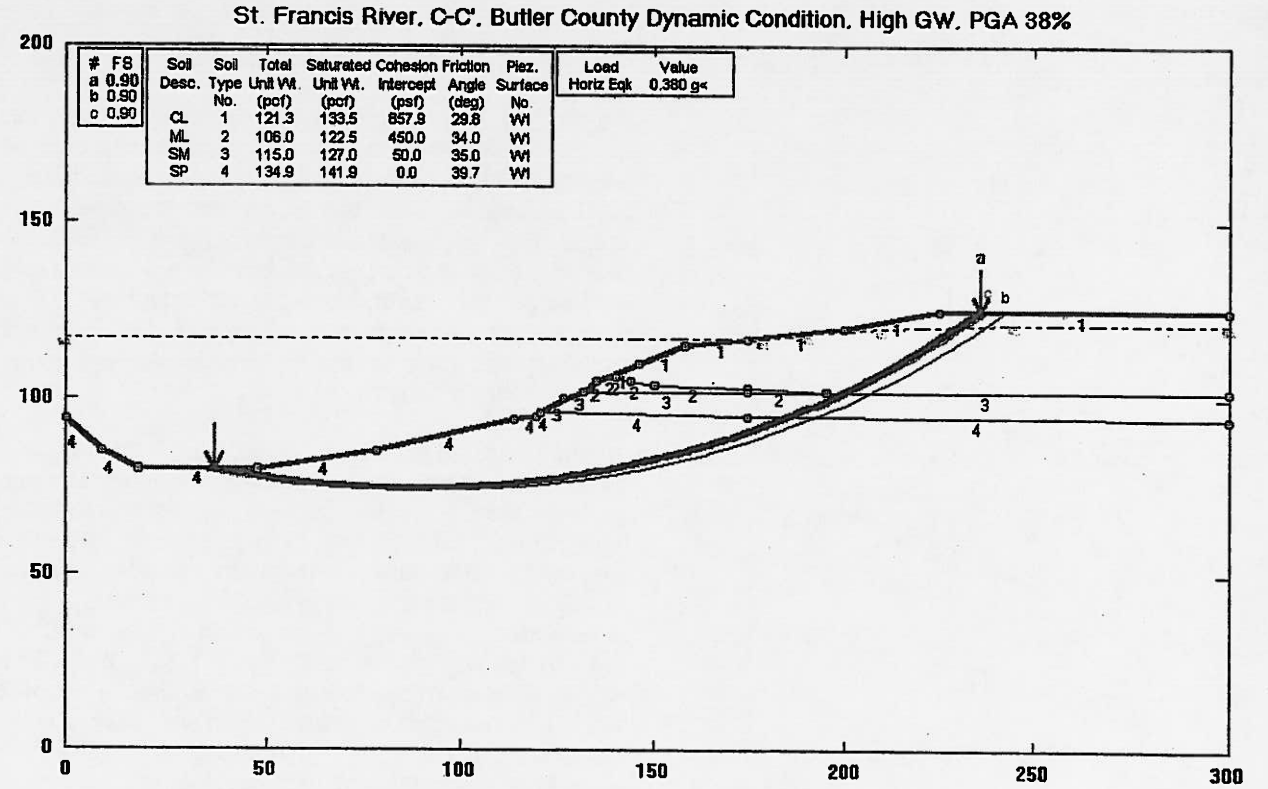

Figure 5 – Seismic Slope Stability Analysis – example.

Table 2 - Factor of Safety for Select Cross-sections

Cross-Section	A - A'	C – C'	F – F'	G – G'
Static				
Low GW	2.63	2.88	1.93	3.96
High GW	3.06	3.48	2.02	2.67
Dynamic* (Low GW)				
10% PE, PGA 21%	1.46	1.52	1.23	2.20
2% PE, PGA 38%	1.03	1.06	0.90 $^{\S\Psi}$	1.56
Dynamic* (High GW)				
10% PE, PGA 21%	1.28	1.41	1.01	1.41
2% PE, PGA 38%	0.83 $^{\S\Psi}$	0.90 $^{\S\Psi}$	0.66 $^{\S\Psi}$	0.99 §

These results indicate that slopes at the St. Francis Bridge site are expected to be stable under small earthquake shaking (10% PE), and unstable at higher levels of shaking (2% PE), regardless of the ground-water level.

A similar set of analyzes were performed for the Wahite Ditch site. The anticipated behavior is similar to that described for the St. Francis Bridge site. The site slopes are expected to be stable under static conditions (F.S. range from 3.48 to 7.76) and under 10% PE (27%g) loads (F.S. range from 1.28 to 2.60) for both low and high ground-water conditions. Under 2% PE (39%g) loads, factors of safety are greater than one for all analyzed sections for low ground-water conditions. Under high water conditions' factors of safety are less than or approximately equal to one for sections A-A', C-C', D-D', E-E', and F-F' (not shown).

Both sites are expected to be stable under small earthquake conditions. The results at the St. Francis Bridge site indicate slightly higher sensitivity to ambient ground-water levels (which are affected by water levels in the river) than at Wahite Ditch. Stability analysis under large earthquake conditions indicates instability at the St. Francis Bridge site, regardless of the ground-water level and instability at Wahite Ditch when ground-water levels are high.

ANALYSIS OF ST. FRANCIS RIVER BRIDGE (1978) SUPERSTRUCTURE

For this preliminary analysis of the older St. Francis River Bridge, soil-structure interaction was not included. All columns were fixed at the centroid of pile caps and, abutments and their supporting soil strata were assumed rigid. The seismic acceleration time history (maximum acceleration: 0.1g) at the elevation of one pile cap of Bent 2 was used as longitudinal input at all boundaries of the bridge model. The maximum responses from such time history analyses were compared with those due to the design earthquake specified in AASHTO.

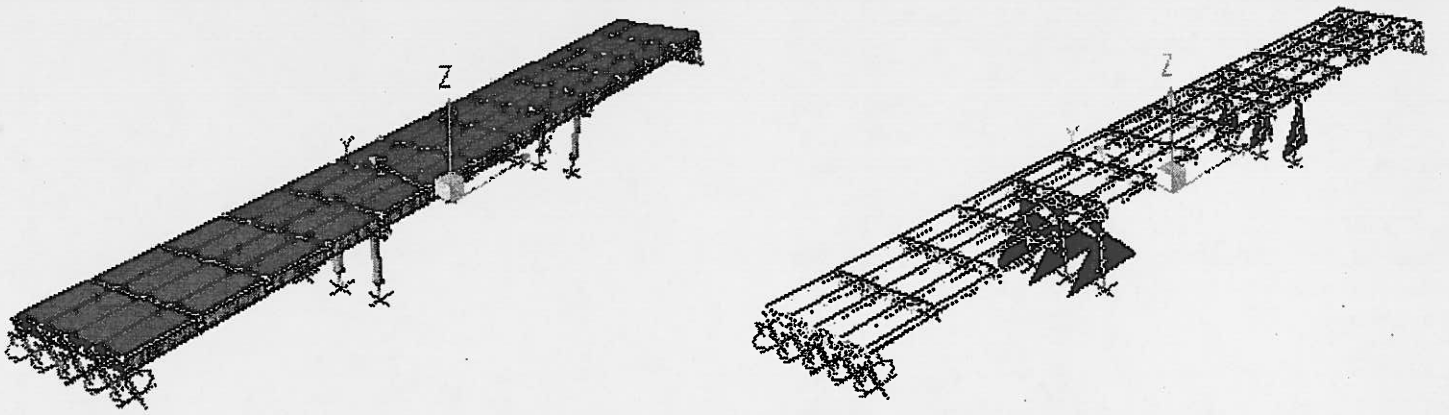

Figure 6 – St. Francis Bridge Structural Dynamic Analysis

Under the site-specific seismic load, the bridge deck experiences about 0.14 in movement, which is less than the existing joint width (2.5 in or 1.875 in). Pounding will not occur in this case. It is observed that the bridge mainly moves in the longitudinal (traffic) direction.

Although there are no seismic forces in the transverse direction, columns are subject to bending in the transverse plane due to the skew effect of the bridge. The maximum moment of column in the transverse plane is only 36% of that in the longitudinal plane. Since its longitudinal movement is restrained at the top of cap beam by fixed bearings, the columns at this bent carry the most seismic load from the superstructure and are thus subject to a significantly larger moment than that of Bent 2. It is also interesting to note that several girders are subject to bending due to the skew effect. For the same reason, those girders carry little axial forces.

Figure 6 shows the computer model performed using SAP 2000 for the structural dynamic analysis and the moments develop in the columns at both bridge bents.

The maximum ground acceleration is about 0.288g according to the AASHTO spectrum, which is significantly higher than the maximum acceleration of the site-specific time history (0.1g). Therefore, the displacement and force of the bridge are much higher under a design earthquake specified in AASHTO than the site-specific earthquake used in analysis. Pounding will not occur under the AASHTO design earthquake.

FLOODING POTENTIAL

Evaluation of the effects of flooding due to failure of levees was based on a series of topographic maps covering the entire study section of US 60. This evaluation was field checked by visual observation of the elevation of the roadway compared to surrounding land. Some of the maps were as old as 1962 vintage without photo-revision, so the estimate of the limits of potential flooding should be considered tentative. Furthermore, the roadway elevation was shown only to 5-foot accuracy, and slight elevations or depressions in the roadway could significantly change the degree of anticipated flooding. In general, the following hydrologic features are expected to be affected during an earthquake, presented in order from west to east: Blue Spring Slough, St. Francis River, Mingo, Cypress Creek Lateral, and Prairie Creek Ditches, Unnamed Creek 1 mile West of Essex, Bess Slough, Six Unnamed Ditches Between Bess Slough and the Castor River, Wahite Ditch. The remaining sections of US 60 to the east of the Wahite Ditch appear to be elevated and are not anticipated to experience flooding due to levee failure.

CLOSING

Overall, the seismic assessment of the critical structures along US60 in the state of Missouri performed satisfactorily for an earthquake event with a PE 10% in 50 years. However, for an event PE 2% in 50 years the structures evaluated, bridge foundations, abutments and embankment fills will be significantly damaged to a level that may render the access routes unusable.

The dynamic structural analysis is preliminary in nature and it does not include the effect of local soil conditions or soil-structure interaction. The bridge structure selected was considered the weakest link or oldest (built in 1978) among the bridges over these crossings, therefore, it was the initial focus of the study. Future analysis will be considering the more modern bridges, which include an integral bridge deck and abutment.

REFERENCES

Anderson, N. et al. (2000), "Earthquake Hazard Assessment Along Designated Emergency Vehicle Access Routes," Report No. R198-043, Missouri Department of Transportation, Jefferson City, Missouri, 65102.

Choudhry, M.S., 1999, Seismic Analysis of Pile Supported Rigid-Bridge Abutments Using Material Geometric Non-linearity: Ph.D. Dissertation, University of Missouri-Rolla.

Monobo, N. and H. Matsuo, (1929), "On the Determination of Earth Pressure During Earthquakes, Proc. World Earthquake Engineering Congress, Tokyo.

NISEE (National Information Service for Earthquake Engineering), University of California, Barkeley. Http://www.eerc.berkeley.edu/

Novak, M., 1974, Dynamics Stiffness and Damping of Piles: Canadian Geotechnical; Journal, Vol 11, 574-598.

Novak, M. and El-Sharnouby, B., 1983, Stiffness and Damping Constants of Single Piles: Journal Geotechnical Engineering, Div., Am. Soc. Civ. Eng. 109(GT-7), 961-974.

Seed, H.B. and Idriss, I.M., 1971, Simplified Procedure for Evaluating Soil Liquefaction Potential: Journal of the Soil Mechanics and Foundation Division, ASCE, Vol. 97, No. SM9, pp. 1249-1273.

Youd, T.L. and Idriss, I.M. (editors.), 1997, Proceeding of the NCEER Workshop on Evaluation of Liquefaction Resistance of Soils: National Center for Earthquake Engineering Research, Technical Report No. NCEER-97-0022, December 31, 1997.

Wen, Y.K. and Wu, C.L., 2000, Generation of Ground Motions for Mid-America Cities: (MAE report currently under review).

Wu, Y., 1999, Displacement-Based Analysis and Design of Rigid Retaining Walls During Earthquake: Ph.D. Dissertation, University of Missouri-Rolla.

The Influence of Tectonic Stress on a Pile Founded Lock and Dam

Jeffrey A. Schaefer, Ph.D., P.E., P.G.[1]

SUMMARY

The presence of very high in-situ horizontal stresses were discovered on the construction site for the Olmsted Locks and Dam project. The Olmsted Locks and Dam project is located on the Ohio River approximately 26.6 km (16.5 mi.) upstream of its confluence with the Mississippi River. It consists of twin 365 m (1200 ft.) locks, five 33.5 m (110 ft.) wide tainter gate bays, a 426.7 m (1400 ft.) wide navigable pass boat-operated wicket gate section, and a 121.9 m (400 ft.) section of fixed weir. The lock will be a monolithic W-frame structure. The project will have a total cost in excess of 1 billion dollars, and is one of the largest civil engineering projects underway in the Corps of Engineers. Figure 1 is a rendering of the completed project. The project is at the northern edge of the Mississippi Embayment and near the New Madrid Seismic Zone (Figure 2). To resist the seismic loads, the foundation for the Locks is constructed with 12,000 steel H-piles driven into a Cretaceous-aged soil deposit known as the McNairy Formation. An extensive pile testing program was conducted within the cofferdam for the construction of the locks. This program included numerous static and dynamic pile load tests. This paper documents a case where the performance of full scale load tests revealed that the capacity of foundation piles were dramatically underestimated. Analysis of the pile test data indicates that the high capacities are due to the large magnitude in-situ horizontal stress. Direct measurments using self-boring pressuremeter (SBPM) tests confirmed the presence of high in-situ horizontal stress. Evidence supporting the theory that the source of the high lateral stress is due to the transfer of tectonic stresses to the soil is presented herein.

SITE CHARACTERISTICS

The Olmsted Locks and Dam project site is located on the Ohio River approximately 26.6 km (16.5 miles) from its confluence with the Mississippi River. Prior to construction, the topography consisted of steep ridges with prevalent landslides on the Illinois bank, a wide riverbed, and generally flat and swampy land on the Kentucky bank. The ground surface is at elevation 136 m (445 ft.) on top of the Illinois ridge, steeply sloping to a terrace at el. 110 m (360 ft.), falling to a bench at el. 98 (320 ft.), and then sloping again to the river bottom at el. 78 m (255 ft.). The river bottom gradually rises across the river to el. 85 m (280 ft.) then up the Kentucky bank to el. 99 m (325 ft.).

[1]Geotechnical Engineer, Civil Engineering Branch, US Army Corps of Engineers, Louisville District, P.O. Box 59, CELRL-ED-T, Louisville, KY 40201-0059, phone (502) 315-6452, fax (502) 315-6454, Email: jeffrey.a.schaefer@LRL02.usace.army.mil

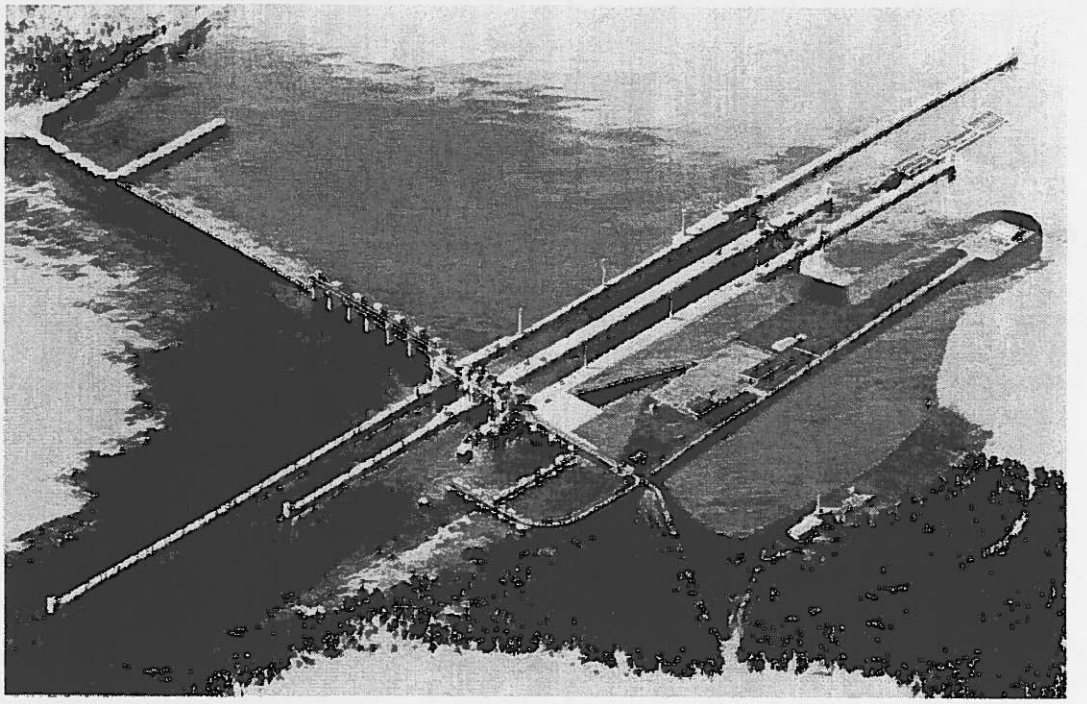

Figure 1- Artist Rendering of Completed Olmsted Project

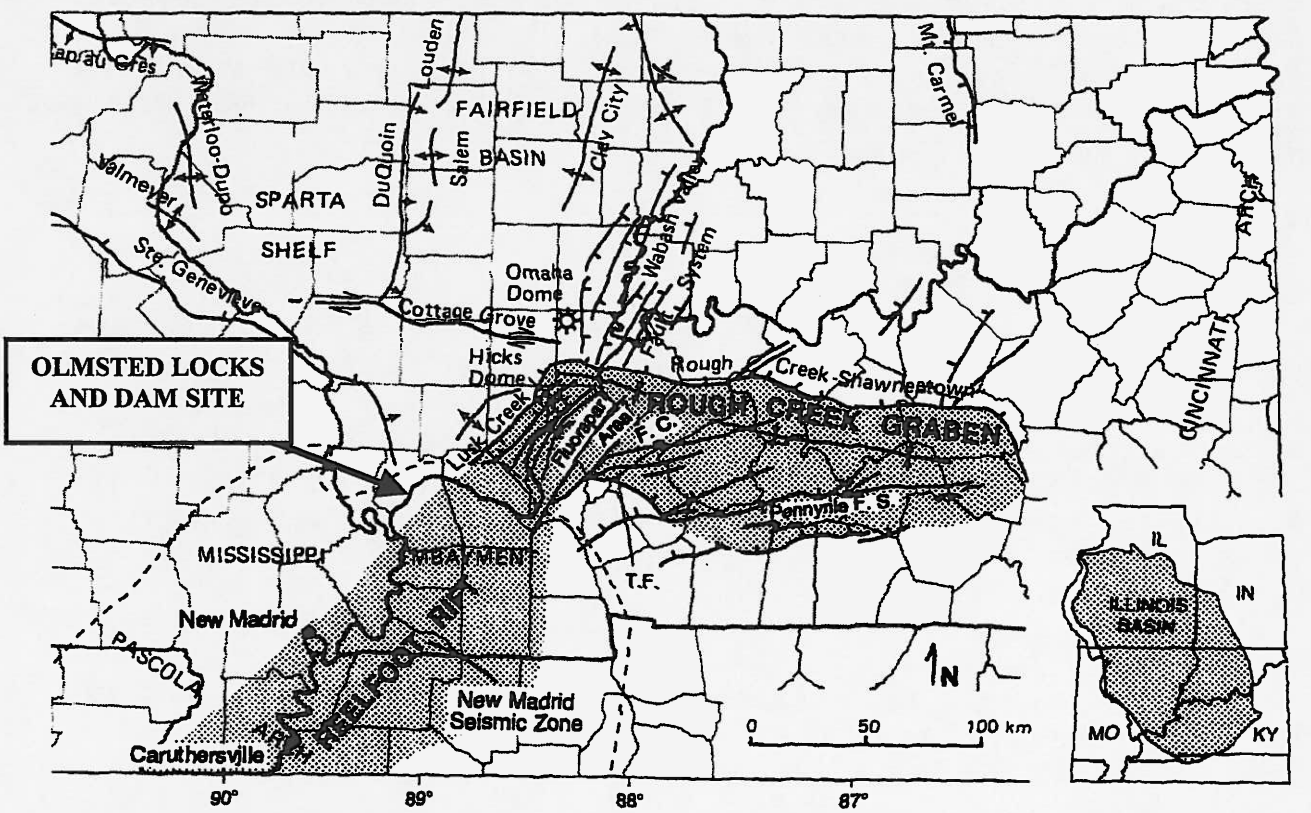

Figure 2 - Site Location Showing Mississippi Embayment Boundary. (Base Map from Kolata and Hildenbrand, 1997)

SUBSURFACE CONDITIONS

The soil stratum of interest in this study is a Cretaceous-aged soil deposit known as the McNairy Formation. The McNairy sediments consist of approximately 80% very fine to fine, dense sands with the remainder consiting of interbedded layers of stiff clays and silts. They were likely deposited in a fluvial deltaic environment. This formation ranges from 13 m (43 ft.) thick in the thalwag of the river, to 36 m (118 ft.) thick on the Illinois bank. The sands were classified according the Unified Soil Classification System as SP. The clays and silts are CL and ML, respectively. The sands are very uniform throughout the formation, with grain sizes predominately ranging from 0.06 mm to 0.3 mm with a mean value of 0.15 mm. The Overconsolidation Ratios (OCR) determined from consolidation tests on clay samples taken from various depths within the McNairy Formation averaged 2.0 having little variation with depth. The void ratios determined from undisturbed sand samples ranged from 0.74 to 0.91. The specific gravity of the sand is between 2.64 and 2.68. The sands have an average drained friction angle (ϕ') of 31 degrees. In the clay layers, peak values of ϕ' range from 19 to 22 degrees with residual values as low as 10 degrees. The average saturated unit weight of the soil is 1,920 kg/m^3 (120 lb/ft^3). The field Standard Penetration Test (SPT) N-values range from 40 to over 100 blows per foot. The groundwater within the McNairy sands is pressurized with heads up to 3 m (10 ft.) above the river surface.

John Nelson of the Illinois Geological Survey and the author evaluated core samples of the material found below the McNairy Formation. It was determined that the Paleozoic rock formation directly underlying McNairy Formation is a leached and silicified Mississippian rock, known as the Fort Payne Formation (John Nelson, personal communication). The Fort Payne is normally a dark-colored, siliceous limestone that contains bands of dark chert. In the Olmsted area, nearly all of the carbonate minerals have been leached or dissolved away and/or replaced with silica, leaving a dark brown silt-like rock that contains occasional bands of hard chert. Several samples of unaltered Fort Payne limestone were obtained. Below the Fort Payne, the Devonian aged New Albany Shale formation was encountered. A deep boring in the New Albany shale also penetrated a fault. Up to 66 m (215 ft.) of variation in the elevation of the top of the New Albany Shale was found within the project limits.

LOCKS FOUNDATION REQUIREMENTS

In order to meet seismic design criteria, numerous high capacity H-piles are required for the lock foundation. The foundation for the locks consist of approximately 12,000, 14x117 H-Piles. The required ultimate compressive capacities ranged from 2,669 to 3,674 kN (600 to 826 kips) while the required tensile capacities ranged from 445 to 1557 kN (100 to 350 kips.) The locks were constructed in a conventional cellular cofferdam as shown in Figure 3. The cofferdam is approximately 610 m (2,000 ft.) long by 305 m (1,000 ft.) wide and 30 m (99 ft.) deep. The cells were constructed with 33 m (109 ft.) long sheets embedded 12 m (40 ft.) into the river bottom

Figure 3 - Locks Cofferdam

CONSTRUCTION PILE TESTING PROGRAM

The testing program was performed to evaluate and optimize the lock's foundation piles. At a cost of approximately $233 per meter ($71 per ft.) for 12,000 piles, it was critical to determine the appropriate driving criteria and lengths needed to obtain the required ultimate capacities. Design calculations indicated that piles needed to be driven 18.3 m (60 ft) to achieve the required compressive and tensile capacities.

The first phase of the testing program was to drive 78 indicator piles throughout the site. Since the depth needed to obtain the required capacities was yet to be determined, the indicator piles were all driven to refusal at depths of approximately 20 meters (67 ft). Three indicator piles were driven in each lock monolith; one under each wall. The indicator piles were driven as production piles in locations selected by the Contractor. The indicator piles were used to evaluate the Contractor's selected driving system prior to installation of the load test and production piling, preview the foundation conditions throughout the site, and aid in selecting appropriate locations for the static load tests. Nine of the indicator piles were monitored with a Pile Driving Analyzer (PDA) during installation. Case Pile Wave Equation Analysis Program (CAPWAP) (Goble et al., 1996) analysis was performed on each of these to determine the end of driving capacity for the piles. Also, a restrike PDA test and CAPWAP analysis were performed after a minimum of seven days to investigate soil strength changes with time. The indicator piles revealed that the foundation conditions were relatively uniform throughout the project site. The

Contractors selected driving system (Delmag D46-32) was found to be very efficient. Locations for compression, tension, and lateral static load tests piles were selected from data gathered by the indicator piles. The areas with the lowest driving resistance were selected for the static load tests.

Static Compression Tests- The static compression tests were performed by applying a load up to 5,338 kN (1,200 kips) to a single pile by jacking against a reaction frame anchored to eight piles driven to refusal. Tests were performed in accordance with the Quick load test requirements of ASTM D-1143 (1994). The jack was placed on the test pile with a load cell to measure applied loads inserted between the jack and the main reaction beam. The movement of the pile head was measured with four dial gauges attached to a reference beams. To determine the elastic compression of the pile and the total tip movement, a 19 mm (3/4 in.) steel rod (tell-tale) was welded to the tip of the pile and monitored throughout the test with a dial gage referenced to the pile head. The tell-tale was isolated from the soil by a steel casing welded to the pile.

Seven full-scale static compression tests were performed. Five of the test piles were loaded to the capacity of the testing frame without failing. The Davisson criterion (Davisson, 1972, 1975, and Fellenius, 1990) was chosen as the method for determining the ultimate capacity of a pile in a compressive Quick load test. These piles (M01-F46, M09-C20, M14-E42, M24-E03, M26-G56) all had a static compressive capacity greater than 5338 kN (1200 kips.) Two of the piles were loaded to the failure criterion. Pile M05-D05 experienced plunging failure at approximately 4003 kN (900 kips) while pile M21-E28 reached the failure criterion at approximately 4448 kN (1000 kips.) See Figure 4 for a typical compressive test result. All of the static compression tests indicated that test piles had a capacity substantially in excess of the required ultimate capacity. An evaluation of the tell-tale data estimated that the piles had a load transfer of approximately 80% friction and 20% end bearing.

Piles driven 12.2 m (40 ft.) with a Delmag D46-32 (2.59 m (8.5 ft.) stroke) to a final blow count of 49 to 66 blows per meter (15 to 20 bpf) were load tested up to 5338 kN (1200 kips) without failure. A summary of static load test results is given in Table 1.

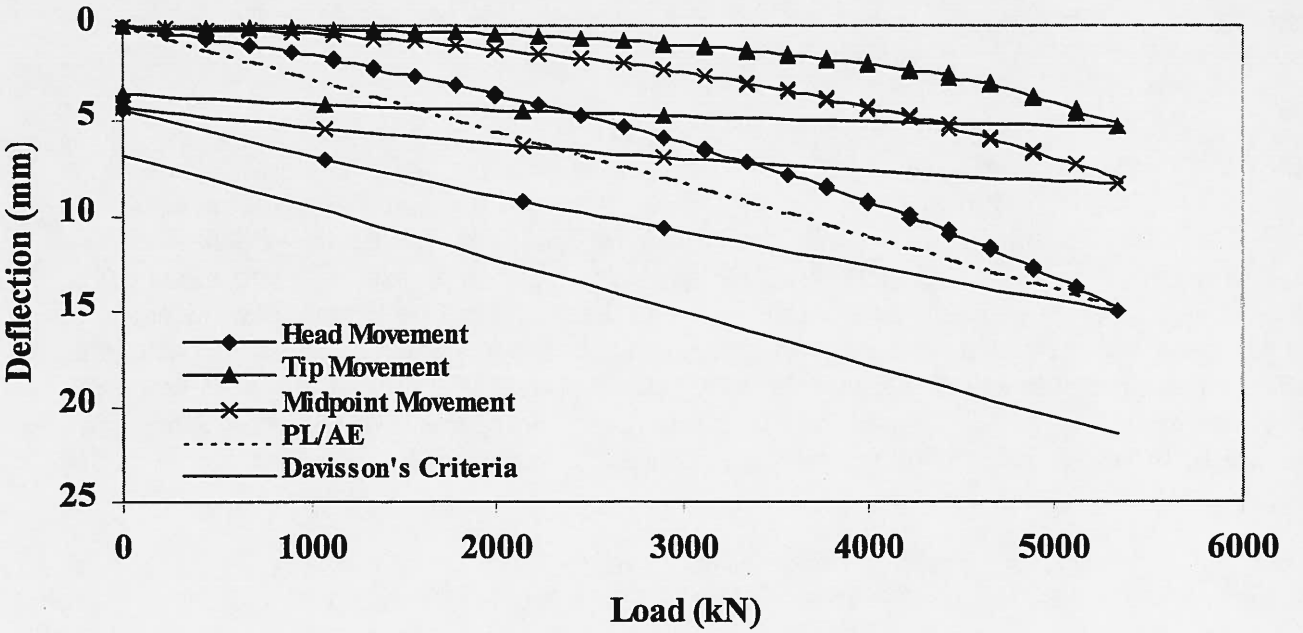

Figure 4 – Typical Compression Test Result

Static Tension Tests - The arrangement for the tension test was very similar to the compression test. The static tension test were performed by loading the piles up to 2224 kN (500 kips) in accordance with the Quick load test requirements of ASTM D-3689 (1990). The jack and load cell were placed on top of the reaction beam. A frame was then welded to the pile and placed over the jack, thus allowing the pile to be loaded in tension. Two methods for providing support for the reaction beam were used. The first was similar to the compression test where reaction piles were driven into the ground and a frame assembly built to attach the main reaction beam. The second method placed the reaction beam on a stack of steel beam cribbing supported on timber mats to distribute the load. All other gages and measurements were the same as the compressive test. A tell-tale was used in the tension test to measure the elongation of the pile during the test.

Six static tension tests were performed on piles M02-B25, M05-F43, M11-B24, M15-H35, M19-E04, and M26-S29. All of the test piles were loaded in tension to 2224 kN (500 kips) (the capacity of the testing frame) without failure. A typical Load - Deflection Curve is shown on Figure 5. The results of the static tension tests are also summarized in Table 1.

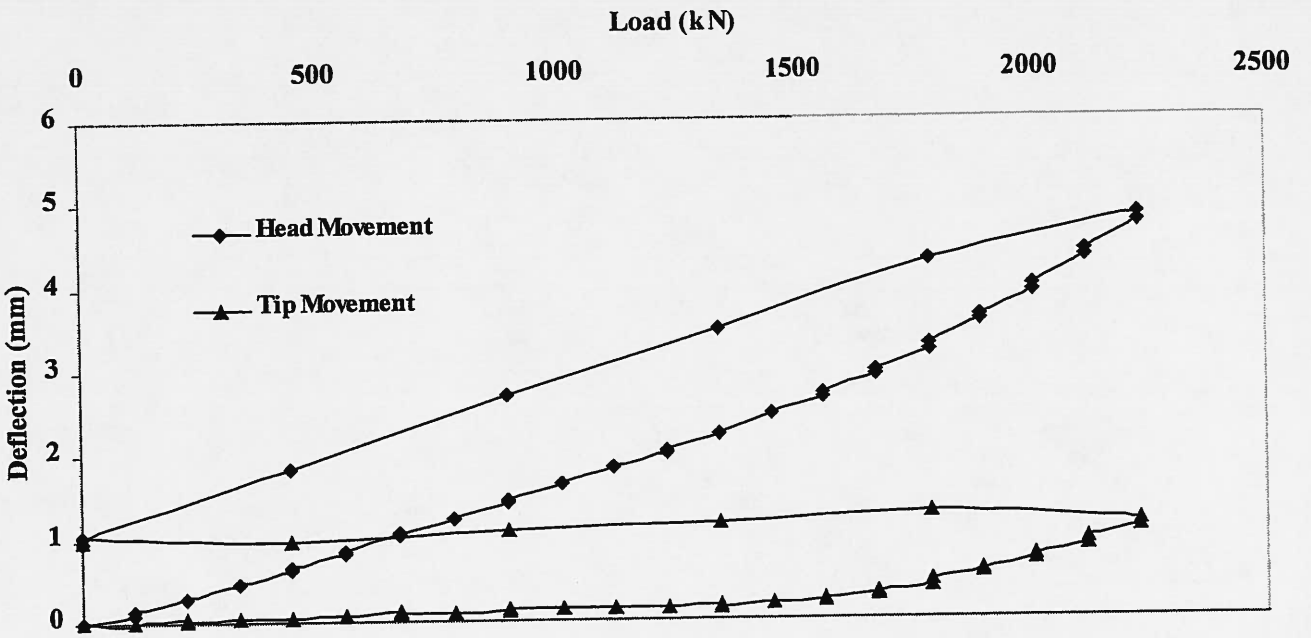

Figure 5 – Typical Tension Test Result

Static Lateral Load Tests - The lateral load tests were performed by simultaneously loading two piles up to 445 kN (100 kips) in accordance with ASTM D-3966 (1990). Two gages were attached to each pile to monitor deflection 152 mm (6 in.) above the ground line at the center of the load application along with two gages placed 457 mm (18 in.) above the ground line. The piles were loaded along their strong axis. An inclinometer was attached to the full length of both piles and monitored at specific load increments to determine the point of fixity and shape of the deflected pile.

A total of four sets of lateral load tests were performed. All of the piles were laterally loaded to 445 kN (100 kips). The deflection at 445 kN (100 kips) ranged from 25.4 mm (1.00 in.) on pile M06-G01 to 40.64 mm (1.6 in.) on pile M25-D25. Typical Lateral Load-Deflection Curves are shown on Figure 6. The point of fixity determined from the inclinometers for all of the piles was at a depth of approximately 3.05 m (10 ft.). A typical inclinometer plot is shown in Figure 7. The lateral deflections measured were all acceptable. Values of N_h (horizontal modulus of subgrade reaction) were calculated by using the deflection measured at the ground line by the dial gages at a load of 445 kN (100 kips). The calculated values of N_h ranged from 1.2×10^6 kg/m^3 (43 lb/in^3) to 2.5×10^6 kg/m^3 (91 lb/in^3). A summary of the results of the static lateral load tests are given in Table 1.

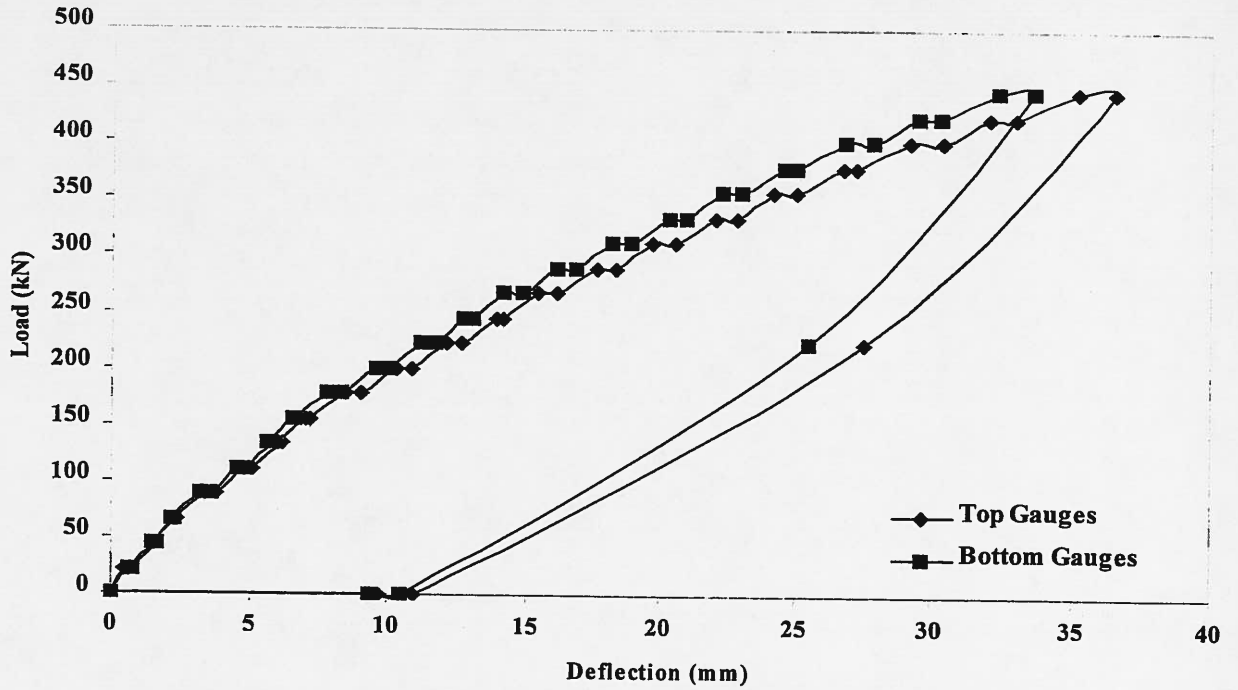

Figure 6 – Typical Lateral Load Test Result

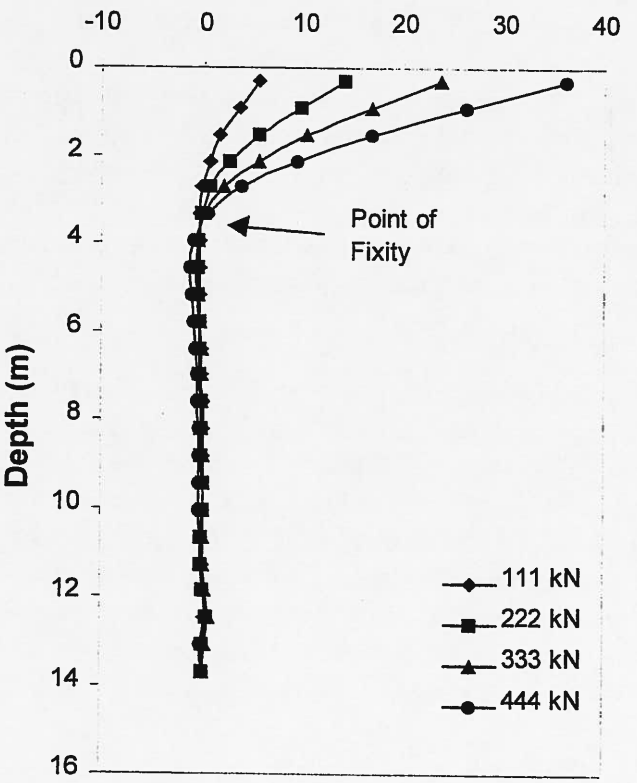

Figure 7- Typical Inclinometer Plot

TABLE 1

Load Test Results

Pile Id	Test Type	Depth Driven m	Days After Driving	Max. Load Applied kN	Tip Movement at Max. Load mm	N_h kg/m^3	Deflection mm
M01-F46	Compression	19.05	14	5338	2.3		--
M05-D05	Compression	12.19	7	4003 *	?		--
M09-C20	Compression	12.19	7	5338	9.30		--
M14-E42	Compression	12.19	10	5338	11.6		--
M21-E28	Compression	12.19	62	4644**	12.1		--
M24-E03	Compression	12.19	10	5338	5.4		--
M26-G56	Compression	12.19	9	5338	5.4		--
M02-B25	Tension	12.19	10	2224	2.6		--
M05-F43	Tension	12.19	12	2224	2.0		--
M11-B24	Tension	12.19	30	2224	1.2		--
M15-H35	Tension	12.19	35	2224	1.7		--
M19-E04	Tension	12.19	72	2224	2.4		--
M26-S29	Tension	12.19	13	2224	2.1		--
M02-C01	Lateral	19.11	9	445	--	2.05×10^6	31.5
M02-C03	Lateral	18.9	9	445	--		32.8
M06-G01	Lateral	20.27	16	445	--	2.52×10^6	25.4
M06-G03	Lateral	19.29	16	445	--		26.7
M13-B41	Lateral	13.72	36	445	--	1.54×10^6	34.3
M13-B43	Lateral	13.72	36	445	--		33.5
M25-D25	Lateral	13.72	13	445	--	1.20×10^6	40.6
M25-D27	Lateral	13.72	13	445	--		34.8

* - Failed (plunged) ** - Failed (reached criterion)

K_0 FROM PILE LOAD TESTS

It is believed that the high capacities reported above are caused by the in-situ effective stress conditions in the foundation soil. The shaft resistance for a low-displacement pile foundation is highly dependent on the effective horizontal stress (the normal force) acting on the sides of the pile. This parameter is commonly expressed in terms of the ratio of effective horizontal stress to effective vertical stress, and is known as the coefficient of earth pressure at rest ($K_0 = \sigma'_h/\sigma'_v$). The determination or estimation of this parameter for use in geotechnical design is one of most difficult tasks in foundation engineering. Often K_0 is erroneously estimated using correlations for normally consolidated soils. Some of the most commonly used empirical formulas are: for normally consolidated soils (Jaky, 1944)

$$K_0 = 1 - Sin\phi'$$

where ϕ' = to the effective friction angle of the soil, for overconsolidated soils (Mayne and Kulhawy, 1982)

$$K_0 = (1 - Sin\phi')OCR^{Sin\phi'}$$

where OCR = the overconsolidation ratio.

As K_0 is dependent on many factors, consequently the use of simple correlations can lead to significant error. Hanna and Ghaly (1992) reported that K_0 is affected by the effective angle of shearing resistance, shape and interlocking of soil particles, amount of fines in the soil, porosity, crushing, modulus of elasticity of the mineral particles, elastic and sliding strains, aging, dilation, densification, compacting method, stress history, and applied stress level.

Since H-piles are low displacement piles and no evidence of plugging was observed during driving, it was assumed that installation effects were negligible. The results of the full-scale pile load tests were used to back-calculate the in-situ horizontal stress in terms of K_0. Back-calculation of K_0 from load tests requires the pile capacity, the load transferred to the soil in skin friction, the distribution of skin friction, the angle of interface friction (δ) between the pile and the soil, and the vertical effective stress profile.

Pile Capacity - Six pile load tests were performed on 14x117 H-piles driven 12.2 m (40 ft.). The piles were driven approximately 1.5 m (5 ft.) in alluvial sand and 10.7 m (35 ft.) into the McNairy formation. The average capacity determined from these tests was at least 5000 kN (1124 kips). Four of the tests were taken to the limit of the testing frame 5338 kN (1200 kips) without reaching failure.

Load Transfer- The load transferred to the soil in friction can be estimated by evaluating tell-tale (displacement) or strain gauge data collected during the test. The tell-tales used for this project were steel rods attached to a specific location on the piles prior to driving. They were isolated from the soil by a protective steel casing and were monitored with dial gauges at the surface during the load tests. Each of the piles tested had a tell-tale attached to the tip of the pile to measure compression of the pile during the tests. An additional tell-tale was attached to one

of the piles at mid-depth. The pile with two tell-tales was used to determine the average load in the pile that resulted in the measured compression. The compression of three segments of the pile was determined from the butt to the tip, the butt to the midpoint, and the midpoint to the tip. The average load in the pile over the length in compression was calculated using the following formula and plotted at the center of each segment in Figure 8.

$$P_{avg} = \frac{A \times E \times \Delta L}{L}$$

Where:

P_{avg} = average load in the pile over the length in compression
A = cross-sectional area of the pile
ΔL = compression of the pile
E = Young's Modulus of the pile
L = length of the pile segment in compression

Graphically, the load remaining in the pile at its tip can be determined by extrapolating a line through the load at the center of each segment to the tip. Figure 8 shows the load remaining in the pile along with the load transferred to the soil (skin friction) determined by subtracting the load in the pile from the total load applied. This procedure indicates that this pile developed at least 4390 kN (986 kips) of skin friction capacity. Since the other piles tested only had one tell-tale, a procedure developed by Leonards and Lovell (1979) and reported by Fellenius (1990) was used to estimate the skin friction. "This method is based on the fact that a plot of butt load versus pile compression results in straight line segments; for this condition it is possible to estimate more reliably the separate contributions to pile compression of point load and shaft friction, and hence to estimate their respective values" (Leonards and Lovell, 1979). An estimate of a ratio (defined as the distance to the centroid of the unit skin friction distribution from the ground surface over the length of embedment) is required to perform this analysis. A uniform distribution would have a ratio of 0.5 while a linear increasing distribution would have a ratio of 0.667. Since the exact shape is not known, this value was back-calculated using the results determined from the pile with two tell-tales. A value of 0.6 was obtained. This value was then used as the ratio for all of the other test piles. The average value of skin friction estimated for the remaining piles was 3880 kN (873 kips). Data was reviewed from a preliminary load test performed in 1988 on a pile instrumented with strain gauges (U.S. Army Corps of Engineers, 1989). This indicated the McNairy formation provided a uniform frictional resistance of approximately 365 kN/m (25 kips/ft) of a 14x117 H-pile. Additionally, an estimate of skin friction is made when performing a CAPWAP analysis on dynamic test data. The CAPWAP analyses that were performed on dynamic data obtained from restrike tests estimated the average skin friction to be 75% of the total capacity. This yields a magnitude of approximately 3750 kN (843 kips). Additionally, six tension tests were performed on this site. The maximum required tension capacity was 1560 kN (350 kips). All of the tension test piles were loaded to 2224 kN (500 kips) (the capacity of the testing frame) without reaching failure. The estimation of horizontal stress from the tension tests can be considered to be a lower bound since the capacity from a tension test is all developed in skin friction and the actual tension capacity is greater than the maximum load applied in the test.

Shape of Distribution- The above analyses all indicate that within the McNairy formation the distribution of skin friction resistance is approximately uniform with depth. The resistance ranges from approximately 350 to 423 kN/m (24 to 29 kips/ft). The upper portion of the pile that is embedded in the alluvial river sand causes the ratio for the overall distribution determined in the Leonards and Lovell (1979) method to be greater than 0.5.

Angle of Interface Friction- The angle of interface friction between the pile and the soil (δ) was estimated to be approximately 25 degrees. δ is normally considered to be approximately 0.66 to 0.75 of the angle of internal friction of the soil (ϕ). The average ϕ for the McNairy soils is approximately 31 degrees. For the subject H-piles, a δ of 25 degrees was chosen for analysis. This was determined by taking an average of 0.66 x ϕ (the interface angle between the steel flanges and soil) and ϕ for the sides adjacent to the web. A true value of interface friction would be difficult to determine due to rearrangement and crushing of sand particles during pile installation and loading. In this particular case, the horizontal stress is so large that this analysis is insensitive to the actual value of δ.

Vertical Effective Stress- The vertical effective stress profile was estimated at each pile location by multiplying the depth and the saturated unit weight of the soil, then subtracting the pore pressure measured by piezometers installed in the foundation subgrade.

Horizontal Effective Stress -For a uniform distribution of skin friction resistance, the horizontal stress can be determined by using the following equation.

$$\sigma'_h = \frac{F_s}{\tan\delta \times A_s}$$

Where:

σ'_h = magnitude of effective horizontal stress
F_s = resistance due to skin friction per unit length of pile
δ = angle of friction between soil and pile
A_s = surface area of pile per unit length

The surface area for an H-pile was determined assuming the pile acts as a rectangular shape rather than an "H". The piles were divided into vertical elements and the above calculation applied to each segment. The upper alluvial sand layer was modeled to have a linearly increasing skin friction distribution while the McNairy was modeled to have a uniform distribution. The values of unit skin resistance were adjusted until the total skin friction resistance matched that determined by the Leonards and Lovell (1979) analysis. Once the effective horizontal stress is determined, the ratio of effective horizontal stress to effective vertical stress (σ'_h / σ'_v) can be calculated. A plot of the effective stress ratio (K_0) verses elevation for each of the compression tests is shown on Figure 9. In addition, K_0 determined from a typical tension test is shown as a lower bound. As discussed earlier, it is important to note that K_0 determined by this method may be slightly greater than the initial in-situ effective stress ratio due to the effects of driving and loading of the pile. The resulting magnitudes of K_0 required to develop the static capacities measured in the pile load tests are quite large.

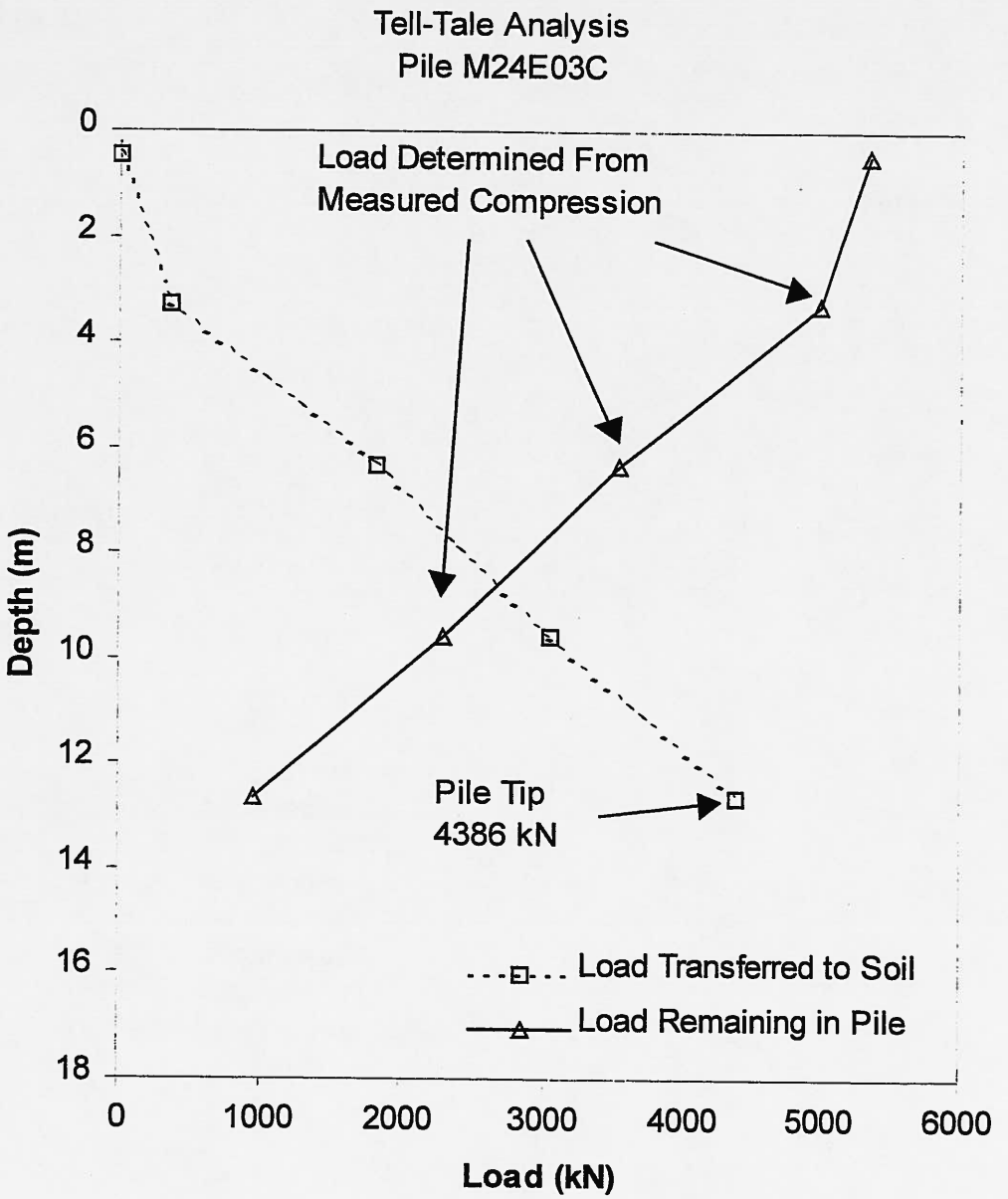

Figure 8- Load Distribution From Tell-Tale

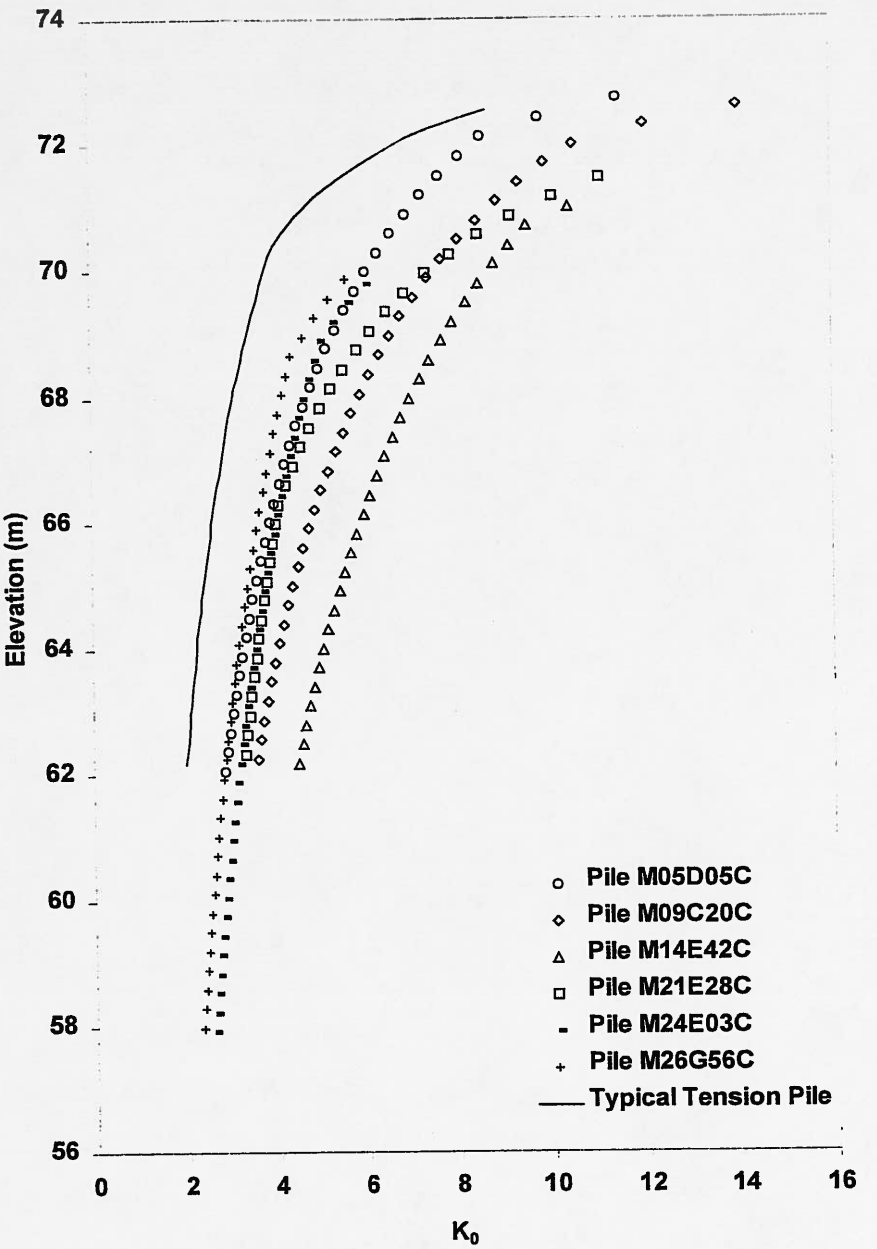

Figure 9 – K_0 From Pile Load Tests

K_0 FROM SELF-BORING PRESSUREMETER TESTS

In conjunction with investigations required for the design of large diameter drilled shafts required for the Lock approach walls, measurements of in-situ stress were made with a self-boring pressuremeter (SBPM). The SBPM is one of the few devices capable of directly measuring in-situ lateral stress and is often used as the baseline method when evaluating other tests (Mayne and Kulhawy, 1990). The testing was performed by Dr. Jean Benoit and associates from the University of New Hampshire.

The measurements were made with a modified English SBPM designed by Dr. Benoit and manufactured by Cambridge In-situ (Figure 10). To measure the movement of the expanding membrane, this SBPM has three sets of strain arms located at the quarter points. At each quarter point, three strain arms are oriented 120 degrees apart. The tests were performed in borings (drilled from a floating plant) located approximately 305 m (1000 ft) upstream and 305 m (1000 ft) downstream of the Olmsted Locks cofferdam. This area is located away from the influence of the pile driving and is assumed to be undisturbed. Borings were advanced to just above the elevation of a test. The SBPM was placed in the bottom of the boring and advanced using one of three different methods: a flat blade bit, a roller bit, or a jetting nozzle. The jetting nozzle provided the best advancement with little disturbance. See Benoit et al. (1995) and Benoit (1995) for more details on advancement methods. After advancement to the desired depth, testing was delayed 45 minutes to allow for the dissipation of pore pressure. The membrane was then pressurized and total pressure verses cavity strain was measured.

The total horizontal stress was determined at each strain arm by inspection of the total corrected pressure vs. cavity strain plots. The pressure at which the membrane lifts off (begins deforming the soil) is equal to the in-situ total horizontal stress. Figure 11 shows a typical test result from one strain arm. All data that indicated significant disturbance were omitted. The effective horizontal stress (σ'_h) was determined by taking the average total horizontal stress at each set of strain arms and subtracting the pore pressure calculated from the height of water above the each test location. A value of K_0 for each elevation of the strain arms was determined by dividing σ'_h by the calculated σ'_v. Figure 12 shows a plot of K_0 verses elevation determined from the SBPM along with K_0 determined from the compressive pile load tests. The shape of the K_0 curve is similar to the curves derived from the pile load tests. However, the magnitude of K_0 determined from the SBPM is lower at depth. The difference is likely due to increases in lateral stress from the installation and loading of the piles and/or possible stress relief from soil disturbance from the SBPM test.

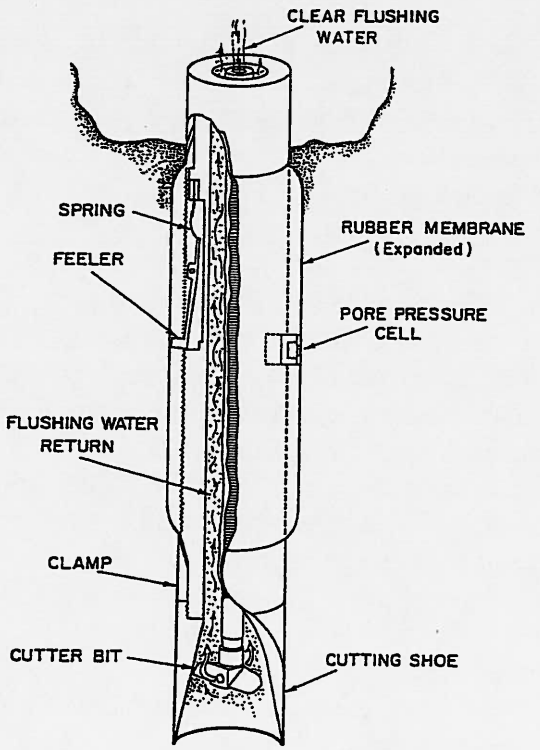

Figure 10 - Self-Boring Pressuremeter (From Benoit, et al., 1995)

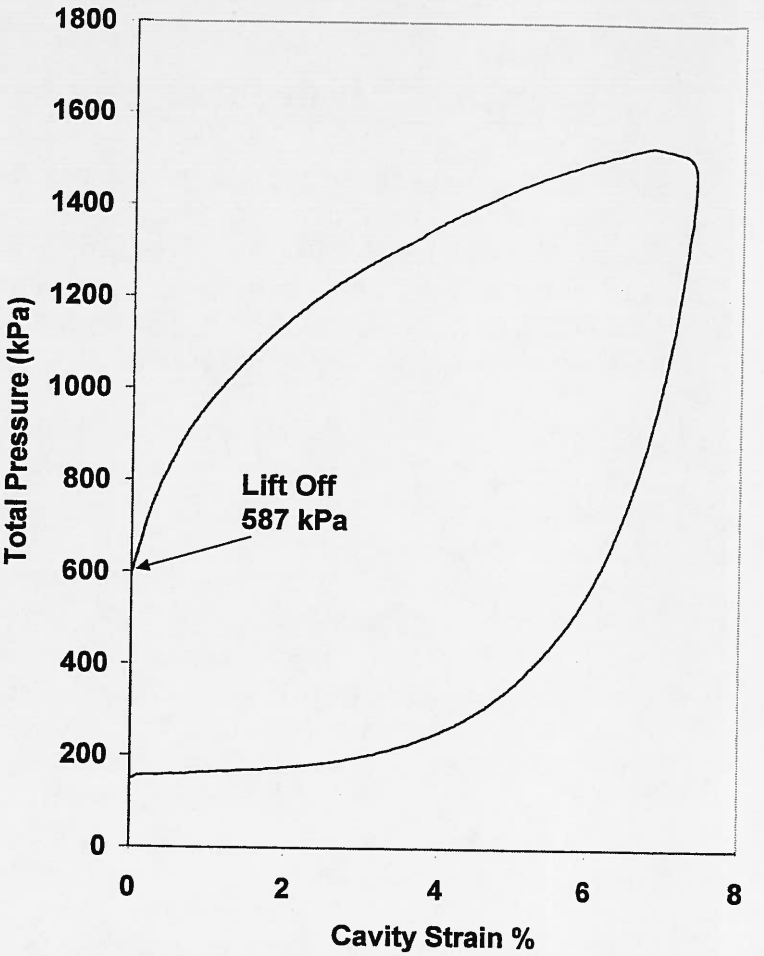

Figure 11 - Typical SBPM Measurements

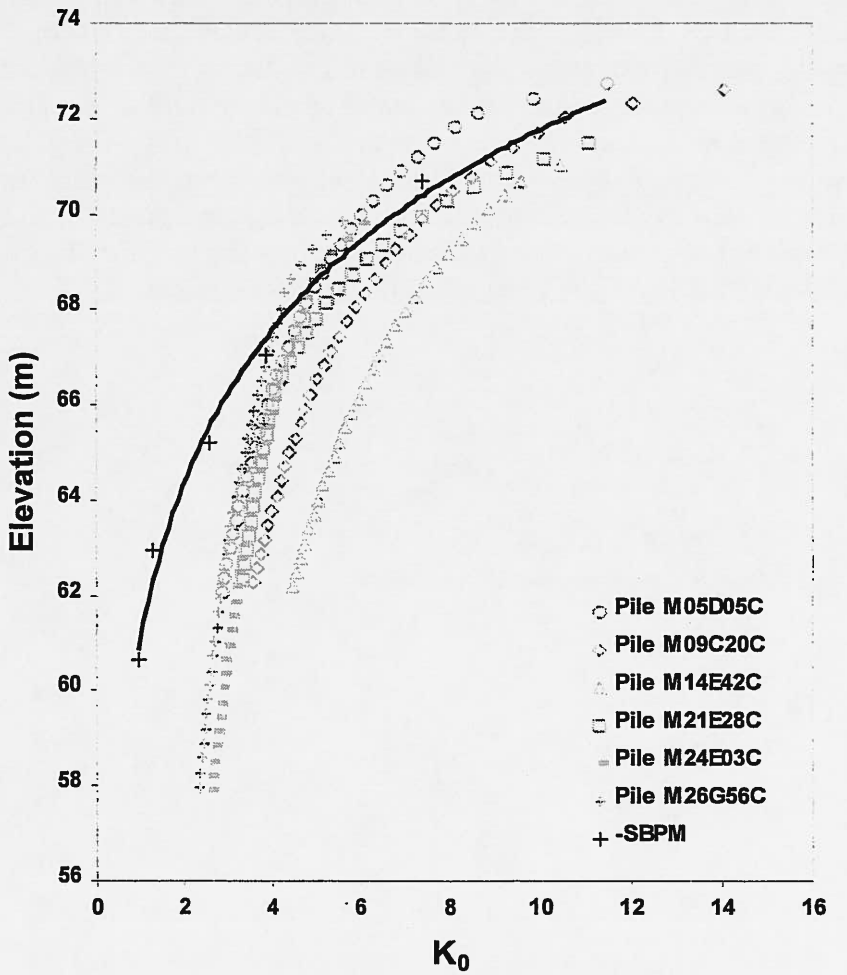

Figure 12 - K_0 from SBPM and Piles

SOURCE OF HIGH HORIZONTAL STRESS

A literature survey reveals many with studies relating K_0 to stress history in terms of the overconsolidation ratio(OCR) (Brooker and Ireland, 1965; Mayne and Kulhawy,1982 and 1990; Kulhawy et al.,1989; Kulhawy and Mayne,1990). The OCR is defined as the maximum past vertical effective stress σ'_p divided by the present vertical effective stress σ'_v. If the main source of high lateral stress is past overburden pressure, using the Mayne and Kulhawy's equation presented earlier, the expected OCR of clay samples obtained from the McNairy would be very high (i.e., greater than 25). Figure 13 shows the OCR vs. depth profile for the study area. These were determined from consolidation tests performed on clay samples taken from the McNairy Formation with a denison sampler. Five of the samples were loaded to 6129 kPa (64 tsf) while two samples were loaded to 3064 kPa (32 tsf). As can be seen, very high past overburden stress

is unlikely to be the main source of the current high lateral stress. Jefferies et al. (1987) documents another case where K_0 was found to be independent of the OCR in the Beaufort Sea clays. In this study, K_0 was also directly measured with a SBPM. Another possible explanation form high horizontal stresses is dynamic loading. Earthquake loading could have caused permanent strain in the soil, which would increase the in-situ state of stress. Zhu and Clark (1993) studied the effect of dynamic loading on lateral stress in sand in the laboratory. They found that the lateral stress in the sand may increase or decrease during vibration, depending on the initial state of stress. When the initial value of K_0 is less than one, the lateral stress increased. When the initial value of K_0 was greater than one, the lateral stress decreased. In both cases, the deviator stress of the soil is reduced towards the isotropic stress state of $K_0 = 1$. Considering this, it is unlikely that dynamic shaking is the source of the high lateral stress.

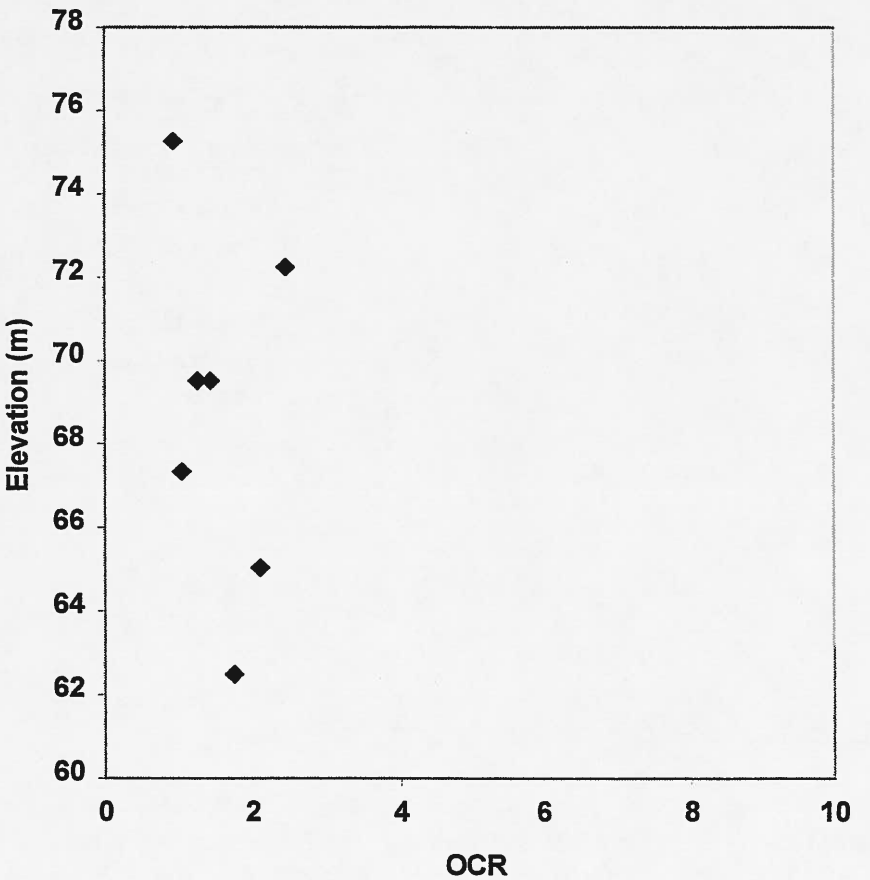

Figure 13 – OCR Profile

Proposed Mechanism - Since the presence of high horizontal stress in the McNairy formation does not appear to be related to stress history, another logical explanation is needed. It is proposed that the high horizontal stress may be related to lateral tectonic loading of the McNairy formation in the study area. Research of the geological literature and subsurface explorations, indicate that the Olmsted project site is located within a graben (a depression caused by two parallel faults) feature. Figure 14 is a contour map taken from Davis et al. (1987) showing the top of Paleozoic bedrock. This shows that the study area lies within a subsurface rock valley. This feature was also found on a map (Figure 15) produced by Ross (1963). The McNairy Formation within the study area is located between elevations 54.8 m (180 ft) and 79.2 m (260 ft). If high stress or displacement is present in the rock valley walls, it would logically be transferred to the infilled soil (McNairy). The presence of this valley feature is also shown on Figure 16 from Schwalb (1969). On this map he associates this feature with a fault. Kolata et al. (1981) describe the valley as the most unusual subcretaceous feature in southern Illinois. It is a northeast-oriented elliptical depression in southeastern Pulaski County that generally coincides with the America Graben (Figure 17). Schwalb (1969) indicates that it may continue southward through Ballard and Carlisle Counties in Kentucky.

The soil could either be loaded from the compressive stresses present in the regional body stress of the rock or by local stresses induced by relative displacements of rock masses associated with local seismicity. Figure 18 depicts a conceptual schematic of the proposed lateral loading of the McNairy Formation. If a soil element subject to horizontal load is allowed to expand vertically, the ratio of horizontal to vertical stress will increase until a state of passive failure exists. Although similar source mechanism theories could not be found in the literature, it is recognized that K_0 is influenced by geologic environment (Kulhawy, et al., 1989).

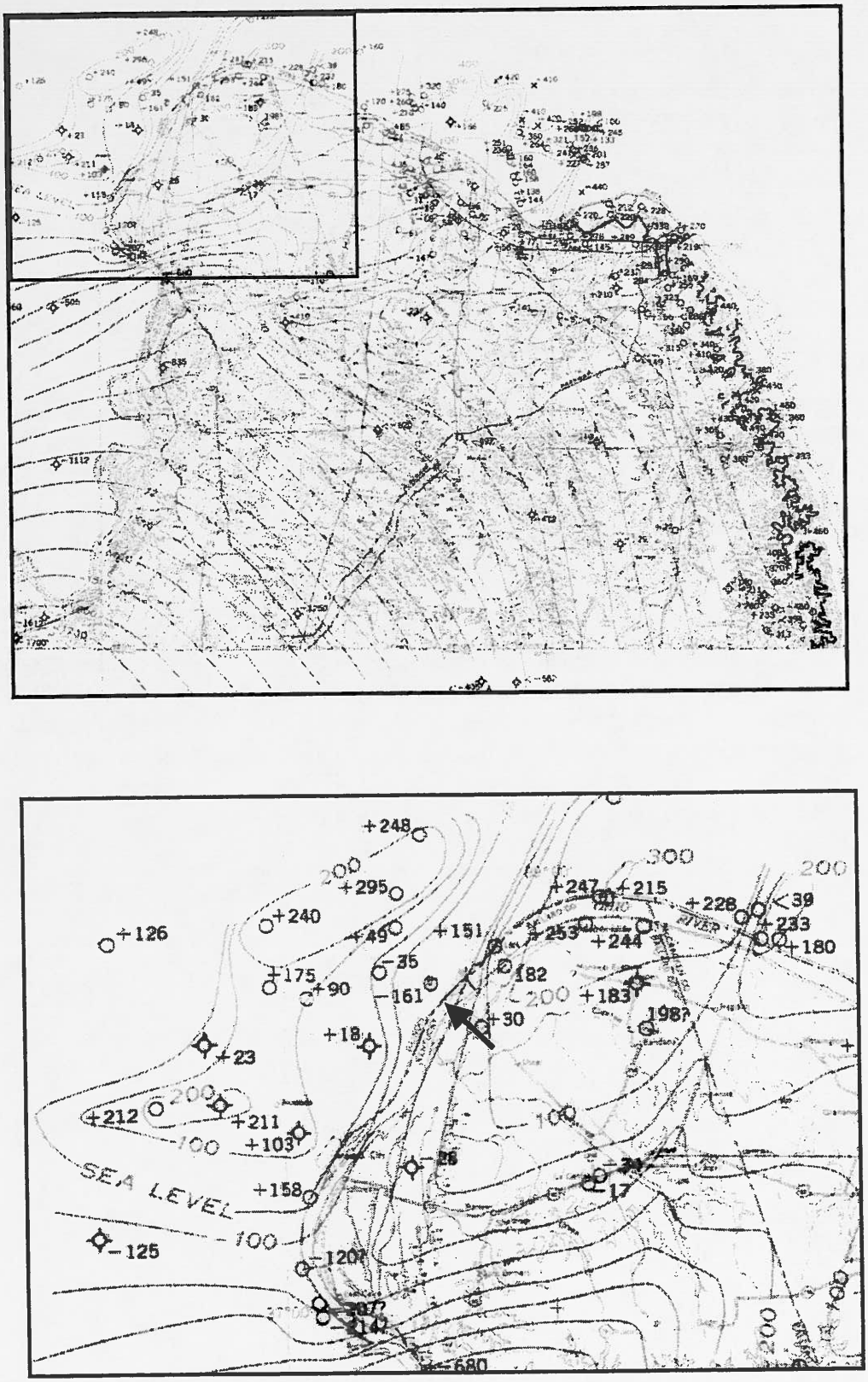

Figure 14 - Top of Paleozoic Rock (From Davis, et. al, 1973)

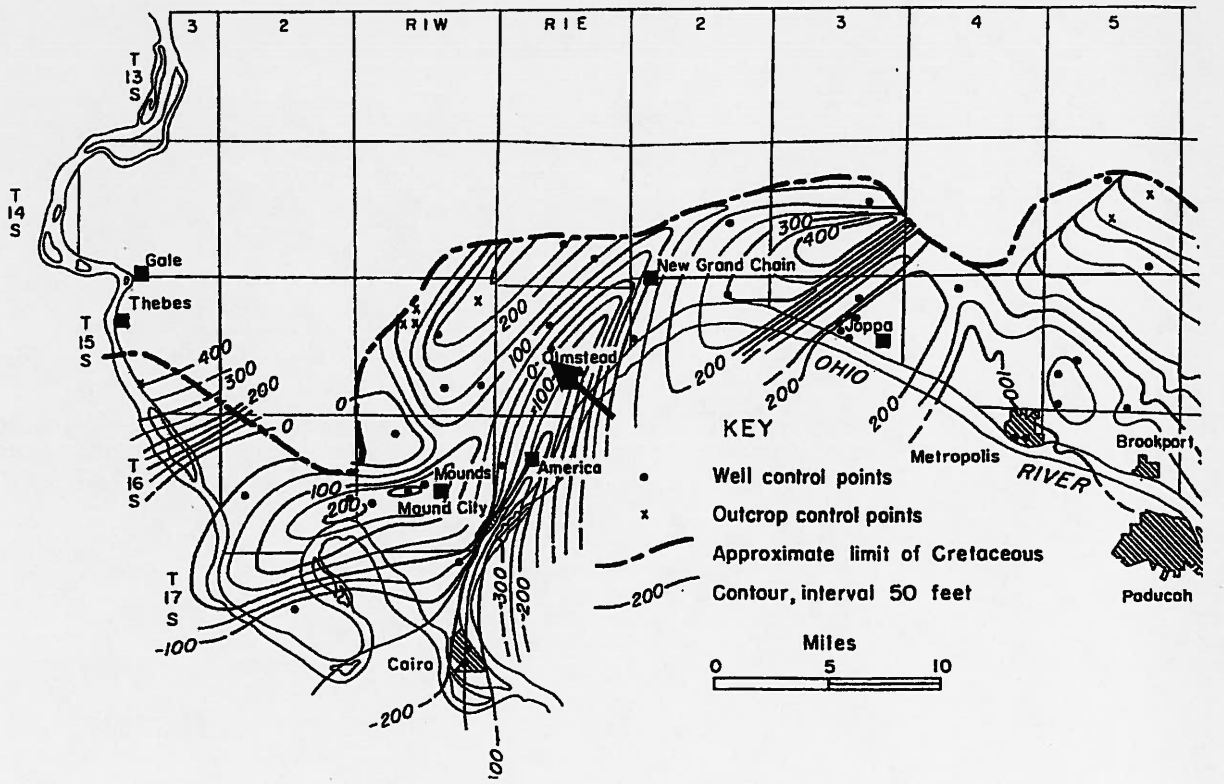

Figure 15 - SubCretaceous Surface (From Ross, 1963)

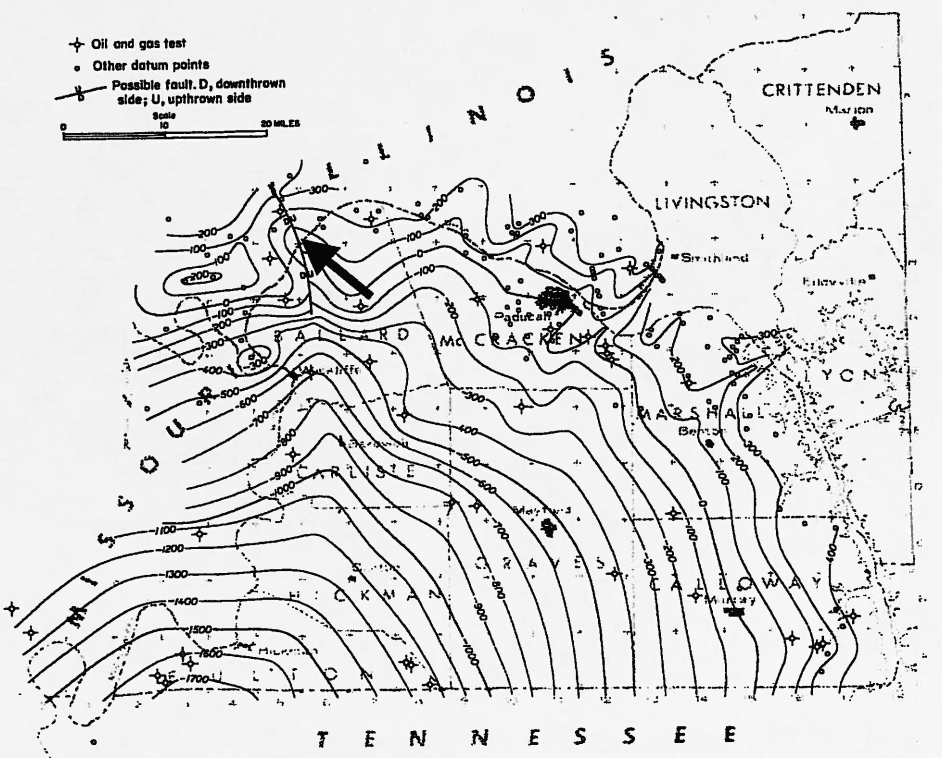

Figure 16 - Paleozoic Bedrock Surface (From Schwalb, 1969)

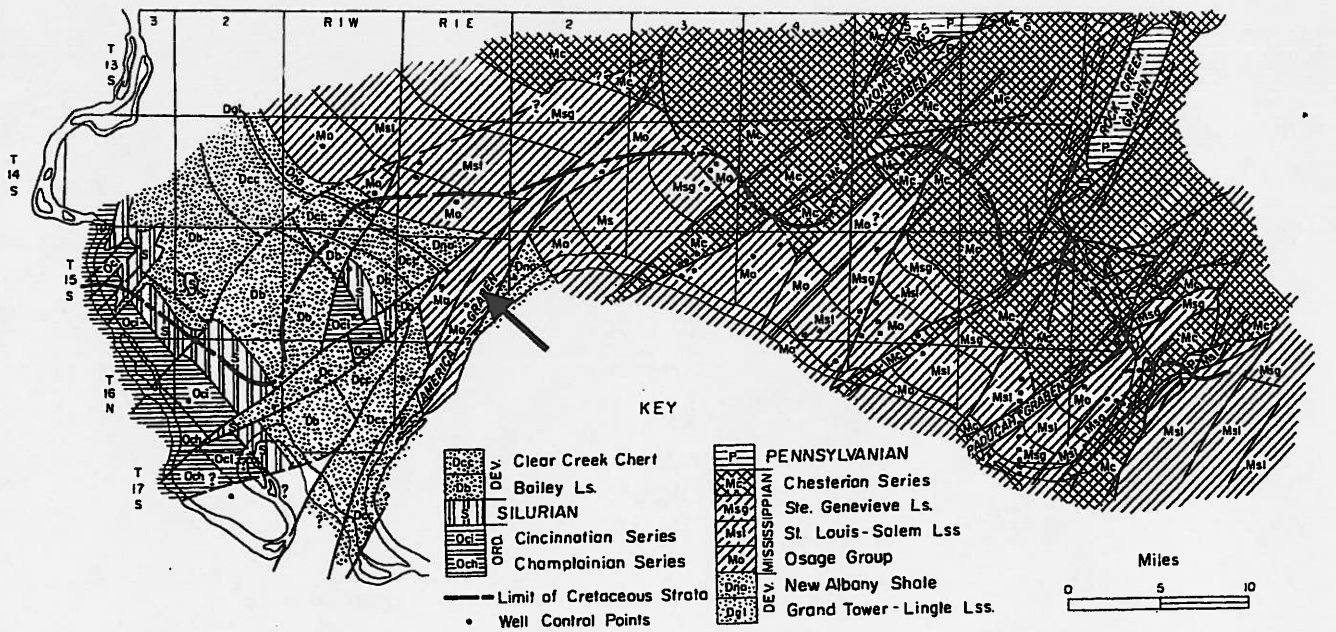

Figure 17 - Map Showing American Graben (From Ross, 1963)

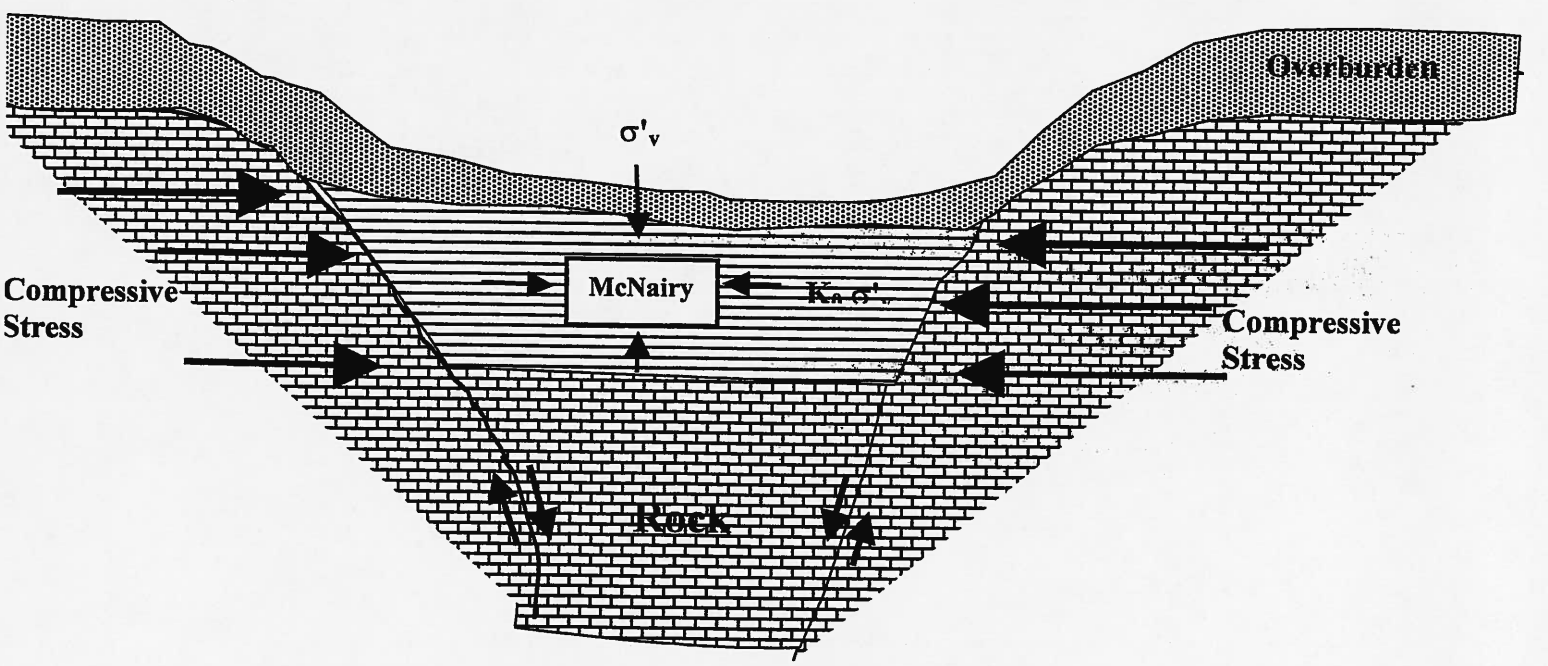

Figure 18 - Proposed Mechanism of Lateral Loading of McNairy (No Scale)

Evidence of Geologic Compressive Stress- The existence of high horizontal stress in the rock within the region is well documented in the geologic literature. Zoback and Zoback (1980, 1989), Nelson and Bauer (1987), Hamburger and Rupp (1988), and Ellis (1994) have compiled stress data and indicators in the New Madrid Seismic Zone (NMSZ) region. Ellis (1994) provides a summary of the crustal stress data. He presents focal mechanism solutions, borehole breakouts, and shallow stress measurements. These data confirm the east-west to northeast-southwest horizontal compressive stress in the region. The ratio of horizontal to vertical stress (K_0) from the compiled measurements ranged from 1.6 to 5.6.

In a report prepared for the U.S. Army Corps of Engineers, Nieto (1991) proposes a linear elastic finite element model of the Mississippi Embayment. His model shows that very high horizontal stress should be expected in the upper Mississippi Embayment. Taylor and Duncan (1991) agree that there are high horizontal stresses in the geologic formations that underly the Olmsted Locks and Dam Site.

Other features found within the Mississippi Embayment substantiate the regional compressive stress regime. These features include the Lake County Uplift consisting of Ridgely Ridge, Tiptonville Dome, and Sikeston Ridge (Russ, 1992) and Charlies Ridge (Hamilton and McKeown, 1988).

The landslide present on the Illinois bank can also be considered as evidence of the presence of high horizontal stresses. The slide was found to be failing along the upper contact of the McNairy Formation. Erosion of the Illinois bank likely created passive failure of this formation. The thin clay layers were then in a state of residual strength making the slope failure possible. This mechanism of failure in areas with high lateral stress has been documented by Brooker and Peck (1993).

Local Seismicity - The Olmsted project is located near the northern edge of the New Madrid Seismic Zone (NMSZ). The NMSZ is the location of North America's greatest earthquake sequence. The New Madrid earthquakes of 1811-1812 are well documented by Fuller (1912), Nuttli (1973), Street (1982), Street and Nuttli (1984, 1990), Johnston and Schweig (1996). It is generally accepted that the current seismic activity is caused by the contemporary stress field acting on previously weakened fault zones associated with the failed Reelfoot rift; however, the actual mechanism is not well understood. The NMSZ remains active today, Figure 19 shows epicentral plots of earthquakes measured between 1974 and 1998. Most activity occurs in the central part of the NMSZ. However, numerous events have occurred near the Olmsted site.

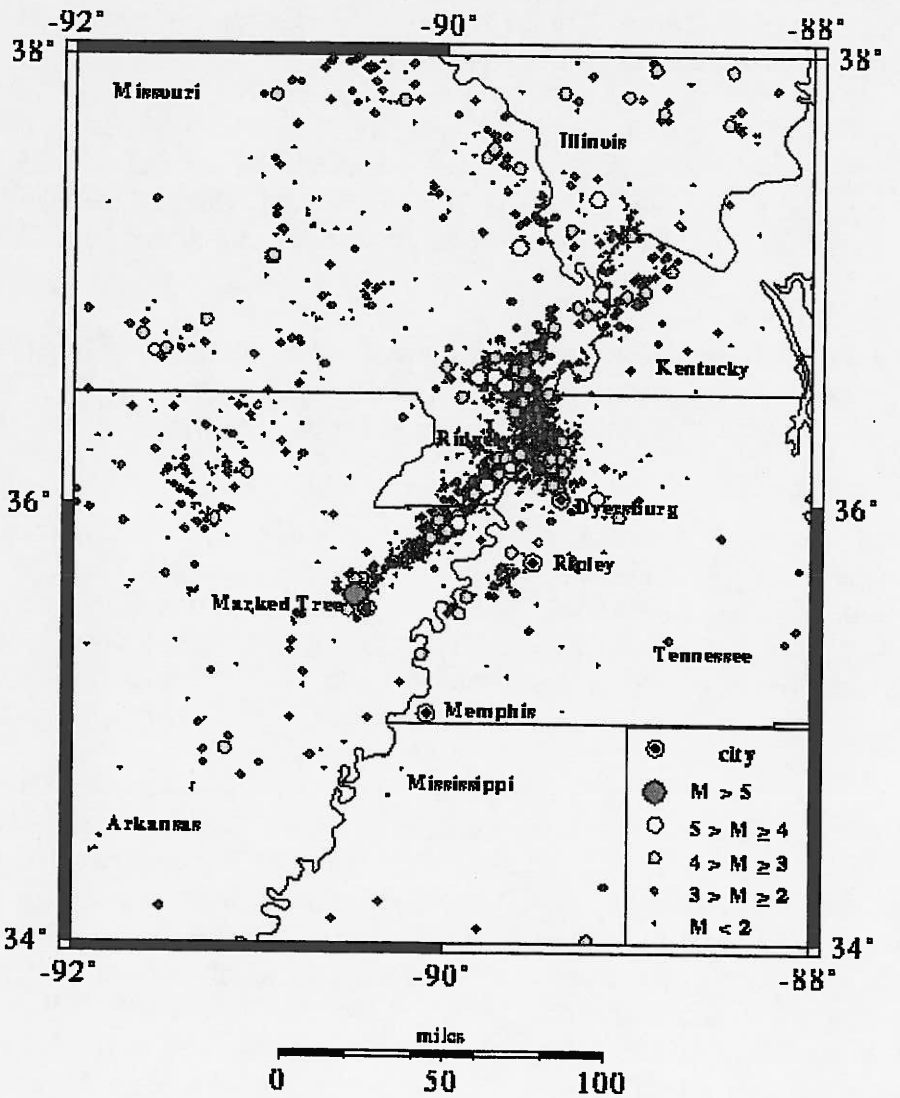

Figure 19 - Recorded Regional Seismic Events (From CERI)

Other Local Geologic Features - The study area lies within the Paducah Gravity Lineament and is very close to the Commerce Geophysical Lineament, Figure 20. There is evidence from the magnetic data presented by Hildenbrand et al. (1982), that the Ste. Genevieve fault in southern Illinois crosses into Kentucky near the study area.

As previously mentioned, the McNairy Formation overlies an altered rock formation (Fort Payne). The unaltered Fort Payne is a highly siliceous and cherty fine grained dolomite or dolomitic limestone. In its altered state, as found in the study area, this formation is dark gray, lightweight rock with layers of hard chert. The current accepted source of this alteration (Nelson et al., 1995; Berg and Masters, 1994) is leaching of the carbonates from the parent rock due to hydrothermal activity. Measured gravity and magnetic anomalies probably represent a mafic igneous intrusion, which was a likely heat source for hydrothermal activity in southern Illinois (Berg and Masters, 1994). The presence of this altered rock formation is additional evidence of deep structures in the region. The local seismicity is likely a result of the reactivation of these structures.

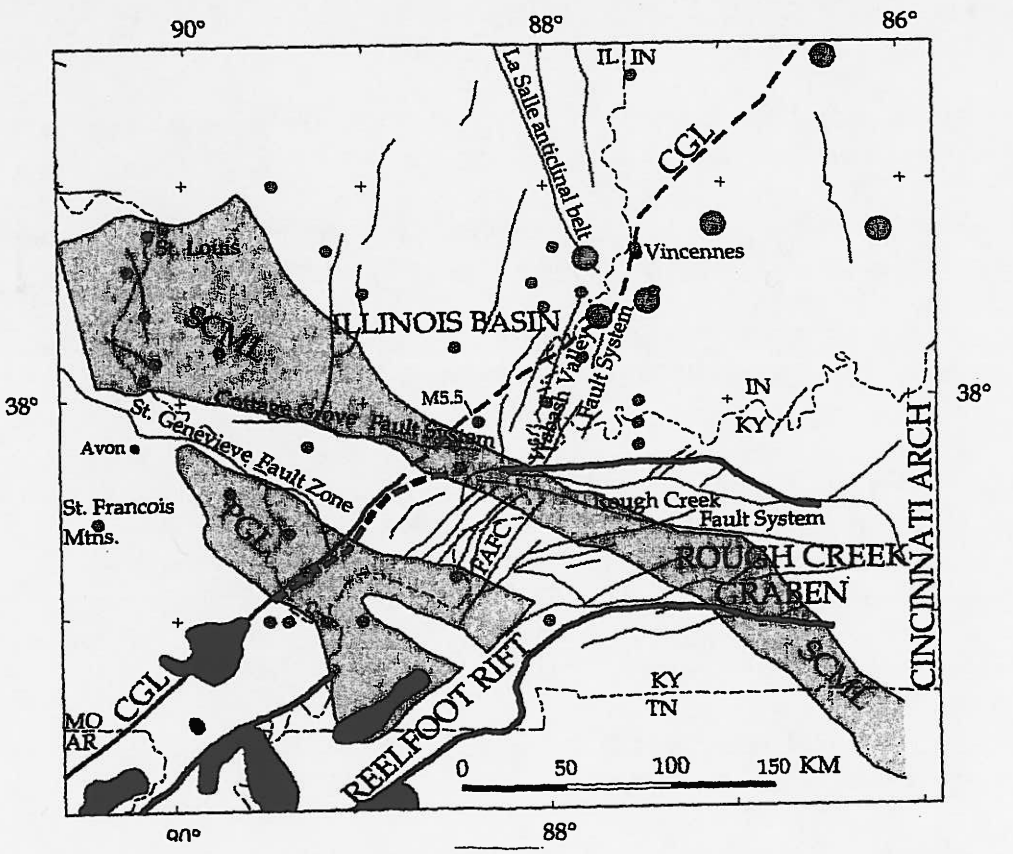

Figure 20 - Site Relative to PGL and SCML. (Base Map from Hildenbrand and Ravat, 1997)

CONCLUSIONS

- A comprehensive study of the Olmsted Locks and Dam site has shown that very high in-situ stress exists in the shallow soils of the upper Mississippi Embayment.
- These stresses have had a dramatic effect on the capacity of the pile foundation for the Olmsted Lock and Dam. Analysis of pile load test results indicate that K_0 ranges from 2 (at the tip of the piles) to greater than 10 near the ground surface.
- Testing with a SBPM was successful in verifying the high lateral stress.
- A logical theory is presented which shows the high in-situ stress in the McNairy formation is the result of tectonic compressive stresses which have been transferred to the soil.
- It is suggested that additional geophysical investigation of the study area should be performed to gain a better understanding of the structure and seismological implications of the features presented in this study.

REFERENCES

ASTM D 1143-81. "Standard test method for piles under axial compressive load." *American Society for Testing and Materials, Annual Book of Standards*, Vol. 04.08.

ASTM D 3689-90. "Standard test method for individual piles under static axial tensile load." *American Society for Testing and Materials, Annual Book of Standards*, Vol. 04.08.

ASTM D 3966-90. "Standard Test Method for Piles Under Lateral Loads." *American Society for Testing and Materials, Annual Book of Standards*, Vol. 04.08.

Bear, G., Rupp, J. and Rudman, A. (1997). "Seismic Interpretation of the Deep Structure of the Wabash Valley Fault System", *Seismological Research Letters*, Vol. 68, 624-640.

Benoit, J. (1995). "Advances in Pressuremeter Technology with Specific Reference to Clays." *The Pressuremeter and Its New Avenues*, Proceedings of the 4th International Symposium, 125-139.

Benoit, J., M.J. Atwood, R.C. Findlay, and B.D. Hillard (1995). "Evaluation of Jetting Insertion for the Self-Boring Pressuremeter." *Canadian Geotechnical Journal*, Vol. 32, 22-39.

Berg, R. B., and Masters, J. M., (1994). "Geology of Microcrystalline Silica (Tripoli) Deposits, Southernmost Illinois", Illinois State Geological Survey, Circular 555, 89 p.

Brooker, E.W., and Ireland, H.O., (1965). "Earth Pressures at Rest Related to Stress History", *Canadian Geotechnical Journal*, vol. II no.1, 1-15

Brooker, E. W., and Peck, R. B. (1993). "Rational design treatment of slides in overconsolidated clays and clay shales," *Canadian Geotechnical Journal*, Vol. 30, No. 3, 526-544.

Davis, R. W., Lambert, T. W., and Hanson, A. J. (1973). "Subsurface Geology and Ground-Water Resources of the Jackson Purchase Region, Kentucky," Geological Survey Water Supply Paper 1987, U.S. Geological Survey.

Davisson, M. T., (1975). "Pile Load Capacity," Proceedings, Design, Construction and Performance of Deep Foundations, ASCE- University of California, Berkeley.

Davisson, M. T., (1972). "High Capacity Piles", Proceedings, Soil Mechanics Lecture Series on Innovations in Foundation Construction, American Society of Civil Engineers, ASCE, Illinois Section, Chicago.

Ellis,W.L., (1994)."Summary and Discussion of Crustal Stress Data In the Region of the New Madrid Seismic Zone," Investigations of the New Madrid Seismic Zone, U.S. Geological Survey Professional Paper 1538-B, B1-B13.

EM-1110-2-2906 (1991). "Design of Pile Foundations." U. S. Army Corps of Engineers, Engineer Manual.

Fellenius, Bengt H. (1990). "Guidelines for the Interpretation and Analysis of the Static Loading Test." Deep Foundations Institute Short Course Text.

Fuller, M. L., (1912). "The New Madrid Earthquake", U.S. Geological Survey Bulletin 494, 118 p.

Goble, Rauche, Likins, and Associates Inc. (1996). "CAPWAP Manual"

Hamilton, R.M., and McKeown, (1988). "Structure of the Blytheville arch in the New Madrid seismic zone, *Seismological Research Letters*, Vol. 59, 117-121.

Hamburger,M. W. and Rupp, J.A. (1988). "The June 1987 southeastern Illinois earthquake: Possible tectonism associated with the La Salle anticlinal belt." *Seismological Research Letters*, Vol. 59, 151-157.

Hanna, A. and Ghaly, A. (1992). "Effects of K_0 and Overconsolidation on Uplift Capacity." *Journal of Geotechnical Engineering.*, ASCE, Vol. 118, No. 7, 1449-1469.

Hildenbrand, T.G., Kane, M.F, and Hendricks, J. D.. (1982). "Magnetic Basement in the Upper Mississippi Embayment Region - A Preliminary Report," Investigations of the New Madrid Earthquake Region, Geological Survey Paper 1236, 39-53

Hildenbrand, T.G., and Hendricks, J.D., (1995). "Geophysical Setting of the Reelfoot Rift and Relations between Rift Structures and the New Madrid Seismic Zone," U.S. Geological Survey Professional Paper 1538-E, E1-E29

Hildenbrand, T.G., and Ravat, D. (1997). "Geophysical Setting of the Wabash Valley Fault System," *Seismological Research Letters*, Vol 68, 567-585.

Jaky, J., (1944). "The coefficient of Earth Pressure at Rest", *Journal of the Society of Hungarian Architects and Engineers*, Budepest, 355-358.

Jefferies, M. G., Crooks, J. H. A., Becker, D. E., and Hill, P. R., (1987). "Independence of geostatic stress from overconsolidation in some Beufort Sea clay", *Canadian Geotechnical Journal*, Vol. 24, 342-356.

Johnston, A. C. and Schweig, E. S., (1996). "The Enigma of The New Madrid Earthquakes of 1811-1812." *Annual Review of Earth and Planetary Sciences*, Vol 24.

Kolata, D. R., Treworgy, J. D., and Masters, J. M. (1981), "Structural Framework of the Mississippi Embayment of Southern Illinois," Illinois State Geological Survey, Circular 516, 72 p.

Kolata, D.R., and Hildenbrand,T.G., (1997). "Structural Underpinnings and Neotectonics of the Southern Illinois Basin: An Overview," *Seismological Research Letters*, Vol. 68, 499-510.

Kulhaway, F. H., and Mayne, P. W.,(1990). "Manual on Estimating Soil Properties for Foundation Design," Electric Power Research Institute, EPRI EL-6800

Kulhaway, F. H., Jackson, C. S., and Mayne, P. W., (1989). "First-Order Estimation of K_0 in Sands and Clays," Foundation Engineering: Current Principles and Practice, ASCE, 121-134.

Kulhaway, F. H., Beech, J. F., and Trautmann, C. J., (1989). "Influence of geologic development on horizontal stress in soil," Foundation Engineering: Current Principles and Practice, ASCE, 43-57.

Leonards, G. A., and Lovell, D. (1979). "Interpretation of Load Tests on High-Capacity Driven Piles." *Behavior of Deep Foundations*, ASTM STP 670, 388-415.

Mayne, P. W., and Kulhawy, F. H.(1990). "Direct and Indirect Determination of In-situ K_o in Clays." *Transportation Research Record* 1278, 141-149.

Mayne, P. W., and Kulhawy, F. H., (1982). "K_o - OCR Relationships in Soils," *Journal of Geotechnical Engineering*, ASCE, Vol. 108, 851-872.

Nelson, W.J., and Bauer, R.A., (1987). "Thrust Faults in Southern Illinois basin- Result of contemporary stress?," Geological Society of America Bulletin, Vol 98, p. 302-307

Nelson, W. J., Devera, J. A., and Masters, J. M., (1995). "Geology of the Jonesboro 15-Minute Quadrangle, Southwest Illinois," Illinois State Geological Survey, Bulletin 101, 57 p.

Nieto, Alberto S., (1991)."Geomechanical Study for USCEORL - Olmsted Dam Site," Supplement to Design Memorandum No. 5, Foundation Design Memorandum, U. S. Corps of Engineers, Louisville District.

Nuttli, O.W., (1973). "The Mississippi Valley Earthquakes of 1811-1812, Intensities, groundmotion, magnitude," *Bulletin of Seismological Society of America*, Vol. 63, 227-248.

Ross, C. A., (1963). "Structural Framework of Southernmost Illinois," Illinois State Geological Survey Circular 351, 27 p.

Russ, D.P. (1982). "Style and Significance of surface Deformation in the Vicinity of New Madrid, Missouri," *Investigations of the New Madrid Missouri, Earthquake Region*, U.S./ Geological Survey Professional Paper 1236, 95-114.

Schwalb, H. R., (1969). "Paleozoic geology of the Jackson Purchase region, Kentucky," Kentucky Geological Survey Report of Investigations 10, 40 p.

Street, R., (1982). "A Contribution to the Documentation of the 1811-1812 Mississippi Valley Earthquake Sequence," *Earthquake Notes*, Vol. 53, 39-52.

Street, R., and Nuttli, O.W., (1984). "The Central Mississippi Valley Earthquakes of 1811-1812," Proceedings of the Symposium on the New Madrid Seismic Zone, U.S. Geological Survey Open File Report 84-770, 33-63.

Street, R., and Nuttli, O.W., (1990). "The Great Central Mississippi Valley Earthquakes of 1811-1812," Kentucky Geological Survey, ser. 11, Special Publication 14, 15 p.

Taylor, T. and Duncan, J.M., (1991). "Review of the Structural Geology of the Olmsted Locks and Dam Area and Possible Consequences for the Project," Supplement to Design Memorandum No. 5, Foundation Design Memorandum, U. S. Corps of Engineers, Louisville District.

U. S. Army Corps of Engineers (1989). Louisville District, "Pile Tests Report," Design Memorandum No. 1, General Design Memorandum, Appendix F.

Zhu, F. and Clark, J. I., (1994). "The Effect of Dynamic Loading on Lateral Stress in Sand," *Canadian Geotechnical Journal*, Vol. 31, 308-311.

Zoback, M. L., and Zoback, M.D., (1980). "State of stress in the conterminous United States", Journal of Geophysical Research, Vol. 85, 6113-6156

Zoback, M. L., and Zoback, M.D., (1989). "Tectonic Stress Field of the Continental U.S.", *Geological Society of America*, Mem. 102, 523-537.

AN OVERVIEW OF CRITERIA USED BY VARIOUS ORGANIZATIONS FOR ASSESSMENT AND SEISMIC REMEDIATION OF EARTH DAMS

Rick Deschamps, P.E., Ph.D.[1] and Greg Yankey, P.E.[2]

ABSTRACT

There are several organizations within North America that are responsible for stability assessment and design of remediation options for seismically deficient earth dams. This paper provides on overview of the criteria and philosophy used by several agencies including: the U.S. Army Corps of Engineers, the U.S. Bureau of Reclamation, the Federal Energy Regulatory Commission, the California Department of Water Resources, and British Columbia Hydro. The methodologies used by the various agencies to evaluate stability, and the criteria adopted to assess different remediation schemes are compared and contrasted. Included is a discussion of the tendency to move to probabilistic risk based approaches by some agencies.

INTRODUCTION

Many earth dams in the United States are undergoing seismic stability assessments because at the time of construction earthquake loading criteria were below current standards, and the potential for liquefaction of alluvial foundations was not fully appreciated. Based on these reviews, most "well constructed" earth dams located in the Midwest and Eastern U.S. have adequate stability against design earthquake loading, provided loose granular alluvium is not present in the foundation. However, when loose granular alluvium is present, a significant risk of liquefaction can be found if the materials are not adequately dense.

Assessing the risk of liquefaction in a dam foundation and the potential for ensuing failure is one of the most challenging problems faced by geotechnical engineers. The mechanisms are extremely complex, the response is very sensitive to minor changes in soil parameters, the results of failure are catastrophic, and the cost of repairs are huge. Many of the important factors influencing liquefaction potential are poorly understood by the profession. The approaches that are commonly used in analyses have severe limitations, however, better methodologies are unavailable. Understandably in this challenging environment, the approaches used by various regulatory agencies and dam owners can be expected to vary.

This paper provides a brief overview of methodologies used to assess the potential for dam failure from liquefaction, and the criteria associated with calculating stability and evaluating remediation options. Only well constructed earth dams are considered in this discussion wherein the potential for the development of liquefaction is limited to the foundation. The approaches and philosophies of several agencies that are responsible for dam safety are described.

BACKGROUND

The impetus for this research started with the need to establish design criteria for seismic remediation of Dewey Dam, a U.S. Army Corps of Engineers (USACE) homogeneous earth dam located in Eastern Kentucky. A liquefaction analysis using the Seed and Idriss

---

[1] Senior Geotechnical Engineer, Fuller, Mossbarger, Scott and May Engineers Inc. Lexington KY.
[2] Associate, Fuller, Mossbarger, Scott and May Engineers Inc. Lexington KY.

approach, as outlined in NCEER (1996), indicated the potential for extensive liquefaction to occur in the foundation alluvium. In this type of analysis the challenges include developing soil strengths as function of the safety factor against liquefaction for use in limit equilibrium analyses, and assessing the applicability and reliability of predicted deformations using either Newmark-type analyses or dynamic numerical modeling. A methodology and criteria are needed to judge the relative stability of the existing structure and to evaluate proposed remediation alternatives. Accordingly, it was decided to review the approaches used by a variety of organizations responsible for dam safety in terms of seismic assessment and remediation.

THE ISSUES

There are several challenging issues regarding the assessment of liquefaction and seismic stability of earth dams. Although an exhaustive discussion of these issues is beyond the scope of this paper, a few brief general statements are made herein to establish a basis for the following discussions. A few of the important factors in the stability assessment include:

Liquefaction Potential Methodology.
The empirical approach developed by Seed, Idriss and their co-workers is employed in most cases. The approach is based on evidence of liquefaction at level ground sites where in-situ test results are available (commonly standard penetration tests or SPTs). Assessment of liquefaction potential in the foundation of an earth dam requires extensive adjustments, or corrections to the database for factors such as earthquake magnitude (duration), confining stress level, hammer energy, fines content, and shear stress level. Many of these corrections are based on interpretations from the extensive database of laboratory tests. The main criticism of this approach is the fact that each of these corrections introduces a significant uncertainty into the interpretation of liquefaction potential. In fact, there is conflicting evidence in some cases as to the effect of the factors including confining stress and initial shear stress.

Another approach that is sometimes used to assess liquefaction potential is to perform laboratory tests on "undisturbed" samples using the steady state concept advocated by Poulos and Castro (Poulos et. al.,1985). The approach is used to determine if the soil is in a contractive state such that a flow failure is possible. The main criticism of this approach is that truly undisturbed samples of granular soils are not possible to obtain requiring that the void ratio be corrected for interpretation. Moreover, the response of the soil is often sensitive to small changes in void ratio.

Although these approaches have significant limitations, they still represent the state-of-art in the assessment of liquefaction potential.

Assessment of Liquefied Soil Residual Strength.
Similar to the assessment of liquefaction potential, there are generally two approaches used to estimate the residual strength of liquefied soils: empirically and from laboratory tests. The empirical approach relates the corrected SPT N-value to back calculated strengths of failed slopes developed by Seed, Idriss and co-workers (See NCEER, 1996). The lab testing approach consists of performing sufficient tests to develop the steady state line and use this relationship to obtain the steady state strength for the estimated in-situ void ratio and confining stress (Poulos et. al. 1985). Recently, British Columbia Hydro (BCH) obtained frozen samples and performed dynamic testing in the laboratory in an attempt to obtain residual strengths directly (See series of papers on Duncan Dam

from Canadian Geotechnical Journal, 1994). A primary criticism of the empirical approach is the reliability of the back calculated strengths given the significant dependence on the assumptions made. Criticisms of the lab testing approaches is related to difficulty in establishing true in-situ conditions, and basing the response of a large volume of typically heterogeneous materials on the results of relatively few lab tests.

Further complicating the assessment of strength is choosing parameters for conditions were only partial liquefaction is expected, i.e. the safety factor against liquefaction is greater than 1.0.

Approaches Used To Assess Deformation.
Newmark type analyses are often employed to estimate seismicly induced slope movements. However, these approaches are recognized as being inapplicable for liquefied soils because they were developed based on rigid, or elastic, blocks. One of the challenges that faces the engineer is to discern when this type of deformation analysis is not valid. For example, below what safety factor against liquefaction should this type of analysis no longer be used, 1.3, 1.2, 1.1?

Over the last 10 to 15 years there has been increasing use of dynamic numerical modeling to perform deformation analyses. These programs and models can be incredibly complex and a significant challenge exists in developing and assigning needed input parameters. In general, the results are sensitive to the input parameters and can be sensitive to the input ground motion. The main criticisms of numerical modeling are that they can be overly complex, they lack verification on actual projects, and the results are sensitive to input parameters.

How to Assess Adequacy of an Existing Structure, or Planned Remediation.
Philosophically, how should the adequacy of a structure be evaluated: based on adequate stability, or on tolerable deformations? Must the safety factor against failure during earthquake loading be somewhat greater than 1.0, or can it be less than 1.0, provided that deformations are tolerable in terms of adequate freeboard, integrity of the drainage systems is maintained, and there is no development of adverse cracks? The answers to these questions depend on the confidence in the analysis procedures, and relates to the degree of conservatism that may have been inherently built into many of the parameters used.

INTERPRETATIONS OF CRITERIA OF VARIOUS AGENCIES

General
The agencies covered in this review include: the United States Army Corps of Engineers (USACE), the United States Bureau of Reclamation (USBR), the Federal Energy Regulatory Commission (FERC), the California Department of Water Resources (CADWR), and British Columbia Hydro (BCH). The general methodology was to obtain and review available documented agency guidelines, and the significant body of related scholarly publications and technical reports. Recognized experts from each of the agencies were contacted in an attempt to better understand the "spirit" of the guidelines and to obtain clarification of specific details. In addition, case histories were sought from each agency that would demonstrate use of the design criteria on specific projects.

Up to as recently as several years ago the overall approach to assessment of seismic stability was very similar among the various agencies, differing primarily in the details. However, two agencies, the USBR and BCH, are making a transition into a "risk" based approach to dam safety. Inherent in the use of risk based analyses is the acceptance of some potential for the loss of life, albeit very small. The models used for seismic assessment remain the same; however, the way that the models are being used and interpreted differs. The risk based approaches used by the USBR and BCH are very much in a state of flux, changing from year to year and project to project. The methodology used on a project last year may not be the same as that used next year.

Approaches Used

The criteria used by all of the agencies includes consideration of design seismicity, exploration and laboratory testing methods, assessment of liquefaction triggering, post-triggering strengths, post-triggering limit equilibrium stability, and post-triggering deformation analyses. Differences among the agencies exist related to preferred: magnitude of the post earthquake limit equilibrium safety factor; approaches used to determine post earthquake strengths; use of total stress or effective stress "triggering" analyses; and approaches used to conduct deformation analyses. Common to all methods is the need for site specific seismic input representative of the Maximum Credible Earthquake (MCE) in terms of earthquake magnitude, peak ground acceleration and associated time history. However, some agencies use deterministically developed MCE's while others use probabilistic. This section will provide a brief outline of the methodologies used by each of the agencies, followed by a discussion of the similarities and differences.

USACE.

For critical structures (potential loss of life), the USACE requires that the dam should survive and remain safe (i.e. no uncontrolled release of the pool) when subjected to the Maximum Credible Earthquake (MCE). The details of the seismic safety and evaluation process are described in detail in Appendix B of ER 1110-2-1155. The USACE guidelines call for a three phase process for seismic evaluation of existing dams: Seismic Safety Review, Phase I Special Studies, and Phase II Special Studies. The three phase approach has been implemented to eliminate those projects that are judged to be safe as early in the evaluation process as possible. The Seismic Safety Review generally consists of examination of existing data and the Periodic Inspections reports. Limited, simple preliminary analyses using existing data are performed when the initial screening indicates possible cause for concern. If the simple analyses indicate the potential for uncontrolled loss of reservoir or other factors leading to a loss of life then a Phase I Special Study is recommended.

The Phase I Special Study consists of developing site specific ground motions and performing field investigations and laboratory studies. Based on the gathered data, preliminary analyses are conducted to estimate the response of the dam to seismic loading and to identify problem areas that are in need of more detailed analyses. The dam response would typically be estimated using one-dimensional dynamic analyses with the program SHAKE. Post earthquake strengths for use in limit equilibrium stability analyses are typically obtained empirically from back analysis of well documented case histories (Seed and Harder, 1990). Deformation analysis is required if post earthquake limit equilibrium safety factors are inadequate. The method of deformation analysis is not specified, but dynamic numerical modeling is commonly used in addition to Newmark type analyses.

The Phase II Special Study is necessary when the Phase I Special Study concludes that potential deficiencies exist in the embankment dam or foundation which could lead to a

sudden uncontrolled loss of reservoir pool or other forms of unacceptable performance likely to cause loss of life. Comprehensive detailed analyses to evaluate seismic stability of the structure and to assess alternative remedial measures, if needed, are performed as part of the Phase II Study.

The recommended engineering approach to analyze an embankment dam and foundation for seismic stability consists of assessing both post earthquake static limit equilibrium slope stability and deformation response using detailed numerical analyses. The steps involved in the Phase II Study include:

1. Obtain deterministic based ground motions representative of the MCE (can be collected during Phase 1).
2. Perform detailed field investigations which may include a wide variety of techniques including SPT, CPT, BPT, geophysical methods, and laboratory tests (can be conducted during Phase 1).
3. Estimate the pre-earthquake stress field in the embankment and foundation.
4. Estimate the dynamic shear moduli of the soils in the embankment and foundation.
5. Estimate the earthquake induced **effective** stresses in the embankment and foundation using an appropriate 2-D or 3-D numerical model and the design time histories.
6. Estimate the liquefaction resistance of the embankment and foundation and the maximum potential residual excess pore water pressure using corrected penetration data and index tests.
7. Map the areal extent of suspect materials, estimate post earthquake shear strengths, and prepare several cross sections for final analyses
8. Perform static limit equilibrium analyses to identify potential zones of the dam and foundation that may require remediation.
9. Estimate the deformation response and post earthquake shape of the embankment using numerical or other appropriate deformation analyses.
10. Recommend remediation when the limit equilibrium safety factor is inadequate or it is concluded that the resulting deformations would lead to a sudden, uncontrolled loss of the reservoir pool and loss of life.
11. Perform additional post earthquake limit equilibrium slope stability and finite element analyses to estimate preliminary remediation needs.
12. Evaluate various preliminary remediation alternatives and select the most appropriate alternatives for cost estimating purposes.
13. Perform additional numerical analyses to estimate expected deformations in both the remediated and non-remediated sections of the dam, overall dam response, and differential deformation.

The minimum required post earthquake limit equilibrium safety factor is 1.0 based on EM 1110-2-1902. The post earthquake strengths for liquefied materials are typically determined using the empirical charts based on corrected standard penetration test N values proposed by Seed and Harder (1990). Deformation analyses are typically conducted using non-linear dynamic numerical analyses.

USBR.

The USBR is in the process of revising their approach to assessing the seismic stability of embankment dams. The following discussion is interpreted from new draft guidelines, and conversations with USBR personnel. As noted earlier, the USBR is in the process of shifting from a deterministic based approach to a risk based approach such that the applicable criteria varies with the interpreted level of risk. The level of risk is determined using a variety of information including the earthquake return period, the number of potential fatalities if a breach occurred, and the confidence in the data. However, the design approach that is used is similar to that used by the USACE.

The USBR lists the following six steps to assess the response of an embankment dam to seismic loading. Details are found in USBR Design Standards for Embankment Dams, Chapter 13: Seismic Design and Analyses, Working Draft (7/3/2001). .

1. Determine the "evaluation earthquake(s)," which include the magnitude and source of that will be used to assess the structure. Both deterministic and/or probabilistic approaches are employed.
2. Determine the ground-motion time histories associated with evaluation earthquakes. As with Step 1, both deterministic and/or probabilistic approaches are used. The frequency content of the design earthquake are "matched' to the frequency of the structure.
3. Determine the properties of the embankment and foundation materials (similar approach as USACE),
4. Determine the liquefaction potential of the foundation and embankment. Unlike the USACE, earthquake induced stresses are evaluated in terms of total stresses.
5. Determine the stability of the embankment if liquefaction would cause loss of strength.
6. Predict the extent of deformations resulting from earthquake shaking and/or loss of strength of materials.

Other considerations include embankment cracking, filter compatibility, and response to fault movements. If the embankment is unstable or predicted deformations exceed tolerable limits, corrective action may be required. The decision to take corrective action is made considering the probability of dam failure and the consequences.

FERC.

The FERC is currently revising "Engineering Guidelines for the Evaluation of Hydropower Projects." A revised draft of Chapter 4, which deals with embankment dams, is expected to be available this year (2001). The FERC has no intention of moving towards a probabilistic risk based approach to assess stability. The charge of the FERC is to review engineering analyses and plans for remedial design submitted by dam owners. Although, they do not preclude use of probabilistic methods of analyses, the results must be consistent with conventional deterministic analyses. Their general approach is similar to the USACE, citing ER 1110-2-1806, and includes the use of deterministic based development of the MCE. It appears that there is more skepticism to the interpretation of deformations from sophisticated numerical deformation analyses. More reliance is placed on Newmark-type analyses.

Although the existing FERC guidelines are being modified, a philosophical change from the 1991 document, which follows the USACE approach, is not expected. There are some specific criteria cited in the document as follows:

- The limit equilibrium safety factor must be greater than 1.0 for post-triggering reduced strength conditions,
- Deformations should not exceed two feet based on a Newmark type analyses (exceptions are made, based on details of dam construction and recommendations of review boards).
- Deformation calculations are applicable only if post-triggering safety factors are greater than 1.0.

CADWR

A discussion of the approach used in seismic assessment of earth dams by the CADWR is described by Babbitt and Verigin (1996). A brief overview drawn from that paper is provided here. The CADWR uses a two-phase approach in the assessment process that is similar in scope to the Phase I and Phase II approach used by the USACE. The first phase utilizes site specific design seismicity, subsurface exploration and laboratory testing, and preliminary analyses. The preliminary analyses include assessment of liquefaction potential using Seed and Idriss's method to assign zones of liquefied materials, and post triggering stability analyses using residual strengths from Seed and Harder (1990). If the analyses indicate a significant risk of instability a more detailed investigation is undertaken. The CADWR reviews analyses prepared by, or for, dam owners and makes independent analyses. The independent analyses performed by CADWR are described as simplified techniques: Seed-Idriss approach to liquefaction potential based on SPT N values and, Newmark and Makdisi-Seed deformation analyses. Other more rigorous methods of analysis, including sophisticated dynamic finite element analyses, are believed to be logically formulated, but have not been substantiated by observed performance of existing dams. Accordingly, these methods are viewed with "conservative skepticism." An outline of the procedure used by CADWR was drawn from Babbitt and Verigin and is similar to the USACE Phase I and II.

1. Obtain design seismicity based on the MCE.
2. Develop an exploration and testing program that is consistent with seismic loading, site geology, dam size, and existing data. The minimum level of exploration and testing should include site inspection by geologist and geotechnical engineer, trenching, continuously sampled and logged drillholes with SPT's obtained at a maximum of five-foot intervals, soil classification tests, determination of in-situ densities, moisture-density tests, and shear strength tests (type dependent on projected needs for later analysis).
3. Perform preliminary analysis of embankment and foundation to identify need for further analysis. A liquefaction potential analysis is performed at this point to locate liquefiable soil units and assign preliminary residual strengths. Preliminary stability analyses are performed and a decision is made that the dam is either stable or further evaluation is required.
4. A plan is designed for a second phase of exploration and testing. Items that will potentially cause stability problems have now been identified and the program is designed to concentrate on these items. A method of analysis considered most appropriate for evaluating the dam stability is selected. It is important to gather all data necessary to perform the analysis. Exploration and laboratory tests that are usually considered at this point are: additional borings and SPT testing, CPT testing, Becker

hammer testing, seismic surveys, undisturbed sampling for triaxial shear testing, a specific shear test required to perform the desired analysis.

5. The next step is to perform the dynamic stability analysis. If dam is judged to be unstable, then proceed to conceptual repair design. If dam is stable then evaluate potential deformations.
6. Next, perform the deformation analysis. Simplistic or rigorous approach may be selected depending on the anticipated deformation magnitudes, size and potential hazard posed by deformations, and applicability of dam characteristics to selected model.
7. Evaluate deformation results and determine the need for additional work required to assure that dam failure will not occur under design seismic loading.

BCH

Although BCH does not publish a design guidelines document, there evolving approach to assessing and dealing with seismic stability is extensively published in the technical literature. The following outline summarizes the approach used by BCH to perform a seismic evaluation.

1. Use a probabilistic approach to the development of MCE ground motions.
2. Perform detailed field investigations.
3. Estimate the pre-earthquake stress field in the embankment and foundation.
4. Estimate the dynamic shear moduli of the soils in the embankment and foundation.
5. Estimate the earthquake induced shear stresses in the embankment and foundation from a total stress analysis using the computer program SHAKE and the design time histories.
6. Estimate the liquefaction resistance of the embankment and foundation and the maximum potential residual excess pore water pressure using corrected penetration data and index tests.
7. Map the areal extent of suspect materials, estimate the post earthquake shear strengths, and prepare several cross sections for final analyses.
8. Perform static limit equilibrium analyses to identify potential zones of the dam and foundation that may require remediation.
9. Estimate the deformation response and post earthquake shape of the embankment using numerical or other appropriate deformation analyses.
10. Recommend remediation when the limit equilibrium safety factor is inadequate or it is concluded that the resulting deformations would lead to a sudden, uncontrolled loss of the reservoir pool and loss of life.
11. Perform additional post earthquake limit equilibrium slope stability and finite element analysis to estimate preliminary remediation needs.
12. Evaluate various preliminary remediation alternatives and select the most appropriate alternatives for cost estimating purposes.
13. Perform additional numerical analyses to estimate expected deformations in both the remediated and non-remediated sections of the dam, overall dam response, and differential deformation.

COMPARISON OF APPROACHES FROM VARIOUS AGENCIES

Table 1 provides a comparison for select factors where information was available.

Table 1. Comparison of Criteria Proposed by Various Agencies.

	USACE	USBR	FERC	CADWR	BCH
Basis for MCE	Deterministic	Both	Deterministic	Deterministic	Probabilistic
Use of Total or Effective Stresses in Stress Analysis	Effective	Total	Effective	Total	Total
Minimum Post-Earthquake Safety Factor	>1.0[1]	1.05 to 1.20[2]	>1.0	>1.0	>1.0
Deformation Analyses by Newmark Type or Numerical Modeling	Both	Both	Newmark	Newmark	Both

[1]Exceptions made on a case by case basis.
[2]SF=1.20 is applicable when best estimate of post-earthquake strengths. SF=1.05 is used for worst case estimate of post-earthquake strengths.

Of the five agencies considered, three are dam owners, USACE, USBR and BCH, while the FERC and CADWR are regulators. Generalizations can be made regarding the philosophical differences between the dam owners and the dam regulators. For example, the FERC and CADWR can be viewed as skeptical of both probabilistic based approaches, and dynamic numerical analyses, while USBR and BCH are moving towards probabilistic methodologies. Moreover, all three dam owners are more likely to use numerical modeling in the deformation analyses.

Regarding risk-based studies, it is possible for regulators to take the view that a probabilistic approach is used solely to make an argument that a dam has adequate stability, when a deterministic approach would indicate that it does not. Conversely, for an owner of many dams the probabilistic approach has many advantages because it allow the quantification and prioritization of risk among many structures. In fact, risk based approaches can sometimes show that the largest earthquake event may not pose the greatest risk. A smaller event with a shorter return period may pose greater risk. Moreover, it may be illustrated that other modes of failure pose greater risk than seismic loading and require more immediate attention.

In terms of deformation analyses, the regulators can be viewed as more skeptical of numerical analyses. The primary concern is that predictions from these methods of analyses have not been substantiated by observed performance. It is natural for an agency that owns many dams to want to advance the state-of-the-art through the use of numerical analyses such that design efficiencies may be realized.

Unlike the USBR, the USACE has not embraced a risk-based design approach. It is the authors perspective that this is due to the history and charge of the two organizations and the resulting subtle philosophical differences that have developed. The primary charge of the USACE regarding dams is related to flood control and navigation (locks), while the USBR has been power supply. The first step in moving toward a risked based assessment is accepting and quantifying the risk of loss of life. This appears to be at conflict with the basic premise governing the civilian efforts of the USACE.

SUMMARY

The geotechnical professions ability to reliably predict the occurrence and extent of liquefaction below an embankment dam is extremely limited because the subject is complex and there is very limited empirical data available to use for guidance. Various approaches have evolved that often lead to very different conclusions, with a significant difference of opinion as to which methods are appropriate. Some of the differences are primarily due to the agencies basic function as an owner or regulator. Obviously, the perspective is much different when you own/operate a facility and when you are merely providing regulatory oversight.

REFERENCES

Babbitt and Verigin, 1996. "General Approach to Seismic Stability Analysis of Earth Embankment Dams," CADWR. Available at http://damsafety.water.ca.gov/tech-ref/dhb%201996%20paper.pdf

Byrne, PM, Imrie, AS, and Morgenstern, NR, (1994). "Results And Implications Of Seismic Performance Studies For Duncan Dam," Canadian Geotechnical Journal, vol 31, nr 6, s 979-988.

Garner, S.J., Hartford, D.N.D, Salmon, G.M., Stewart, R.A., and Turner, F.P.P (1998). "Seismic Risk Management in the Pacific Northwest Utility," ASCE Geotechnical Publication No. 75, p141-151.

Liao S.S.C., and Lum, K.Y. (1998). Statistical Analysis and Application of the Magnitude Scaling Factor in Liquefaction Analysis," ASCE Geotechnical Publication No. 75, p410-422.

NCEER, Proceedings of the National Center for Earthquakes Research Workshop on Evaluation of Liquefaction Resistance of Soils, 1996.

Pillai, VS, and Salgado, FM, 1994. "Post-Liquefaction Stability And Deformation Analysis Of Duncan Dam," Canadian Geotechnical Journal, vol 31, nr 6, s 967-978.

Pillai, VS, and Stewart, RA , "Evaluation Of Liquefaction Potential Of Foundation Soils At Duncan Dam," Canadian Geotechnical Journal, vol 31, nr 6, s 951-966.

Plewes, HD, Pillai, VS, Morgan, MR, and Kilpatrick, BL, 1994. "In Situ Sampling, Density Measurements, And Testing Of Foundations Soils At Duncan Dam,' Canadian Geotechnical Journal, vol 31, nr 6, s 927-938.

Poulos, SJ, Castro, G, and France, JW (1985). "Liquefaction Evaluation Procedure," Journal of Geotechnical Engineering, vol 111, nr 6, s 772-792.

Sego, DC, Robertson, PK, Sasitharan, S, Kilpatrick, BL, and Pillai, VS, 1994. "Ground Freezing And Sampling Of Foundation Soils At Duncan Dam," Canadian Geotechnical Journal, vol 31, nr 6, s 939-950.

Vick, S.G. and Stewart, R.A. (1996). "Risk Analysis in Dam Safety Practice," ASCE Geotechnical Publication No. 58, p586-603.

APPENDIX
PAST OHIO RIVER VALLEY SOILS SEMINARS

ORVSS I	*BUILDING FOUNDATION DESIGN AND CONSTRUCTION*, October 16, 1970, Lexington, KY.
ORVSS II	*EARTHWORK ENGINEERING, START TO FINISH*, October 15, 1971, Louisville, KY.
ORVSS III	*LATERAL EARTH PRESSURES*, October 27,1972, Fort Mitchell, KY.
ORVSS IV	*GEOTECHNICS IN TRANSPORTATION ENGINEERING*, October 5,1973, Lexington, KY.
ORVSS V	*ROCK ENGINEERING*, October 18, 1974, Clarksville, IN.
ORVSS VI	*SLOPE STABILITY AND LANDSLIDES*, October 17, 1975, Fort Mitchell, KY.
ORVSS VII	*SHALES AND MINE WASTES: GEOTECHNICAL PROPERTIES, DESIGN, AND CONSTRUCTION*, October 8, 1976, Lexington, KY.
ORVSS VIII	*EARTH DAMS AND EMBANKMENTS: DESIGN, CONSTRUCTION, AND PERFORMANCE*, October 14, 1977, Louisville, KY.
ORVSS IX	*DEEP FOUNDATIONS*, October 27, 1978, Fort Mitchell, KY.
ORVSS X	*GEOTECHNICS OF MINING*, October 5, 1979, Lexington, KY.
ORVSS XI	*EARTH PRESSURES AND RETAINING STRUCTURES*, October 10, 1980, Clarksville, IN.
ORVSS XII	*GROUNDWATER: MONITORING, EVALUATION, AND CONTROL*, October 9, 1981, Fort Mitchell, KY
ORVSS XIII	*RECENT ADVANCES IN GEOTECHNICAL ENGINEERING PRACTICE*, October 8,1982, Lexington, KY.
ORVSS XIV	*FOUNDATION INSTRUMENTATION AND GEOPHYSICAL EXPLORATION*, October 14, 1983, Clarksville, IN.
ORVSS XV	*PRACTICAL APPLICATION OF DRAINAGE IN GEOTECHNICAL ENGINEERING*, November 2, 1984, Fort Mitchell, KY.
ORVSS XVI	*APPLIED SOIL DYNAMICS*, October 11, 1985, Lexington, KY.
ORVSS XVII	*NATURAL SLOPE STABILITY AND INSTRUMENTATION*, October 17, 1986, Clarksville, IN.

APPENDIX
PAST OHIO RIVER VALLEY SOILS SEMINARS

ORVSS XVIII	*LIABILITY ISSUES IN GEOTECHNICAL ENGINEERING AND CONSTRUCTION*, November 6, 1987, Fort Mitchell, KY.
ORVSS XIX	*CHEMICAL AND MECHANICAL STABILIZATION OF SOIL SUBGRADES*, October 21, 1988, Lexington, KY.
ORVSS XX	*CONSTRUCTION IN AND ON ROCK*, October 27, 1989, Louisville, KY.
ORVSS XXI	*ENVIRONMENTAL ASPECTS OF GEOTECHNICAL ENGINEERING*, October 26, 1990, Fort Mitchell, KY.
ORVSS XXII	*DESIGN AND CONSTRUCTION WITH SYNTHETICS*, October 18, 1991, Lexington, KY.
ORVSS XXIII	*IN-SITU SOIL MODIFICATION*, October 16, 1992, Louisville, KY.
ORVSS XXIV	*GEOTECHNICAL ASPECTS OF INFRASTRUCTURE RECONSTRUCTION*, October 15, 1993, Fort Mitchell, KY.
ORVSS XXV	*RECENT ADVANCES IN DEEP FOUNDATIONS*, October 21, 1994, Lexington, KY.
ORVSS XXVI	*SITE INVESTIGATIONS: GEOTECHNICAL AND ENVIRONMENTAL*, October 20, 1995, Clarksville, IN.
ORVSS XXVII	*FORENSIC STUDIES IN GEOTECHNICAL ENGINEERING*, October 11, 1996, Cincinnati, OH.
ORVSS XXVIII	*UNCONVENTIONAL FILLS: DESIGN, CONSTRUCTION, AND PERFORMANCE*, October 10, 1997, Lexington, KY.
ORVSS XXIX	*PROBLEMATIC GEOTECHNICAL MATERIALS*, October 16, 1998, Louisville, KY.
ORVSS XXX	*VALUE ENGINEERING IN GEOTECHNICAL CONSULTING AND CONSTRUCTION*, October 1, 1999, Cincinnati, OH.
ORVSS XXXI	*INSTRUMENTATION*, September 15,2000, Lexington, KY.